

1-1-1990

**Surface modification of poly(tetrafluoroethylene-co-hexafluoropropylene) ; Surface initiated graft polymerization ; Surface chemistry of fibrillar carbon/**

Robert Charles Bening  
*University of Massachusetts Amherst*

Follow this and additional works at: [https://scholarworks.umass.edu/dissertations\\_1](https://scholarworks.umass.edu/dissertations_1)

---

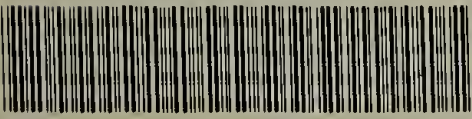
**Recommended Citation**

Bening, Robert Charles, "Surface modification of poly(tetrafluoroethylene-co-hexafluoropropylene) ; Surface initiated graft polymerization ; Surface chemistry of fibrillar carbon/" (1990). *Doctoral Dissertations 1896 - February 2014*. 768.  
<https://doi.org/10.7275/qd1n-x369> [https://scholarworks.umass.edu/dissertations\\_1/768](https://scholarworks.umass.edu/dissertations_1/768)

This Open Access Dissertation is brought to you for free and open access by ScholarWorks@UMass Amherst. It has been accepted for inclusion in Doctoral Dissertations 1896 - February 2014 by an authorized administrator of ScholarWorks@UMass Amherst. For more information, please contact [scholarworks@library.umass.edu](mailto:scholarworks@library.umass.edu).



UMASS/AMHERST



312066007778586



I. SURFACE MODIFICATION OF  
POLY(TETRAFLUOROETHYLENE-CO-HEXAFLUOROPROPYLENE)  
II. SURFACE INITIATED GRAFT POLYMERIZATION  
III. SURFACE CHEMISTRY OF FIBRILLAR CARBON

A Dissertation Presented  
by  
ROBERT CHARLES BENING Jr.

Submitted to the Graduate School of the  
University of Massachusetts in partial fulfillment  
of the requirements for the degree of

DOCTOR OF PHILOSOPHY

September 1990

Polymer Science and Engineering

© Copyright by Robert Charles Bening Jr. 1990

All Rights Reserved



I. SURFACE MODIFICATION OF  
POLY (TETRAFLUOROETHYLENE-CO-HEXAFLUOROPROPYLENE)  
II. SURFACE INITIATED GRAFT POLYMERIZATION  
III. SURFACE CHEMISTRY OF FIBRILLAR CARBON

A Dissertation Presented

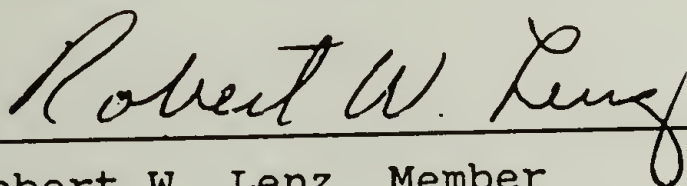
by

ROBERT CHARLES BENING Jr.

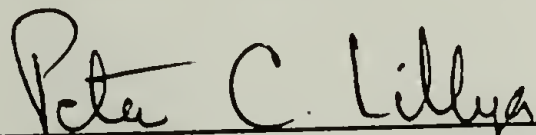
Approved as to style and content by:



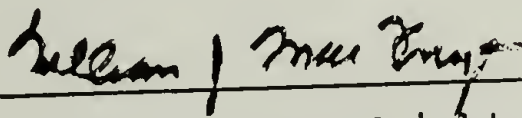
Thomas J. McCarthy, Chair



Robert W. Lenz, Member



Peter C. Lillya, Member



William J. MacKnight, Department Head  
Polymer Science and Engineering

## ACKNOWLEDGEMENTS

There are many people whose help and encouragement have made my successful completion of this graduate program possible. The guidance and enthusiasm offered by my advisor, Dr. Thomas McCarthy has been invaluable. The atmosphere created in this group gave me the right blend of direction and freedom to progress from performing experiments to doing research. I would also like to acknowledge the efforts of my committee, Professors Lenz and Lillya.

Nothing I can say can begin to do justice to the encouragement and assistance that Ginger has given me. Her love, patience and typing have been truly "above and beyond the call of duty".

I would also like to thank the students of McCarthy's group, past and present, especially Joan, Rick, Nicole, Molly, Damo, Brant and Elisa, whose conversations and comments have been very helpful. I would also like to thank Dave Waldman for his advice on spectroscopy, Dwight and all of the members of Professor Uden's group for their help with gas chromatography and Dave Martin and John Reffner for their help with SEM and TEM.

I would also like to recognize Dr. Dave Cotts and Dr. Andrea Chow and everybody at SRI International for making my "Pre-Doc" at SRI such valuable preparation for graduate school.



## ABSTRACT

I. SURFACE MODIFICATION OF  
POLY(TETRAFLUOROETHYLENE-CO-HEXAFLUOROPROPYLENE)

II. SURFACE INITIATED GRAFT POLYMERIZATION

III. SURFACE CHEMISTRY OF FIBRILLAR CARBON

ROBERT CHARLES BENING Jr., B.A. UNIVERSITY OF  
CALIFORNIA, BERKELEY

Ph.D. UNIVERSITY OF MASSACHUSETTS

Directed by: Professor Thomas J. McCarthy

Part I of this dissertation deals with the surface modification of poly(tetrafluoroethylene-co-hexafluoropropylene) (FEP). The reduction of FEP using sodium naphthalide was studied with regard to the kinetics of reaction and the product structure. The thickness of the resulting modified surface layer could be controlled, using reaction time and temperature, in the ranges of 45-90 and 250-800 Å. The air-sensitive reduction product contained carbon-carbon double and triple bonds, aliphatic C-H bonds, alcohols, carbonyls and very little fluorine. Hydroboration/oxidation introduced hydroxyl groups in high yield to the surface. The alcohols exhibited low reactivity in esterification reactions in the absence acylation catalysts. Treatment of

this surface with ethylene oxide in the presence of LDA rendered a more reactive, primary alcohol-containing, surface. Reaction of the hydroxyl surface produced by hydroboration and oxidation with 1,4-toluene diisocyanate or isophorone diisocyanate resulted in surface-bound isocyanate groups. The reactivity of these surfaces towards nucleophiles was investigated.

Part II deals with graft polymerization from surface-confined initiator species. Halogenated surfaces were prepared by treating reduced FEP with chlorine or bromine. Treatment of these surfaces with silver trifluoromethanesulfonate in the presence of tetrahydrofuran (THF) resulted in the polymerization of THF from the surface. Initiation at temperatures less than  $-10^{\circ}\text{C}$ , followed by polymerization at  $-10^{\circ}\text{C}$ , resulted in a relatively thick, homogeneous overlayer of the graft polymer. Neopentyl and *n*-propyl alcohol groups were introduced to the surface of poly(chlorotrifluoroethylene) (PCTFE) by reaction with the appropriate protected alcohol-containing lithium reagent. The corresponding tosylate surfaces were prepared and the reaction of these surfaces with 2-methyloxazoline was studied. Acrylamide monomers were polymerized from hydroxyl surfaces derived from FEP using ceric ion redox initiation. The introduction of trimethylsilyl ketene acetal groups to polymer surfaces was also investigated.



Part III deals with the surface chemistry of fibrillar carbon. Oxidation and reactions with carbenes were studied as a means of introducing functional groups to the surface. X-ray photoelectron spectroscopy was used to characterize the products; chemical derivatization was used to determine the functional group composition of the oxidized surface.

# TABLE OF CONTENTS

	Page
ACKNOWLEDGEMENTS.....	iv
ABSTRACT.....	v
LIST OF TABLES.....	xvi
LIST OF FIGURES.....	xix
LIST OF EQUATIONS.....	xxii
PART I	
SURFACE MODIFICATION OF POLY(TETRAFLUOROETHYLENE -CO-HEXAFLUOROPROPYLENE).....	1
Chapter	
I. INTRODUCTION.....	2
Chemical Modification of Fluoropolymer Surfaces.....	3
Surface Chemistry of PTFE.....	3
Chemical and Structural Properties of FEP. Structure-Reactivity Characteristics of Functionalized Polymers.....	4
Reactions of Nucleophilic Surfaces with Multifunctional Electrophiles.....	5
Surface Analytical Techniques.....	7
Contact Angle Measurements.....	7
X-Ray Photoelectron Spectroscopy (XPS). Attenuated Total Reflectance IR Spectroscopy (ATR-IR).....	8
Gravimetric Analysis.....	9
Ultraviolet-Visible Light Spectroscopy.	12
References.....	13
II. EXPERIMENTAL SECTION.....	14
Methods.....	15
Inert Atmosphere Techniques.....	18
Analytical Techniques.....	19
Purification of Solvents and Reagents.....	21
Preparation and Characterization of Reduced FEP Surfaces.....	24
Kinetics of the Reduction of FEP with Sodium Naphthalide (FEP-C).....	24



Reaction of FEP with Benzoin Dianion.....	26
Reaction of PTFE with Sodium Naphthalide..	27
Oxidation of Reduced Surfaces with KClO <sub>3</sub> /H <sub>2</sub> SO <sub>4</sub> .....	27
Preparation of FEP-C Using Sublimed Naphthalene.....	28
Preparation of FEP-C Using Non-Aqueous Work Up.....	28
Preparation of FEP-C Using D <sub>2</sub> O Rinsing....	29
Preparation of FEP-C Using THF-d <sub>8</sub> .....	29
Preparation of FEP-C Using D <sub>2</sub> O "Spiked" THF.....	30
Preparation of FEP-C in a PTFE Reactor...	30
Preparation of FEP-C in an OD-Enriched Glass Reactor.....	31
Preparation of FEP-C Using Naphthalene-d <sub>8</sub> .....	32
Preparation of FEP-C Using Only Deuterated Reagents.....	32
Reaction of FEP-C with Oxygen and Air.....	33
Reaction of FEP-C with Aryl Hydrazines....	34
Reaction of FEP-C with Heptafluorobutyryl Chloride.....	34
Preparation of FEP-C for Further Modifications.....	35
Hydroboration and Subsequent Oxidation of FEP-C (FEP-OH).....	35
Reaction of FEP-OH with Aryl Hydrazines...	36
Reaction of FEP-OH with HFBC in THF.....	36
Reaction of FEP-OH with HFBC in Pyridine..	37
DMAP Catalyzed Reaction of FEP-OH with HFBC in Pyridine.....	38
DMAP Catalyzed Reaction of FEP-OH with HFBC in THF.....	38
Reaction of FEP-OH with Ethylene Oxide and LDA (FEP-EO-OH).....	39
Reaction of FEP-EO-OH with HFBC.....	40
Reaction of FEP-OH with Ethylene Oxide and DBU.....	40
Reaction of the Ethylene Oxide/DBU Product with HFBC.....	40
Reaction of FEP-C with Methanol and Benzoyl Peroxide.....	41
Reaction of the BPO/Methanol Product with HFBC.....	41
Reaction of FEP-C with 9-BBN (FEP-9BBN)...	41
Carbonylation and Basic Work Up of FEP-9BBN (FEP-CH <sub>2</sub> OH).....	42
Reaction of FEP-CH <sub>2</sub> OH with HFBC.....	43

Reaction of Hydroxylated Surfaces with Multifunctional Electrophiles.....	43
Preparation of PCTFE-OH.....	44
Reaction of FEP-OH and PCTFE-OH with Cyanuric Chloride.....	45
Reaction of FEP-OH with 2,4-Toluene Diisocyanate (FEP(TDI)-NCO).....	46
Reaction of FEP-OH with Isophorone Diisocyanate (FEP(IPDI)-NCO).....	47
Reaction of PCTFE-OH with TDI (PCTFE(TDI)-NCO).....	48
Reaction of PCTFE-OH with IPDI (PCTFE(IPDI)-NCO).....	48
Reaction of FEP-OH with Hexamethylene Diisocyanate (FEP(HMDI)-NCO).....	49
Reaction of Isocyanate Surfaces with 3-Bromo-1-Propanol.....	49
Reaction of Isocyanate Surfaces with 4-Bromophenylethyl Alcohol.....	50
Reactions of Isocyanate Surfaces with Methanol.....	50
References.....	51
III. RESULTS AND DISCUSSION.....	52
Sodium Naphthalide Reduction of FEP.....	52
Kinetics and Structure of FEP-C.....	52
Variable Angle XPS.....	57
Functional Group Composition.....	60
Origin of OH, C=O and C-H Groups.....	64
Conclusions.....	67
Other Reductions.....	68
Synthesis and Reactivity of FEP-OH.....	75
Preparation of FEP-OH.....	77
Reactions of FEP-OH with HFBC.....	80
Other Approaches to Hydroxylated FEP.....	84
Reactions of Hydroxyl Surfaces with Multifunctional Electrophiles.....	93
Reactions with Cyanuric Chloride.....	93
Reactions with Diisocyanates.....	95
References .....	107
IV. CONCLUSIONS AND SUGGESTIONS.....	110



PART II	
SURFACE INITIATED GRAFT POLYMERIZATION.....	114
V. INTRODUCTION.....	115
References.....	120
VI. EXPERIMENTAL SECTION.....	121
Methods.....	121
Purification of Solvents and Reagents.....	122
Attempted Polymerization of MMA from FEP-C.....	126
Attempted Polymerization of MMA from FEP-OH.....	126
Ce <sup>IV</sup> Initiated Polymerization of Acrylamides.....	127
Aluminoporphyrin-Initiated Ring Opening Polymerizations.....	129
Preparation of TPP-Al-Et.....	129
Preparation of TPP-AlO- <i>i</i> Pr.....	129
Preparation of TPP-AlO- <i>t</i> Bu.....	130
Model Polymerizations.....	130
Reaction of PCTFE-OH with TPP-Al-Et (PCTFE-OAl-TPP).....	131
Reaction of PCTFE-OAl-TPP with Epoxide Monomers.....	132
TPP-Al-Cl Initiated Polymerization in the Presence of PCTFE-OH.....	133
Adsorption of TPP-H <sub>2</sub> by PCTFE-OH.....	135
Cationic Ring Opening Polymerization of THF.....	135
Chlorination of FEP-C.....	135
Room Temperature Initiation from FEP-Cl.....	136
Reaction of Graft Surfaces with Heptafluorobutyryl Chloride.....	137
Bromination of FEP-C (FEP-Br).....	138
Low Temperature Initiation from FEP-Br.....	139
Low Temperature Initiation from FEP-Cl.....	140
Preparation of Neopentyl Alcohol Surfaces.	141

Preparation of 3-Bromo-2,2-Dimethyl- propyl Ethyl Acetaldehyde Acetal (BrDiMePrOP) .....	141
Reaction of LidiMePrOP with Acetone....	142
Reaction of LidiMePrOP with PCTFE Film (PCTFE-diMe-OP) .....	142
Deprotection of PCTFE-diMe-OP (PCTFE-diMe-OH) .....	145
Reaction of PCTFE-diMe-OH with HFBC....	145
Attempted Preparation of Triflate Surfaces.	145
Reaction of PCTFE-OH with Trifluoromethanesulfonyl Chloride.....	145
Reaction of PCTFE-diMe-OH with Trifluoromethanesulfonic Anhydride.....	147
Reaction of PCTFE-diMe-OH with Trifluoromethanesulfonyl Chloride.....	148
Cationic Ring Opening Polymerization of 2-Methyloxazoline .....	149
Reaction of PCTFE-OH with Toluenesulfonyl Chloride (PCTFE-OTos) .....	149
Reaction of PCTFE-diMe-OH with TosCl (PCTFE-diMe-OTos) .....	150
Reaction of Tosylate Surfaces with 2-Methyloxazoline .....	150
Group Transfer Polymerizations .....	152
Reaction of PCTFE-OH with Isobutyryl Chloride (PCTFE-OC(=O)-iBu) .....	152
Reaction of PCTFE-OC(=O)-iBu with Trimethylsilyl Chloride and LDA .....	152
Reaction of PCTFE-OC(=O)-iBu with Trimethylsilyl Chloride and Triethylamine in DMF .....	153
Reaction of PCTFE-OC(=O)-iBu with TEA and Trimethylsilyl Triflate .....	154
Reaction of Ethyl Phenylacetate with TEA and TMSOTf .....	154
1-Ethoxy-1-(Trimethylsilyloxy)-2-Phenyl Ethylene Initiated Polymerization of MMA .....	156
Reaction of PCTFE-OH with Phenylacetyl Chloride (PCTFE-OC(=O)CH <sub>2</sub> Ph) .....	156
Reaction of PCTFE-OC(=O)CH <sub>2</sub> Ph with TEA and TMSOTf .....	157



Reaction of PCTFE-diMe-OH with Phenylacetyl Chloride (PCTFE-diMe-OC(=O)CH <sub>2</sub> Ph) .....	157
Reaction of PCTFE-diMe-OC(=O)CH <sub>2</sub> Ph with TEA and TMSOTf .....	158
Attempted Initiation of MMA from Surfaces Treated with TMSOTf and TEA...	159
Preparation of 3-Bromo-2,2-Dimethyl-1-Propyl Isobutyrate (BrPri <u>Bu</u> ) .....	160
Reaction of BrPri <u>Bu</u> with LDA and Trimethylsilyl Chloride (BrPrTMSKA) ....	161
Reaction of LiPrTMSKA with PCTFE .....	162
Reaction of LiPrTMSKA with PEEK .....	163
Polymerization of $\epsilon$ -Caprolactam from Isocyanate Surfaces .....	163
Attempted Room Temperature Polymerization of $\epsilon$ -Caprolactam .....	164
VII. RESULTS AND DISCUSSION .....	166
Ce <sup>IV</sup> Initiated Polymerization of Acrylamides .....	167
Aluminoporphyrin-Initiated Ring Opening Polymerization .....	176
Polymerization of THF from Halogenated Surfaces .....	189
Attempted Preparation of Triflate Surfaces and Preparation of Neopentyl Alcohol Surfaces .....	208
Ring Opening Polymerization of 2-Methyloxazoline .....	219
Group Transfer Polymerizations .....	228
Polymerization of $\epsilon$ -Caprolactam from Isocyanate Surfaces .....	250
References .....	257
VIII. CONCLUSIONS AND SUGGESTIONS .....	260
References .....	267
PART III	
SURFACE CHEMISTRY OF FIBRILLAR CARBON .....	268
IX. INTRODUCTION .....	269
Fibrillar Carbon .....	269
Chemical Modification of Graphitic Carbon .....	273
Chemical Composition of Oxidized Carbon ...	274

Titrametric Studies.....	275
Spectroscopic Studies.....	277
Derivitization Experiments.....	277
Overall Conclusions.....	278
Objectives.....	279
References .....	281
X. EXPERIMENTAL SECTION.....	283
Methods.....	283
Purification of Solvents and Reagents.....	285
KClO <sub>3</sub> Oxidation.....	287
Lithium Triethylborohydride Reduction.....	288
Reaction with Thallium Ethoxide.....	289
Reaction of Tl-Labeled Surfaces with Heptafluorobutyryl Chloride.....	289
Preparation of Trifluoromethyldiazomethane.	290
Reaction of CF <sub>3</sub> CHN <sub>2</sub> with Benzoic Acid in Dichloromethane.....	292
Boron Trifluoride Etherate Catalyzed Reaction with CF <sub>3</sub> CHN <sub>2</sub> .....	292
Reaction with 2,4-Dinitrophenylhydrazine..	293
Reaction with Heptafluorobutyryl Chloride.	294
Reaction with DCC and p-Bromophenylethanol.	295
Reaction with Carbonyldiimidazole.....	295
DBU Catalyzed Reactions with Electrophiles.	296
Reaction with Sodium Methoxide.....	296
Reaction with Thionyl Chloride.....	297
Titration.....	297
Reactions of Fibrillar Carbon with Carbenes.....	298
Cu Catalyzed Reaction with CF <sub>3</sub> CHN <sub>2</sub> .....	298
Cu Catalyzed Reaction with Ethyl Diazoacetate.....	299
Thermal Decomposition of Ethyl Diazoacetate in the Presence of Fibril Samples.....	300
Amidation of Ester Surfaces.....	301
XI. RESULTS AND DISCUSSION.....	302
Oxidation and Reduction.....	302
Labeling Reactions.....	308
Titration Results.....	324
Functional Group Composition.....	327
Reactions of Fibrillar Carbon with with Carbenes.....	329
Effect of Oxidation on Fibril Morphology..	335

References .....	338
XII. CONCLUSIONS AND SUGGESTIONS.....	341
APPENDICES	
A. SUMMARY OF GC-MS AND GC-IR DATA FOR LidiMeProp MODEL REACTIONS.....	345
B. SUMMARY OF GC-MS DATA FOR THE PREPARATION OF 1-ETHOXY-1-(TRIMETHYLSILYLOXY) -2-PHENYL ETHYLENE.....	347
C. SUMMARY OF GC-MS AND GC-IR DATA FOR LiPrTMSKA PREPARATION AND REACTIONS....	348
BIBLIOGRAPHY.....	349



# LIST OF TABLES

Table		Page
1	XPS atomic composition data for labeling of FEP-C.....	63
2	XPS atomic composition data for acylation of FEP-OH with heptafluorobutyryl chloride.....	81
3	XPS atomic composition data for primary hydroxyl surfaces derived from ethylene oxide.....	86
4	XPS atomic composition data for other primary hydroxyl surfaces.....	90
5	XPS atomic composition data for reaction with cyanuric chloride.....	94
6	XPS atomic composition data for reaction with isophorone diisocyanate.....	97
7	XPS atomic composition data for reaction with toluene diisocyanate.....	102
8	XPS atomic composition data for Ce <sup>IV</sup> initiated graft polymerizations.....	170
9	XPS atomic composition data for alumino-porphyrin surfaces and aluminoporphyrin initiated graft polymerizations.....	184
10	XPS atomic composition data for room temperature-initiated graft polymerizations of THF.....	191
11	XPS atomic composition data for HFBC labeling of graft THF surfaces.....	195
12	XPS atomic composition data for low temperature-initiated THF graft polymerizations.....	200
13	XPS atomic composition data for reactions of PCTFE-OH with TfCl.....	210
14	XPS atomic composition data for PCTFE-diMe-OH surfaces.....	214

15	XPS atomic composition data for reactions of PCTFE-diMe-OH surfaces with TfCl and Tf <sub>2</sub> O...	220
16	XPS atomic composition data for tosylate surfaces.....	222
17	XPS atomic composition data for 2-methyloxazoline graft polymerizations.....	225
18	XPS atomic composition data for reactions of isobutyrate surfaces.....	232
19	XPS atomic composition data for phenylethyl ester surfaces.....	240
20	XPS atomic composition data for reactions of phenylethyl ester surfaces.....	242
21	XPS atomic composition data for attempted surface-initiated GTP polymerizations.....	244
22	XPS atomic composition data for reactions with LiPrTMSKA.....	247
23	XPS atomic composition data for reactions of isocyanate surfaces with ε-caprolactam.....	253
24	XPS atomic composition data for fibril oxidations.....	304
25	XPS atomic composition data for reduced fibrils.....	308
26	XPS atomic composition data for Tl-labeled fibrils.....	312
27	XPS atomic composition data for reactions of Tl-labeled surfaces with HFBC.....	314
28	XPS atomic composition data for BF <sub>3</sub> ·OEt <sub>2</sub> catalyzed reactions of fibril samples with CF <sub>3</sub> CHN <sub>2</sub> .....	316
29	XPS atomic composition data for hydrolysis (1N HCl) of CF <sub>3</sub> CHN <sub>2</sub> labeled fibrils.....	318
30	XPS atomic composition data for HFBC labeled fibrils.....	319
31	XPS atomic composition data for DNPH labeled fibrils.....	320

32	XPS atomic composition data for reactions of fibrils using CDI and DCC.....	322
33	XPS atomic composition data for DBU catalyzed reactions of fibrils with electrophiles.....	323
34	Results of titration #1.....	324
35	Results of titration #2.....	325
36	Summary of titration results.....	326
37	Summary of chemical composition estimates based on fibril reactivity.....	327
38	XPS atomic composition data for reactions with $\text{CF}_3\text{CHN}_2$ in the presence of $\text{CuAc}_2 \cdot \text{H}_2\text{O}$ ...	331
39	XPS atomic composition data for reaction with ethyl diazoacetate.....	334



# LIST OF FIGURES

Figure		Page
1	Schlenk tube.....	20
2	Trap-to-trap apparatus.....	20
3	UV-visible spectrum of FEP-C (4 h, 0°C).....	54
4	Reaction depth versus reaction time for sodium naphthalide reduction of FEP at 0°C (□,●) and -78°C (■).....	56
5	XPS spectra (C <sub>1s</sub> region) of FEP, FEP-C (-78°C, 4 h) and FEP-C (0°C, 4 h) recorded at 15° and 75° takeoff angles.....	58
6	ATR-IR spectra of (a) FEP, (b) FEP-C, H <sub>2</sub> O/THF, (c) FEP-C, THF/H <sub>2</sub> O/THF, (d) FEP-C, fully deuterated.....	61
7	Reaction depth versus reaction time for sodium naphthalide reduction of PTFE at 0°C (■) and -78°C (●).....	70
8	XPS spectra (C <sub>1s</sub> region) of sodium naphthalide-reduced PTFE (-78°C, 4 h) recorded at 15° (a) and 75° (b) takeoff angles.....	71
9	Reaction depth versus time for benzoin dianion reduction of FEP at 50°C (□,▲), FEP at 21°C (Δ) and PTFE at 50°C (●).....	73
10	XPS spectra (C <sub>1s</sub> region) of benzoin dianion-reduced FEP (50°C, 4 h) recorded at 15° (a) and 75° (b) takeoff angles.....	76
11	ATR-IR spectra of (a) FEP-OH; (b) FEP-OH reacted with HFBC, THF/pyridine; (c) FEP-OH reacted with HFBC, pyridine/DMAP.....	78
12	XPS spectra (C <sub>1s</sub> region) of (a) FEP-OH (b) FEP-OH reacted with HFBC, THF/pyridine (c) FEP-OH reacted with HFBC, pyridine/DMAP.....	79
13	IR spectrum of (4-dimethylamino)pyridinium heptafluorobutyrate.....	83

14	ATR-IR spectra of (a) FEP-EO-OH (b) FEP-EO-OH reacted with HFBC (c) FEP-C, reacted with BPO and methanol.....	87
15	ATR-IR spectra of (a) FEP-9BBN (b) FEP-CH <sub>2</sub> OH.....	91
16	ATR-IR spectra of (a) FEP(IPDI)-NCO and FEP(IPDI)-NCO reacted with (b) BrPrOH (c) BrPhEtOH (d) BrPhEtOH and MeOH.....	98
17	ATR-IR spectra of (a) PCTFE(IPDI)-NCO and PCTFE(IPDI)-NCO reacted with (b) BrPrOH (c) MeOH.....	100
18	ATR-IR spectra of (a) FEP(TDI)-NCO and FEP(TDI)-NCO reacted with (b) BrPrOH (c) BrPhEtOH (d) BrPhEtOH and MeOH.....	103
19	ATR-IR spectra of (a) PCTFE(TDI)-NCO and PCTFE(TDI)-NCO reacted with (b) BrPrOH (c) MeOH.....	104
20	ATR-IR spectra of (a) FEP-OH; (b) FEP-g-pAA, high [Ce <sup>IV</sup> ]; (c) FEP-g-pAA, low [Ce <sup>IV</sup> ]; (d) FEP-g-pAA, high [Ce <sup>IV</sup> ], extracted.....	171
21	SEM micrograph of FEP-g-pdMAA.....	175
22	ATR-IR spectra of (a) PCTFE-OH; (b) PCTFE-OH + TPP-Al-Cl/P.O. ....	188
23	ATR-IR spectra of (a) FEP-Cl; (b) FEP(Cl)-g-THF, reacted at room temperature..	192
24	ATR-IR spectra of (a) FEP(Cl)-g-THF, reacted at room temperature; FEP(Br)-g-THF reacted at: (b) -78°C/-10°C, (c) -23°C/-10°C, (d) -10°C; (e) FEP(Cl)-g-THF, reacted at -23°C/-10°C.....	199
25	XPS spectra (C <sub>1s</sub> region) of (a) FEP-Br; (b) FEP(Br)-g-THF, -78°C/-10°C; (c) FEP(Br)-g-THF, -78°C/-10°C, <sup>3</sup> He <sup>+</sup> ion etched.....	202
26	Curve fitting results (XPS, C <sub>1s</sub> region) for FEP(Br)-g-THF, -78°C/-10°C.....	203
27	<sup>3</sup> He <sup>+</sup> ion etching results for FEP(Br)-g-THF, reacted at -78°C/-10°C.....	204

28	ATR-IR spectra of (a) PCTFE-OH, (b) PCTFE-OH + TfCl in pyridine.....	211
29	ATR-IR spectra of PCTFE-diMe-OH prepared by reaction for (a) 5.5 h at 0°C in 0.7:1 THF/hept.; (b) 6.5 h at -30°C in 1.7:1 Et <sub>2</sub> O/ hept.; (c) 4 h at -20°C in 5:1 THF/hept.....	215
30	ATR-IR spectra of (a) PCTFE-OH; (b) PCTFE-OTos, #4; (c) PCTFE-g-2MO, #1; (d) PCTFE-g-2Mo, #4; (e) PCTFE control.....	224
31	ATR-IR spectra of (a) PCTFE-OC(=O) <u>i</u> Bu; PCTFE-OC(=O) <u>i</u> Bu reacted with (b) LDA/TMSCl, (c) TEA/TMSCl, (d) TEA/TMSOTf.....	231
32	ATR-IR spectra of (a) PCTFE-OC(=O)CH <sub>2</sub> Ph, (b) PCTFE-OC(=O)CH <sub>2</sub> Ph + TEA/TMSOTf.....	238
33	ATR-IR spectra of PCTFE-diMe-OC(=O)CH <sub>2</sub> Ph prepared in (a) pyridine, (b) THF/pyridine/DMAP; (c) reaction of product (b) with TMSOTf/TEA in benzene, (d) reaction of product (b) with TMSOTf/TEA in TCE.....	241
34	ATR-IR spectrum of PCTFE reacted with LiPrTMSKA.....	248
35	ATR-IR spectra of (a) FEP-CL, prepared in THF, (b) FEP-g-CL prepared in THF, (c) FEP-CL prepared in the melt, (d) FEP-g-CL prepared in the melt.....	254
36	TEM micrograph of graphite fibrils.....	272
37	Schlenk-type filter apparatus.....	284
38	XPS spectra (C <sub>1s</sub> region) of (a) "as received" and (b) oxidized carbon fibrils...	305
39	XPS spectra (O <sub>1s</sub> region) of (a) "as received" and (b) oxidized carbon fibrils...	306
40	XPS spectra of "as received" fibrils reacted with CF <sub>3</sub> CHN <sub>2</sub> in the presence of CuAc <sub>2</sub> ·H <sub>2</sub> O.....	332



# LIST OF EQUATIONS

Equation		Page
1	Reaction of FEP-OH with LDA and ethylene oxide.....	84
2	Ceric ion initiated polymerization of acrylate monomers.....	168
3	Aluminoporphyrin initiated "immortal" polymerization of epoxide monomers.....	177
4	Preparation of TPP-Al-Et and reaction of TPP-Al-Et with alcohols.....	178
5	The effect of temperature on the reaction of AgOTf and THF with PSBr.....	196
6	Effect of ion etching on low temperature-initiated THF graft surfaces.....	205
7	Elimination of PCTFE-OH in the presence of TfCl and pyridine.....	209
8	Polymerization of 2-methyloxazoline.....	221
9	Group transfer polymerization.....	228
10	Charge delocalization in 1-ethoxy-1-(trimethylsilyloxy)-2-phenyl ethylene.....	236
11	Preparation of LiPrTMSKA.....	245
12	Activated monomer polymerization of $\epsilon$ -caprolactam.....	251
13	Half reaction for chlorate oxidation.....	302
14	Half reaction for perchlorate oxidation.....	303
15	Reaction of graphitic carbon with carbenes..	330

PART I

SURFACE MODIFICATION OF POLY(TETRAFLUOROETHYLENE-  
CO-HEXAFLUOROPROPYLENE)

## CHAPTER I

### INTRODUCTION

Most, if not all technological applications of polymers involve polymer interfaces. As a result, understanding interface structure-property relationships has become an important research topic in polymer science. Phenomena such as wetting, wear and adhesion are critically dependent on the chemical and physical properties of the interfacial region.<sup>1</sup> For a variety of applications, it would be desirable to modify the chemical structure of polymer surfaces. A variety of methods have been employed, including plasma modification, oxidation, reduction, surface graft polymerization and vapor deposition of metals.<sup>2</sup> Many of these modifications result in chemically-complex surfaces and/or offer little control over the depth to which the modification occurs.

Much of the research in this group has focused on the goal of using organic solution chemistry to introduce chemically-well defined functional groups to a precisely controlled depth on polymeric substrates.<sup>3</sup> Much of this work has been focused on chemically-resistant polymer surfaces. In addition to being technologically important,<sup>4</sup> these materials offer a number of advantages as substrates. The unmodified surfaces are stable to normal laboratory conditions. They are generally insoluble in common solvents at moderate temperatures, but the degree of swelling of the



interface, hence the ease of reagent penetration, can be controlled through choice of solvent and temperature. In addition, a variety of further reactions can be performed on the functional groups that are introduced without affecting the bulk.

### Chemical Modification of Fluoropolymer Surfaces

This section provides background on relevant aspects of the chemistry and surface modification of poly(tetrafluoroethylene-co-hexafluoropropylene) (FEP) and poly(tetrafluoroethylene) (PTFE), a similar polymer which has been studied more extensively.

### Surface Chemistry of PTFE

It has been known for some time that PTFE reacts with strong reducing agents<sup>5,6</sup>, resulting in a crosslinked, carbonaceous surface containing unsaturation,<sup>7</sup> oxygen-containing functional groups (hydroxyls, carbonyls) and C-H bonds.<sup>8</sup> These reduction products have been shown to be somewhat electronically conductive.<sup>9,10</sup> Sodium naphthalide-reduced films that have not been washed with water exhibit conductivities between  $10^{-5}$  and  $10^{-4} \Omega \text{ cm}^{-1}$ <sup>11</sup>. C.A. Costello and T.J. McCarthy have studied the reduction of PTFE with potassium benzoate dianion in DMSO. These conditions have been shown to result in a highly conjugated surface that is metallic gold in appearance. Doping of the

reduced layer resulted in high electronic conductivity.<sup>12</sup> These products were shown to undergo a variety of olefin reactions. Average modification depths in the 150-2000 Å range were reproducibly obtained. However, the reduction was corrosive; virgin polymer remained in the outer angstroms of deeply modified surfaces<sup>13</sup>.

#### Chemical and Structural Properties of FEP

FEP is a copolymer of tetrafluoroethylene and hexafluoropropylene (hexafluoropropylene comprises ~8% of the monomer feed). The copolymers are thermoplastic (mp=260°C) while maintaining the low surface energy and chemical resistance generally associated with PTFE. The most significant difference between FEP and PTFE is the extent of crystallinity. PTFE is highly crystalline (on the order of 98%<sup>14</sup>) while FEP is only 35-45% crystalline.<sup>15</sup> This has the effect of making FEP films semi-transparent, rather than opaque. In addition, while crystalline phase transitions are observed in PTFE<sup>16</sup>, no such transitions occur for FEP.<sup>17</sup> This suggests that crystalline regions may be less well ordered in FEP. Like PTFE, FEP reacts with reducing agents to yield a carbonaceous product. Although these surfaces have not been extensively characterized, their chemical structure appears to be generally similar to reduced PTFE.<sup>18</sup> One important difference appears to be in the conductivity of the product. The conductivity of sodium

naphthalide-reduced FEP is almost an order of magnitude lower.<sup>19</sup> This appears to be another result of the decreased crystallinity.

One objective of this work was to produce reduced fluoropolymer surfaces with sharper transitions between modified and unmodified polymer. It was suspected that the crystallinity of PTFE played an important role in the modification kinetics. One consistent explanation for the corrosive reaction of PTFE is reduction of bulk fluoropolymer by electrons transported along the eliminated polymer backbone; the reducing agent effectively acts as the dopant. Reaction would be expected to occur faster in regions where chains were in a favorable (extended) conformation and crystallinity was well developed. The kinetics of the reduction of FEP with sodium naphthalide in THF were studied, and the chemical composition of the reduced product was compared to reduced PTFE.<sup>20</sup> FEP was chosen as the substrate as its chemistry should resemble a hypothetical low crystallinity form of PTFE.

### Structure-Reactivity Characteristics of Functionalized Polymers

Although a wide variety of functional groups have been introduced to polymer surfaces, and a substantial number of further reactions have been performed using these groups, little systematic attempt has been made to determine how



steric and electronic factors affect the reactivity of functional groups on a surface.<sup>21</sup> Such studies have been hampered by the unavailability of suitable model surfaces. The chemical structure, and thus the chemical reactivity, of most modified surfaces cannot be represented by a single functional group. Recently, surfaces of well defined reactivity have been produced. A surface containing primary alcohols, separated from the polymer backbone by three methylene groups, has been prepared from poly(chlorotrifluoroethylene) (PCTFE). Quantitative esterification of this surface occurs under reasonably mild conditions.<sup>22</sup> The reactivity of hydroxyl groups on this surface does not appear to be much lower than primary hydroxyl groups on soluble species. Hydroboration of reduced FEP was found to produce a surface containing predominately secondary alcohol groups attached directly to the polymer backbone. These groups proved very difficult to acylate. A variety of acylation conditions were studied, and reactions were performed to introduce primary hydroxyl groups to this surface.<sup>23</sup> Comparison between increases in the yield due to catalysis for the surface and soluble species allows some correlation to be made between the reactivity of surface functional groups and their solution counterparts. Comparison of the reactivity of primary alcohol surfaces from FEP with those derived from PCTFE will help to determine if, in

general, primary alcohol-containing surfaces would be expected to be reactive towards electrophiles.

## Reactions of Nucleophilic Surfaces with Multifunctional Electrophiles

Of all of the polymer modification reactions studied, reactions that introduce hydroxyl functionality have been among the most successful.<sup>24</sup> These reactions provide a chemically versatile nucleophilic surface. Conversion of these surfaces to surfaces containing acid chloride or isocyanate groups would greatly extend the scope of polymer surface chemistry. Reaction with a multifunctional electrophile possessing sites of differing reactivity (cyanuric chloride) has been used to introduce electrophilic functionality to oxidized carbon, presumably through the reaction of phenolic groups.<sup>25</sup> Reactions of hydroxyl surfaces with cyanuric chloride and diisocyanates were investigated.

## Surface Analytical Techniques

This section describes the major surface analytical techniques employed in this research. All of these methods have been extensively reviewed in the literature. The fundamental principles will be briefly reviewed here and aspects of particular importance to this work will be discussed in detail.

Contact Angle Measurements. Contact angle measurements provide information about the surface energy of the outer few angstroms of appropriate substrates. While this technique does not provide direct atomic composition or functional group analysis, it is very sensitive to changes in surface polarity due to reaction.<sup>26</sup> In this research, the dynamic (advancing and receding) contact angles of water were measured. Advancing contact angles ( $\theta_a$ ) were measured while water was being added to the drop and receding angles ( $\theta_r$ ) while water was being removed. Low energy surfaces, such as fluoropolymers, exhibit high water contact angles ( $>90^\circ$ ). The introduction of polar groups lowers these values; very polar surfaces have receding contact angles approaching  $0^\circ$ .

The contact angle hysteresis ( $\theta_a - \theta_r$ ) provides information about the chemical and morphological heterogeneity.<sup>27</sup> Introduction of relatively few polar groups to a non-polar surface is expected to decrease  $\theta_r$  when water is the probe liquid to a much greater extent than  $\theta_a$ , while the introduction of relatively few non-polar groups to a polar surface is expected to increase  $\theta_a$  much more than  $\theta_r$ . The effect of roughness can be similar to the effect of chemical heterogeneity, although extreme roughness tends to impart non-wetting character to surfaces and eventually decrease the contact angle hysteresis. Experimental evidence suggests that these effects only become dominant for extremely rough



surfaces, exhibiting topological changes by SEM.<sup>28</sup> In the work reported here, no changes due to film modification could generally be observed by SEM and the FEP films themselves were featureless. Contact angle measurements are reported for those surfaces expected to be relatively stable to air and water. The interpretation of results for reactive surfaces is difficult since it is unclear if the measured values reflect the results of the initial modification. Since the sampling depth of contact angle measurements is much shallower than that of any of the other analytical techniques, it is not possible to provide verification that changes in the surface composition were not induced by reaction with water.

X-Ray Photoelectron Spectroscopy (XPS). XPS or ESCA (Electron Spectroscopy for Chemical Analysis) has been one of the most widely applied techniques for analysis of polymer surfaces.<sup>29</sup> The experiment provides a great deal of information and, in most cases, does relatively little damage to the sample. Samples are irradiated with soft X-rays (generally  $MgK_{\alpha}$  or  $AlK_{\alpha}$ ) in an ultrahigh vacuum and photoelectrons emitted from core states are detected. The resulting spectrum consists of a plot of the number of electrons emitted per energy interval ( $N(E)/E$ ) versus binding energy. The kinetic energy (KE) of the photoelectron is related to the

binding energy (BE) of the electron in the orbital from which it is emitted according to:

$$KE = h\nu - BE - \Phi_s$$

Where  $h\nu$  is the energy of the incident photon and  $\Phi_s$  is the spectrometer work function (both known). Thus, the kinetic energy is characteristic of a particular atom. The intensity (I) of the signal (obtained by integration) is related to the concentration (n, in atoms  $\text{cm}^{-3}$ ) according to:

$$n = \frac{I}{S}$$

where S, defined as the atomic sensitivity factor, can be calculated from known quantities related to the instrument and the sample. As the exact sampling volume is not easily defined, quantitative data is usually expressed in terms of relative concentrations calculated according to:

$$C_x = \frac{n_x}{\sum (n_i)} = \frac{I_x/S_x}{\sum I_i/S_i}$$

This has the additional advantage of correcting for variations in S due to differing sample matrices; the ratios of matrix-related quantities that contribute to S vary less than the quantities themselves.<sup>30</sup> Since the energy of core states is influenced by energy levels of valence states, the exact kinetic energy of a photoelectron will depend on the electronic environment around an atom, as well as its atomic number. Factors that decrease the electron density,

such as the presence of electron withdrawing substituents, increase the binding energy, while factors such as electron donating substituents or resonance (in the case of oxygen in carbonyl groups) that increase the electron density lower the binding energy. In practice, this often results in multiple peaks and shoulders in high resolution (narrow binding energy range) scans.<sup>31</sup> Interpretation of the exact binding energy values must be made with caution due to charging.<sup>32</sup> Often corrections for differences in charging can be made empirically for samples before and after modification from the relative shift in the energies of photoelectron lines from an element whose position is not expected to change substantially due to the modification, such as the  $F_{1s}$  line<sup>33</sup> of residual fluorine in reduced fluoropolymer samples.

The sampling depth of XPS is dependent on the mean free path ( $\lambda$ ) of photoelectrons in the sample matrix and the photoelectron kinetic energy. Experimental measurement of  $\lambda$  in polymeric materials has proven difficult; best estimates are in the range of 10 Å for low kinetic energy (high binding energy) electrons and 30 Å for high kinetic energy electrons. 95% of the intensity comes from a depth of  $3\lambda$ , this translates to an effective sampling depth range on the order of 30 Å to 90 Å; for carbon (binding energy of about 300 eV), this translates to a sampling depth of about 40 Å. By varying the angle between the sample and the detector,



the distance that an electron must travel through the sample before being detected can be increased, decreasing the effective sampling depth. A takeoff angle of  $15^\circ$  reduces the sampling depth for carbon to about  $10 \text{ \AA}$ <sup>34</sup>.

XPS labeling refers to reaction with a functional group-specific reagent that contains a characteristic XPS feature (a heteroatom absent from the sample, for example). This procedure can be used to verify the presence of a particular functional group and to provide an estimate of it's relative abundance, although a secondary confirmation of quantitative reaction is generally desirable.<sup>35</sup>

#### Attenuated Total Reflectance IR Spectroscopy (ATR-IR).

Attenuated total reflectance (also known as internal reflectance) infrared spectroscopy allows rapid identification of functional groups on surface-modified materials.<sup>36</sup> In favorable cases, this technique provides information complementary to XPS in the same way that IR compliments NMR and microanalysis results in solution chemistry.

In this experiment, polymer films are placed in close contact with a high refractive index optical element. Reflection sets up a standing wave that decays exponentially into the rarer medium (polymer sample). This evanescent wave can interact with dipoles in the surface region, resulting in a spectrum of the surface material. The sampling depth ( $d_p$ ) for this technique can be expressed as:

$$d_p = \frac{\lambda_o}{2\pi n_1 (\sin^2 \theta - n_{21}^2)^{1/2}}$$

Where  $\theta$  is the angle of incidence between the beam and the normal to the surface ( $45^\circ$  for this work),  $\lambda_o$  is the wavelength and  $n_{21}$  is the ratio of the refractive index of the sample to the refractive index of the internal reflectance element. Sampling depths are dependent on the wavelength; 90% of the signal comes from depths between  $0.22 \mu$  ( $3000 \text{ cm}^{-1}$ ) and  $0.41 \mu$  ( $1600 \text{ cm}^{-1}$ ) for a typical polymer sample (PCTFE) using a Ge element at  $45^\circ$  incidence. The contribution is greater for dipoles at the surface. These depths are much greater than the sampling depth of XPS; rather deeply modified films are required to obtain lucid spectra of the modified region. In addition, absolute intensities depend critically on film contact, which is difficult to reproduce.<sup>37</sup> As a result, it is generally best to compare peak ratios between spectra. In this research, ATR-IR results were used only for qualitative analysis.

Gravimetric Analysis. In general, obtaining modification depths using gravimetric analysis requires relatively deep reaction (to obtain significant weight changes) and stoichiometric assumptions must be made.<sup>38</sup> Fluoropolymer reductions have the advantage that oxidation quantitatively removes the reduced layer<sup>39</sup>, eliminating the need for stoichiometric assumptions and increasing the mass loss for a

given depth of modification. Film samples offer advantages in handling and static charge-build up could be avoided by neutralization with a polonium source. FEP samples had a further advantage in that polymers were not swollen by the reaction solvent. The samples were dried under vacuum (0.02-0.03 mm) at 75°C and weighed on three consecutive days; the samples generally reached constant mass ( $\pm 1 \mu\text{g}$ ) on the first day.

Ultraviolet-Visible Light Spectroscopy. FEP films are essentially transparent at wavelengths above 200 nm, allowing changes due to reduction to be easily monitored. Two FEP film samples were placed in sample holders, and the difference spectrum was recorded. Films were well matched; no significant difference in absorbance was observed between FEP samples. One film was modified, and the spectrum was recorded relative to FEP. For quantitative measurements, the absorbance of FEP (air background) was read off the LED meter at 250, 290 and 300 nm. The average of measurements for four FEP film samples agreed (at a given wavelength) to within 0.004 a.u. The absorbance of modified films was measured similarly, and the difference determined by subtraction. The difference at each wavelength was comparable. The values for 250 nm were used in conjunction with gravimetric data, to calculate reaction depths.



## References

1. Clark, D.T.; Feast, W.J. *Polymer Surfaces*, Wiley-Interscience: New York, 1978.
2. Ward, W.J.; McCarthy, T.J. In *Encyclopedia of Polymer Science and Engineering*, 2nd ed.; Supplement, Wiley: New York, 1989; pp 674-689.
3. See reference 2, pp 680-686 and the references contained therein.
4. Fluoropolymer surfaces are often modified to increase the surface energy in order to promote adhesion, improve wetting and decrease thrombogenic activity when these polymers are used in prostheses. See, for example, Benderly, A.A. *J. Appl. Poly. Sci.* **1962**, *6*, 221.; Andrade, J.D.; Hlady, V.; *Adv. Poly. Sci.* **1986**, *79*, 1.
5. Nelson, E.R.; Kilduff, T.J.; Benderly, A.A. *Ind. Eng. Chem.* **1985**, *50*, 329.
6. Chakrabarti, N.; Jacobus, J. *Macromolecules* **1988**, *21*, 3011.
7. Dwight, D.W.; Riggs, W.J. *J. Colloid Interface Sci.* **1974**, *47*, 650.
8. Borisova, F.K.; Galkin, G.A.; Kiselev, A.V.; Korolev, A.; Lygin, V.I. *Colloid J. USSR (Eng.)* **1965**, *27*, 265.
9. Varma, A.J.; Jog, J.P.; Nadkarni, V.M. *Makromol. Chem., Rapid Commun.* **1983**, *4*, 715.
10. Barker, D.J.; Brewis, D.M.; Dahm, R.H.; Hoy, L.R. *Polymer* **1978**, *19*, 856.
11. Yoshino, K; Yanagida, S.; Sakai, T.; Azuma, T.; Inuishi, Y.; Sakurai, H. *Jpn. J. Appl. Phys.* **1982**, *21*, L301.
12. Costello, C.A. Ph.D. Dissertation, pp 125-130.
13. Costello, C.A.; McCarthy, T.J. *Macromolecules* **1987**, *20*, 2819.
14. Gangal, S.V. In *Encyclopedia of Polymer Science and Technology*, vol.16, Wiley: New York, 1987; p 583.
15. See reference 14, p 601.
16. See reference 14, pp 583-584.

17. See reference 14, p 604.
18. See reference 7.
19. See reference 9.
20. Bening, R.C.; McCarthy, T.J. *Macromolecules* **1990**, *23*, 2648.
21. See reference 2, pp 680-686.
22. Lee, K.-W.; McCarthy, T.J. *Macromolecules* **1988**, *21*, 2318.
23. See reference 20.
24. See references 20 and 2.
25. Murray, R.W. *Electroanal. Chem.* **1984**, *13*, 280-282.
26. Adamson, A. *Physical Chemistry of Surfaces*, 4th ed., Wiley: New York, 1982.
27. Johnson, R.E.Jr.; Dettre, R.H. *J. Phys. Chem.* **1964**, *68*, 1744.
28. Morra, M.; Occhiello, E.; Garbassi, F. *Langmuir* **1989**, *5*, 872.
29. Andrade, J.D. In *Surface and Interfacial Aspects of Biomedical Polymers*, vol 1. Andrade, J.D. ed., Plenum: New York, 1985, pp 105-195.
30. Wagner, C.A.; Riggs, W.M.; Davis, L.E.; Moulder, J.F.; *Handbook of X-ray Photoelectron Spectroscopy*, Muilenberg, G.E. ed., Perkin-Elmer: Eden Prairie Minn., 1979, pp21-22.
31. See reference 29, pp 143-151.
32. See reference 29, pp 119-121.
33. See reference 30, p 44.
34. See reference 29, pp 175-184.
35. See reference 29, pp 163-169.
36. Harrick, N.J. *Internal Reflectance Spectroscopy*, Harrick Sci. Corp.: New York, 1979.

37. Mirabella, F.M. *J. Polym. Sci. Phys. Ed.* **1982**, *20*, 2309.
38. Bonafini, J.A.; Dias, A.J.; Guzdar, Z.A; McCarthy, T.J. *J. Polym. Sci., Polym. Lett. Ed.* **1985**, *23*, 33.
39. See reference 13.



## CHAPTER II

### EXPERIMENTAL SECTION

#### Methods

Inert Atmosphere Techniques. Many of the products and reagents discussed in this dissertation are sensitive to oxygen and moisture. Appropriate precautions were taken to minimize contact with the laboratory environment. Standard inert atmosphere techniques were employed<sup>1</sup> and will be discussed only briefly here.

Nitrogen atmosphere was employed unless otherwise specified. Pre-purified grade (Linde) nitrogen was further purified by passage through columns of indicating Drierite ( $\text{CaSO}_4$ ), phosphorous pentoxide, and BASF BTS catalyst to remove water and oxygen, respectively. Unless otherwise specified, reactions were performed in standard Schlenk glassware. Figure 1 depicts a typical example; liquids were transferred via stainless steel cannula or gas-tight (Hamilton) syringe through septum-capped joints. Air sensitive solids were handled in a nitrogen atmosphere (Vacuum Atmosphere) glove box. Solvents and reagents were stored in Schlenk type storage flasks.

Drying of samples and other vacuum line procedures were performed on a vacuum manifold of a standard design, provided with a liquid nitrogen-cooled trap. The vacuum was provided by a Precision D150 pump and monitored using a

Teledyne-Hasting vacuum gauge. The typical operating pressure was 0.02-0.05 mm. Pressure during distillations was maintained with a Manowatch (I<sup>2</sup>R) manostat and monitored with a mercury manometer. Trap-to-trap distillations were performed using the apparatus shown in figure 2 or, in cases where it was desirable to distill directly into the reactor vessel, using two vessels linked to the vacuum line through a yoke. When bumping was expected, a bump trap, similar to those used for roto-vap distillations was placed between the pot and the distillation apparatus.

Analytical Techniques. The details pertinent to surface analytical techniques are discussed in Chapter I. Gravimetric analysis was performed with a Cahn 29 electrobalance. XPS was performed with a Perkin-Elmer-Physical Electronics 5100 spectrometer (MgK<sub>α</sub>, 300 W, base pressure of  $\sim 10^{-8}$  torr), using pass energies of 71.5 eV or 35.75 eV. ATR-IR spectra were recorded on an IBM 38 or IBM 44 FTIR using a 45° Ge microsampling internal reflection element. UV-vis spectra were recorded in air using a Perkin-Elmer Lambda 3A spectrophotometer. Dynamic advancing and receding contact angles were measured with a Rame'-Hart telescopic goniometer while adding or removing water (pH of 5-7) using a Gilmont syringe. IR spectra of solids were obtained as KBr mulls using the IBM 38 FTIR.

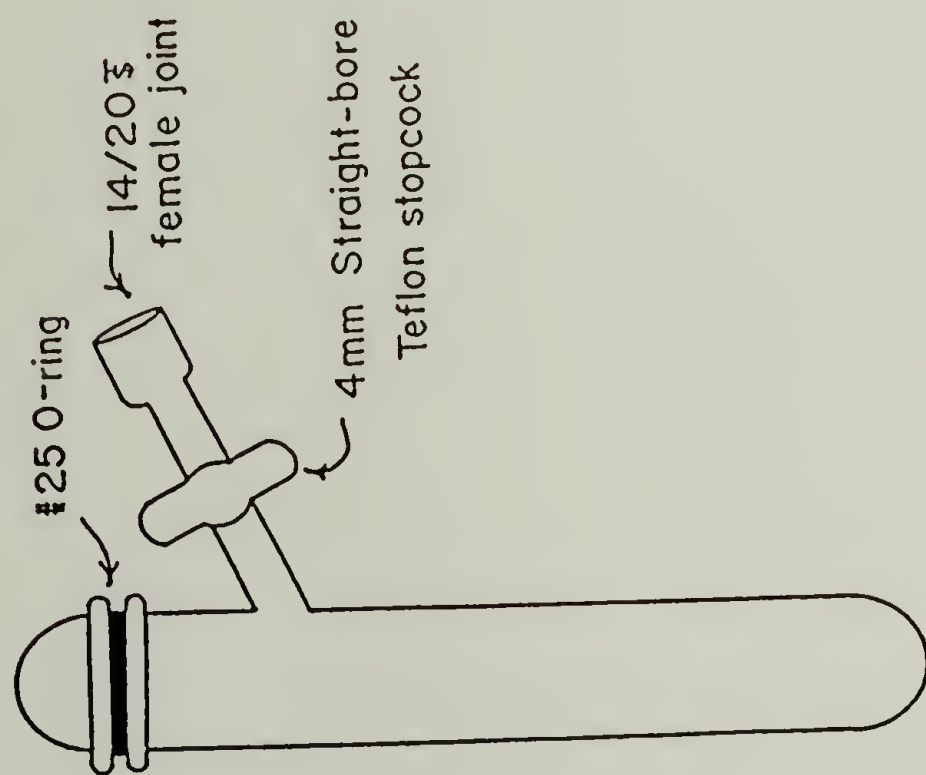


Figure 1. Schlenk tube

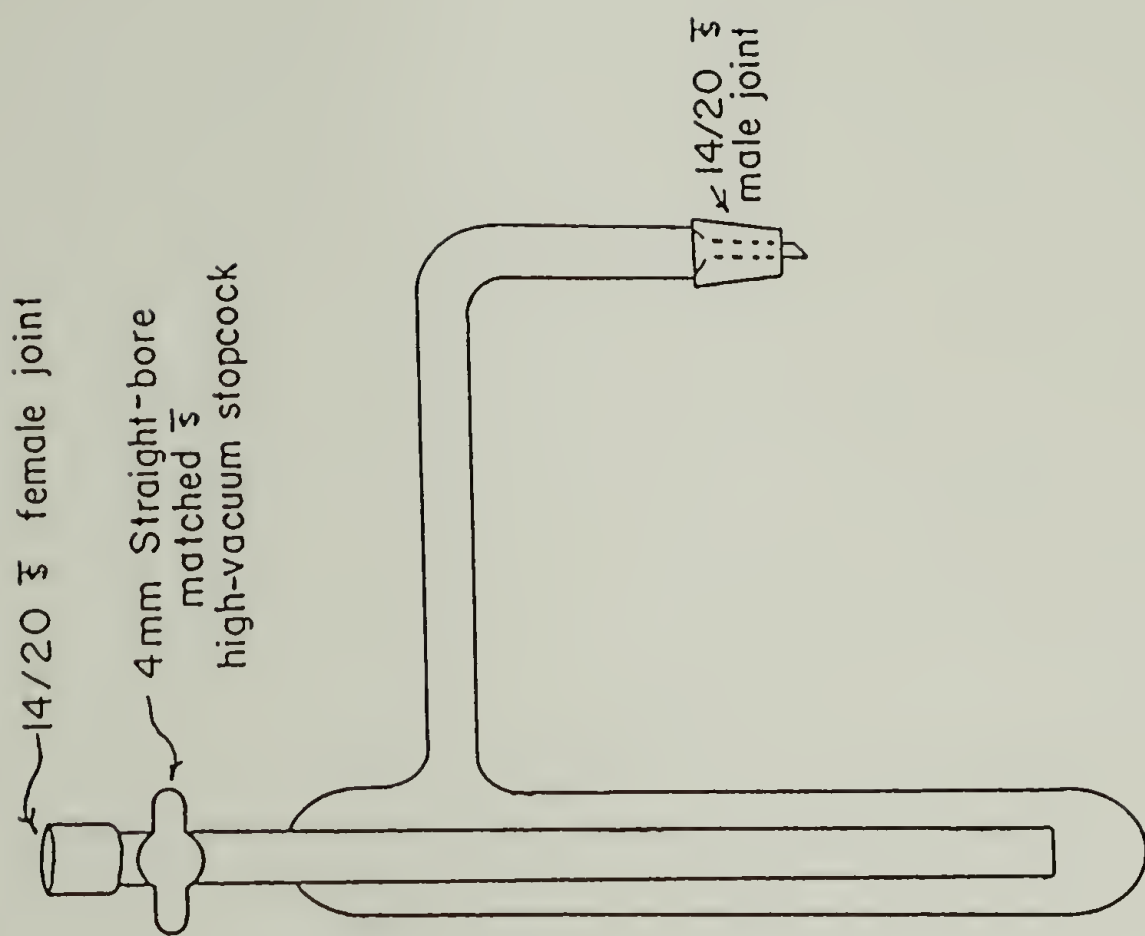


Figure 2. Trap-to-trap apparatus



## Purification of Solvents and Reagents

**Poly(tetrafluoroethylene-co-hexafluoropropylene)** (FEP, DuPont, 5-mil) film samples were extracted with THF (Soxhlet extractor) for 24 hours and dried (0.02 mm, 75°C) overnight. Films could be stored in tightly sealed containers under ambient atmosphere without being contaminated.

**Poly(tetrafluoroethylene)** (PTFE, Berghoff, 1/16") film samples were also extracted with THF and dried under a vacuum (0.02 mm, 75°C).

**Poly(chlorotrifluoroethylene)** (PCTFE, Allied, 5-mil) film samples were extracted (Soxhlet extractor) overnight with methylene chloride and dried at room temperature under vacuum.

**Tetrahydrofuran** (Aldrich, anhydrous) was dried over activated 3A molecular sieves (Linde, activated at 150°C, 0.02 mm for 24 hours), distilled from sodium benzophenone dianion and stored under nitrogen.

**Methanol** (Fisher, spectrophotometric grade) was refluxed over and distilled from magnesium turnings and stored under nitrogen.

**Ethanol** (Pharmco, anhydrous) was refluxed over and distilled from magnesium turnings and stored under nitrogen.

**Water** was doubly distilled in a Gilmont still and deoxygenated by sparging with nitrogen for about 1 hour for each 100 mL immediately prior to use.

**2,4-Dinitrophenylhydrazine** (Aldrich) was recrystallized from petroleum ether.

**Pyridine** (Fisher) was distilled from calcium hydride under vacuum (54°C, 100 mm) and stored under nitrogen.

**Heptafluorobutyryl chloride** (Aldrich) was distilled at 0.05 mm, trap-to-trap, and stored under nitrogen.

**Ethylene oxide** (Eastman) was distilled from calcium hydride under reduced pressure (50 mm), trap-to-trap, and stored under nitrogen in a refrigerator.

**Sodium** (Fisher) was washed with two portions of hexane and cut under nitrogen.

**1,8-Diazabicyclo[5.4.0]undec-7-ene** (DBU, Alfa) was distilled from calcium hydride (80°C, 0.6 mm) and stored under vacuum.

**Dimethylsulfoxide** (DMSO, Aldrich) was distilled from calcium hydride under vacuum (75°C, 13 mm) and stored under nitrogen.

**Potassium-t-butoxide** (Aldrich) was purified by sublimation (210°C, 0.04 mm) and stored under nitrogen.

**Benzoin** (Aldrich) was recrystallized twice from 95% ethanol to give white crystals (mp=135.5-136.5°C).

**3-Bromo-1-propanol** (Aldrich) was vacuum distilled from potassium carbonate (60-65°C, 5 mm) and stored under nitrogen.

**Ethyl vinyl ether** (Aldrich) was distilled under nitrogen (to remove inhibitors) immediately prior to use.

**t-Butyllithium** (1.7 M in pentane, Aldrich) was standardized by titration with biphenylmethanol in diethyl ether at -20°C.

**Diethyl ether** (Fisher) was distilled from benzophenone dianion and stored in a refrigerator under nitrogen.

**Benzene** (Aldrich) was distilled from calcium hydride and stored under nitrogen.

**Heptane** (Aldrich) was distilled from benzophenone dianion. Approximately 10% (v/v) Diglyme (2-methoxyethyl ether) was added to solubilize the anion.

The following reagents were used without further purification: naphthalene (Fisher), borane-tetrahydrofuran (1.0 M, Aldrich), potassium chlorate (Alfa), hydrogen peroxide (30%, VWR), D<sub>2</sub>O (Aldrich), THF-d<sub>8</sub> (Aldrich), lithium diisopropylamide (LDA, Aldrich), 4-(dimethylamino)pyridine (DMAP, Aldrich), 9-BBN (0.5 M in THF, Aldrich), LiAlH<sub>4</sub> (1.0 M in THF, Aldrich), benzoyl peroxide (Aldrich), dichloromethane (Fisher), calcium hydride (Aldrich), sulfuric acid (ACS concentrated, Fisher), sodium deuterioxide (40 wt% in D<sub>2</sub>O, Aldrich), naphthalene-d<sub>8</sub> (Aldrich), hydrochloric acid (ACS concentrated, Fisher), 1,4-toluene diisocyanate (Aldrich), isophorone diisocyanate (Fluka), dibutyl tin dilaurate (Aldrich), 4-bromophenylethyl alcohol (Aldrich), 1,4 diaza-bicyclo(2.2.2)-octane (DABCO, Aldrich), carbon monoxide (Linde), DCl (37 wt.% in D<sub>2</sub>O, Aldrich), 2-methoxyethyl ether



(Aldrich), oxygen (pre-purified, Linde), 2,5-dichlorophenylhydrazine (Aldrich), sodium hydroxide (Fisher), dichloroacetic acid (Aldrich), potassium carbonate (Fisher), cyanuric chloride (Aldrich), hexamethylene diisocyanate (Aldrich).

## Preparation and Characterization of Reduced FEP Surfaces

This section describes the reduction of FEP with sodium naphthalide to produce eliminated surfaces of varying thicknesses. Isotopic labeling and XPS labeling reactions are also described. Reactions with PCTFE and benzoin dianion, performed for comparative purposes, are also included in this section.

## Kinetics of the Reduction of FEP with Sodium Naphthalide (FEP-C)

(b1p2,27,111) Sodium naphthalide was prepared by adding a stir bar and 5 g (40 mmol) of naphthalene to a 500 mL sidearm flask. The flask was purged with nitrogen and 250 mL of THF was added. About 1.7 g (74 mmol) of sodium was cut into the mouth of the flask while purging with nitrogen. After stirring for about 3 hours under nitrogen, the dark green solution was transferred, via cannula, to a nitrogen-purged storage flask. (b1p18-22,27-29,39) Deeply modified surfaces for kinetics studies were prepared by placing a  $7.5 \times 4 \text{ cm}^2$  and a  $1.5 \times 1.5 \text{ cm}^2$  FEP sample in a

nitrogen-purged Schlenk tube. 10 mL of THF was added and the tube was equilibrated at 0°C for at least 15 minutes, and then 15 mL of the sodium naphthalide reagent (at room temperature) was added. Reaction was allowed to proceed for the desired time (2 minutes to 11 hours). At the end of this time, the reagent was removed, and the films were washed sequentially with ten, 10 mL portions each of deoxygenated water and THF. Washing entailed transferring a portion of the desired solvent into the reaction tube, agitation for about 60 seconds on a Vortex-Genie, and removal of the solvent by cannula. The resulting films were brown and somewhat shiny, but lacked the metallic luster of PTFE-C<sup>2</sup>. The films were dried under vacuum. (b1p47-50,57, 61) Shallower surfaces for kinetic studies were obtained by reacting at -78°C. Reactions were performed as described above, except that the reaction tube was equilibrated in a dry ice-acetone bath, and the sodium naphthalide reagent was cooled to the reaction temperature prior to addition. As the reaction proceeds, the characteristic dark green color is lost; a brownish solid precipitates, leaving a clear supernatant. The green color is restored by warming the reaction vessel, suggesting that the solubility of the sodium naphthalide complex is reduced at low temperatures. The films produced at -78°C were much less colored.

## Reaction of FEP with Benzoin Dianion

(b1p89,93,102) FEP was reduced with benzoin dianion under the conditions used by C. Costello to prepare PTFE-C<sup>3</sup>. A 7.5 x 4 cm<sup>2</sup> and a 1.5 x 1.5 cm<sup>2</sup> film sample were placed in a Schlenk tube and the tube was purged with nitrogen and equilibrated in an oil bath at 50 °C. 2 g of potassium t-butoxide and a stir bar were added to a 100 mL round bottom flask in a drybox and 60 mL of DMSO were added. Benzoin (0.54 g) was added to a 50 mL round bottom flask; the flask was capped with a septum and purged with nitrogen. 10 mL of DMSO was added to dissolve the solid. This solution was transferred onto the base; a dark purple solution formed immediately. An equal portion of this solution was transferred onto each of three film samples and reactions were allowed to proceed for the desired time (1 hour, 6 hours, or 8 hours). Alternately, single portions of this reagent could be prepared using 1 g of potassium t-butoxide in 30 mL of DMSO and 0.22 g of benzoin. The films were washed with five 10 mL portions of DMSO, five 20 mL portions of deoxygenated water and five 20 mL portions of THF. The films were dull black before washing with water and became somewhat shiny but did not develop gold, metallic color. When PTFE was reacted under identical conditions, gold, metallic looking films were produced, as expected.

(b1p102,106) FEP and PTFE films were also reduced with benzoin dianion at room temperature for 1, 4 and 8 hours.



FEP reduction products were less colored than the 50°C products and PTFE reduction products appeared "blotchy", with light purple colored patches, indicating inhomogeneous reaction of the film surface. The metallic character observed for the 50°C reaction product was entirely absent.

#### Reaction of PTFE with Sodium Naphthalide

(b1p107,117) PTFE films were reacted with sodium naphthalide at 0°C and -78°C, as described previously for FEP. The films produced by reaction at 0°C were dull black, not metallic, but appeared homogeneously reacted, while the -78°C films appeared "blotchy", like the products of room temperature benzoin reduction.

#### Oxidation of Reduced Surfaces with $\text{KClO}_3/\text{H}_2\text{SO}_4$

(b1p23,30,53,89,102,107) The reduced layer was removed by oxidation with a solution of 1 g  $\text{KClO}_3$  in 50 mL of sulfuric acid at room temperature in an open beaker. Typically, equal portions of this reagent were transferred into each of three beakers containing the samples to be oxidized. Reaction for 2-3 hours was generally sufficient to remove the oxidized layer. The films were washed with five 10 mL portions each of distilled water and THF, and dried under vacuum (0.02 mm, 45°C). After oxidation, the films appeared identical to the virgin polymer.

## Preparation of FEP-C Using Sublimed Naphthalene

(b2p45,51,57-58) Naphthalene was sublimed ( $90^{\circ}\text{C}$ , 0.05 mm); 0.3 g was loaded into a Schlenk tube in a drybox. The solid was dissolved in 15 mL of THF. Approximately 5 g of sodium was loaded into a nitrogen-purged Schlenk tube containing a stir bar. The naphthalene solution was transferred onto the sodium, stirred for 1 hour, and the dark green solution was transferred to a Schlenk storage tube. 10 mL of this solution was later transferred to a tube containing an FEP sample and 10 mL of THF, equilibrated at  $0^{\circ}\text{C}$ . Reaction was allowed to proceed for 1 hour, the reagent was removed, and the film sample was washed with two 10 mL portions of THF, five 20 mL portions of deoxygenated water and four 20 mL portion of THF, and then dried under vacuum (0.03 mm). The films remained dull black in color prior to washing with water. The following week, 5 mL of the above sodium naphthalide solution was transferred to a tube containing an FEP film sample and 10 mL of THF at  $0^{\circ}\text{C}$ . After 6 hours, the film was worked up as described above.

## Preparation of FEP-C Using Non-Aqueous Work Up

(b1p149;b2p4) Reduction of two FEP film samples was carried out at  $0^{\circ}\text{C}$  for 4 hours as described previously. One film sample was washed with three 10 mL portions of THF, five 20 mL portions of DMSO, and three 20 mL portions of THF; the second was washed with five 20 mL portions of

methanol, three 20 mL portions of THF, and two 10 mL portions of heptane. Both films remained dull black. The films were dried at room temperature under vacuum (0.03 mm).

#### Preparation of FEP-C Using D<sub>2</sub>O Rinsing

(b1p67) An FEP sample was prepared by reduction at 0°C for 4 hours, as described previously. The reagent was removed, 10 mL of D<sub>2</sub>O was added, and the film was allowed to stand in D<sub>2</sub>O for 30 minutes. The sample was washed with five 20 mL portions of THF and then dried under vacuum (0.03 mm) at room temperature. The films were shiny and brown colored.

#### Preparation of FEP-C Using THF-d<sub>8</sub>

(b1p152) Sodium naphthalide reagent was prepared in THF-d<sub>8</sub> as follows: 6 mL of THF-d<sub>8</sub> was added to a nitrogen-purged Schlenk tube containing 0.16 g of naphthalene. This solution was transferred to a tube containing approximately 1 g of sodium. After two hours, the dark green solution was transferred to a nitrogen-purged Schlenk storage flask. The following day, this solution was reacted with two 1.5 x 1.5 cm<sup>2</sup> FEP samples for 6 hours at 0°C. The reagent was removed and the films were washed with two 10 mL portions of THF, five 20 mL portions of deoxygenated water and four 20 mL portions of THF, and then dried under vacuum at room temperature.



### Preparation of FEP-C Using D<sub>2</sub>O "Spiked" THF

(b1p120) D<sub>2</sub>O "spiked" THF was prepared as follows: 1 mL of D<sub>2</sub>O was added to 100 mL of distilled THF in a nitrogen-purged sidearm flask containing a stir bar. With the septum removed and nitrogen flowing through the sidearm, 10 g of benzophenone and 3 g of sodium were added. The solution was stirred under nitrogen. Two more aliquots of sodium were added over a three hour period, resulting in a characteristically purple colored solution. A still head was mounted on the flask; the solution was refluxed for 30 minutes and then distilled into a nitrogen-purged storage flask. This solvent was used to prepare the sodium naphthalide reagent and an FEP sample was reduced (0°C, 6 hours) as described previously. The reagent was removed and the films were washed with five 20 mL portions of water and five 20 mL portions of D<sub>2</sub>O-spiked THF, and then dried under vacuum at room temperature.

### Preparation of FEP-C in a PTFE Reactor

(b2p21) An FEP film sample was placed in a PTFE round bottom flask equipped with a 14/20 joint (Berghoff). A septum was used to cap the flask. The reactor was purged with nitrogen and 10 mL of THF was added. The flask was equilibrated at 0°C for 15 minutes, sodium naphthalide reagent was added, and the reaction was allowed to proceed for 3.5 hours. The reagent was removed, and the films were

washed with two 20 mL portions of THF, five 20 mL portions of deoxygenated water, and three 20 mL portions of THF. The flask was evacuated for 30 minutes (0.75 mm) through the septum by means of a needle attached to the vacuum line using rubber tubing and a Luer adapter. The film was then transferred to a Schlenk tube (in the drybox) and returned to the vacuum line to finish drying (0.02 mm, room temperature).

#### Preparation of FEP-C in an OD-Enriched Glass Reactor

(b1p144) The surface of a glass reactor was enriched in OD groups by H-D exchange<sup>4</sup> as follows: A Schlenk tube containing approximately 5 g of small pieces of clean glass was heated under nitrogen with a heat gun and cooled to room temperature under nitrogen; 10 mL of 40 wt.% NaOD in D<sub>2</sub>O was added and the solution was allowed to remain in the tube for 48 hours at room temperature. This solution was removed and replaced by a solution of 2 mL of 37% DCl in 20 mL of D<sub>2</sub>O. This solution was removed 24 hours later, and the tube was washed with 10 mL of D<sub>2</sub>O and two 20 mL portions of THF. An FEP-C sample was prepared in this tube by reduction at 0°C for 3 hours. The sample was washed with five 20 mL portions each of water and THF, and dried at room temperature under vacuum.

### Preparation of FEP-C Using Naphthalene-d<sub>8</sub>

(b2p49) Sodium naphthalide-d<sub>8</sub> reagent was prepared as follows: 0.3 g of naphthalene-d<sub>8</sub> was weighed into a round bottom flask in a drybox and capped with a septum. The solid was dissolved in 15 mL of THF and cannulated onto approximately 0.5 g of sodium in a nitrogen-purged Schlenk tube and allowed to react for 1 h. This reagent was transferred to a Schlenk tube containing an FEP-C sample in 10 mL of THF at 0°C. After 4 hours the solution was removed, and the films were washed with two 10 mL portions of THF, five 20 mL portions of deoxygenated water and four 20 mL portions of THF, and then dried at room temperature under vacuum.

### Preparation of FEP-C Using Only Deuterated Reagents

(b2p46-47) Sodium naphthalide reagent was prepared as follows; unless otherwise specified all procedures were carried out in a nitrogen atmosphere drybox: 0.3 g of naphthalene-d<sub>8</sub> was added to a 100 mL round bottom flask with a stir bar; 15 mL of THF-d<sub>8</sub> was added. Approximately 2 g of sodium was placed in a Schlenk tube (outside of the dry box), and washed with three 10 mL portions of heptane by cannulating the solvent onto the sodium, agitating with a Vortex-Genie, and removing the solvent. The tube containing sodium was evacuated on the vacuum line for 10 minutes prior to introduction to the drybox. Sodium was cut to expose fresh surface and 0.7 g were added to the naphthalene solu-



tion. After stirring for 3 hours, the dark green solution was transferred via gas-tight syringe to a storage tube. Three 1 x 1.5 cm<sup>2</sup> FEP samples were placed in a small PTFE beaker in a Schlenk tube; the Schlenk tube top was put in place, the reagent was added, and the reaction was allowed to proceed in the drybox refrigerator (approximately 10 °C) for 5 hours. The reagent was removed using a gas-tight syringe. The films were washed by transferring solvents into the PTFE beaker, shaking gently, and removing the solvent using a gas-tight syringe. Four 5 mL portions of D<sub>2</sub>O and one portion of THF-d<sub>8</sub> were used. The films, in the Schlenk tube, were removed from the drybox and dried under vacuum (0.02 mm) at room temperature. These films were very dark, suggesting deep reaction.

#### Reaction of FEP-C with Oxygen and Air

(b2p2-3,6,11) FEP-C was prepared by reduction of three 1.5 x 3 cm<sup>2</sup> samples at 0°C for 5.5 hours, as described previously, and washed with two 10 mL portions of THF, five 20 mL portions of methanol, and four 20 mL portions of THF. One film was then exposed to ambient atmosphere for about two weeks. The other two film samples were placed in a Schlenk tube that was purged with oxygen, and allowed to stand for 7 days; the tube was then purged with nitrogen.

## Reaction of FEP-C with Aryl Hydrazines

(b1p125-126,130-131) The general procedure employed for labeling carbonyl groups was as follows: 0.2 g of 2,4-dinitrophenylhydrazine (DNPH) or 2,5-dichlorophenylhydrazine was added to a graduated cylinder which was then capped with a septum and purged with nitrogen. 20 mL of THF, 1 mL of deoxygenated water and 2-3 drops of HCl were added to dissolve the solid. This solution was transferred to the film sample, and reaction was allowed to proceed at room temperature for 48 hours. The films were washed with five 10 mL portions each of THF and methanol, and two 10 mL portions of heptane, and dried under vacuum. FEP-C films produced by reaction at  $-78^{\circ}\text{C}$  for 6 hours and washed with water, and then THF, were reacted with DCPH. FEP-C films reacted at  $0^{\circ}\text{C}$  for 4 hours and washed with water, and then THF, were reacted with DNPH.

## Reaction of FEP-C with Heptafluorobutyryl Chloride

(b1p125,130,b2p21) The general procedure employed for labeling hydroxyl groups was as follows: 1 mL of heptafluorobutyryl chloride (HFBC) was dissolved in 10 mL of THF and transferred onto the film sample. 0.1 mL of pyridine was added. The reaction was allowed to proceed for 20 hours. The solution developed a pale yellow color. The reagent was removed, and the films were washed with five 20 mL portions each of ethanol, THF and heptane. FEP-C films

prepared by reaction at (1)  $-78^{\circ}\text{C}$  for 6 hours and (2)  $0^{\circ}\text{C}$  for 4 hours and washed with water and THF, and films prepared by reaction at  $0^{\circ}\text{C}$  for 3 hours and washed sequentially with THF, water and THF, were labeled using this reaction.

#### Preparation of FEP-C for Further Modifications

(b1p149) Unless otherwise specified, FEP-C used in further modifications was prepared as follows: Four  $1.5 \times 4 \text{ cm}^2$  film samples were placed in a glass Schlenk tube equipped with glass dividers (prepared by cutting a groove half the length of each of two microscope slides, and nesting them together in the shape of an X), the tube was purged with nitrogen and 10 mL of THF was added. The tube was equilibrated at  $0^{\circ}\text{C}$  for at least 15 minutes, and then 15 mL of sodium naphthalide reagent (at room temperature) was introduced. The reaction was allowed to proceed for 4-6 hours. The reagent was removed and the films were washed with two 10 mL portions of THF, five 20 mL portions of deoxygenated water, and four 20 mL portions of THF, and then dried at room temperature under vacuum.

#### Hydroboration and Subsequent Oxidation of FEP-C (FEP-OH)

(b1p128,136,b2p14-15,30,39) FEP-C film samples (typically four  $1.5 \times 4 \text{ cm}^2$  films, separated by glass dividers) were reacted with 0.5 M borane-THF complex overnight (typically 18 to 20 hours) at room temperature. The reagent was



removed and the hydroborated films were washed with three 20 mL portions of THF. The films became slightly lighter colored. 1.2 g of sodium hydroxide was added to a graduated cylinder, the top was capped with a septum, and 20 mL of deoxygenated water was added. This solution was cooled to 0°C and 10-20 mL of 30% hydrogen peroxide was added. This solution was transferred onto the films and reaction was allowed to proceed for 3 hours at 0°C. The reagent was removed and the films were washed with five 20 mL portions each of dilute aqueous NaOH, dilute aqueous HCl, water and methanol, and three 20 mL portions of THF. The films were dried under vacuum (0.03 mm) at room temperature. After hydroboration the film samples appeared "bleached".

#### Reaction of FEP-OH with Aryl Hydrazines

(b1p137,146) FEP-OH samples were reacted with DCPH and DNPH for 24 hours using the same conditions employed in labeling FEP-C surfaces.

#### Reaction of FEP-OH with HFBC in THF

Several minor variations of this reaction were employed to label hydroxyl groups: (b1p137) (A) A solution containing 1 mL of pyridine in 10 mL of THF was added to a nitrogen-purged Schlenk tube containing the film sample and 0.05 mL of HFBC was added. The reaction was allowed to proceed for 26 hours at room temperature. The reagent was removed, and

the film was washed with five 10 mL portions each of ethanol, THF and heptane, and then dried at room temperature under vacuum. (b2p90-92) (B) 2 mL of HFBC was dissolved in 20 mL of THF. This solution was transferred onto the film samples and 0.05 mL of pyridine was added. The tube was agitated on a vortex mixer for 24 hours at room temperature. An unusual amount of suspended white solid was present. The films were washed with two 20 mL portions each of THF, methanol, and THF. The films were extracted with THF (Soxhlet, 24 hours) after XPS indicated an unusually high fluorine content. (b4p53) (C) 0.5 mL of HFBC was added to 20 mL of THF. This solution was transferred to a Schlenk tube containing the FEP-OH sample and a stir bar. 0.1 mL of pyridine was added, and the reaction was allowed to proceed for 72 hours. The reagent was removed and the films were washed with three 20 mL portions of THF, five 20 mL portions of methanol, and a further five 20 mL portions of THF, and then dried at room temperature under vacuum.

#### Reaction of FEP-OH with HFBC in Pyridine

(b2p14-16) 15 mL of pyridine was added to a Schlenk tube containing a stir bar and the film sample. 0.5 mL (3.3 mmol) of HFBC was introduced. Gas was evolved, and a pale yellow precipitate formed. After stirring for about 2 hours, the precipitate dissolved, resulting in a bright yellow solution. After 48 hours the solution was removed

and the films were washed with two 20 mL portions of THF, five 20 mL portions of methanol and three 20 mL portions of THF, and then dried at room temperature under vacuum.

#### DMAP Catalyzed Reaction of FEP-OH with HFBC in Pyridine

(b2p14-16) 0.082 g (0.7 mmol, 21 mole percent relative to HFBC) of DMAP was dissolved in 20 mL of pyridine and added to a Schlenk tube containing the film samples and a stir bar. 0.5 mL of HFBC was added with vigorous stirring. Gas evolved, and a white precipitate was formed. Over time, some of the precipitate dissolved, resulting in a yellow-orange solution. After 48 hours, the reagent was removed and the films were washed with two 20 mL portions of THF, five 20 mL portions of methanol and four 20 mL portions of THF; methanol dissolved all of the remaining precipitate. The films were dried under vacuum at room temperature.

#### DMAP Catalyzed Reaction of FEP-OH with HFBC in THF

(b2p23) 0.082 g of DMAP was dissolved in 20 mL of THF. 1.3 mL of pyridine (16 mmol, 230% relative to DMAP) was added, and the solution was transferred to a Schlenk tube containing the film samples and a stir bar. 0.5 mL of HFBC was added with vigorous stirring. A white precipitate formed, some of which dissolved over time, resulting in a pale yellow solution. After 48 hours, the reagent was removed and the films were washed with two 20 mL portions of



THF, five 20 mL portions of methanol and four 20 mL portions of THF; methanol dissolved all of the remaining precipitate. The films were dried under vacuum at room temperature.

#### Reaction of FEP-OH with Ethylene Oxide and LDA (FEP-EO-OH)

(b2p19,86-89) 0.25 g (4.7 mmol) of LDA was loaded into a graduated cylinder in the drybox and capped with a septum. 25 mL of THF was added, and the cylinder was agitated on the Vortex-Genie. A small amount of the solid remained suspended. This solution was cooled to 0°C, and 5 mL of ethylene oxide (100 mmol) was added. The solution was transferred to a Schlenk tube containing film samples and a stir bar. The reaction was allowed to proceed for 4.5 hours at 0°C, the reagent was removed, and the films were washed with one 20 mL portion of methanol, five 20 mL portions of THF, and three 10 mL portions of heptane, and then dried (room temperature, 0.05 mm). Some suspended LDA remained, but no increase in the viscosity was observed. The reaction was repeated on new film samples; this time the reaction was allowed to proceed at 5°C for 68 hours. A significant amount of fluffy, white solid was observed. The reagent was removed, the solid was isolated by filtration and the films were washed as described above. White solid remained on the surface, so the films were extracted for 24 hours in THF (Soxhlet extractor), and then dried under vacuum (0.03 mm) at 45°C.

#### Reaction of FEP-EO-OH with HFBC

(b2p90,92) The 68 hour reaction product was labeled according to procedure B described in the section on reactions of FEP-OH with HFBC in THF. This surface also exhibited an unusually high fluorine content after washing and was extracted with THF.

#### Reaction of FEP-OH with Ethylene Oxide and DBU

(b2p76-77,86-90) An FEP-OH film sample was placed in a Schlenk tube and cooled to 0°C. 7 mL of ethylene oxide and 4 mL of DBU were added. The solution was warmed to 5°C and allowed to react for 48 hours. The reagent was removed and the films were washed with 20 mL of THF, two 20 mL portions of methanol, and four 20 mL portions of THF, and then dried under vacuum at room temperature. No precipitate was formed. This reaction was repeated, with the reaction time increased to 68 hours.

#### Reaction of the Ethylene Oxide/DBU Product with HFBC

(b2p80,90,92) The 48 hour reaction product was labeled by reaction with 1 mL of HFBC in 10 mL of THF and 0.1 mL of pyridine for 18 hours. The film sample was washed with two 20 mL portions each of THF and methanol. The 68 hour reaction product was labeled according to procedure B, described in the section on reactions of FEP-OH with HFBC in THF.

### Reaction of FEP-C with Methanol and Benzoyl Peroxide

(b2p109) A solution of 0.5 g of benzoyl peroxide (BPO) in 25 mL of methanol was added to a Schlenk tube containing FEP-C film samples. The reaction was allowed to proceed at 50°C for 24 hours. The reagent was removed and the films were washed with five 20 mL portions of methanol, extracted overnight (Soxhlet extractor) with methylene chloride, and dried under vacuum at 45°C. The films remained dark colored.

### Reaction of the BPO/Methanol Product with HFBC

(b1p109) Hydroxyl groups introduced by reaction with BPO and methanol were labeled by reaction with 1.0 mL of HFBC and 0.05 mL of pyridine in 10 mL of THF for 22 hours. The films were washed with two 20 mL portions of THF, five 20 mL portions of methanol, and three 20 mL portions of THF, and then dried at room temperature under vacuum.

### Reaction of FEP-C with 9-BBN (FEP-9BBN)

(b2p131,137) 15 mL of 0.5 M 9-BBN in THF was transferred into a Schlenk tube containing FEP-C film samples. The reaction was allowed to proceed overnight (approximately 16 hours), the reagent was removed, and the films were washed with two 20 mL portions of THF, and then dried under vacuum at room temperature. Alternately, FEP-C was hydroborated in refluxing THF as follows: FEP-C film samples



were placed in a sidearm flask equipped with a condenser. Nitrogen purge was maintained through a bubbler, connected to the top of the condenser by a needle through a septum. 15 mL of 0.5 M 9-BBN in THF was added through the sidearm; the flask was placed in an oil bath and heated to reflux. After 16 hours, the flask was cooled to room temperature. The films were transferred (incurring brief air exposure) to a nitrogen-purged Schlenk tube and washed with two 10 mL portions of THF, and then dried at room temperature under vacuum. All of the film samples remained much darker colored than those hydroborated with borane-THF.

#### Carbonylation and Basic Work Up of FEP-9BBN (FEP-CH<sub>2</sub>OH)

(b3p1-2) An FEP-9BBN film sample (prepared at room temperature) was placed in a nitrogen-purged Schlenk tube. LiAlH(OMe)<sub>3</sub> was prepared as follows: 1.7 mL (43 mmol) of methanol and 16 mL of THF were added to a nitrogen-purged Schlenk tube. 14 mL of 1.0 M (14 mmol) LiAlH<sub>4</sub> in THF was added slowly. Heat was evolved and a milky white suspension was formed. This solution was transferred to the tube containing FEP-9BBN. A long stainless steel needle was passed through the septum into the solution and carbon monoxide was bubbled through the solution for 10 minutes. The stopcock was closed under a positive pressure of carbon monoxide. Four hours later the tube was repressurized with CO. After 22 hours at room temperature, the reagent was

removed and the films were washed with two 20 mL portions of THF. A solution of 2.1 g KOH in 30 mL of ethanol was added and the tube was placed in an oil bath at 60°C for 45 minutes. The tube was cooled to room temperature, the reagent was removed, and the film sample was washed with five 20 mL portions each of dilute methanolic HCl, methanol, and dichloromethane, and then dried under vacuum at 60°C. The films did not exhibit the "bleached" appearance observed for FEP-OH.

#### Reaction of FEP-CH<sub>2</sub>OH with HFBC

(b3p3) Hydroxyl groups introduced by hydroboration and carbonylation were labeled by reaction with 1 mL of HFBC in 10 mL of THF and 0.1 mL of pyridine for 24 hours. The films were washed with three 20 portions each of methanol and THF, and then dried at room temperature under vacuum.

#### Reaction of Hydroxylated Surfaces with Multifunctional Electrophiles

This section describes the reaction of FEP-OH with multifunctional electrophiles containing functional groups of differing reactivity. The resulting electrophilic surfaces were reacted with various nucleophiles. These reactions were also performed on PCTFE-OH surfaces for comparison. The preparation of PCTFE-OH surfaces is also described.

Preparation of PCTFE-OH. (b3p68,b4p122,134) The procedure for preparing PCTFE-OH surfaces is described in detail elsewhere<sup>5,6</sup> and will be reviewed only briefly here. Acetaldehyde bromopropyl ethyl acetal (BrPrOP) was prepared by reacting 26 g (187 mmol) of 3-bromo-1-propanol with 22.6 g (314 mmol) of ethyl vinyl ether in the presence of 0.5 mL of  $\text{CHCl}_2\text{CO}_2\text{H}$  overnight at room temperature. Excess ethyl vinyl ether was removed under vacuum and the product was stirred over potassium carbonate for about 20 hours. The product was distilled from potassium carbonate ( $50^\circ\text{C}$ , 1 mm) and stored under nitrogen over  $\text{K}_2\text{CO}_3$ . Approximately 1.1 g (5 mmol) of BrPrOP was added to a nitrogen-purged, tared round bottom flask. The exact amount of BrPrOP added was determined, 15 mL of heptane was added and the flask was cooled to  $-78^\circ\text{C}$  (dry ice/acetone). A solution containing an equimolar amount of *t*-butyllithium was prepared by adding the appropriate amount of standardized solution (approximately 2.5 mL) to 10 mL of heptane. This solution was cooled to  $-78^\circ\text{C}$  and added to the BrPrOP solution with stirring. Reaction was allowed to proceed at  $-78^\circ\text{C}$  for 15 minutes, the solution was warmed to  $-20^\circ\text{C}$  (Haake constant temperature bath) for 15 minutes, and then cooled back to  $-78^\circ\text{C}$ . A white (sometimes pale yellow) solid formed. 20 mL of THF (at room temperature) was slowly added. The reaction was stirred to dissolve this solid, resulting in a colorless to pale yellow solution. This solution was transferred onto



four 1.5 x 4 cm<sup>2</sup> film samples in a nitrogen-purged Schlenk tube (equipped with glass dividers) equilibrated at -20°C. After the desired reaction time (2 hours for deep modification, 45 minutes for shallower surfaces) the reagent was removed, and the films were washed with two portions of methanol. The resulting acetal surface was hydrolyzed by refluxing in a mixture of 5 mL of HCl, 30 mL of water and 65 mL of methanol for three hours, washed with three 20 mL portions each of water, methanol and THF, and dried (room temperature, 0.03 mm).

Reaction of FEP-OH and PCTFE-OH with Cyanuric Chloride.

(b3p71,77,79-80) FEP-OH and PCTFE-OH film samples were reacted with cyanuric chloride (CC) using one of the following procedures: (A) 5 g of CC was dissolved in 40 mL of THF, resulting in a pale yellow solution. Half of this solution was transferred into each of two Schlenk tubes containing a PCTFE-OH and an FEP-OH film sample. The reaction was allowed to proceed for 23 hours, the reagent was removed and the films were washed with three 20 mL portions of THF, and then dried at room temperature under vacuum. Both films appeared white colored and hazy. (B) 1.25 g of CC was dissolved in benzene and added to a Schlenk tube containing a sample of FEP-OH and PCTFE-OH. The reaction was allowed to proceed for 3 hours, the reagent was removed, and the films were washed with two 10 mL portions each of benzene and THF,

and then dried under vacuum. No visible changes in the films occurred due to reaction. (C) 1.25 g of CC was added to 15 mL of pyridine and the suspension was transferred to a Schlenk tube containing an FEP-OH sample. Over time, the solution turned yellow, then black. After 19 hours, the solution was clear, but a black precipitate had settled out. The films were washed with THF and methanol. The precipitate was insoluble in THF, but dissolved somewhat in methanol, resulting in a blue solution. The films were dried at room temperature under vacuum.

#### Reaction of FEP-OH with 2,4-Toluene Diisocyanate

(FEP(TDI)-NCO). (b4p116,128) FEP-OH was reacted with 2,4-toluene diisocyanate (TDI) using one of the following procedures: (A) 0.1 mL (1.2 mole percent relative to TDI) of dibutyl tin dilaurate was added to 20 mL of THF under nitrogen. This solution was transferred to a nitrogen-purged Schlenk tube containing the film sample, and then 2 mL (14 mmol) of TDI was added, resulting in a clear colorless solution. The reaction was allowed to proceed at room temperature for 22 hours, the reagent (still colorless) was removed and the films were washed with five 20 mL portions of THF, and then dried at room temperature under vacuum.

(B) 0.12 g of DABCO (5 mole percent relative to TDI) was dissolved in 20 mL of THF. 0.6 mL of dibutyl tin dilaurate (5 mole percent relative to TDI) was added and the solution

was transferred to a Schlenk tube containing an FEP-OH sample and 2.8 mL (20 mmol) of TDI was added. The tube was covered in foil and reacted in a constant temperature bath at 50°C for 45 hours. The solution became bright yellow and a white solid deposited on the side of the tube, just above the meniscus. The reagent was removed and the films were washed with five 20 mL portions of THF, and then dried at room temperature under vacuum.

#### Reaction of FEP-OH with Isophorone Diisocyanate

(FEP(IPDI)-NCO). (b4p116,128) FEP-OH was reacted with isophorone diisocyanate (IPDI) using one of the following procedures: (A) A solution of 0.1 mL (1.7 mole percent relative to IPDI) of dibutyl tin dilaurate in THF was added to a Schlenk tube containing an FEP-OH film sample. 2 mL (10 mmol) of IPDI was added, resulting in a clear, colorless solution. The reaction was allowed to proceed at room temperature for 23 hours, the reagent was removed and the film samples were washed with five portions of THF, and then dried (0.03 mm, room temperature). (B) A solution containing 0.12 g of DABCO and 0.6 mL of dibutyl tin dilaurate (both 5 mole percent relative to IPDI) in THF was added to a Schlenk tube containing an FEP-OH film sample. 4.2 mL (20 mmol) of IPDI was added and the reaction was allowed to proceed at 50°C for 45 hours. The reagent (which remained



colorless) was removed and the films were washed with five 20 mL portions of THF and dried as before.

Reaction of PCTFE-OH with TDI (PCTFE(TDI)-NCO). (b4-p126,134) PCTFE-OH was reacted with TDI using one of the following procedures: (A) 0.1 mL of dibutyl tin dilaurate was dissolved in 20 mL of THF. The solution was transferred to a Schlenk tube containing FEP-OH samples and 2 mL of TDI was added. After 20 hours at room temperature, the solution was removed and the films were washed with five 20 mL portions of THF and dried (0.03 mm, room temperature). (B) 0.6 mL of dibutyl tin dilaurate was added to 20 mL of THF. The solution was transferred to a Schlenk tube containing FEP-OH samples, 2.8 mL of TDI was added, and the reaction was allowed to proceed for 48 hours in the dark at room temperature. The solution developed a pale yellow color. The films appeared somewhat swollen at the end of 48 hours. The film samples were washed with five 20 mL portions of THF, and then dried (0.03 mm, 55°C).

Reaction of PCTFE-OH with IPDI (PCTFE(IPDI)-NCO). (b4-p123,134) PCTFE-OH was reacted with IPDI using one of the following procedures: (A) 0.1 mL of dibutyl tin dilaurate in 20 mL of THF was transferred to a Schlenk tube containing a PCTFE-OH film sample. 2.0 mL of IPDI was added and the reaction was allowed to proceed at room temperature for 24

hours. The films were washed with five 20 mL portions of THF and dried (room temperature, 0.03 mm). (B) 0.6 mL of dibutyl tin dilaurate was dissolved in 20 mL of THF, this solution was transferred onto the film samples and 4.2 mL of IPDI was added. The reaction was allowed to proceed for 48 hours at room temperature. The solution remained colorless, but the films appeared to be somewhat swollen. The reagent was removed and the films were washed with five 20 mL portions of THF and dried at 55°C under vacuum.

Reaction of FEP-OH with Hexamethylene Diisocyanate (FEP(HMDI)-NCO). (b4p118) 0.1 mL of dibutyl tin dilaurate in 20 mL of THF was added to a Schlenk tube containing an FEP-OH film sample. 2 mL of hexamethylene diisocyanate (HMDI) was added. The reaction was allowed to proceed for 19 hours. The reagent was removed, and the films were washed with five 20 mL portions of THF and dried (0.03 mm, room temperature).

Reaction of Isocyanate Surfaces with 3-Bromo-1-Propanol. (b4p117,121,125,127) Isocyanate surfaces were reacted with 1 mL of 3-bromo-1-propanol (BrPrOH) in 20 mL of THF and 0.05 mL of dibutyl tin dilaurate for 24 hours. The films were washed with five 20 mL portions of THF and dried at room temperature under vacuum. This reaction was performed on the following surfaces: FEP(TDI)-NCO, procedure A;

PCTFE(TDI)-NCO, procedure A; FEP(IPDI)-NCO, procedure A;  
PCTFE(IPDI)-NCO, procedure A; FEP(HMDI)-NCO.

Reaction of Isocyanate Surfaces with 4-Bromophenylethyl Alcohol. (b4p132) Isocyanate film samples were reacted with 1 mL of 4-bromophenylethyl alcohol (BrPhEtOH) and 0.05 mL of dibutyl tin dilaurate in 20 mL of THF for 20 hours. The film samples were washed with five 20 mL portions of THF and dried (room temperature, 0.03 mm). This reaction was performed on the following samples: FEP(TDI)-NCO, procedure B; FEP(IPDI)-NCO, procedure B.

Reactions of Isocyanate Surfaces with Methanol. (b4p-132,136) Isocyanate film samples were reacted with 2 mL of methanol and 0.6 mL of dibutyl tin dilaurate in 20 mL of THF for 48 hours. The films were washed with five 20 mL portions of THF and dried under vacuum. Surfaces treated with BrPhEtOH and isocyanate surfaces (TDI and IPDI) from the reaction of PCTFE-OH using procedure B were reacted under these conditions.



## References

1. Shriver, D.F.; Drezdon, M.A. *Manipulation of Air Sensitive Compounds*, 2nd. ed., Wiley Interscience: New York, 1986.
2. Costello, C.A.; McCarthy, T.J. *Macromolecules* **1987**, *20*, 2819.
3. See reference 2.
4. Holland, L. *The Properties of Glass Surfaces*, Chapman and Hall: London, 1966.
5. Dias, A.J.; McCarthy, T.J. *Macromolecules* **1987**, *20*, 2068.
6. Lee, K.-W.; McCarthy, T.J. *Macromolecules* **1988**, *21*, 2318.

### CHAPTER III

#### RESULTS AND DISCUSSION

##### Sodium Naphthalide Reduction of FEP

Kinetics and Structure of FEP-C. FEP film reacts rapidly with THF solutions of sodium naphthalide at room temperature as evidenced by an instantaneous blackening of the initially clear white film. Film samples were reacted with 0.2 M sodium naphthalide in THF at 0°C and -78°C. Films produced by reaction at 0°C were much darker, suggesting deeper reaction. Kinetics (depth of reaction vs. time) were determined using a combination of gravimetric analysis and UV-visible spectroscopy. Accurate measurements of reaction depth could be made without stoichiometric assumptions for samples reacted at 0°C. Film samples (5-mil, 1.5 x 1.5 cm<sup>2</sup>) were weighed, reacted for the desired length of time, oxidized with KClO<sub>3</sub>/H<sub>2</sub>SO<sub>4</sub> and reweighed. XPS spectra confirmed complete removal of the reduced layer. The reduced-then-oxidized surface differed from virgin FEP by the presence of 2-3 % oxygen. Reaction times ranged from 2 minutes to 11.5 hours. Reactions were terminated promptly by adding deoxygenated water immediately after the reagent was removed. The depth of reaction (thickness of the carbonaceous layer) can be directly determined using the following formula:

$$d_{rxn} = \frac{M_v - M_o}{2.15A}$$

where  $M_v$  is the mass of the virgin film sample,  $M_o$  is the mass of the reduced-then-oxidized film sample, and  $A$  is the surface area (neglecting edges) of the sample; 2.15 is the density of FEP (in g/cc). The surface area,  $A$ , can be determined conveniently from the mass of the virgin polymer sample according to the following formula:

$$A = \frac{M_v}{2.15t}$$

where  $t$  is the sample thickness, easily measured with a micrometer. The UV-visible spectrum of FEP-C, shown in figure 3, exhibits a broad absorbance, tailing out to 700 nm, with a distinct local maximum at 266 nm. Comparision of the increase in absorbance that occurs at 250 nm to the reaction depth obtained by gravimetric analysis reveals that these quantities are directly proportional to one another, with a proportionality constant of  $80 \pm 5 \text{ Å/au}$ . No significant weight loss occurred upon removal of the reduced layer for  $-78^\circ\text{C}$  reaction products, indicating much shallower reaction. However, if it assumed that the proportionality constant determined at  $0^\circ\text{C}$  is valid for  $-78^\circ\text{C}$  reduction, the reaction depth can be determined from the UV-visible data. The similarity of the spectra of the products prepared at



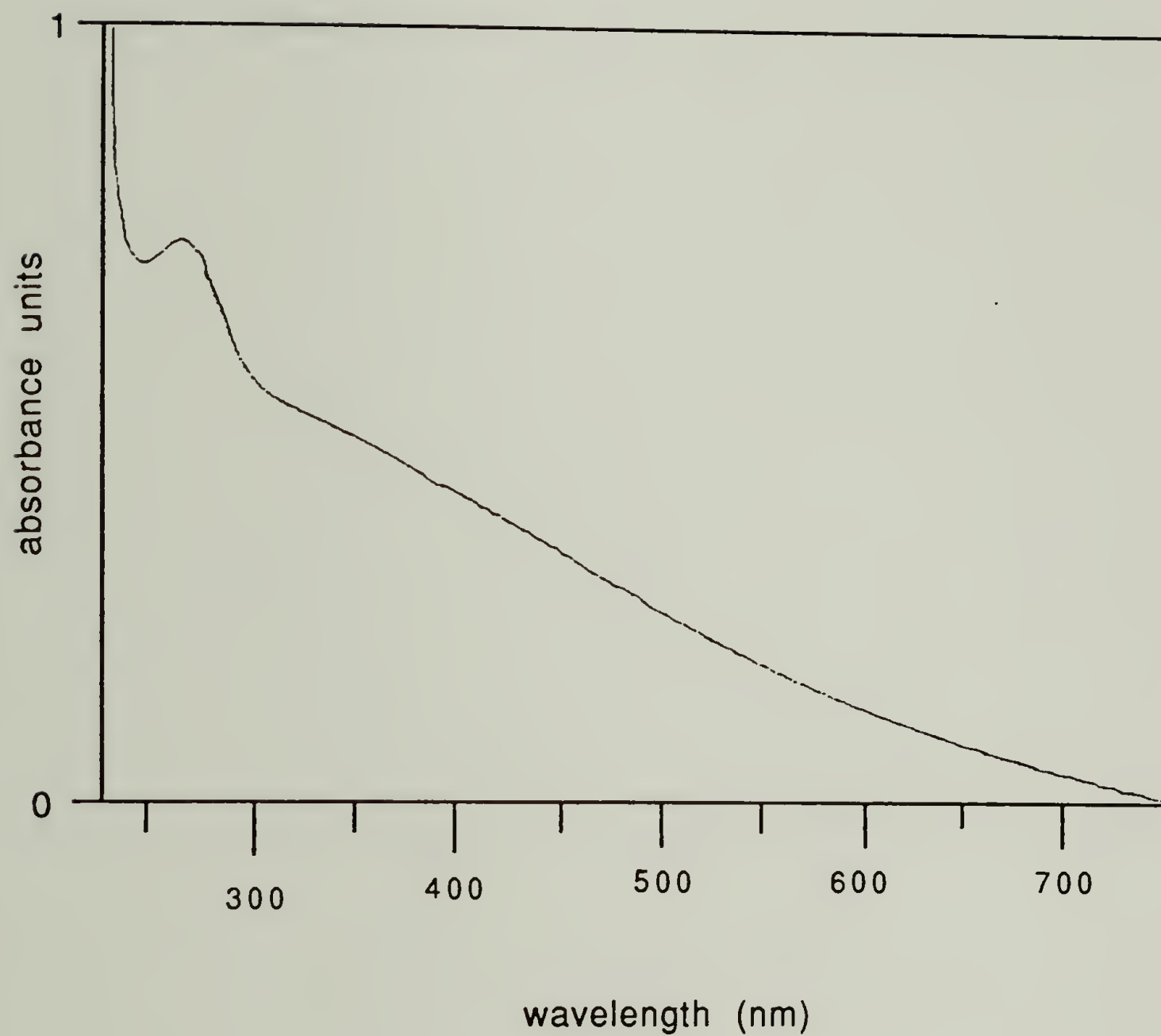


**Figure 3.** UV-visible spectrum of FEP-C (4 h, 0°C).

these temperatures, described in detail in latter sections, suggests that this assumption is valid.

Figure 4 summarizes the kinetics data for FEP reduction at 0°C and -78°C. At 0°C, the reaction proceeds rapidly (less than 2 minutes) to a depth of about 250 Å, and then slows. This trend in reaction depth with time differs somewhat from what was observed for the reduction of PTFE with benzoin dianion<sup>1</sup>, where reaction depth increased more uniformly with time. At -78°C the initial rapid reaction renders a shallower modified surface (approximately 45 Å) and is followed by a very slow reaction, more like the autoinhibitive reactions of polyvinylidene fluoride and PCTFE described by Dias<sup>2,3</sup>. While these results do not constitute a careful mechanistic study, they are consistent with two different mechanisms, one responsible for the initial, nearly instantaneous, reduction, and a second responsible for the subsequent slower modification. A variety of factors such as differences in swelling of the interface region or partitioning of reducing agent into the polymer, in addition to differences in the conductivity of the reduced product, may account for the differences between this reaction and the reduction of PTFE with benzoin dianion. Solubility of the reagent (precipitation at -78°C) undoubtedly plays an important role in the temperature dependence of this reaction, but other factors such as

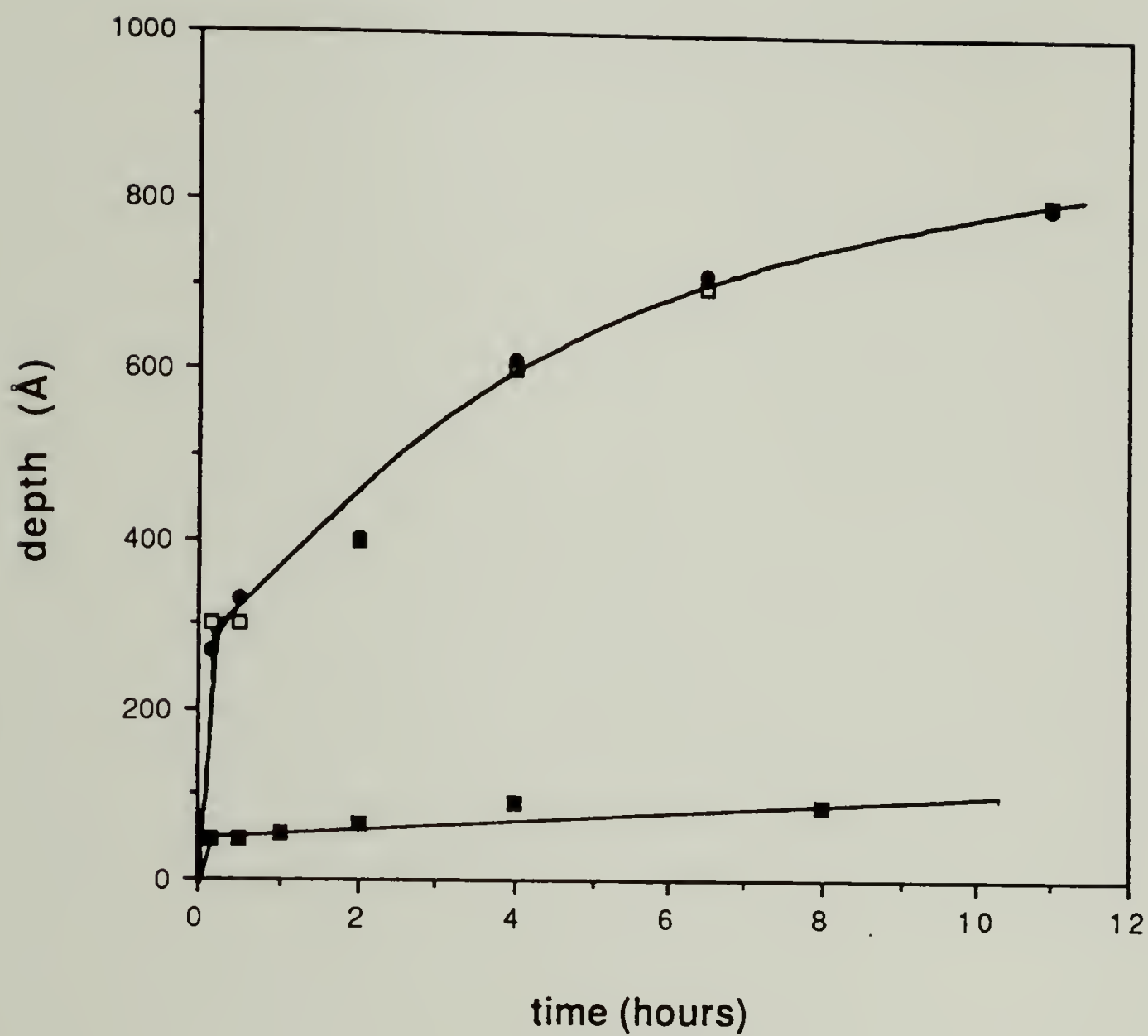


**Figure 4.** Reaction depth versus reaction time for sodium naphthalide reduction of FEP at 0°C (□,●) and -78°C (■). (□) determined from gravimetric data; (●) determined from absorbance at 250 nm.



thermal activation of the reduction and polymer chain mobility may be important as well.

Variable Angle XPS. The reaction depths obtained from gravimetric and UV-vis data represent average values. The data says nothing about the sharpness of the interface; unreacted polymer may be present in the modified region, either as "islands" or "peninsulas". Variable angle XPS yields information about the atomic composition and chemical homogeneity (as a function of depth) of the outer approximately 40 Å of the film sample. Comparing the data obtained at a 15° takeoff angle to that obtained at a 75° takeoff angle reveals changes in the film's composition that occur between the outer 10 and 40 Å. Figure 5 displays the  $C_{1s}$  region of XPS spectra (corrected for differential charging) of FEP and FEP-C prepared at 0°C (4 hours) and -78°C (4 hours). When the reduction was carried out at 0°C, the high binding energy peak, which is due to  $CF_2$  and  $CF_3$ , in the FEP spectrum is replaced by a peak at lower binding energy due to more highly reduced carbon species. No high binding energy carbon was observed at a 75° takeoff angle; identical spectra resulted for reaction times as short as 2 minutes. Empirical formulas of  $C_{100}F_{4\pm3}O_{17\pm3}$  (at a 15° takeoff angle) and  $C_{100}F_{5\pm3}O_{16\pm3}$  (at a 75° takeoff angle) are obtained from the atomic composition data. The similarity in the data ob-

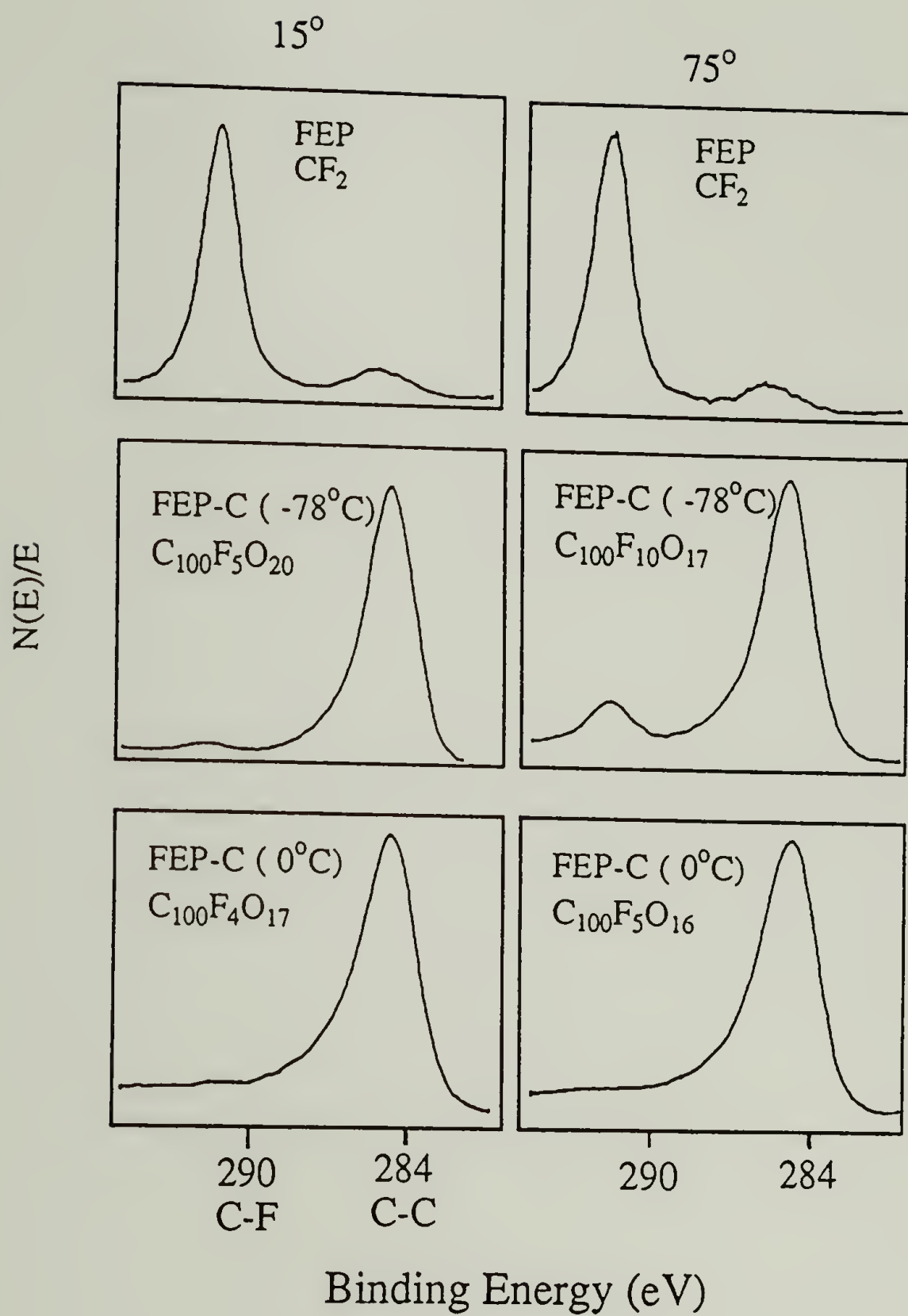


**Figure 5.** XPS spectra (C<sub>1s</sub> region) of FEP, FEP-C (-78°C, 4 h) and FEP-C (0°C, 4 h) recorded at 15° and 75° takeoff angles.

tained at different angles shows that the composition is similar throughout the outer 40 Å of the film sample. The XPS data for samples prepared at  $-78^{\circ}\text{C}$  indicates that the composition of the outer 10 Å is similar to that obtained at  $0^{\circ}\text{C}$ ; no high binding energy carbon is present and the composition can be represented as  $\text{C}_{100}\text{F}_{3.5\pm 2}\text{O}_{20\pm 1.5}$ . However, at a  $75^{\circ}$  takeoff angle (40 Å), a small peak due to  $\text{CF}_2/\text{CF}_3$  was observed and the F:C ratio increased ( $\text{C}_{100}\text{F}_{10\pm 4}\text{O}_{17\pm 4}$ ). All samples prepared at  $-78^{\circ}\text{C}$  lacked high binding energy carbon in the  $15^{\circ}$  takeoff angle spectrum, but the relative size of the  $\text{CF}_2/\text{CF}_3$  peak did not decrease smoothly with increasing reaction depth;  $\text{CF}_2/\text{CF}_3$  carbon was still present in a samples possessing an average modification depth of 90 Å. These data indicate that the transition from FEP-C to the interphase region (containing both FEP and FEP-C) first occurs at approximately the same depth as the average modification depth (45 Å), suggesting a relatively sharp interface. The lack of systematic change in the ratio of reduced to high binding energy carbon observed at a  $75^{\circ}$  takeoff angle with reaction depth, however, suggests that the interphase region spans at least 40 Å.

These results are in sharp contrast with those of PTFE-C. High binding energy carbon, indicative of unreacted polymer, was present in the outer 10 Å of much deeper modified surfaces. While these results do not verify that the reduction of FEP is less corrosive due to decreased conduc-



tivity of the reduction product, they are consistent with this explanation. The decreased crystallinity of FEP, as a result of the introduction of  $\text{CF}_3$  groups along the polymer chain, undoubtedly plays a role in its more homogeneous reactivity. Reduction would be expected to proceed more rapidly through crystalline regions if most of the reaction occurs as a result of "pumping" electrons from the solution to the unreacted polymer. Conversely, crystalline regions may react more slowly if most reduction occurs as a result of diffusion of the reducing agent into the bulk polymer.

Functional Group Composition. The large fluorine loss, shift in the  $\text{C}_{1s}$  binding energy and broad UV-vis absorbance imply significant unsaturation and conjugation. The intense absorbance at higher wavelengths (centered about 580 nm), observed for PTFE- $\text{C}^4$  is lacking, consistent with the expected shorter conjugation length of FEP-C. XPS also indicates that a significant amount of oxygen is incorporated into the reduced polymer. Given the atomic composition of the product, the higher binding energy tail in the  $\text{C}_{1s}$  region of FEP-C probably consists of both C-O and C-F species. More information about the functional group composition of these surfaces was obtained by ATR-IR spectroscopy. Figure 6 shows the spectra of FEP and FEP-C. The only feature present in FEP above  $1210\text{ cm}^{-1}$  is a weak overtone at  $2360\text{ cm}^{-1}$ . In FEP-C, unsaturation, in the form of  $\text{C}=\text{C}$



Figure 6. ATR-IR spectra of (a) FEP, (b) FEP-C, H<sub>2</sub>O/THF, (c) FEP-C, THF/H<sub>2</sub>O/THF, (d) FEP-C, fully deuterated.

(1597  $\text{cm}^{-1}$ ),  $\text{C}\equiv\text{C}$  (2115  $\text{cm}^{-1}$ ) and aromatic  $\text{C}=\text{C}$  (1462  $\text{cm}^{-1}$ , may include methylene bending contributions), is present and alcohols (3400  $\text{cm}^{-1}$ ), carbonyl groups (1720  $\text{cm}^{-1}$ ) and aliphatic hydrocarbon groups (2930, 2960  $\text{cm}^{-1}$ ) are also present. Unlike PTFE- $\text{C}^5$ , no  $\text{sp}^2$  C-H stretching ( $>3000$   $\text{cm}^{-1}$ ) is observed. The absorbance at 2930  $\text{cm}^{-1}$  is most likely due to methylenes and the band at 2960  $\text{cm}^{-1}$  is most likely due to methyls, although methines in a suitably electron withdrawing environment could, in principle, absorb at this wavelength.<sup>6</sup> Reduction at  $-78^\circ\text{C}$  resulted in the same absorbances, but the intensities were much weaker.

Further evidence for the presence of hydroxyl groups and carbonyl groups was provided by XPS labeling. Hydroxyl groups were labeled with heptafluorobutyryl chloride (HFBC). Carbonyl groups were labeled with 2,4-dinitrophenylhydrazine (DNPH) or 2,5-dichlorophenylhydrazine (DCPH). The results of these experiments are summarized in table 1. Attenuated total reflectance (ATR) IR spectroscopy was used to determine if the majority of the functional groups in the modified layer react with the label. Reaction with HFBC should result in disappearance of the hydroxyl band while reaction with DNPH or DCPH should result in disappearance of the carbonyl band.



**Table 1.** XPS atomic composition data for labeling  
of FEP-C.

<u>Sample</u>	<u>Label</u>	<u>Takeoff angle</u>	<u>C</u>	<u>F</u>	<u>O</u>	<u>N</u>	<u>Cl</u>
FEP-C	HFBC	15°	100	22	18	--	--
(0°C)		75°	100	21	9	--	--
FEP-C	DNPH	15°	100	5	15	3.5	--
(0°C)		75°	100	9	12	3.6	--
FEP-C	HFBC	15°	100	17	11	--	--
(-78°C)		75°	100	19	7	--	--
FEP-C	DCPH	15°	100	5	20	3	3
(-78°C)		75°	100	10	11	2	2

Labeling results were similar for both products and indicate that only approximately 8% of the oxygen reacts as carbonyl groups and 15% as hydroxyl groups. The ATR-IR spectra of HFBC labeled films show features due to the label (heptafluorobutyryl carbonyl at  $1780\text{ cm}^{-1}$ ), but the hydroxyl band is clearly still present. The carbonyl band also remained in the ATR-IR spectrum of aryl hydrazine labeled films. While these reactions confirm the presence of hydroxyl and carbonyl groups, labeling is too inefficient to be used to provide quantitative estimates of their relative abundance.

Origin of OH, C=O and C-H Groups. These analyses of FEP-C reveal that, in addition to the expected unsaturation, carbon-oxygen and carbon-hydrogen species result from the reaction. These side products compromise the utility of FEP-C as a substrate for further modification reactions. The potential sources of these side products were considered (THF, naphthalene and adventitious impurities in the reduction, water and THF in the rinsing, and air during handling), and a series of experiments were performed to determine the source(s), with the goal of preparing a more suitable surface for functionalization.

Four different rinsing procedures were studied: When  $D_2O$  was substituted for water, a weak O-D absorbance at  $2580\text{ cm}^{-1}$ , as well as the usual OH absorbance, was observed. When methanol or DMSO was substituted for water, the intensity of the carbonyl absorbance was substantially decreased while the OH region remained essentially unchanged, but a large increase was observed in the O:C ratio. In addition, a significant amount of sodium and fluoride was observed, as evidenced by a peak in the  $F_{1s}$  region, 4 eV lower in binding energy. These results, along with the dull black color of the film samples, suggest that ionic impurities, particularly NaF, were not removed. The results of the  $D_2O$  rinsing experiment suggest that the reaction of sodium naphthalide with water in the rinsing step may be responsible for some of the hydroxyl groups. Hydroxyl ions that are formed may

add to conjugated olefins and alkynes, leading to carbonyl groups, as well. Removal of the sodium naphthalide by washing with THF decreased the oxygen content in the outer 40 Å slightly. In general, films prepared according to this procedure (see figure 6c) exhibited a somewhat more dramatic decrease in the hydroxyl and carbonyl intensities by ATR-IR than would have been expected based on the XPS results. However, the carbonyl intensity was found to vary substantially from sample to sample. These results suggest that the majority of oxygen-containing functional groups are present in the outer 40 Å, most likely due to reaction of the air-sensitive surface with oxygen and adventitious moisture during drying and transfer. Recent work by Ha and Garten<sup>7</sup> supports this conclusion. To study the reaction of FEP-C with air, FEP-C films were prepared by washing with methanol instead of water to minimize the initial carbonyl concentration. These films were exposed to laboratory atmosphere or dry oxygen. In both cases, a substantial increase in the carbonyl intensity was observed. The increase in the hydroxyl intensity was much greater for films exposed to laboratory atmosphere. This suggests that moisture in the air contributes to hydroxyl group formation, however, it should be noted that this sample may have been a poor choice since NaF is hygroscopic. Some of this band may be due to adsorbed moisture. None of these changes resulted in differences in the C-H region and no evidence of C-D



stretch was observed, although weak absorbances may be obscured by the broad  $C\equiv C$  band.

In an effort to determine the source(s) that contribute to C-H bond formation, a series of reactions was performed in which one of the following changes was made in the reaction conditions: THF was "spiked" with  $D_2O$  prior to distillation, THF- $d_8$  was substituted for THF, naphthalene- $d_8$  was substituted for naphthalene, the reaction flask was treated with NaOD/ $D_2O$  prior to reduction and reduction was carried out in a PTFE vessel. The last two procedures were employed to assess the importance of soluble silanol species as proton sources. Such species might be formed as a result of attack on the glass surface of the Schlenk tube by fluoride ions. The intensity of the C-H bands relative to the C-F bands remained essentially unchanged and no C-D absorbances were observed. No OD stretch was observed, and the relative intensity of the carbonyl band varied from sample to sample, as observed previously. These results provide further evidence that the majority of oxygen-containing functional groups were introduced subsequent to the reduction, but failed to identify a primary source of hydrogen.

An unusual result occurred when sublimed naphthalene was used to prepare sodium naphthalide. The first time the reaction was performed only very weak hydroxyl and carbonyl absorbances were observed. No XPS spectrum of the product

was taken. When the experiment was repeated, the product exhibited the usual hydroxyl and carbonyl intensities.

In an attempt to gauge the importance of adventitious impurities, the reaction was run under the cleanest possible conditions, using only deuterated reagents. The resulting spectrum is shown in figure 6d. Although the features due to unsaturation ( $1550, 1470, 2120 \text{ cm}^{-1}$ ) are quite intense, as expected for reaction at  $-10^{\circ}\text{C}$ , the features due to side reactions are quite weak. No carbonyl absorbance was observed, a weak OD stretch was observed at  $2560 \text{ cm}^{-1}$ , and weak C-H bands were observed in the usual positions ( $2960, 2930 \text{ cm}^{-1}$ ). It was unclear if any OH or C-D groups were present; weak C-D absorbances may be obscured by the intense  $\text{C}\equiv\text{C}$  absorbance. Clearly, at least some of the C-H groups result from reaction with adventitious impurities. XPS reveals that the product still contained a substantial amount of oxygen in the outer  $40 \text{ \AA}$ ; the atomic composition data yields empirical formulas of  $\text{C}_{100}\text{F}_3\text{O}_9$  ( $15^{\circ}$  takeoff angle) and  $\text{C}_{100}\text{F}_7\text{O}_7$  ( $75^{\circ}$  takeoff angle). These results also support the idea that most of the oxygen is present in the outer angstroms.

Conclusions. Reduction of FEP with sodium naphthalide offers substantial control over the modification depth; reaction depths in the ranges of  $45\text{-}90 \text{ \AA}$  and  $250\text{-}800 \text{ \AA}$  can be reproducibly obtained. The interface between FEP-C and

FEP is relatively sharp; all FEP is removed from the outer 10 Å for average modification depths as shallow as 45 Å. The reduction product is similar to PTFE-C chemically, but less extensively conjugated and lacking  $sp^2$  C-H. As with PTFE-C, the presence of oxygen-containing functional groups, primarily alcohols and carbonyls, could not be avoided, although washing films with THF to remove the sodium naphthalide prior to washing with water did decrease their abundance.

FEP-C films prepared by reaction for 4 to 6 hours at 0°C and washing with THF, deoxygenated water, and then THF were used for further modification reactions. The procedure reproducibly yields a 600-700 Å-thick modified surface with an atomic composition that can be represented as  $C_{100}F_{4\pm2}O_{13\pm3}$  in the outer 40 Å. These surfaces are free of ionic impurities and possess thick enough modified regions that reactions can easily be followed by ATR-IR.

Other Reductions. These results show clear differences in the kinetics and product structure between sodium naphthalide-reduced FEP and benzoin dianion-reduced PTFE. It was of interest to determine the extent to which the choice of the reducing agent influences the results of reduction. It was also of interest to compare the changes in reduction kinetics due to changes in temperature for the two films.



The following series of experiments was performed to study these issues.

PTFE film samples were reduced with sodium naphthalide under conditions identical to those used for FEP reduction. The results are summarized in figure 7. The reaction resulted in significantly deeper modification; reaction for one hour at  $-78^{\circ}\text{C}$  and  $0^{\circ}\text{C}$  resulted in reaction depths (by gravimetric analysis) of 120 Å and 2000 Å, respectively. Reaction times of less than one hour were not studied, so it is not clear if an initial "burst" of modification occurs, as was observed for FEP. XPS analysis of surfaces reacted for four hours resulted in empirical formulas of  $\text{C}_{100}\text{F}_4\text{O}_{24}$  ( $15^{\circ}$  takeoff angle) and  $\text{C}_{100}\text{F}_{14}\text{O}_{13}$  ( $75^{\circ}$  takeoff angle) for  $0^{\circ}\text{C}$  (2480 Å) reduction, and  $\text{C}_{100}\text{F}_{14}\text{O}_{20}$  ( $15^{\circ}$  takeoff angle) and  $\text{C}_{100}\text{F}_{23}\text{O}_{17}$  ( $75^{\circ}$  takeoff angle) for  $-78^{\circ}\text{C}$  (170 Å) reduction. Figure 8 shows the  $\text{C}_{1s}$  region at  $15^{\circ}$  and  $75^{\circ}$  takeoff angles for PTFE reduced at  $-78^{\circ}\text{C}$  for 4 hours. Relatively little carbon due to  $\text{CF}_2$  is present. These results are comparable to those obtained for reduction with benzoin dianion to similar depths<sup>8</sup>. Slightly more oxygen was introduced using sodium naphthalide. The ATR-IR spectrum of the  $0^{\circ}\text{C}$  reduction product resembles that of FEP-C much more than that of PTFE-C from benzoin dianion reduction. The  $\text{sp}^2$  C-H absorbance was absent and a significant hydroxyl absorbance was observed. It is also important to note that the films were black, not metallic gold in appearance, consistent with

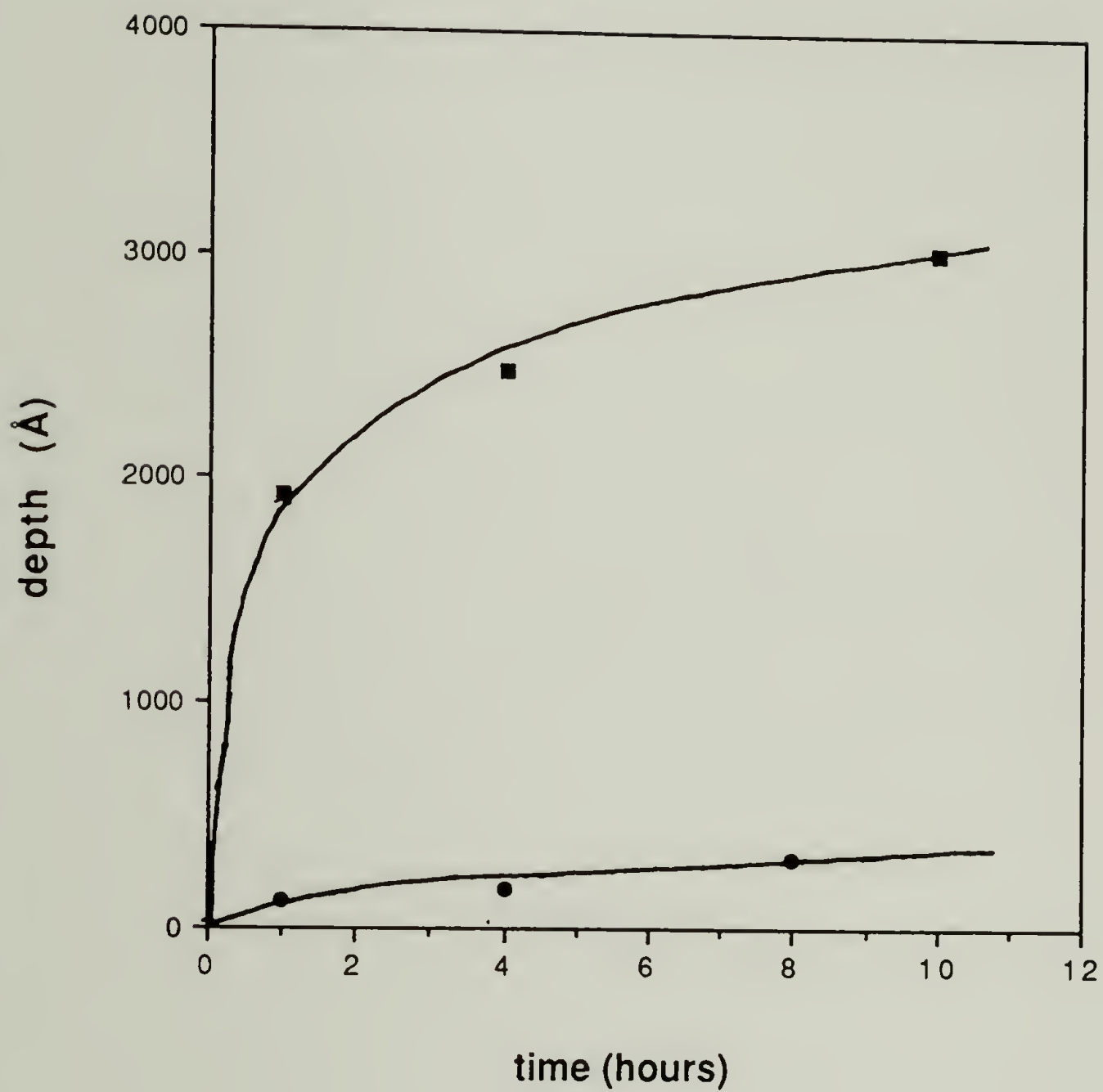


Figure 7. Reaction depth versus reaction time for sodium naphthalide reduction of PTFE at 0°C (■) and -78°C (●).

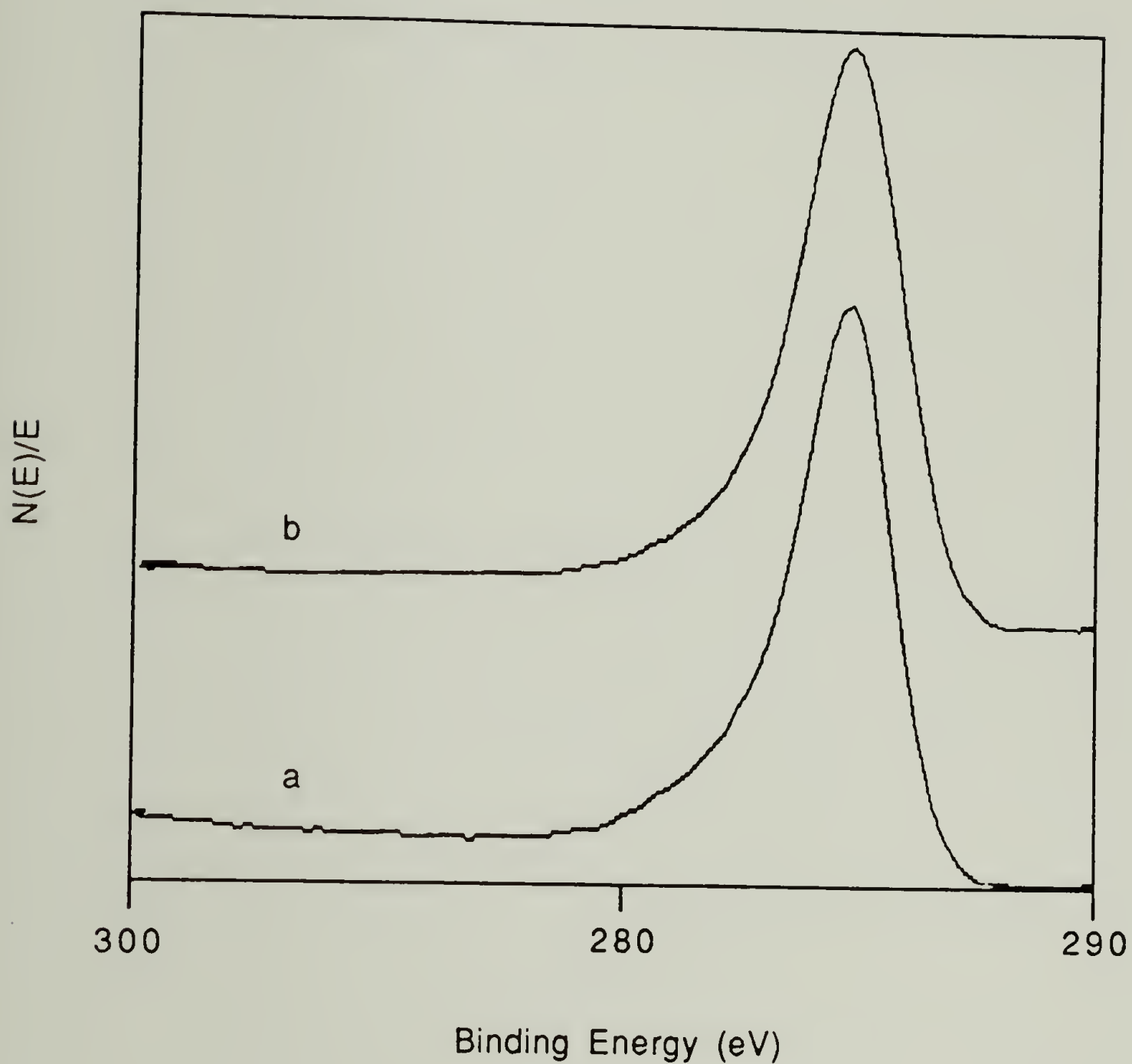
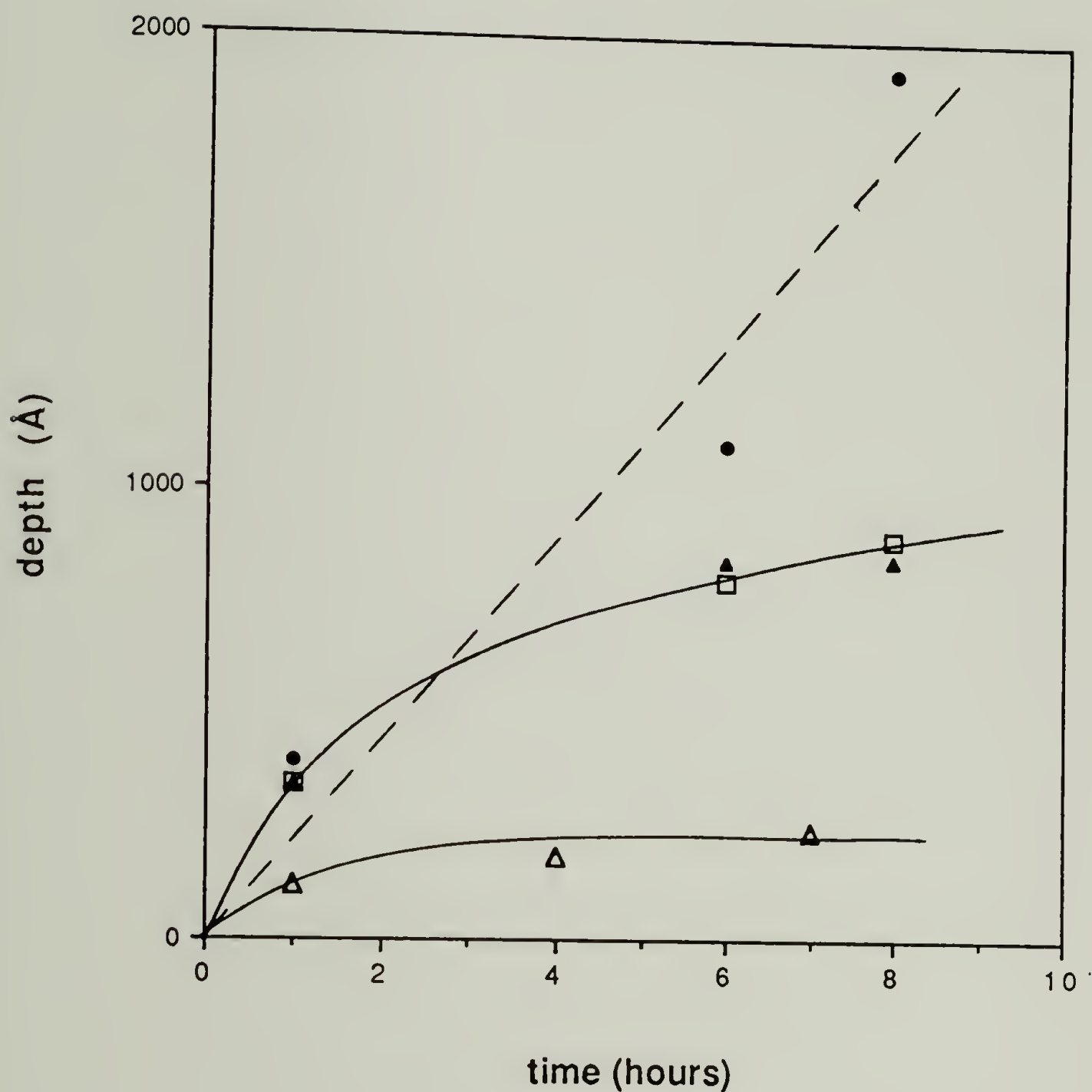


Figure 8. XPS spectra ( $C_{1s}$  region) of sodium naphthalide-reduced PTFE ( $-78^{\circ}\text{C}$ , 4 h) recorded at  $15^{\circ}$  (a) and  $75^{\circ}$  (b) takeoff angles.



previous reports for the sodium naphthalide reduction of PTFE<sup>9</sup>. The relative decrease in reaction depths obtained for lowering the reaction temperature to -78°C was comparable to that observed for FEP, consistent with changes in reagent solubility and/or other film-insensitive phenomena being the key factor in the temperature dependence of this reaction. Reduction was relatively fast, even at 0°C, for the sodium naphthalide system; the depth of modification that was observed for reaction at 0°C for 10 hours was comparable to that which was observed for reaction with benzoin dianion at 50°C for 10 hours. The most important difference between the two systems appears to be the increased conjugation of the benzoin reduction product; it is not clear if the presence of  $sp^2$  C-H is associated with increased conjugation.

The results of reducing PTFE with benzoin dianion in DMSO at 50°C, shown in figure 9, were comparable to those reported by C. Costello. The reaction depth increases almost linearly with time over an eight hour period; films were metallic in appearance, contained significant  $CF_2$  in the outer angstroms, and exhibited the characteristic  $sp^2$  C-H absorbance in their ATR-IR spectrum. FEP was reduced under identical conditions and the depth was monitored by UV-vis and gravimetric analysis; PTFE films were too opaque to yield useful UV-vis spectra. Reaction times less than



**Figure 9.** Reaction depth versus time for benzoin dianion reduction of FEP at 50°C (□,▲), FEP at 21°C (Δ) and PTFE at 50°C (●). (□) determined from gravimetric data; (▲) determined from absorbance at 250 nm.

one hour were not studied, as a result, it could not be determined if an initial "burst" of modification occurred.

FEP was reacted with benzoin dianion under comparable conditions. Modification depths for this system (figure 9) were comparable to those obtained for the reaction of FEP at 0°C with sodium naphthalide, and significantly shallower than those obtained for the reaction of PTFE at 0°C with sodium naphthalide or the reaction of PTFE at 50°C for reaction times greater than 1 hour. Reduced FEP films were similar in appearance to those obtained from sodium naphthalide reduction. It is interesting to note that the gravimetric depth to absorbance proportionality constant for this system was much larger ( $1051 \pm 59 \text{ \AA/au}$ ), suggesting that fewer conjugated groups absorbing at 250 nm were introduced as a function of depth. These films also lacked the intense longer wavelength absorbance characteristic of PTFE-C. The films contained somewhat less oxygen and more fluorine than those produced by reduction with sodium naphthalide; the XPS data leads to an empirical formula of  $C_{100}F_{6.7 \pm 0.8}O_{10 \pm 1.5}$  at a 15° takeoff angle and  $C_{100}F_{5 \pm 0.7}O_{9 \pm 0.6}$  at a 75° takeoff angle. The ATR-IR spectra were identical to those obtained for FEP-C prepared using sodium naphthalide; no  $sp^2$  C-H was observed.

FEP was also reduced with benzoin dianion in DMSO at room temperature (approximately 21°C). Not only was the average modification depth substantially reduced (see figure



9), but the reaction was also observed to proceed less uniformly across the surface. The films had a blotchy, purple appearance. Examination of the  $C_{1s}$  region of the 4 hour reduction product, shown in figure 10, reveals the presence of  $CF_2/CF_3$  in the outer angstroms, despite an average modification depth of 180 Å. Similar results were reported by C. Costello<sup>10</sup> for the reaction of PTFE with benzoin dianion in THF. This suggests that the influence of reaction temperature on solvation of the anion, or some related phenomenon, is responsible for these results.

From these results, it can be concluded that the structure of FEP, not the choice of reducing conditions, leads to greater surface selectivity and decreased conjugation of the product. Choice of reducing conditions is critical, however, to obtaining metallic appearance in reduced PTFE.

#### Synthesis and Reactivity of FEP-OH

The results of the previous sections show that reduction of FEP with sodium naphthalide offers precise control over modified layer thickness, but, the functional group composition, and thus the chemical behavior, of the resulting surface is rather complex. It would be desirable to convert this surface to one whose chemistry is dominated by the reactions of a single functional group. Alcohol functionality was chosen because hydroxyl groups comprise a large percentage of the oxygen-containing functional groups

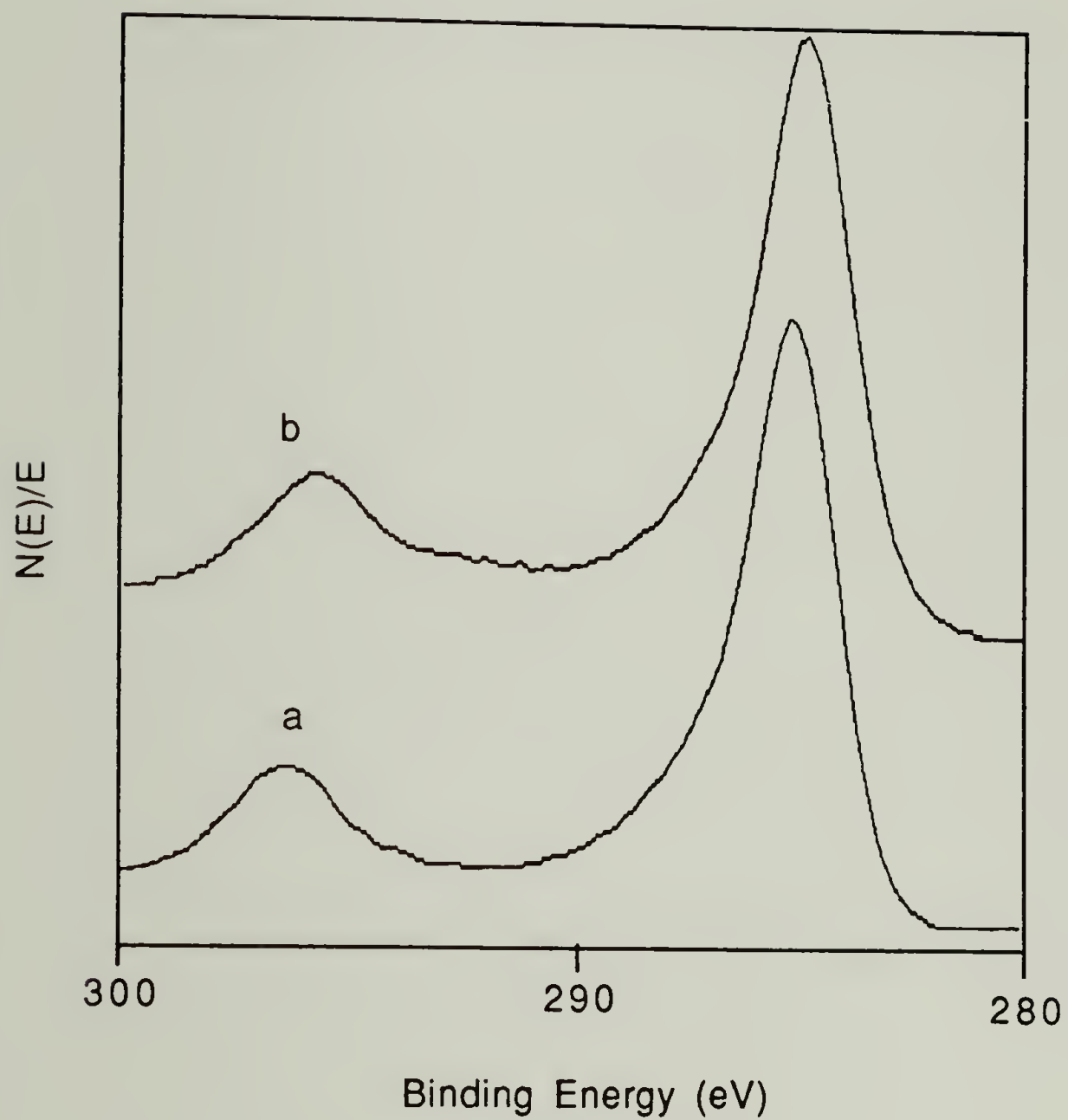


**Figure 10.** XPS spectra (C<sub>1s</sub> region) of benzoin dianion-reduced FEP (50°C, 4 h) recorded at 15° (a) and 75° (b) takeoff angles.

on FEP-C; the remainder consist primarily of carbonyl groups, which can, in principle, be reduced to alcohols. Further, the chemistry of surface-confined hydroxyl groups is quite versatile.<sup>11</sup>

Preparation of FEP-OH. Treatment of PTFE-C with borane-THF complex, followed by oxidation with basic peroxide, produces film samples exhibiting little of the color present in FEP and properties and spectra consistent with the introduction of hydroxyl groups. Contact angle measurements indicate polar groups are introduced;  $\theta_a/\theta_r$  values for FEP-OH are  $59^\circ \pm 2^\circ/30^\circ \pm 3^\circ$ . FEP initially exhibits very high contact angles ( $108^\circ/100^\circ$ ), characteristic of a fluoropolymer surfaces. Changes in the ATR-IR spectrum (compare figure 6c to 11a) are consistent with the addition of alcohol groups to unsaturation; the intensity of the OH absorbance ( $\sim 3300\text{ cm}^{-1}$ ) increases dramatically while the C=C absorbance at  $1597\text{ cm}^{-1}$  decreases in intensity and the C $\equiv$ C absorbance at  $2120\text{ cm}^{-1}$  disappears. The C=O band shifts from  $1720$  to  $1710\text{ cm}^{-1}$ , suggesting that carbonyl groups previously present were reduced and new ketones were formed by hydroboration /oxidation of alkynes. XPS indicates a substantial increase in oxygen; the surface can be represented by an empirical formula of  $\text{C}_{100}\text{F}_{1.5\pm.5}\text{O}_{27\pm3}$  at  $15^\circ$  takeoff angle and  $\text{C}_{100}\text{F}_{1.5\pm.5}\text{O}_{26\pm3}$  at a  $75^\circ$  takeoff angle. Figure 12 shows the  $\text{C}_{1s}$  spectrum of FEP-OH; the increase in the size



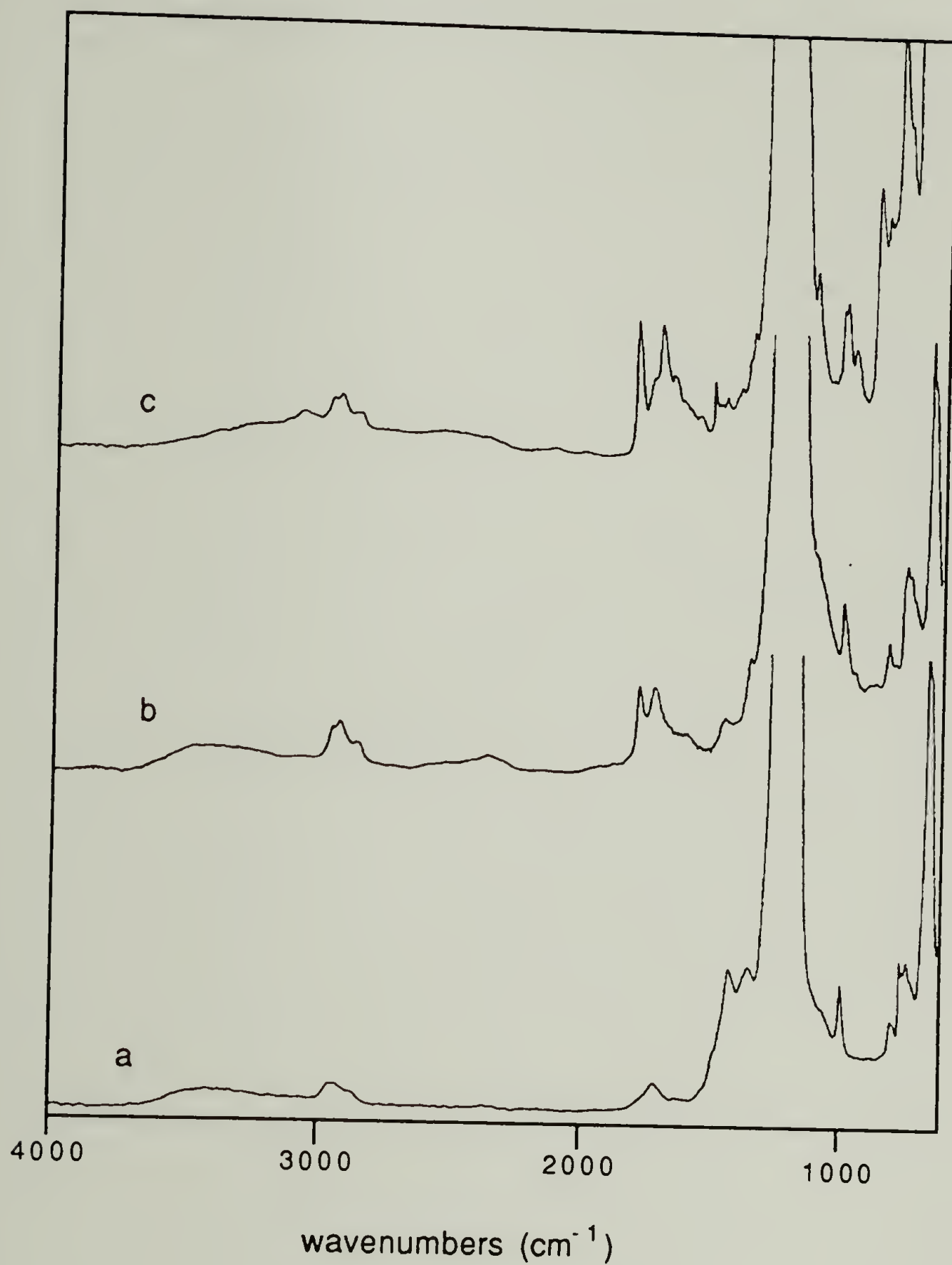
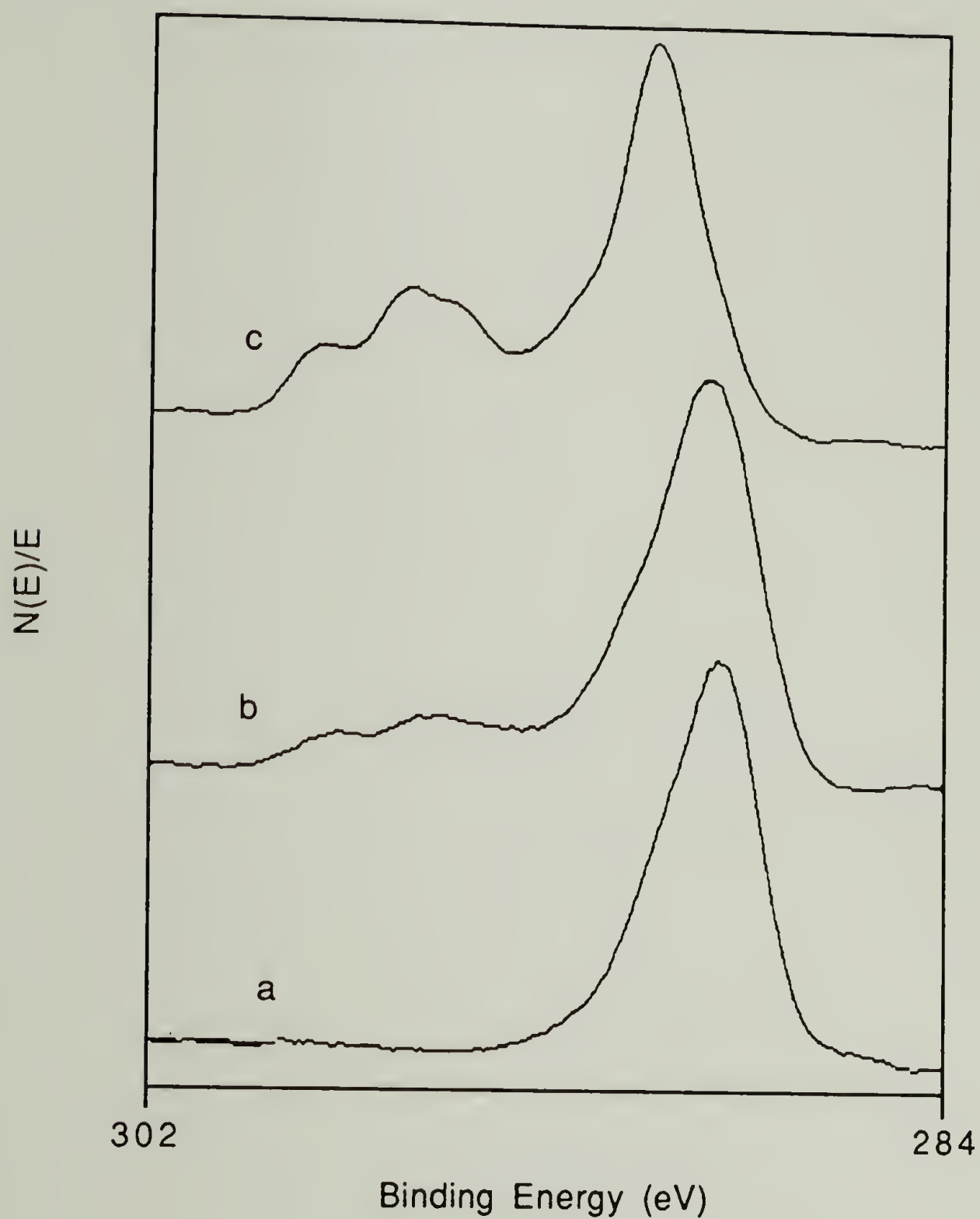


Figure 11. ATR-IR spectra of (a) FEP-OH; (b) FEP-OH reacted with HFBC, THF/pyridine; (c) FEP-OH reacted with HFBC, pyridine/DMAP.



**Figure 12.** XPS spectra ( $C_{1s}$  region) of (a) FEP-OH (b) FEP-OH reacted with HFBC, THF/pyridine (c) FEP-OH reacted with HFBC, pyridine/DMAP. Recorded at a  $15^\circ$  takeoff angle.

of the high binding energy shoulder is consistent with the introduction of hydroxyl groups.

Reactions of FEP-OH with HFBC. Esterification with heptafluorobutyryl chloride was chosen as the test reaction for studying the reactivity of FEP-OH. Reaction in THF in the presence of pyridine resulted in a rather poor yield of the heptafluorobutyrate. The XPS atomic composition data, summarized in table 2, indicates that only about 30% of the oxygen on the surface reacts to form the ester. The ATR-IR spectrum of the product, shown in figure 11b, exhibits the characteristic heptafluorobutyrate carbonyl absorbance at  $1780\text{ cm}^{-1}$ , but the intensity of the hydroxyl band decreases only slightly. In contrast, hydroxyl groups on PCTFE-OH surfaces were quantitatively acylated under milder conditions.<sup>12</sup> Structural differences probably account for the difference in reactivity. The hydroxyl groups in PCTFE-OH are primary and separated from the polymer backbone by three methylene units, while the majority of hydroxyl groups in FEP-OH are expected to be secondary and directly attached to the polymer backbone. In addition, FEP-OH surfaces are probably crosslinked, making swelling of the interface region more difficult.

It was of interest to determine how effectively strategies used to increase acylation yields in solution could be applied to film reactions. Using pyridine as the solvent



Table 2. XPS atomic composition data for acylation of  
FEP-OH with heptafluorobutyryl chloride.

<u>Sample</u>	<u>Acylation Conditions</u>	<u>Takeoff Angle</u>	<u>Carbon</u>	<u>Fluorine</u>	<u>Oxygen</u>	<u>% Esterification<sup>a</sup></u>
FEP-OH	-----	15°	100	1.4 +/- .5	27 +/- 3	-----
		75°	100	1.5 +/- .5	26 +/- 3	-----
FEP-OCOC <sub>3</sub> F <sub>7</sub>	THF, Pyridine, 24 h.	15°	100	42	29	46
		75°	100	27	22	30
FEP-OCOC <sub>3</sub> F <sub>7</sub>	THF, Pyridine, 48 h.	15°	100	23	28	25
		75°	100	18	26	20
FEP-OCOC <sub>3</sub> F <sub>7</sub>	THF, Pyridine, 72 h.	15°	100	39	29	43
		75°	100	25	27	27
FEP-OCOC <sub>3</sub> F <sub>7</sub>	Pyridine, 48 h.	15°	100	36	16	40
		75°	100	31	15	35
FEP-OCOC <sub>3</sub> F <sub>7</sub>	Pyridine, DMAP, 48 h.	15°	100	82	23	91
		75°	100	53	20	58
FEP-OCOC <sub>3</sub> F <sub>7</sub>	THF, Pyridine, DMAP, 48 h.	15°	100	42	26	46
		75°	100	37	21	41

<sup>a</sup>calculation based on the C:F ratio relative to C<sub>3</sub>.7-OCOC<sub>3</sub>F<sub>7</sub> (C<sub>100</sub>F<sub>91</sub>O<sub>26</sub>)

resulted in no significant increase in the yield. DMAP catalysis had a significant effect on the yield; the XPS atomic composition of the product was consistent with nearly quantitative reaction in the outer 10 Å when pyridine was used as the solvent. The ATR-IR spectrum of this product (figure 11c) shows an intense heptafluorobutyrate carbonyl at  $1778\text{ cm}^{-1}$  and nearly complete disappearance of the O-H stretching band. Additional bands at 3070, 1688, and  $1645\text{ cm}^{-1}$  indicate the presence of (dimethylamino)pyridinium heptafluorobutyrate, the spectrum of which is shown in figure 13. No nitrogen was observed by XPS, indicating that this salt had been washed from the outer 40 Å. The XPS spectrum of the  $C_{1s}$  region clearly shows the presence of  $CF_3$ ,  $CF_2$  and C=O groups. Comparison of 1-3-10b with 1-3-10c clearly illustrates the increase in conversion due to DMAP catalysis. Contact angles for labeled surfaces showed an increase, as expected for adding low surface energy  $C_3F_7$  groups. Contact angles for reaction in pyridine ( $99^\circ \pm 3^\circ / 60^\circ \pm 2^\circ$ ) were essentially the same as those obtained using DMAP catalysis in pyridine ( $95^\circ \pm 3^\circ / 54^\circ \pm 2^\circ$ ), indicating that the outer surface coverage of  $C_3F_7$  groups was about the same in both cases. In addition to confirming that most of the oxygen in FEP-OH is present as hydroxyl groups, these results indicate that catalysts used to increase the yield of reactions with sterically hindered functional groups in solution may serve the same purpose for surface-confined

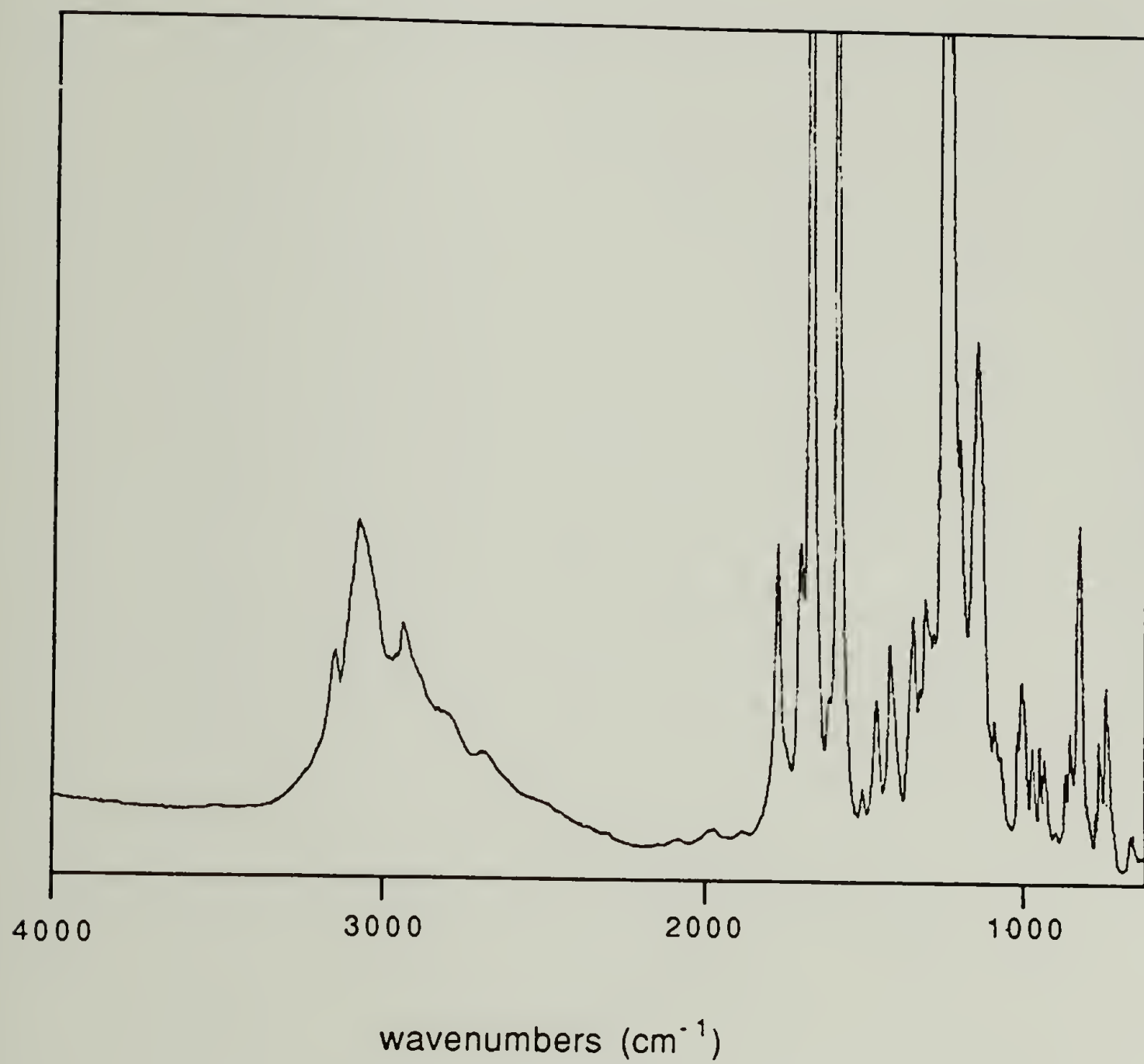


Figure 13. IR spectrum of (4-dimethylamino)pyridinium heptafluorobutyrate.

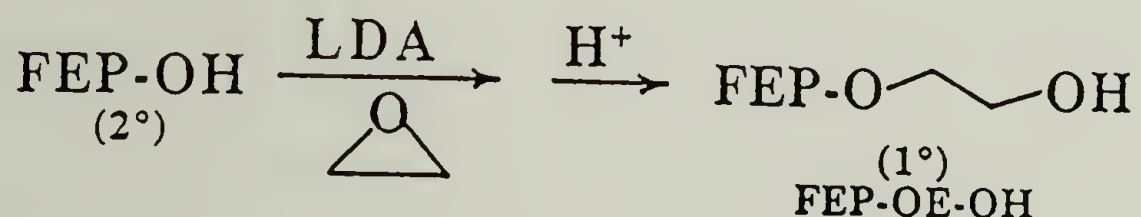


functional groups. Comparison with the results of solution acylation studies<sup>13</sup> suggests that highly hindered alcohols, such as 1-methylcyclohexanol, provide a reasonable model for the reactivity of FEP-OH.

#### Other Approaches to Hydroxylated FEP

Although hydroxyl groups were introduced in good yield by hydroboration, their low reactivity limits the usefulness of the resulting surface. Work was done aimed at converting hydroxyl groups on FEP-OH to primary groups and on the direct introduction of methylol groups to FEP-C.

FEP-OH was treated with LDA in ethylene oxide in an attempt to prepare hydroxyethyl ether surfaces according to equation 1. There are several reasons why this reaction



**Equation 1.** Reaction of FEP-OH with LDA and ethylene oxide.

may not proceed as written. Although LDA is basic enough, in principle, to quantitatively deprotonate FEP-OH, this may not occur. Other reactions, such as ring opening of ethylene oxide by LDA, may be more facile. Even if the lithium

alkoxide is formed, it may not react with ethylene oxide due to steric effects or the covalent nature of the O-Li bond; lithium alkyls generally do not polymerize ethylene oxide due to the inability of the lithium alkoxide to open the epoxide ring.<sup>14</sup> The formation of ethylene oxide oligomers cannot be ruled out; XPS cannot distinguish between primary alcohols, secondary alcohols and ethers. The XPS atomic composition data for this reaction is summarized in table 3. The carbon to oxygen ratio changes from 3.7:1 to 2.9:1, consistent with the addition of one ethylene oxide unit to each surface oxygen. The ATR-IR spectrum, shown in figure 14a, reveals a small increase in the relative intensity of the methylene absorbance. The advancing contact angle ( $50^{\circ} \pm 2^{\circ}$ ) was essentially unchanged, while the receding contact angle ( $15^{\circ} \pm 2^{\circ}$ ) decreased slightly. The white solid that was isolated from the 68 hour reaction was analyzed by FTIR. The results were consistent with  $(i\text{-Pr})_2\text{NCH}_2\text{CH}_2\text{OH}$  suggesting that ring opening had occurred and the insoluble lithium salt was isolated; protonation occurred during isolation and analysis. Addition of HFBC to the hypothetical hydroxyethyl ether surface results in a predicted composition of  $\text{C}_{100}\text{F}_{72}\text{O}_{30}$ . When the 68 hour reaction product was labeled (under conditions that minimize reaction with secondary FEP-OH hydroxyls), the composition of the product was consistent with approximately 90% acylation. ATR-IR of the product (figure 14b) revealed a substantial number of

**Table 3.** XPS atomic composition data for primary hydroxyl surfaces derived from ethylene oxide.

<u>Sample</u>	<u>Takcoff Angle</u>	<u>Carbon</u>	<u>Fluorine</u>	<u>Oxygen</u>	<u>Nitrogen</u>	<u>% Conversion</u>
FEP-C + EO (LDA, 68 h)	15° 75°	100 100	2 2	35 33	----- -----	
FEP-C + EO (LDA, 45 h)	15° 75°	100 100	7 7	31 29	----- -----	
FEP-C + EO (DBU)	15° 75°	100 100	2 1	30 27	2 2	
C <sub>3</sub> .7-OCH <sub>2</sub> CH <sub>2</sub> OH		100	-----	35	-----	
FEP-C + EO (LDA, 68 h)	15° 75°	100 100	66 62	26 28	----- -----	92 <sup>b</sup> 86 <sup>b</sup>
HFBC <sup>a</sup>						
FEP-C + EO (DBU)	15° 75°	100 100	44 40	19 20	----- -----	48 <sup>c</sup> 43 <sup>c</sup>
HFBC <sup>a</sup>						

<sup>a</sup>in THF, pyridine, 48 h.

<sup>b</sup>calculation based on the C:F ratio relative to C<sub>3</sub>.7-OC<sub>2</sub>H<sub>4</sub>OCOC<sub>3</sub>F<sub>7</sub>

<sup>c</sup>calculation based on the C:F ratio relative to C<sub>3</sub>.7-OCOC<sub>3</sub>F<sub>7</sub>



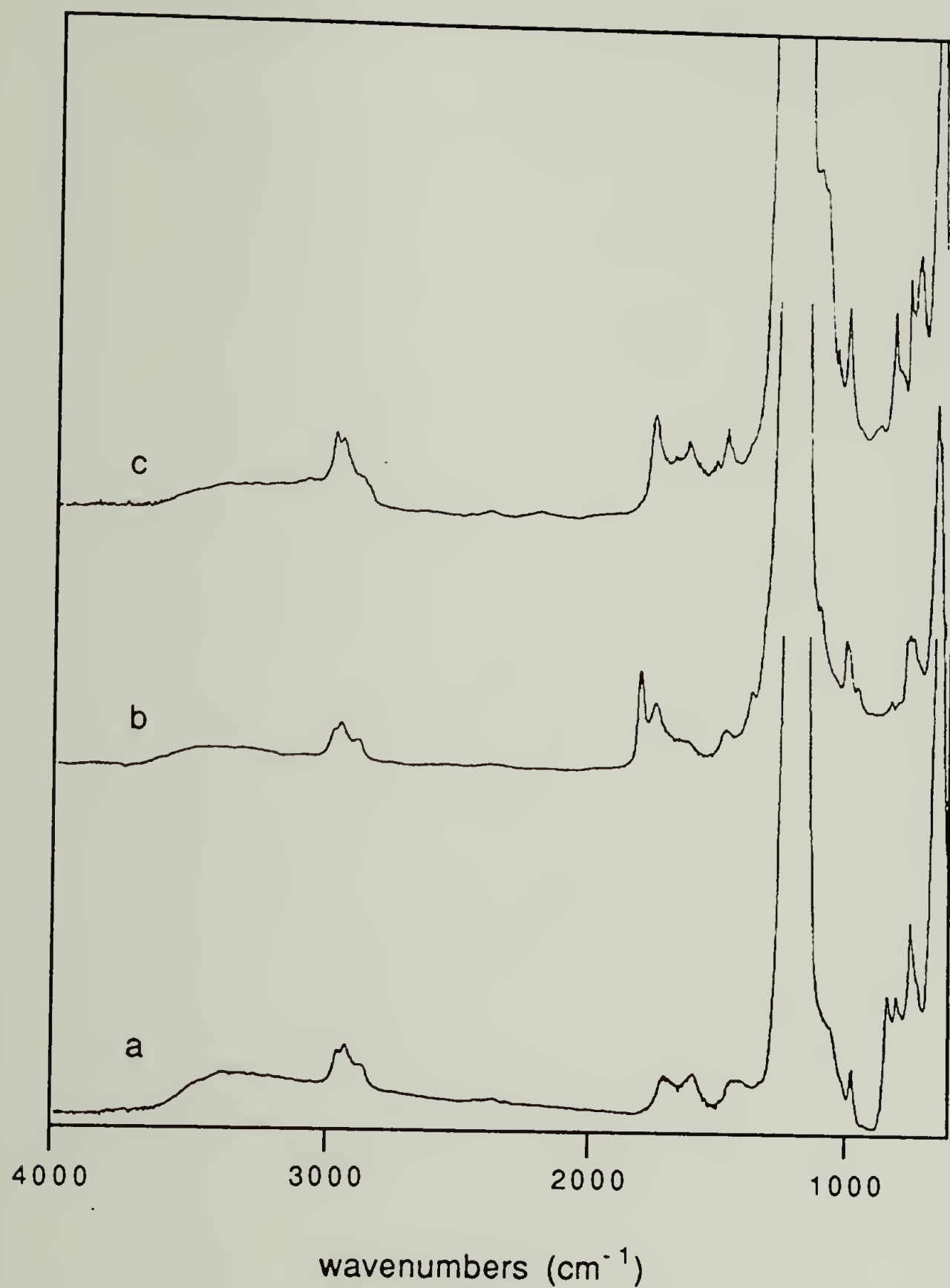


**Figure 14.** ATR-IR spectra of (a) FEP-EO-OH (b) FEP-EO-OH reacted with HFBC (c) FEP-C, reacted with BPO and methanol.

unreacted hydroxyl groups; XPS results do not represent deeper regions. These results also confirm that oligomerization was not extensive; this would have resulted in less enhancement of the reactivity as fewer primary hydroxyl groups would have been represented by the increase in oxygen. One plausible explanation for this behavior is that surface lithium alkoxides are unable to form aggregates. These aggregates have been cited as the cause for the low reactivity of lithium alkoxides<sup>15</sup>. When an ethylene oxide unit is added, enough mobility may be imparted to allow such aggregation to occur, resulting in the addition of only one ethylene oxide unit.

A similar reaction was attempted using DBU, a strong non-nucleophilic, non-ionic base. It was hoped that reaction would occur between the equilibrium concentration of surface alkoxide groups that should be generated and ethylene oxide in solution. No evidence of reaction was obtained; there was no enhancement of reactivity with HFBC for these surfaces.

An attempt was made to introduce primary hydroxyl groups in the form of methanol groups by the reaction of the eliminated surface with methylol radicals generated from methanol and benzoyl peroxide. This procedure has been reported to enhance the hydroxyl reactivity of other "carbonaceous" surfaces, namely carbon black.<sup>16</sup> The reaction results in a significant increase in oxygen by XPS, as shown

in table 4, but the ATR-IR spectrum (figure 14c) shows only a weak hydroxyl absorbance, and a strong carbonyl absorbance at  $1730\text{ cm}^{-1}$ . Reaction with HFBC (table 4) indicates that very little of this oxygen is introduced as hydroxyl groups. The ATR-IR spectrum and the labeling behavior are consistent with the introduction of benzoyloxy groups by the reaction of  $\text{PhC(=O)O}\cdot$  radicals with the surface. Hydrolysis of corresponding surfaces obtained from reaction with eliminated  $\text{PVF}_2$  generated alcohols<sup>17</sup>, confirming this explanation.

Hydroboration of olefins with 9-BBN, carbonylation and reduction<sup>18</sup> offers a potential route to a methylol surface. Reaction of the hydroboration product of 9-BBN has the potential to introduce a variety of functional groups to unsaturated surfaces<sup>19</sup>. Despite the presence of the large nonane ring, reactions with highly hindered olefins,<sup>20</sup> and olefin-containing polymers<sup>21</sup> are reported to occur in good yield, although at least one vinyl proton is required for successful carbonylation<sup>22</sup>. Hydroboration with 9-BBN was less efficient than with  $\text{BH}_3\cdot\text{THF}$ , as evidenced by the XPS results shown in table 4. Correcting for the fact that 9 carbons are associated with each boron in the 9-BBN product still gives a ratio of 1 boron per 17 surface carbons versus 1 per 10 for surfaces hydroborated with  $\text{BH}_3\cdot\text{THF}$ . The ATR-IR spectrum of the 9-BBN product (shown in figure 15) shows the expected increase in the methylene absorbance, but the intensity at  $1650\text{ cm}^{-1}$  remains high, indicating a signif-



Table 4. XPS atomic composition data for other primary hydroxyl surfaces.

<u>Sample</u>	<u>Takeoff Angle</u>	<u>Carbon</u>	<u>Fluorine</u>	<u>Oxygen</u>	<u>% Conversion</u>
FEP-C + HFBC <sup>a</sup>	15° 75°	100 100	17 15	12 12	19 17
FEP-C + BPO/MeOH	15° 75°	100 100	3 3	27 24	
FEP-C + BPO/MeOH HFBC <sup>a</sup>	15° 75°	100 100	13 10	26 22	15 <sup>b</sup> 11 <sup>b</sup>
FEP-B	15° 75°	100 100	2 2	21 21	<u>Boron</u> 10 10
FEP-9BBN (room temp.)	15° 75°	100 100	1 2	8 7	3 3
FEP-9BBN (THF reflux)	15° 75°	100 100	3 6	20 18	5.5 5.7
FEP-CH <sub>2</sub> OH	15° 75°	100 100	3 4	13 13	<u>Chlorine</u> 3 1.5
FEP-CH <sub>2</sub> OH HFBC <sup>a</sup>	15° 75°	100 100	33 29	15 14	3 1 55 <sup>c</sup> 48 <sup>c</sup>

<sup>a</sup>in THF, pyridine, 48 h.

<sup>b</sup>calculation based on the C:F ratio relative to C<sub>3</sub>.8-OCOC<sub>3</sub>F<sub>7</sub>

<sup>c</sup>calculation based on the C:F ratio relative to C<sub>7</sub>.7-OCOC<sub>3</sub>F<sub>7</sub>

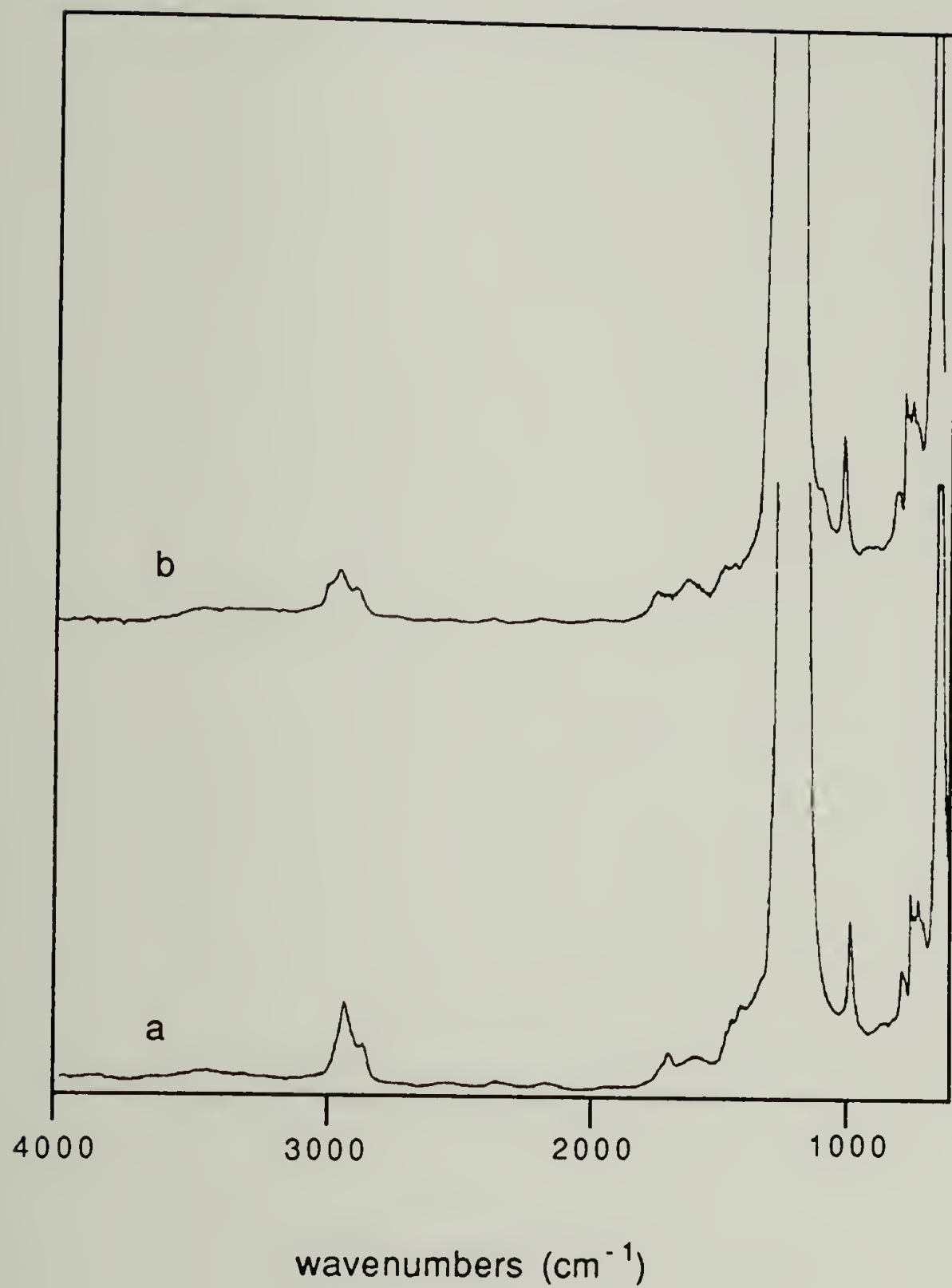


Figure 15. ATR-IR spectra of (a) FEP-9BBN (b) FEP-CH<sub>2</sub>OH.

ificant concentration of unreacted double bonds. Hydroboration in refluxing THF is reported to result in higher yields<sup>23</sup>, but oxidation of FEP-C, as evidenced by a significant increase in the O:C ratio (table 4), occurred under these conditions. As a result, room temperature hydroboration was used to prepare surfaces for carbonylation. Carbonylation and reduction with  $\text{LiAlH}(\text{OCH}_3)_3$  resulted in no significant increase in oxygen over the amount present in FEP-C (table 4) and, chlorine for some unknown reason, appeared in the XPS sampling depth, however, all of the boron was removed from the XPS sampling depth and a noticeable increase in the methylene absorbance was observed by ATR-IR, suggesting the presence of methylol groups. Reaction with HFBC revealed a significant enhancement in surface reactivity. From these results, it is unclear if carbonylation occurred as reported in the literature or if some other reaction, such as reduction by  $\text{LiAl}(\text{OMe})_3\text{H}$ , resulted in the increase in the reactivity of the surface oxygen. However, it is clear from the yield of the hydroboration step that, at best, new functional groups would be introduced in amounts comparable to the oxygen already present on the surface. As the goal of this work was to produce surfaces of single functional group reactivity, no further work was done on FEP-9BBN.



## Reaction of Hydroxyl Surfaces with Multifunctional Electrophiles

Reactions with Cyanuric Chloride. Cyanuric chloride (the cyclic trimer of cyanogen chloride) has been used extensively to introduce electrophilic sites onto carbon and metal oxide surfaces<sup>24</sup>. Despite the rather low electrophilicity of cyanuric chloride<sup>25</sup> and the low nucleophilicity of these surfaces, extensive surface coverage has been reported.<sup>26</sup> Subsequent reactions with nucleophiles suggest that, on average, one of the three electrophilic sites remains unreacted.<sup>27</sup> Table 5 summarizes the XPS atomic composition results for the reactions of FEP-OH and PCTFE-OH with cyanuric chloride. Relatively little reaction occurred by XPS; no significant increase in high binding energy carbon was observed<sup>28</sup> and no significant changes were observed by ATR-IR for reactions in benzene. Reaction in THF seemed to result in dissolution of the modified layer; the C-H and O-H absorbances disappeared. This was particularly surprising for FEP-OH, since crosslinking was expected to occur, stabilizing the modified layer. Cyanuric chloride reacted with pyridine to yield an insoluble product.<sup>29</sup> One explanation that accounts for these results is the ability of cyanuric chloride to form polymeric species.<sup>30</sup> These graft surfaces may be soluble in THF. Reaction with cyan-

**Table 5.** XPS atomic composition data for reaction with cyanuric chloride.

<u>Sample</u>	<u>Solvent</u>	<u>Takeoff Angle</u>	<u>C</u>	<u>F</u>	<u>O</u>	<u>N</u>	<u>Q</u>	<u>% Conversion<sup>a</sup></u>
FEP-OH	THF	150°	100	3	27	7.1	2.4	24
		750°	100	7	26	7.3	1.6	24
PCTFE-OH	THF	150°	100	26	34	5	6.7	23
		750°	100	26	27	4	2.9	19
FEP-OH	benzene	150°	100	3	27	3.6	1.3	(4.8 Si)
		750°	100	3	27	3.6	1.3	
PCTFE-OH	benzene	150°	100	27	25	1.5	1	7
		750°	100	37	19	0.6	6	2
FEP-OH	pyridine	150°	100	2	28	9.5	0.7	2
		750°	100	2	29	7	0.7	2

<sup>a</sup>calculation based on the N:C ratio, assuming difunctional reaction  
 FEP-OH: C100O20N29Cl9.5  
 PCTFE-OH: C100F21O21N31Cl10

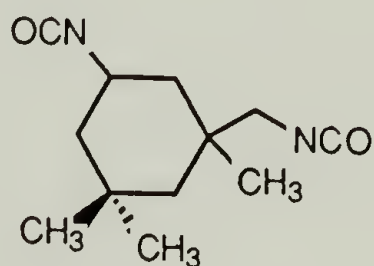
uric chloride does not appear to be a practical way to introduce electrophilic sites to hydroxyl film surfaces.

Reactions with Diisocyanates. Reactions with diisocyanates possessing isocyanate groups of substantially different reactivity have not been investigated as extensively as a means of introducing electrophilic sites to surfaces, but this approach has been commonly used to produce telechelic isocyanates from telechelic diols.<sup>31</sup> Earlier work in this group has shown that hexamethylene diisocyanate, a flexible diisocyanate with roughly equal reactivity of both isocyanate groups, reacts difunctionally with PCTFE-OH<sup>32</sup>. Difunctional reaction may have been facilitated by the mobility of hydroxyl groups (attached to the backbone by a three methylene chain) on this surface. PCTFE-OH and FEP-OH surfaces were reacted with two different diisocyanates, isophorone diisocyanate (IPDI) and 2,4-toluene diisocyanate (TDI); FEP-OH was reacted with hexamethylene diisocyanate for comparison. Diisocyanates have a number of advantages over diacid chlorides. The extent of reaction of isocyanate groups can be easily followed by ATR-IR due to their intense absorbance at 2270-2275 cm<sup>-1</sup> and their reactivity can be increased over a thousand-fold using organotin compounds<sup>33</sup>, which cannot reduce PCTFE the way some amine bases can. Although reactions between isocyanate groups, (to form the cyclic trimer) and between isocyanates



and urethane (carbamate) groups (to form the allophanate) are known, these reactions tend to be suppressed in the presence of organotin catalysts.<sup>34</sup> Reactions with a number of nucleophiles were performed to determine the reactivity of isocyanate groups on the resulting surfaces.

Isophorone diisocyanate, shown below, is often used when differential reactivity is required<sup>35</sup>. Table 6



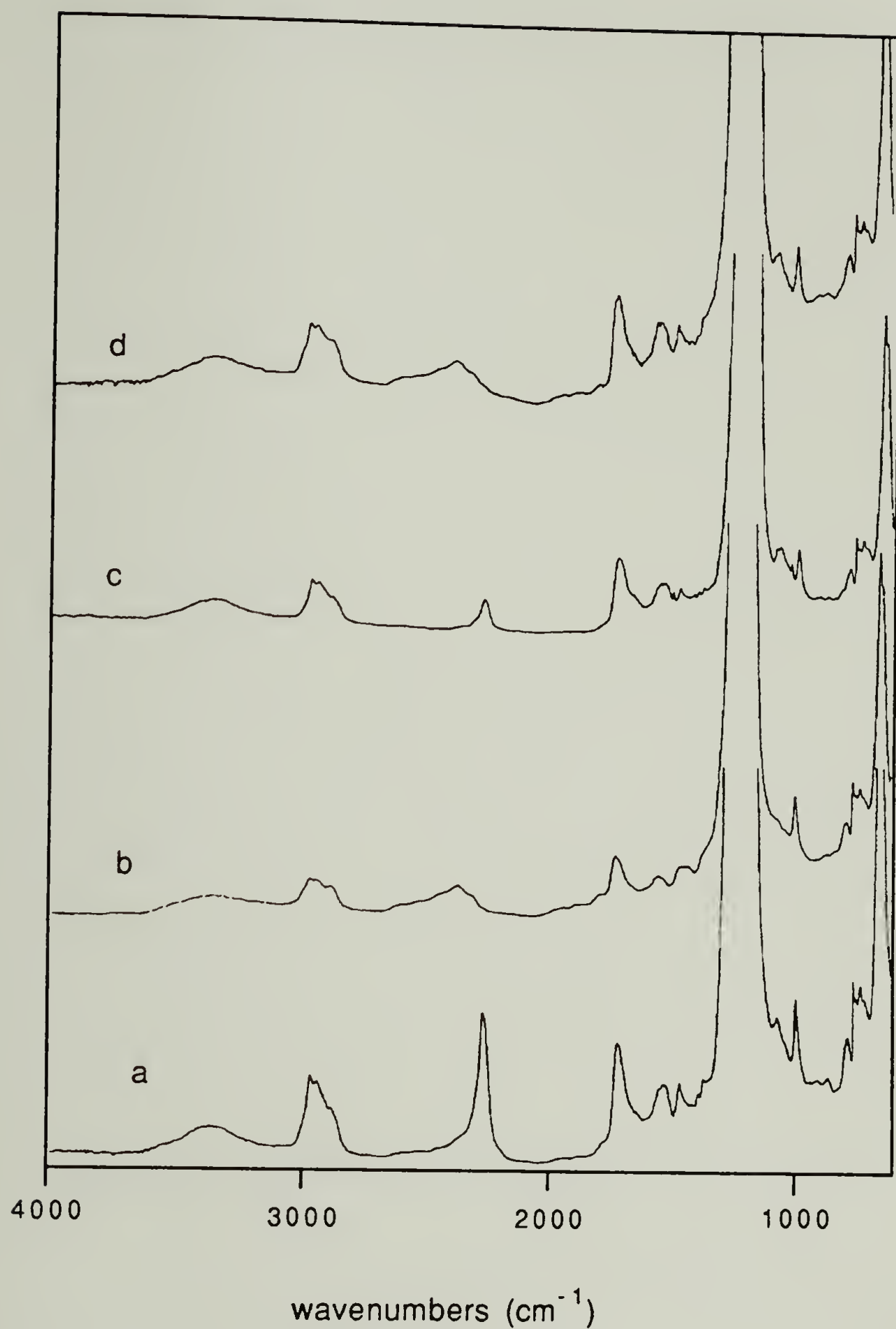
summarizes the XPS atomic composition data for reactions of the hydroxyl surfaces with IPDI in the presence of dibutyl tin dilaurate. Extensive reaction occurred for both surfaces. Although the reaction with PCTFE-OH was more extensive, unlike most previous reactions with PCTFE-OH, the reaction was not quantitative. Increasing the dibutyl tin dilaurate concentration and the reaction time had no effect on the yield for reaction with PCTFE-OH. Adding DABCO as a co-catalyst<sup>36</sup> resulted in only a marginal increase in the extent of reaction with FEP-OH. The ATR-IR spectrum of FEP(IPDI)-NCO shown in figure 16 supports primarily mono-functional reaction. Reaction with IPDI results in both carbamate (at  $1714\text{ cm}^{-1}$ ), N-H ( $\alpha$  to C=O, at  $1540\text{--}1520\text{ cm}^{-1}$ ) and isocyanate (at  $2262\text{ cm}^{-1}$ ) absorbances, as well as an

Table 6. XPS atomic composition data for reaction with isophorone diisocyanate.

Sample	Catalyst	Label	Takeoff Angle	C	F	O	N	Br	% Conversion <sup>a</sup>
FEP-OH	dBSndL	-----	15°	100	1	24	6.7	--	56 <sup>a</sup>
			75°	100	2	25	5.5	--	44 <sup>a</sup>
FEP-OH	dBSndL	BrPrOH	15°	100	3	26	3.8	1.9	100 <sup>c</sup>
			75°	100	8	25	3.6	1.9	100 <sup>c</sup>
PCTFE-OH	dBSndL 24 h.	-----	15°	100	10	12	9	--	80 <sup>b</sup>
			75°	100	10	12	9	--	80 <sup>b</sup>
PCTFE-OH	dBSndL 24 h.	BrPrOH	15°	100	12	14	9	.8	17 <sup>c</sup>
			75°	100	12	15	10	1	20 <sup>c</sup>
FEP-OH	dBSndL DABCO	-----	15°	100	2	25	9.5	--	75 <sup>a</sup>
			75°	100	2	17	6.7	--	53 <sup>a</sup>
FEP-OH	dBSndL DABCO	BrPhEtOH	15°	100	23	16	5.4	0.7	13 <sup>c</sup>
			75°	100	26	17	4.3	0.7	16 <sup>c</sup>
PCTFE-OH	dBSndL 48 h.	-----	15°	100	9	20	9	--	80 <sup>b</sup>
			75°	100	9	16	8	--	75 <sup>b</sup>

calculation based on the N:C ratio, assuming: <sup>a</sup>C<sub>100</sub>O<sub>18</sub>N<sub>12</sub>; <sup>b</sup>C<sub>100</sub>F<sub>8</sub>O<sub>17</sub>N<sub>11</sub>

<sup>c</sup>calculation based on the N:Br ratio; 2:1 indicating complete reaction



**Figure 16.** ATR-IR spectra of (a) FEP(IPDI)-NCO and FEP(IPDI)-NCO reacted with (b) BrPrOH (c) BrPhEtOH (d) BrPhEtOH and MeOH.



increase in the intensity of the methyl and methylene absorbances. A significant absorbance is present in the hydroxyl region ( $3300\text{--}3500\text{ cm}^{-1}$ ). It should be noted that the N-H stretching band in carbamates generally appears at  $3335\text{ cm}^{-1}$ , but is much sharper. This band most likely contains contributions due to both N-H and O-H stretching. Similar results were obtained for the reaction of PCTFE-OH with IPDI (figure 17) but the  $\sim 3300\text{ cm}^{-1}$  absorbance is significantly less intense.

Table 6 summarizes the XPS atomic composition data for the reactions of these surfaces with nucleophiles. The XPS atomic composition data suggests that FEP(IPDI)-NCO reacts quantitatively with 3-bromo-1-propanol in the outer 40 Å. The ATR-IR spectrum of this surface (figure 16b) suggests that the reaction was nearly complete throughout the modified region; the isocyanate absorbance appears to have vanished, although a weak absorbance may be hidden in the shoulder of the overtone band. The use of a less reactive nucleophile, 4-bromophenylethyl alcohol, resulted in incomplete reaction in the outer 40 Å, as evidenced by the XPS atomic composition, and throughout the modified region, as evidenced by the persistence of the isocyanate band in the ATR-IR spectrum (figure 16c). Subsequent treatment of this surface with methanol in the presence of dibutyl tin dilaurate (figure 16d) resulted in the disappearance of this absorbance, suggesting that carbamates were formed from the

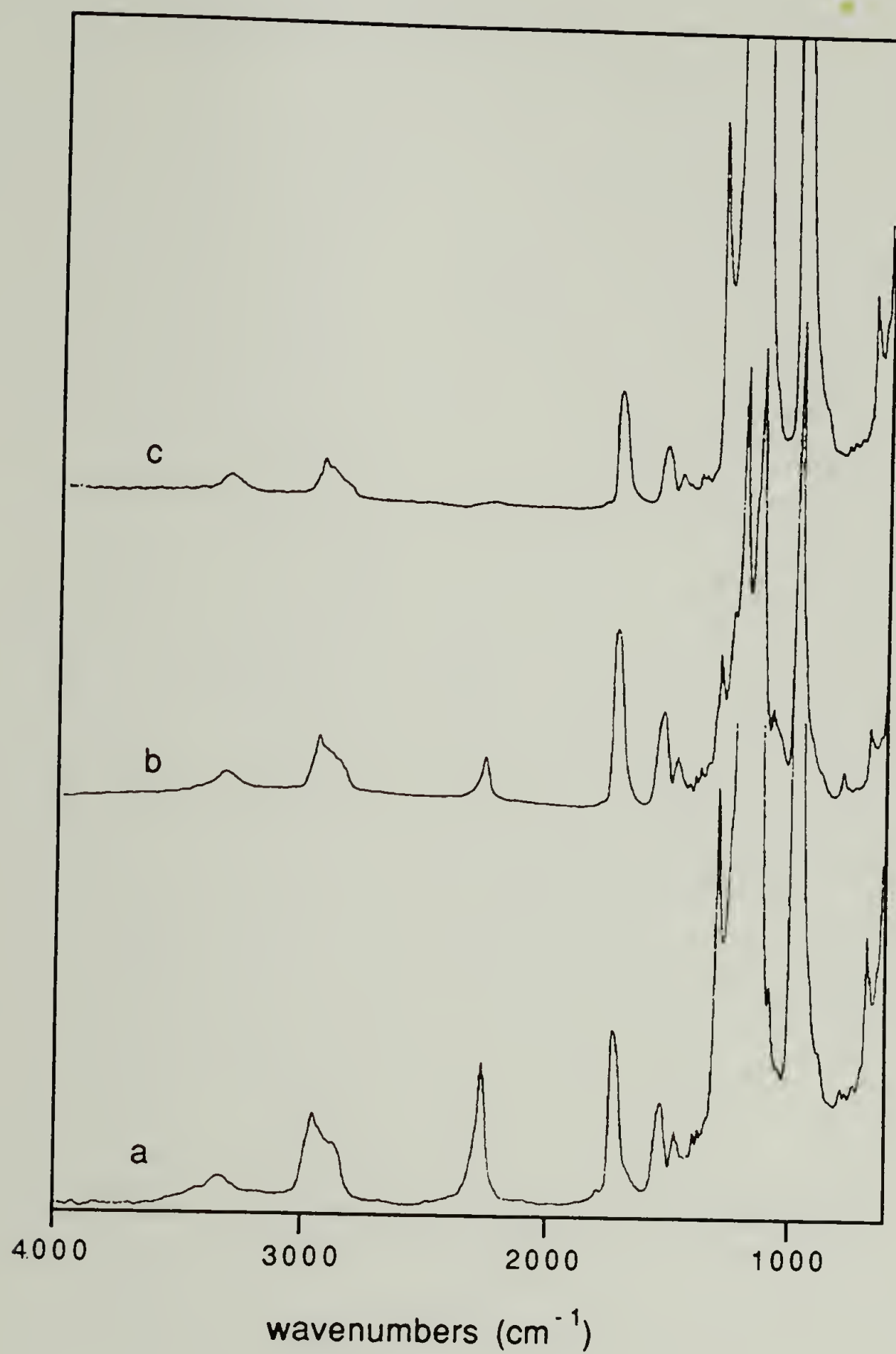


**Figure 17.** ATR-IR spectra of (a) PCTFE(IPDI)-NCO and PCTFE(IPDI)-NCO reacted with (b) BrPrOH (c) MeOH.

remaining isocyanates. Some hydrolysis of isocyanates, resulting in primary amines ( $3350\text{ cm}^{-1}$  and  $1615\text{ cm}^{-1}$ ) cannot be ruled out. Much less reaction occurred between 3-bromo-1-propanol and PCTFE(IPDI)-NCO surfaces, as evidenced by the XPS atomic composition data (summarized in table 6) and the persistence of the isocyanate absorbance (figure 17b).

Treatment of the isocyanate surface with methanol (figure 17c) also resulted in disappearance of the isocyanate band.

FEP-OH and PCTFE-OH surfaces were also reacted with TDI. The reactivity difference between the two different isocyanate groups of this reagent is significantly smaller; the isocyanate in the 2 position is reported to be approximately 25 times less reactive<sup>37</sup>. Aryl isocyanates are also expected to be somewhat more reactive than alkyl isocyanates, although the difference becomes less pronounced when organotin catalysts are used<sup>38</sup>. Table 7 summarizes the XPS atomic composition data. The extent of reaction of TDI with both surfaces was comparable to that observed for the reaction with IPDI. Similar trends were observed by ATR-IR as well. Bands due to the isocyanate stretch ( $2274\text{ cm}^{-1}$ ), urethane carbonyl ( $1722\text{ cm}^{-1}$ ), N-H ( $\alpha$  to C=O,  $1530\text{ cm}^{-1}$ ) and aromatic C=C bands ( $1590\text{--}1650\text{ cm}^{-1}$ ) were observed after the reaction of FEP-OH (figure 18) and PCTFE-OH (figure 19) with TDI. XPS and ATR-IR results for the reactions of isocyanate surfaces derived from FEP-OH suggest nearly quantitative reaction occurred with 3-bromo-1-propanol and incomplete



**Table 7.** XPS atomic composition data for reaction with  
toluene diisocyanate.

Sample	Catalyst	Label	Takeoff Angle	C	F	O	N	Br	% Conversion <sup>a</sup>
FEP-OH	dBSndL	-----	15°	100	3	33	3.7	--	23 <sup>a</sup>
			75°	100	3	28	3.5	--	20 <sup>a</sup>
FEP-OH	dBSndL	BrPrOH	15°	100	2	31	3.9	1.5	100 <sup>c</sup>
			75°	100	2	28	3.2	1.6	100 <sup>c</sup>
PCTFE-OH	dBSndL 24 h.	-----	15°	100	13	17	12	--	86 <sup>b</sup>
			75°	100	12	16	12	--	86 <sup>b</sup>
PCTFE-OH	dBSndL 24 h.	BrPrOH	15°	100	16	25	11	1	20 <sup>c</sup>
			75°	100	14	24	11	.9	18 <sup>c</sup>
FEP-OH	dBSndL DABCO	-----	15°	100	10	24	11	--	65 <sup>a</sup>
			75°	100	15	16	9	--	52 <sup>a</sup>
FEP-OH	dBSndL DABCO	BrPhEtOH	15°	100	1	24	10	1	25 <sup>c</sup>
			75°	100	1	24	10	0.9	25 <sup>c</sup>
PCTFE-OH	dBSndL 48 h.	-----	15°	100	11	22	11	--	80 <sup>b</sup>
			75°	100	12	20	12	--	85 <sup>b</sup>

calculation based on the N:C ratio, assuming: <sup>a</sup>C<sub>100</sub>O<sub>25</sub>N<sub>16</sub>; <sup>b</sup>C<sub>100</sub>F<sub>10</sub>O<sub>21</sub>N<sub>14</sub>  
<sup>c</sup>calculation based on the N:Br ratio; 2:1 indicating complete reaction

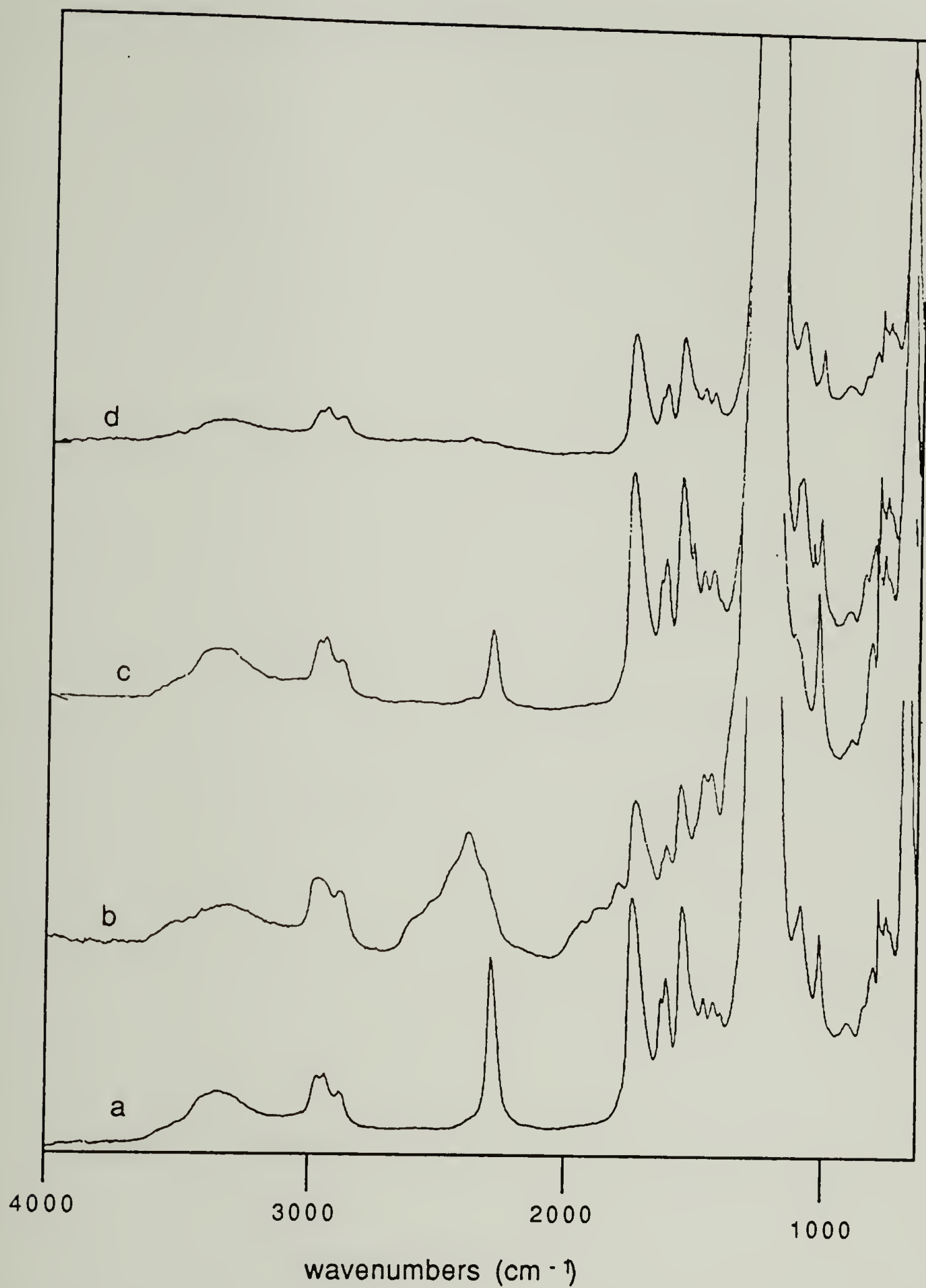


**Figure 18.** ATR-IR spectra of (a) FEP(TDI)-NCO and FEP(TDI)-NCO reacted with (b) BrPrOH (c) BrPhEtOH (d) BrPhEtOH and MeOH.

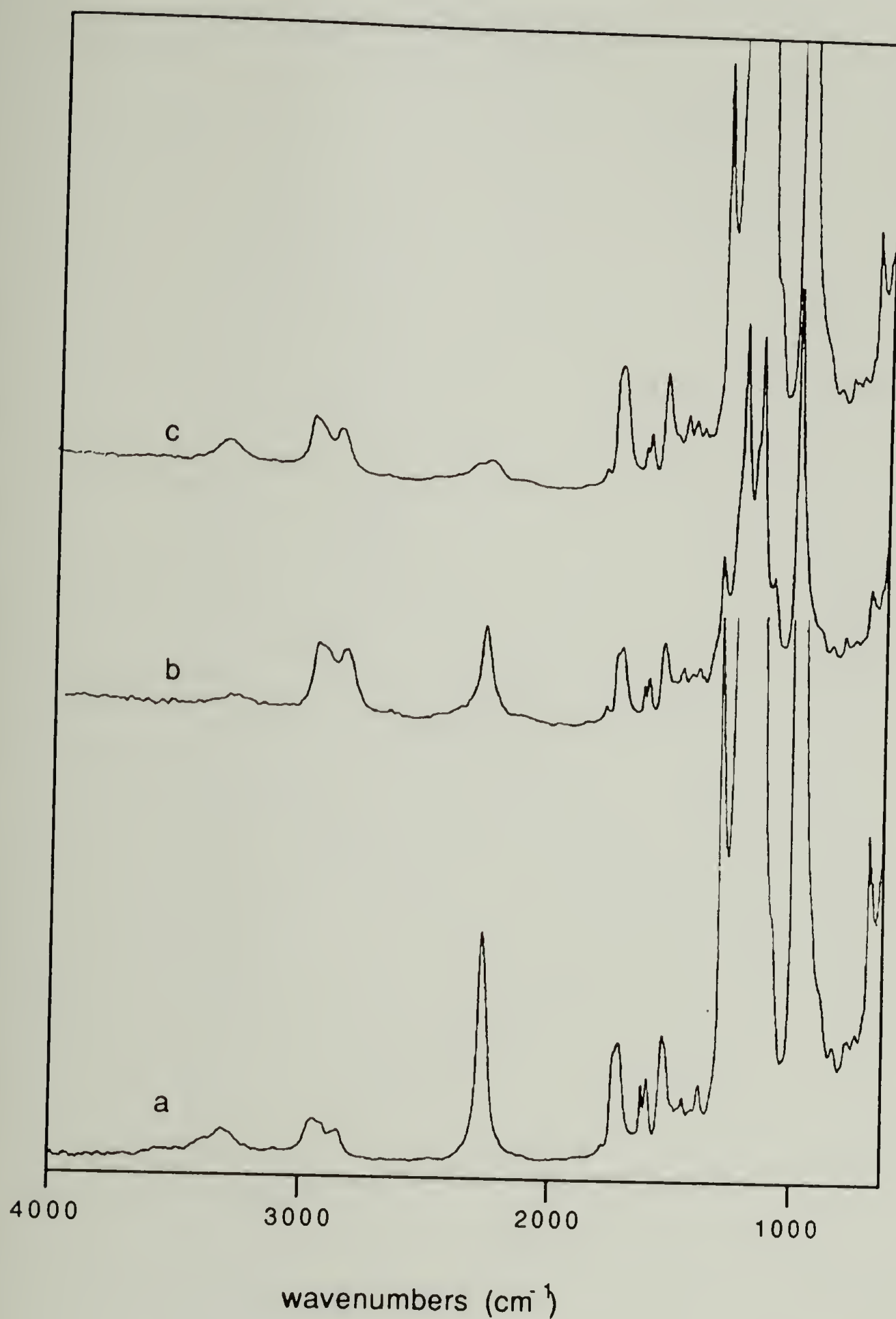


**Figure 19.** ATR-IR spectra of (a) PCTFE(TDI)-NCO and PCTFE(TDI)-NCO reacted with (b) BrPrOH (c) MeOH.



reaction occurred with 4-bromophenylethyl alcohol. The remaining isocyanate groups appeared to react with methanol. PCTFE(TDI)-NCO surfaces reacted poorly with 3-bromo-1-propanol, but appeared to react quantitatively with methanol.

Taken together, these results suggest that factors related to the film and/or film-reagent interface are more important for determining the extent of reaction than the identity of the diisocyanate. The extent of reaction of both IPDI and TDI with surface hydroxyls was about the same for a given film, and, as expected, both reacted more extensively with PCTFE-OH. Similar behavior was observed for subsequent reactions of the surface-bound isocyanates. Although the remaining isocyanate group in IPDI is expected to be considerably less reactive than the corresponding group in TDI, the yields were independent of the choice of isocyanate for a given film. What was surprising was the low reactivity of the isocyanate groups on PCTFE-OH. Although unreacted isocyanate groups were undoubtedly present, the occurrence of some crosslinking via difunctional reaction cannot be ruled out. The increased rigidity of the modified surface would account for the decreased reactivity, although, it seems unusual that such a profound effect would be manifest in the outer 10 Å.

The reaction of FEP-OH with hexamethylene diisocyanate (HMDI) appeared to result in a mixture of monofunctional and difunctional reaction. In addition, reaction appeared to be

confined primarily to the outer 40 Å. The XPS atomic composition of the product leads to an empirical formula of  $C_{100}F_1O_{34}N_5$  at a 15° takeoff angle and  $C_{100}F_3O_{31}N_{4.4}$  at a 75° takeoff angle. Labeling of this product with 3-bromo-1-propanol resulted in an atomic composition represented by  $C_{100}F_2O_{34}N_{3.4}Br_{0.6}$  at a 15° takeoff angle and  $C_{100}F_5O_{32}N_{2.5}Br_{0.7}$  at a 75° takeoff angle. These results suggest 35% monofunctional reaction at approximately 10 Å and 56% at approximately 40 Å. However, no changes could be observed by ATR-IR. It seems probable that crosslinking of the surface by HMDI units sealed off the surface to further reaction.

## References

1. Costello, C.A.; McCarthy, T.J. *Macromolecules* **1987**, *20*, 2819.
2. Dias, A.J.; McCarthy, T.J. *Macromolecules* **1984**, *17*, 2529.
3. Dias, A.J.; McCarthy, T.J.; *Macromolecules* **1985**, *18*, 1826.
4. See reference 1.
5. See reference 1.
6. Methine in  $\alpha, \alpha, \alpha', \alpha', 2, 3, 5, 6$ -octachloro-p-xylene absorbs at  $2940\text{ cm}^{-1}$ .
7. Ha, K.; Garton, A. *Polym. Preprints (Am. Chem. Soc., Div. Polym. Chem.)* **1990**, *31(1)*, 326.
8. Costello, C.A. Ph.D. dissertation pp 90-101.
9. Dwight, D.W.; Riggs, W.J. *J. Colloid Interface Sci.* **1974**, *47*, 650.
10. See reference 1.
11. Lee, K.-W.; McCarthy, T.J. *Macromolecules* **1988**, *21*, 2318.
12. See reference 11.
13. Steglich, W.; Höfle, G. *Angew. Chem. Intern. Ed.* **1969**, *8*, 981.
14. Quirk, R.P.; Seung, N.S. In *Ring Opening Polymerization*, McGrath, J.E. ed.; ACS Symposium Series 286: Washington DC, 1985.
15. Halaska, V.; Lochmann, L.; Lim, D. *Coll. Czech. Chem. Commun.* **1968**, *23*, 3245.
16. Tsubokawa, N.; Fujiki, K.; Sone, Y. *J. Polym. Sci., Polym. Chem. Ed.* **1986**, *24*, 191.
17. Brennan, J. unpublished results, this laboratory.
18. Brown, H.C.; Knights, E.F.; Coleman, R.A. *J. Am. Chem. Soc.* **1969**, *91*, 2144.



19. Cragg, G. *Organoboranes in Organic Synthesis*, Dekker: New York, 1973.
20. Knights, E.F.; Brown, H.C. *J. Am. Chem. Soc.* **1968**, *90*, 5281.
21. Ramakrishnan, S.; Berluche, E.; Chung, T.C. *Macromolecules* **1990**, *23*, 378.
22. See reference 18.
23. Lane, C.F.; Brown, H.C. *J. Organometal. Chem.* **1971**, *26*, C51.
24. Murray, R.W. *Electroanal. Chem.* **1984**, *13*, 191.
25. Smolin, E.M.; Rapapport, L. *S-Triazenes and their Derivatives*, Interscience Pub.: New York, 1959.
26. Yacynych, A.M.; Kuwana, T. *Anal. Chem.* **1978**, *50*, 640.
27. Tse, D.C.S.; Kuwana, T.; Royer, G.P. *J. Electroanal. Chem.* **1979**, *98*, 345.
28. See reference 26, p 643.
29. A similar reaction was reported to occur in wet pyridine, see Saure, S. *Chem. Ber.* **1950**, *83*, 335.
30. Dautartas, M.F.; Evans, J.F.; Kuwana, T. *Anal. Chem.* **1979**, *51*, 104.
31. For example, see Allen, W.T.; Eaves, D.E. *Angew. Makromol. Chem.* **1977**, *58/59*, 321.
32. See reference 11.
33. Reegen, S.L.; Frisch, K.C. In *Advances in Urethane Science and Technology*, vol. 1, Frisch, K.C.; Reegen, S.L. eds., Technomic Pub. Co.: Stamford Conn., 1971, Chapter 1.
34. Wong, S.-W.; Frisch, K.C. In *Advances in Urethane Science and Technology*, vol. 10, Frisch, K.C.; Klempner, D. eds., Technomic Pub. Co.: Stamford Conn., 1987, pp 49-75.
35. Holubka, J.W. *Reactive Oligomers*, ACS Symposium Series 282, American Chemical Society: Washington DC, p 117.
36. See reference 33.



37. Ferstandig, L.L.; Scherrer, R.A. *J. Am. Chem. Soc.* **1959**, *81*, 4838.
38. Farkas, A.; Mills, G.A. In *Advances in Catalysis* vol 13, Eley, D.D.; Selwood, P.W.; Weisz, P.B. eds., Academic Press: New York, 1962, pp 419-425.

## CHAPTER IV

### CONCLUSIONS AND SUGGESTIONS

The research presented in this section has extended the knowledge of fluorocarbon surface modification and organic surface chemistry into a number of new areas. In the first part of this work, the details of reductive surface modification were studied for poly(tetrafluoroethylene-co-hexafluoropropylene) (FEP), a fluoropolymer whose chemical composition is similar to that of Teflon (PTFE), but differs substantially in crystallinity. This was found to have a number of effects on the surface modification kinetics and the structure of the reduced layer. The proper choice of reaction time and temperature for reduction with sodium naphthalide in THF produced modified layer depths in the ranges of 45-90 Å and 250-800 Å. Reaction depths of less than 150 Å could not be reproducibly obtained by reduction of PTFE with benzoin dianion. In addition, the surface selectivity of the reduction was substantially improved. Surfaces with average modification depths as shallow as 45 Å contained no  $\text{CF}_2/\text{CF}_3$  in the outer 10 Å. While the chemical composition of the reduced layer was generally similar to benzoin dianion-reduced PTFE, a number of significant differences were observed. FEP-C lacked the metallic gold appearance associated with PTFE-C (even when FEP was reduced with benzoin dianion) and exhibited substantially decreased

conjugation, as evidenced by UV-vis spectroscopy. In addition, ATR-IR spectroscopy revealed no  $\text{sp}^2$  C-H.

Spectroscopic results revealed that the surface of FEP-C is chemically complex. In addition to unsaturation ( $\text{C}=\text{C}$ ,  $\text{C}\equiv\text{C}$ ), the presence of oxygen-containing functional groups ( $\text{OH}$ ,  $\text{C}=\text{O}$ ) could not be avoided. Hydroboration, followed by basic peroxide work up, resulted in a surface containing hydroxyl groups as the major reactive functionality. Consideration of the structure of the reduction products predicts that most of these groups will be secondary and attached directly to the polymer backbone. Solution chemistry suggests that these groups will be very difficult to acylate, and this was found to be the case. As in acylation reactions in solution, catalysis with DMAP was found to increase the yield substantially. Surfaces containing primary hydroxyl groups separated from the polymer backbone are known to be easily acylated. As a result, attempts were made to introduce primary hydroxyl groups to FEP. When FEP-OH film samples were treated with LDA in ethylene oxide, these conditions appeared to result in a surface containing both primary and secondary hydroxyl groups. Hydroboration with 9-BBN appears to be a viable way to introduce functional groups to the eliminated surface, however, yields are low. The number of new functional groups expected to be introduced is comparable to the number of oxygen-containing functional groups already present in FEP-C.

Reaction with an appropriate multifunctional electrophile is a viable way to produce electrophilic surfaces from nucleophilic (hydroxyl) surfaces. FEP-OH and PCTFE-OH reacted in high yield with both TDI and IPDI when the appropriate catalysts were employed, however, not even PCTFE-OH reacted quantitatively. Surprisingly the remaining isocyanate groups on both FEP-OH-derived surfaces were much more reactive than those on PCTFE-OH-derived surfaces; no significant difference due to the choice of isocyanate was observed. Only small, reactive nucleophiles (methanol) appear to react quantitatively with isocyanate surfaces derived from PCTFE-OH. One possible explanation for this is that crosslinking due to multifunctional reaction occurs, decreasing reagent access to the surface, although it is not clear that this should effect the outer 10 Å enough to account for the observed results.

Research in this group has resulted in a number of functionalized surfaces that approach, to varying degrees, a uniform distribution of a well defined organic functional group in a layer of uniform and precisely defined dimensions on a chemically inert surface. Surfaces prepared from FEP-C have a number of advantages, including a fairly well defined and uniform modified layer thickness and a highly inert substrate (compared to PCTFE, for example). Where these properties are desirable, FEP-C and surfaces derived from modification of FEP-C will be of great utility. Hydroboration



introduces hydroxyl groups to this surface in good yield, however, the reactivity of these groups is low, compared, for example, to PCTFE-OH. The unavoidable presence of OH and C=O groups also compromises the utility of the FEP-C surface. Some further applications of these materials have been developed and are discussed in the next section of this thesis.

The work described here only begins to address the surface structure-reactivity properties of modified polymer surfaces. A great deal more quantitative work remains to be done in this area. In addition, the contribution that these and other model surfaces produced in this group can make to elucidating surface structure-physical properties relationships has yet to be realized. These surfaces provide excellent substrates for studying the effect of chemical and physical structure (layer thickness, rigidity) on interfacial phenomena such as friction, adhesion, and adsorption.

PART II  
SURFACE INITIATED GRAFT POLYMERIZATION

## CHAPTER V

### INTRODUCTION

It would be desirable for a variety of applications to graft polymer chains to the surface of another, chemically dissimilar, polymer. In addition to providing an alternate way to modify the chemical composition and surface energy of the polymer surface, graft polymerization has the potential to modify the mechanical properties of the interface in a controlled way. While the majority of the research in this area has focused on introducing graft polymers to lower the thrombogenic activity of surfaces used in biomedical applications,<sup>1</sup> graft polymerizations have also been studied as a means of improving the adhesion of fibers and particulate fillers to polymer matrices<sup>2</sup>. In addition, surfaces in which the chains are covalently attached have value as model systems for studying the dynamics of chains at polymer-solvent interfaces. In principle, a variety of solvent and temperature conditions could be studied that would result in desorption of polymers from the interface if non-covalent interactions alone anchored the chains to the surface.

An ideal system would result in: (1) Complete coverage of the polymer substrate with a graft polymer overlayer of uniform thickness, (2) a sharp interface between the polymer substrate and the graft polymer layer, (3) the introduction of well defined (low polydispersity, no crosslinking or branching) polymer molecules of controlled molecular weight.

Two general strategies for introducing graft polymers to polymer surfaces have been used. The most common procedure involves polymerization from initiator sites generated by relatively non-specific reactions of the polymer film substrate. In most cases, monomers are polymerized by radicals resulting from bombardment of the surface with ionizing radiation. In general, well defined polymer overlayers are not formed. Radicals are generated deep within the polymer substrate, generally resulting in a diffuse interface between the graft polymer and the substrate. In addition, radical polymerizations offer little control over the molecular weight and suffer from a variety of side reactions. Coupling reactions result in crosslinking of both the substrate and the graft polymer. Chain transfer results in solution polymerization of the monomer and, if the surface is swollen by the monomer, may result in the formation of polymer chains that are entrapped in, rather than grafted to, the interface region<sup>3</sup>. Graft polymerizations have also been reported in which the graft polymers are introduced to unsaturated surfaces (produced by the reduction of PTFE) by chain transfer of the polymer radical to the surface. While control of the reduced layer thickness allowed control of the thickness of the interface region, the efficiency of grafting was low; little polymer was added to the surface<sup>4</sup>. Radical polymerizations have also been initiated on surfaces using chemically-generated radicals. Radicals generated by



the oxidation of alcohol groups on carbon black surfaces<sup>5</sup> and urethane groups on poly(ether urethane)<sup>6</sup> surfaces with ceric ions have been used initiate the polymerization of acrylamide and hydroxyacrylate monomers. While these conditions offer somewhat more control over the initiation site, the reaction still allows no control over the molecular weight and the polydispersity of the product is expected to be relatively high. It was also unclear from these data if uniform coverage of the polymer surface had occurred.

An alternative that has received less attention is the reaction of functional group-terminated polymers with polymer surfaces. This strategy has the advantage of allowing substantial control over the molecular characteristics of the graft polymer. In one recent study, (polystyrylthio)-lithium was shown to react with poly(chlorotrifluoroethylene) in THF to produce a graft polymer surface. The thickness of the modified layer could be controlled by changing the reaction time and temperature. Under the appropriate conditions, surfaces could be produced that contained predominately polystyrene in the outer 3000 Å. The reaction resulted in a very rough surface and the sharpness of the PCTFE-PS interface was difficult to determine from the data<sup>7</sup>.

The research that will be discussed in the following sections represents a refinement of the "grafting from" procedure for preparing graft polymer surfaces. The objec-

tive of this work was to extend the knowledge of the functionalization of chemically-resistant polymers to include the introduction of functional groups capable of initiating polymerization from polymer surfaces and to identify systems that could be used to produce a relatively thick, uniform graft polymer overlayer. Chemically resistant polymer surfaces were chosen in order to minimize problems with swelling and reaction of the polymer substrate. There are a number of potential problems with this approach. A very small number of initiator species are expected to be present (on the order of picomoles). Termination by adventitious impurities is expected to be unusually difficult to avoid. In addition, very high local chain concentrations are expected to be present early in the reaction. Intermolecular reactions that tend to be important only in the later stages of polymerization may occur throughout the reaction. In many cases, these reactions lead to chain degradation as well as crosslinking and branching. An ideal system would allow the surface-selective introduction of the initiator species to the polymer surface. The resulting initiator surface would be stable enough to isolate and characterize. Initiation would be rapid and quantitative; polymerization would be fast, living, tolerant of protic impurities and occur under mild conditions. No polymerization mechanism satisfies all of these requirements perfectly. Systems were chosen for study that satisfied one or more of these re-

quirements. A number of polymerizations were studied. Of these, cationic ring opening polymerization of tetrahydrofuran (THF) by triflate groups generated by the reaction of halogenated precursor surfaces with silver triflate gave results that were closest to ideal. The polymer surface was covered to a depth of at least 40 Å with poly(THF); ATR-IR results suggested that the average depth was substantially greater. Taken together, the results of this study help to identify characteristics of the polymerization reaction and the initiator surface that are most conducive to successful surface-initiated graft polymerization.

## References

1. Britton, R.A.; Merrill, E.W.; Gilland, E.R.; Salzman, E.W.; Austen, W.G.; Kemp, D.S. *J. Biomed. Mater. Res.* **1968**, *2*, 429.
2. Donnet, J.-B.; Bansal, R.C. *Carbon Fibers*, Marcel Dekker: New York, 1984.
3. Ward, W.J.; McCarthy, T.J. In *Encyclopedia of Polymer Science and Engineering*, 2nd. ed; Supplement, Wiley: New York, 1989, pp 678-680.
4. Miller, M.L.; Postal, R.H.; Sawyer, P.N.; Martin, J.G.; Kaplit, M.J. *J. Appl. Polym. Sci.* **1970**, *14*, 257.
5. Tsubokawa, N.; Fujiki, K.; Sone, Y. *J. Polym. Sci., Polym. Chem. Ed.* **1986**, *24*, 191.
6. Qiu, K.Y.; Fang, F.L.; Huang, Z.X.; Feng, X.J.; Feng, X.D. *Polym. Commun.* **1982**, *2*, 81.
7. Kolb, B.U.; Patton, P.A.; McCarthy, T.J. *Macromolecules* **1990**, *23*, 366.



## CHAPTER VI

### EXPERIMENTAL SECTION

#### Methods

Unless otherwise specified, the same inert atmosphere techniques described in part I were used here. The surface analytical techniques employed in this study were described in detail in the introduction to part I. Contact angle measurements were obtained using a Ramé-Hart goniometer. XPS spectroscopy was performed with a Perkin-Elmer-Physical Electronics 5100 spectrometer ( $\text{MgK}_\alpha$  excitation, 300 W) using a pass energy of 71.5 eV or 35.75 eV. Ion beam etching experiments were performed using a Perkin-Elmer-Physical Electronics DN4000 spectrometer equipped with a Perkin-Elmer-Physical Electronics 04-300 differential ion gun. Analysis was carried out using  $\text{MgK}_\alpha$  excitation (400 W) and a pass energy of 71.5 eV. Gravimetric analysis was performed with a Cahn 29 electrobalance equipped with a polonium source. The samples were stored under vacuum at 75°C between weighing and charge neutralized with a Zerostat (Aldrich), just prior to weighing. The samples were weighed at 24 hour intervals until a constant mass ( $\pm 1 \mu\text{g}$ ) was obtained. ATR-IR spectra were recorded using an IBM 38 ATR-IR and a 45° Ge microsampling internal reflection element. In addition, SEM micrographs of several samples were taken using a JEOL 35CF SEM.

The following techniques were employed to characterize reagents and model reaction products in solution: Infrared spectra were recorded of thin films cast on NaCl plates using an IBM 38 FTIR. Proton NMR spectra were obtained using a Varian XL300 or a Bruker AC80 NMR. GPC chromatograms were obtained using Polymer Laboratories PL gel columns ( $10^4$ ,  $10^3$ ,  $10^2$  Å), a Rainin Rabbit pump and a Knauer 98 DRI detector. GPC chromatograms were analyzed using Micro-ware GPC software on an Apple IIe computer. Packed column GC chromatography was performed using an Analabs Superpak II column on a Hewlett Packard 5790A gas chromatograph equipped with an FID detector. Capillary column chromatography was performed using a Supelco SDB-1 0.53 mm ID silica column and a splitless injection system on the same instrument. GC-MS data were obtained using a Hewlett Packard 5890 gas chromatograph equipped with a 5970 mass selective detector and a non-polar stationary phase (comparable to Supelco SPB-1) capillary column. GC-IR data were obtained using a Mattson Cygnus 100IR and a Perkin-Elmer Sigma 3B gas chromatograph. Chromatography was performed using a non-polar stationary phase (DBI) capillary column and IR spectra were recorded at  $16\text{ cm}^{-1}$  resolution.

#### Purification of Solvents and Reagents

Purification of the following solvents and reagents is described in part I, chapter 2: FEP, PCTFE, tetrahydrofuran,

methanol, water, pyridine, heptafluorobutyryl chloride, ethylene oxide, sodium, 3-bromo-1-propanol, ethyl vinyl ether, t-butyllithium, benzene and heptane.

**Methyl methacrylate** (Aldrich) was distilled from calcium hydride under reduced pressure (46°C, 100 mm) and stored in the dark under nitrogen at 4°C.

**Dichloromethane** (Fisher), was distilled from calcium hydride and stored under nitrogen.

**Acrylamide** (Fisher), was recrystallized from acetone.

**Isopropanol** (Fisher) was refluxed over, and distilled from Mg turnings and stored under nitrogen.

**t-Butanol** (Fisher) was refluxed over, and distilled from Mg turnings in the presence of a small amount of iodine and stored under nitrogen.

**Propylene oxide** (Aldrich) was distilled from calcium hydride under reduced pressure (50 mm), trap-to-trap, and stored in a refrigerator under nitrogen.

**Bromine** (Aldrich) was degassed using four freeze-pump-thaw cycles, distilled under vacuum (trap-to-trap) and stored under nitrogen.

**Carbon tetrachloride** (Fisher) was degassed using four freeze-pump-thaw cycles, distilled under vacuum (trap-to-trap) and stored under nitrogen.

**Acetone** (Fisher) was stored over anhydrous potassium carbonate.



**Diethyl ether** (Fisher) was distilled from sodium benzo-phenone and stored under nitrogen.

**2-methyloxazoline** (2MO, Aldrich) was stirred over calcium hydride, distilled under vacuum (trap-to-trap) and stored under nitrogen.

**Triethylamine** (TEA, Aldrich) was stirred over calcium hydride, distilled under vacuum (100 mm, trap-to-trap) and stored under nitrogen.

**Dimethylformamide** (DMF, Aldrich) was refluxed over calcium hydride and distilled under reduced pressure (70°C, 40 mm) and stored under nitrogen.

**Ethyl phenylacetate** (Aldrich) was stirred over calcium hydride, distilled under vacuum (trap-to-trap) and stored under nitrogen.

**1,1,1-Trichloroethane** (Aldrich) was stirred over calcium hydride, distilled under vacuum (trap-to-trap) and stored under nitrogen.

**Phenylacetyl chloride** (Aldrich) was distilled under reduced pressure (trap-to-trap) and stored under nitrogen.

**Diisopropylamine** (Aldrich) was stirred over and distilled from calcium hydride and stored under nitrogen.

**n-Butyllithium** (~1.6 M in hexanes, Aldrich) was standardized by titration with biphenylmethanol in THF at room temperature.



**Poly(ether ether ketone)** (PEEK, ICI Chemical) was washed with dichloromethane and dried under vacuum at room temperature.

**ε-Caprolactam** (Fluka) was distilled under vacuum (145°C, 10 mm). The temperature of the entire stillhead had to be maintained above 85°C to prevent freezing of the product. This was accomplished by running 85°C water through the condenser and heating with a heat gun.

The following reagents were used without further purification: naphthalene (Fisher), borane-tetrahydrofuran (1.0 M, Aldrich), hydrogen peroxide (30%, VWR), calcium hydride (Aldrich), hydrochloric acid (ACS concentrated, Fisher), 1,4-toluene diisocyanate (Aldrich), lithium diisopropylamide (LDA, Aldrich), dibutyl tin dilaurate (Aldrich), DABCO (Aldrich), sodium hydroxide (Fisher), potassium carbonate (Fisher), ceric ammonium nitrate (Fisher), N,N-dimethylacrylamide (Aldrich), nitric acid (ACS concentrated, Fisher), 5,10,15,20-tetraphenyl-21H,23H-porphine (TPP-H<sub>2</sub>, Aldrich), triethylaluminum (Aldrich, 7% alkylaluminum chlorides), diethylaluminum chloride (Aldrich), chlorine (Aldrich), silver trifluoromethanesulfonate (Aldrich), dibutylmagnesium (0.85 M in hexanes, Alfa), 4-Dimethylaminopyridine (DMAP, Aldrich), 3-bromo-2,2-dimethyl-1-propanol (Aldrich), trifluoromethanesulfonyl chloride (Aldrich), trifluoromethanesulfonic anhydride (Aldrich), 2,2,2-trichloroethanol (Aldrich), toluenesulfonyl chloride (Aldrich), acetonitrile

(Fisher), isobutyryl chloride (Aldrich), trimethylsilyl chloride (Aldrich), trimethylsilyl trifluoromethanesulfonate (Petrarch), D<sub>2</sub>O (Aldrich), tris(dimethylamino)sulfur (trimethylsilyl)bifluoride (TAS·TMSF<sub>2</sub>, Aldrich), calcium chloride (Fisher), biphenylmethanol (Aldrich), methyl iodide (Aldrich), phenyl isocyanate (Aldrich), dichloroacetic acid (Aldrich).

#### Attempted Polymerization of MMA from FEP-C

(b2p76-77) FEP was reduced with sodium naphthalide at 0°C for 5 1/2 hours as described in part I, chapter 2. The films were rinsed with one 10 mL portion of THF, 20 mL of MMA was added, and the reaction allowed to proceed for approximately 16 hours at room temperature in the dark. The reagent was removed, and the films were washed with two 20 mL portions each of THF and methanol and four 20 mL portions of THF, and then dried under vacuum at room temperature.

#### Attempted Polymerization of MMA from FEP-OH

(b1p128, b2p7, b2p23-24) The graft polymerization of methyl methacrylate (MMA) from hydroxyl surfaces was attempted by each of the following procedures: (a) FEP was reduced with sodium naphthalide (-78°C, 2 h) and hydroborated as described in part I, chapter 2. The film was treated with 0.5 M n-butyllithium in THF for 1 hour, the reagent was removed and the films were washed with two 20 mL

portions of dry THF. Then approximately 20 mL of MMA was transferred onto the film. After about 6 hours, the MMA was removed and the films were washed with five 20 mL portions each of THF, dichloromethane and heptane. (b) the experiment was repeated using deeply modified FEP-OH surfaces produced by reduction at 0°C for 4 hours. (c) An FEP-OH film sample (produced by reaction at 0°C for 6 hours) was placed in a nitrogen-purged Schlenk tube and a solution of 0.5 g of LDA in THF was added. The tube was cooled to -78°C in a dry ice/ethanol bath and 11.0 mL (100 mmol) of MMA was added. Polymerization, as evidenced by an increase in viscosity, began immediately. After one hour, the films were washed with two 20 mL portions each of THF, methanol and heptane. No visible changes occurred to the film during any of the reactions.

#### Ce<sup>IV</sup> Initiated Polymerization of Acrylamides

(b2p37-39,42-44,60-61) FEP-OH (0°C, 6 h) was reacted with acrylamide (AA) as follows: (a) A 4 x 1.5 cm<sup>2</sup> FEP-OH film sample was placed in a nitrogen-purged Schlenk tube at 30°C. 0.015 g of ceric ammonium nitrate was dissolved in 20 mL of 0.1 N aqueous HNO<sub>3</sub>. The pale yellow-orange solution was transferred onto the film. After 10 minutes, 0.5 g (6 mmol) of acrylamide in approximately 2 mL of water was transferred to the reaction tube. The reaction was allowed to proceed for 4 hours at 30°C, the reagent was removed, and



the films were washed with four 20 mL portions each of dilute aqueous sodium hydroxide, water and THF, and then dried under vacuum at room temperature. The film surface was slightly hazy. (b) A solution of 1.98 g ceric ammonium nitrate in 1.0 N aqueous  $\text{HNO}_3$  was transferred onto a 1.5 x 4  $\text{cm}^2$  film sample in a nitrogen-purged Schlenk tube at 30°C. After 4 hours, the reagent was removed, and the films were washed with five 20 mL portions each of dilute aqueous NaOH, water and THF, and then dried (room temperature, 0.03 mm). The film samples were lighter colored and appeared to have white solid on the surface. A portion of each sample was also extracted with THF prior to analysis. FEP-OH films were also reacted with N,N-dimethylacrylamide (DMAA) as follows; a tared 1.5 x 1.5  $\text{cm}^2$  sample was included for gravimetric analysis: One set of FEP-OH samples was reacted using 0.015 g of ceric ammonium nitrate in 0.1 N  $\text{HNO}_3$  and 6 mmol (0.6 mL) of DMAA for 4 hours at 30°C as described in (a) above. The second set was reacted with 2.2 g of ceric ammonium nitrate and 95 mmol (9.8 mL) of DMAA for 4 hours at 30°C, as described in (b) above. As in the previous reaction, the films reacted using procedure (a) showed little visible evidence of reaction while those reacted using procedure (b) were hazy and white. The weight gain for gravimetric samples was determined, and the samples were extracted (Soxhlet, 24 h) with water and then THF, and dried



at 70°C under vacuum. The weight loss due to extraction was determined and the samples were analyzed by XPS and ATR-IR.

### Aluminoporphyrin-Initiated Ring Opening Polymerizations

Preparation of TPP-Al-Et. (b2p122) 0.32 g (0.5 mmol) of 5,10,15,20-tetraphenyl-21H,23H-porphine (TPP-H<sub>2</sub>) was dissolved in 25 mL of dichloromethane in a nitrogen-purged Schlenk tube. 0.6 mL (0.49 mmol) of triethylaluminum (Et<sub>3</sub>Al) was added dropwise (via syringe) with rapid stirring, resulting in a dark green-purple solution. The solvent and volatiles were removed using a rotary evaporator under vacuum, resulting in a dark green solid, that was stored in a dry box.

Preparation of TPP-AlO-iPr. (b2p94,102-103) 1 mmol (0.61 g) of TPP-H<sub>2</sub> was added to a Schlenk tube, the tube was purged with nitrogen and 25 mL of dichloromethane was added, resulting in a dark purple solution. 0.14 mL (1 mmol) of Et<sub>3</sub>Al was added with stirring. After stirring for 1 hour, the solution was green at the meniscus but seemed purple throughout. An additional 0.01 mL of Et<sub>3</sub>Al was added, and the reaction was allowed to proceed for another hour; the solution became dark green. The solvent and volatiles were removed under vacuum, using a trap-to-trap apparatus, leaving a dark green solid.

The solid was redissolved in 25 mL of dichloromethane and 2.5 mL (5 x excess relative to TPP-H<sub>2</sub>) of isopropanol was added. The reaction was allowed to proceed overnight. The solution was refluxed (40°C) under nitrogen for four hours. The solution became somewhat red-purple, but stayed green at the meniscus. The solvent and excess isopropanol were removed (using a rotary evaporator) under vacuum, resulting in a purple crystalline solid. Note- may contain (i-PrO)<sub>3</sub>Al.

Preparation of TPP-AlO-tBu. (b2p103-104) TPP-AlO-tBu was prepared analogously to TPP-AlO-iPr. 1.0 mmol of TPP-H<sub>2</sub> was reacted with 0.32 mL (4.5 mmol) of Et<sub>3</sub>Al in dichloromethane. The solution was still green after three hours. The solvent was removed, resulting in dark purple crystals. The solid was redissolved in dichloromethane and 5 mL (8.5 mmol) of t-butanol was added. The solution was refluxed overnight and the solvent and excess alcohol were removed under vacuum, resulting in dark purple crystals. Note- product may contain (RO)<sub>n</sub>Al(OR')<sub>3-n</sub>, R=Me, R'=tBu.

Model Polymerizations. (b2p113,121) The polymerization of ethylene oxide using TPP-AlO-tBu was performed as follows: 0.63±.01 g (0.08 mmol) of the TPP-AlO-tBu product was added to a Schlenk tube in a dry box. 20 mL of dichloromethane was added and the dark purple solution was cooled to

0°C.  $8.7 \pm 0.1$  mL (176 mmol) of ethylene oxide was added and the reaction was allowed to proceed overnight. GPC of the product indicated that the molecular weight was far lower than predicted (Theoretical:  $\langle DP_n \rangle \sim 219$ ,  $\langle M_n \rangle \sim 9,650$ ), therefore the reaction temperature was increased to 25°C. After 24 hours, the solution had increased in viscosity. The product was poured into 200 mL of methanol and the volatiles were removed under vacuum using a rotary evaporator, resulting in a tough green film. Ethylene oxide was polymerized using TPP-AlO-*i*Pr in a similar fashion;  $0.3 \pm 0.05$  g (4.3 mmol) was reacted with 2.1 mL of ethylene oxide for 24 hours at 20°C (Theoretical:  $\langle M_n \rangle = 7,500$ ,  $\langle DP_n \rangle = 170$ ). Removal of the solvent resulted in a green, powdery solid.

Reaction of PCTFE-OH with TPP-Al-Et (PCTFE-OAl-TPP).

(b2p116-117,124) Deeply modified PCTFE-OH surfaces were prepared by the reaction of LiPrOP with PCTFE at -15°C (ethylene glycol/dry ice) for 30 minutes as described in part I, chapter 2. PCTFE-OH surfaces were reacted with TPP-Al-Et by one of the following procedures: (a) 0.62 g (1 mmol) of TPP-H<sub>2</sub> was dissolved in 25 mL of dichloromethane and 1.0 mmol (0.14 mL) of Et<sub>3</sub>Al was added. After 1 hour the volatiles were removed under vacuum using a rotary evaporator. The dark purple solid was redissolved in 20 mL of dichloromethane. Equal portions of this solution were then transferred to each of three nitrogen-purged Schlenk tubes



(equipped with reflux condenser jackets) containing PCTFE-OH film samples. One tube was reacted at reflux for 24 hours, the second for 39 hours and the third for 65 hours. Much of the solvent evaporated from all of the tubes. The surfaces were washed with two 10 mL portions of dichloromethane, five 20 mL portions of methanol and three 10 mL portion of dichloromethane. The resulting films were green colored and somewhat hazy, (b) 0.32 g (5.4 mmol) of TPP-H<sub>2</sub> was dissolved in 25 mL of dichloromethane, 4.9 mmol (0.65 mL) of Et<sub>3</sub>Al was added and the reaction was allowed to proceed for 1 hour. The dark green solution was transferred to a nitrogen-purged Schlenk tube (equipped with a reflux condensor jacket) containing PCTFE-OH samples. The reaction was allowed to proceed at 40°C for 24 hours. The reagent was removed and the films were washed with ten 10 mL portions of dichloromethane, and extracted with dichloromethane in a Soxhlet extractor for 24 hours. The resulting films were dark green colored and less hazy. Washing with dilute methanolic HCl resulted in the loss of both the haziness and the green color.

Reaction of PCTFE-OAl-TPP with Epoxide Monomers. (b2-p118-119,124-129) PCTFE-OAl-TPP surfaces prepared using procedure (a) and reaction times of (1) 24 hours and (2) 65 hours were placed in a Schlenk tube in a dry box. 5 mL of dichloromethane was added and the tube was cooled to 10°C.



2 mL of ethylene oxide was added and the tube was warmed to 20°C. The reaction was allowed to proceed for 44 hours, the reagent was removed, and the films were washed with two 10 mL portions of dichloromethane, one 10 mL portion of methanol, two 20 mL portions of dilute methanolic sodium hydroxide, four 20 mL portions of methanol and three 10 mL portions of dichloromethane. The films were greenish and hazy. PCTFE-OAl-TPP surfaces prepared by procedure (b) were reacted with 5 ml of propylene oxide at 25°C for 65 hours. The reagent was removed and the films were washed with five 20 mL portions each of dilute methanolic HCl, methanol and dichloromethane, and then dried at room temperature under vacuum.

TPP-Al-Cl Initiated Polymerization in the Presence of PCTFE-OH. (b2p132-133,139-140,142-143,146-150) Attempts were made to graft polymer to the surface of PCTFE-OH by chain transfer to the hydroxyl surface using one of the following procedures: (a) 0.323 g (5.2 mmol) of TPP-H<sub>2</sub> was dissolved in 20 ml of dichloromethane and reacted with 5.1 mmol of Et<sub>2</sub>AlCl (0.5 ml of 1 M solution in heptane) for 1 hour. The volatiles were removed under vacuum (rotary evaporator) and the purple solid was dissolved in 20 ml of dichloromethane. 0.6 mL (0.156 mmol TPP-Al-Cl) of this solution was diluted with 10 mL of dichloromethane and transferred to a Schlenk tube containing PCTFE-OH films

(prepared at  $-15^{\circ}\text{C}$ , 45 minutes). 5 mL (0.1 moles) of ethylene oxide in 10 mL of dichloromethane was added to the tube. The reaction was allowed to proceed at  $25^{\circ}\text{C}$  for 72 hours and the films were washed with five 20 mL portions each of methanolic HCl, methanol and dichloromethane. The solution was analyzed by GPC (theoretical:  $\langle M_n \rangle = 28,000$ ). (b) The corresponding reaction was carried out using propylene oxide (5 mL, 0.07 moles) and 0.8 mL (0.21 mmol) of TPP-Al-Cl solution. The solution was analyzed by GPC (theoretical:  $\langle M_n \rangle = 19,500$ ). (c) 0.32 g (0.52 mmol) of TPP- $\text{H}_2$  was dissolved in 20 mL of dichloromethane. 0.62 mmol of  $\text{Et}_2\text{AlCl}$  was added as a 1.0 M solution (0.62 mL). After 1 hour the dark purple solution was transferred to a Schlenk tube containing a PCTFE-OH film sample (prepared at  $-15^{\circ}\text{C}$ , 45 minutes). A solution of 5 mL (0.07 moles) of propylene oxide in 5 mL of dichloromethane was added and the reaction was allowed to proceed for 45 hours. The reagent was removed and the films were washed as described previously. The solution was analyzed by GPC (theoretical:  $\langle M_n \rangle = 7,500$ ). (d) TPP- $\text{H}_2$  was dried at  $150^{\circ}\text{C}$  under vacuum (0.05 mm) and used to prepare TPP-Al-Cl. 0.26 mmol of this reagent was reacted with propylene oxide (0.036 moles) for 42 hours according to procedure (c); the molecular weight of the polymer is predicted to be 8,030 amu. All of the films were colorless and clear.



Adsorption of TPP-H<sub>2</sub> by PCTFE-OH. (b2p126) A solution of 0.3 g of TPP-H<sub>2</sub> in 25 mL of dichloromethane was transferred to a Schlenk tube (equipped with a reflux condenser jacket) containing a PCTFE-OH film sample (prepared at -15°C, 45 minutes). The tube was heated to 40°C for 17 hours and the film was washed with six 15 mL portions of dichloromethane and dried at 45°C under vacuum. The films were clear and green colored.

#### Cationic Ring Opening Polymerization of THF

Chlorination of FEP-C. (b2p144,151;b3p6,11,28-29,122) FEP-C film samples were prepared as described in part I, chapter 2. The films were placed in a nitrogen-purged Schlenk tube, chlorine gas was flushed through the tube for about 5 minutes, the tube was sealed under positive chlorine pressure and the reaction was allowed to proceed in the dark for 1 hour at 0°C. At the end of this time, the tube was purged with nitrogen to remove the chlorine and the films were washed with two 15 mL portions of THF, and then dried at room temperature under vacuum. The films were less dark colored than they were prior to chlorination and pale yellow colored.

Room Temperature Initiation from FEP-Cl. (b2-

p145,152;b3p19-20,34-35) Tetrahydrofuran (THF) was graft polymerized from FEP-Cl surfaces using one of the following procedures: (a) An FEP-Cl film sample was placed in a Schlenk tube and 0.17 g (6.5 mmol) of silver trifluoromethanesulfonate (AgOTf) was loaded into a graduated cylinder in a dry box. The graduated cylinder was capped with a septum and both the tube and the cylinder were wrapped in foil (AgOTf is light sensitive) and 20 mL of dry THF was added to the tube via cannula. 5 mL of THF was added to dissolve the AgOTf and the clear, colorless solution was transferred to the reaction tube via cannula. The reaction was allowed to proceed for 66 hours, the reagent was removed, and the film was washed with two 20 mL portions of THF, five 20 mL portions of water, three 20 mL portions of methanol and two 20 mL portions of THF, and then dried under vacuum at 50°C.

(b) The reaction was carried out as described in procedure (a) using 0.89 g (3.5 mmol) of AgOTf for 72 hours. The films were washed sequentially with two 20 mL portions of methanol, five 20 mL portions each of dilute aqueous HCl and water, and two 20 mL portions each of methanol and THF and dried under vacuum at 50°C. A tared 1.5 x 1.5 cm<sup>2</sup> FEP-Cl film sample was included for gravimetric analysis. A second sample of the graft product was extracted for 24 hours with THF prior to analysis. (c) A Schlenk tube with a constricted neck was prepared, allowing the tube to be sealed with a



torch. The FEP-Cl film samples were loaded into the tube in a dry box. Also in the dry box, 0.85 g of AgOTf was placed in a graduated cylinder and the cylinder was capped with a septum. Both vessels were covered with foil. THF was further purified by distillation from dibutylmagnesium immediately prior to use. 20 mL of THF was added to the reaction tube; the AgOTf was dissolved in 5 mL of THF and the solution was transferred to the reaction tube. The tube was placed on a vacuum line and the solution was frozen with liquid nitrogen. The tube was evacuated and then sealed with a torch. The tube was warmed to room temperature and the reaction was allowed to proceed for four days. The seal was broken, the reagent was poured out, and the films were transferred to a nitrogen-purged Schlenk tube. The film was washed and dried as described in (b). (d) The reaction was carried out according to procedure (b) using 1.29 g of AgOTf and THF distilled from dibutylmagnesium. The reaction was allowed to proceed for 4 days. The solution was unusually dark; dibutylmagnesium may have bumped into the THF during distillation. The films lost some of the yellow color, but no other visible changes occurred.

Reaction of Graft Surfaces with Heptafluorobutyryl Chloride. (b3p23-24,39-40) Films prepared according to procedure (c) were labeled with heptafluorobutyryl chloride (HFBC) as follows: A solution of 1 mL of HFBC in 20 mL of

THF was transferred to a Schlenk tube containing the film sample. 0.5 mL of pyridine was added and the reaction was allowed to proceed for 20 hours at room temperature. The reagent was removed and the film was washed with five 20 mL portions each of THF, methanol and THF and dried under vacuum at room temperature. Films prepared according to procedure (d) were labeled as follows: (a) A solution of 0.5 mL of HFBC in 20 mL of THF was added to a Schlenk tube containing the graft reaction product and an FEP-Cl sample. 0.2 mL of pyridine was added. The reaction was allowed to proceed for 48 hours and the films were washed as described above. (b) A solution of 0.2 mL of pyridine and 0.082 g of DMAP in 20 mL of THF was transferred to a Schlenk tube containing the graft reaction product and an FEP-Cl sample. 0.5 mL of HFBC was added and the reaction was allowed to proceed for 48 hours. The films were washed as described above and extracted with THF (24 h, Soxhlet) and dried at room temperature under vacuum.

Bromination of FEP-C (FEP-Br). (b3p96) FEP-C samples were prepared as described in part I, chapter 2. 0.13 mL (4 mmol) of bromine dissolved in 20 mL of carbon tetrachloride was transferred to a nitrogen-purged Schlenk tube containing four FEP-C samples equilibrated at 0°C. The reaction was allowed to proceed for 16 hours at 0°C in the dark. The reagent was removed and the films were washed with three 20

mL portions each of carbon tetrachloride, dichloromethane and THF, and then dried at room temperature under vacuum. The films were nearly as dark in color as FEP-C. The films were stored under nitrogen in the dark.

Low Temperature Initiation from FEP-Br. (b3p98-100, 109,121) The following procedures were used to prepare THF graft surfaces from FEP-Br: (a) A Schlenk tube was built with a necked section to allow it to be sealed with a torch. 1.67 g (6.5 mmol) of AgOTf and an FEP-Br film sample were loaded into the tube in a dry box. The tube was covered with foil, cooled in liquid nitrogen and 20 mL of THF was distilled directly from dibutylmagnesium into the reaction tube (trap-to-trap). The tube was sealed under vacuum with a torch, warmed to  $-78^{\circ}\text{C}$  (dry ice/acetone) and allowed to react for 20 hours. The AgOTf dissolved easily at  $-78^{\circ}\text{C}$ . The tube was then warmed to  $-10^{\circ}\text{C}$  (Haake low temperature bath) and allowed to react for 72 hours. The seal was broken, the reaction was killed with dilute aqueous HCl and the reagent was removed. Polymerization occurred in solution upon addition of the proton source. The films were transferred to a Schlenk tube and washed with five 20 mL portions each of dilute aqueous HCl, water and methanol, and two 20 mL portions of THF, and dried at room temperature under vacuum. The surface of the film had an iridescent sheen. After ATR-IR analysis, the film was extracted with



THF. (b) An FEP-Br film sample was reacted as described in procedure (a) except that an initial reaction temperature of  $-23^{\circ}\text{C}$  (Haake bath) was used and the reagent was removed, and the films were then washed with three 20 mL portions of THF prior to adding the aqueous acid. The surface of this film had an iridescent sheen as well. (c) An FEP-Br sample was reacted with 0.5 g of AgOTf in 20 mL of THF in a sealed tube as described above, except that the reaction temperature was maintained at  $-10^{\circ}\text{C}$  for the full 70 hours of reaction. The seal was broken, the reagent was removed and the film was washed with three 20 mL portions of THF, and then transferred to a Schlenk tube and washed with five 20 mL portions each of dilute aqueous HCl, water, methanol and THF. The film was dried at room temperature under vacuum. The film exhibited a greenish tint, but was not as dramatically colored as those prepared in procedures (a) and (b).

Low Temperature Initiation from FEP-Cl. (b3p122,125)

FEP-Cl films were reacted with AgOTf in THF according to procedure (b) in the previous section. The resulting films lacked the iridescent color observed for the FEP-Br products.

## Preparation of Neopentyl Alcohol Surfaces

### Preparation of 3-Bromo-2,2-Dimethylpropyl Ethyl

#### Acetaldehyde Acetal (BrDiMePrOP). (b3p95,101-110;b4p47)

BrDiMePrOP was prepared analogously to BrPrOP, as described in part I, chapter 2. 0.2 moles (24.6 mL) of 3-bromo-2,2-dimethyl-1-propanol was added to a nitrogen-purged 150 mL round bottom flask equipped with a sidearm and capped with a septum. The flask was cooled to 0°C and 0.334 mole (32 mL) of ethyl vinyl ether was added. 0.3 mL of dichloroacetic acid was added via syringe. The reaction was allowed to proceed at 0°C for 1 hour, and then warmed to room temperature. After 20 hours, the septum was removed (under nitrogen through the sidearm) and 2 scoops of potassium carbonate were added. After stirring for approximately 6 hours, the excess ethyl vinyl ether was stripped off and the product was isolated by vacuum filtration. The product was stirred over potassium carbonate for an additional 24 hours, distilled (6mm, 80°C), and stored over potassium carbonate under nitrogen. GC indicated complete conversion and IR and NMR spectra were consistent with the expected product, although the presence of two weak absorbances in the carbonyl region suggests that small amounts of dichloroacetic acid and potassium dichloroacetate were present.

Reaction of LidiMePrOP with Acetone. (b3p149-150) 1.4 mL (239.1 amu, 1.16 g/cc, 5 mmol) of BrdiMePrOP was added to a nitrogen-purged, septum-capped round bottom flask via syringe. 15 mL of diethyl ether was added and the flask was cooled to  $-78^{\circ}\text{C}$  (dry ice/acetone). 3.0 mL (5 mmol) of pale yellow 1.7 M *t*-butyllithium solution was transferred to a nitrogen-purged Schlenk storage tube and cooled to  $-78^{\circ}\text{C}$ . The *t*-butyllithium solution was transferred into the flask with vigorous stirring. The solution was clear and pale yellow colored. After 15 minutes, the solution was warmed to  $-20^{\circ}\text{C}$  for 15 minutes, and then cooled back to  $-78^{\circ}\text{C}$ . 0.3 mL (6 mmol) of acetone was added via syringe. The solution immediately turned cloudy and white. The solution was warmed to room temperature. An hour later, the solution was washed (separatory funnel) with dilute aqueous potassium carbonate and water. The organic phase became clear. The ether layer was dried over calcium chloride, then filtered. The mixture was analyzed by GC-MS and GC-IR.

Reaction of LidiMePrOP with PCTFE Film (PCTFE-diMe-OP). (b3p103-105, 119-120, 131-133; b4p1-2, 16-17, 21-25, 37-38, 48, 56) Initially, reactions were performed under conditions similar to those used to prepare PCTFE-OH, described in part I, chapter 2. (a) 0.9 g (3.8 mmol) of BrdiMePrOP was dissolved in 15 mL of heptane and cooled to  $-78^{\circ}\text{C}$ . 3.8 mL (3.6 mmol) of 0.95 M *t*-butyllithium was diluted to 10 mL with heptane



and cooled to  $-78^{\circ}\text{C}$ . The *t*-butyllithium solution was added to the acetal, resulting in a pale yellow solution. After 15 minutes, the solution was warmed to  $-20^{\circ}\text{C}$ , resulting in a white precipitate. After 15 minutes the solution was cooled to  $-78^{\circ}\text{C}$  and approximately 20 mL of THF was added. The addition of THF resulted in a transitory bright yellow color. The solid dissolved, resulting in a clear, pale yellow solution. This solution was transferred to a Schlenk tube containing PCTFE films equilibrated at the reaction temperature, in this case,  $-45^{\circ}\text{C}$  (dry ice/acetonitrile). The reaction was allowed to proceed for 2 hours, the reagent was removed, and the films were washed with three 20 mL portions each of methanol and THF, and dried at room temperature under vacuum. (b) PCTFE films were reacted according to procedure (a) at  $-20^{\circ}\text{C}$  for 45 minutes. (c) PCTFE films were reacted according to procedure (a) at  $-45^{\circ}\text{C}$  (cryostat) for 24 hours. Analysis of the films revealed that only shallow modification occurred. A series of reactions was also performed in which diethyl ether was substituted for THF. (d) 1.5 mL of BrdiMePrOP (7.3 mmol) was dissolved in 15 mL of diethyl ether and cooled to  $-78^{\circ}\text{C}$ . 4.3 mL (7.3 mmol) of 1.7 M *t*-butyllithium solution was cooled to  $-78^{\circ}\text{C}$  and transferred into the reaction flask; the resulting diethyl ether:hydrocarbon ratio was 0.26:1. The reaction was allowed to proceed at  $-78^{\circ}\text{C}$  for 15 minutes and  $-20^{\circ}\text{C}$  for 15 minutes, and then the tube was cooled back to  $-78^{\circ}\text{C}$ . No

precipitate formed; the resulting clear, pale yellow solution was transferred onto the film samples at  $-45^{\circ}\text{C}$ . After 2 hours, the reagent was transferred to a nitrogen-purged flask containing 1 mL of acetone equilibrated at  $-78^{\circ}\text{C}$ . The reaction with acetone was allowed to proceed for 1 hour at room temperature and the products were isolated and analyzed as described in the previous section. The films were washed with methanol and THF, and dried at room temperature under vacuum. (e) Film samples were reacted at  $-20^{\circ}\text{C}$  for 4 hours in 0.19:1 diethyl ether/hydrocarbon according to procedure (d). (f) Films were reacted at  $-30^{\circ}\text{C}$  (o-xylene/dry ice) for 6.5 hours in 0.6:1 diethyl ether/hydrocarbon. Once again, only shallow surfaces were obtained. Deeper surfaces, suitable for further modification, were obtained by the following procedure: (g) 1.5 mL (7.2 mmol) of BrdiMePrOP was dissolved in 20 mL of THF and cooled to  $-78^{\circ}\text{C}$ . An equimolar amount of t-butyllithium in hexanes (~4 mL) was cooled to  $-78^{\circ}\text{C}$  and added (slowly) to the reaction flask. A bright yellow color developed, which faded in 1-2 minutes, resulting in a clear, nearly colorless solution. This solution was transferred to a Schlenk tube containing film samples equilibrated at  $-20^{\circ}\text{C}$ . The reaction was allowed to proceed for 4-6 hours, the reagent was removed, and the films were washed with methanol and THF. When the reaction was first performed, the reagent used to modify the films was reacted with acetone, the THF was removed (rotovap) and the products

were redissolved in diethyl ether and isolated and analyzed as described in (d).

Deprotection of PCTFE-diMe-OP (PCTFE-diMe-OH). (b3p103 105,119-120,131-133;b4p1-2,5-6,16-17,21-25,37-38,48,56)

Acetal groups were hydrolyzed using the same procedure employed for the preparation of PCTFE-OH. The films were refluxed in a solution of 65 mL of methanol, 30 mL of water and 5 mL of concentrated HCl for 3 hours, washed with five 20 mL portions each of water, methanol and THF and dried at room temperature under vacuum.

Reaction of PCTFE-diMe-OH with HFBC. (b4p26-27) A film sample prepared by procedure (g) was reacted with 0.5 mL of HFBC in 15 mL of pyridine for 26 hours. The reagent was removed and the film sample was washed with three 20 mL portions each of THF, methanol and THF and dried at room temperature under vacuum.

#### Attempted Preparation of Triflate Surfaces

Reaction of PCTFE-OH with Trifluoromethanesulfonyl Chloride. (b3p22,25,31-32,36) PCTFE-OH film samples were prepared by reaction for 45 minutes at  $-20^{\circ}\text{C}$  as described in part I, chapter 2, and then reacted with trifluoromethanesulfonyl chloride (TfCl) using one of the following proce-



dures: (a) 20 mL of pyridine was added to a nitrogen-purged Schlenk tube containing PCTFE-OH film samples. 0.4 mL (4 mmol) of TfCl was added via syringe at room temperature. A white precipitate formed, which dissolved to yield a clear yellow solution after shaking. The reaction was allowed to proceed at approximately  $-5^{\circ}\text{C}$  (freezer) for 55 hours. The reagent was removed and the films were washed with five 20 mL portions of dichloromethane, and then dried at room temperature under vacuum (0.03 mm). (b) A solution containing 0.3 mL (3.8 mmol) of pyridine in 20 mL of dichloromethane was added to a Schlenk tube containing PCTFE-OH film samples and the tube was cooled to  $-78^{\circ}\text{C}$  (dry ice/acetone). 0.4 mL (4 mmol) of TfCl was added, resulting in a clear colorless solution, and the reaction was allowed to proceed at  $-78^{\circ}\text{C}$  for 2 hours. The reagent was removed and the films were washed with five 20 mL portions of dichloromethane, which had been equilibrated at  $-78^{\circ}\text{C}$ . The reaction tube was then evacuated (still at  $-78^{\circ}\text{C}$ ) for ~10 minutes and dried at room temperature under vacuum. (c) A solution containing 1.12 mL (14 mmol) of pyridine in 20 mL of dichloromethane was added to a Schlenk tube containing PCTFE-OH film samples and the tube was cooled to  $-15^{\circ}\text{C}$  (dry ice/acetonitrile). 1.7 mL of TfCl (16 mmol) was added, resulting in a pale yellow solution. The reaction was allowed to proceed at  $-15^{\circ}\text{C}$  for 15 hours. The reagent was removed and the films were washed with five 20 mL portions of dichloromethane at

0°C and dried at room temperature under vacuum. This film had a hazy white appearance.

Reaction of PCTFE-diMe-OH with Trifluoromethanesulfonic Anhydride. (b4p32,42) Relatively deeply modified PCTFE-diMe-OH surfaces, prepared according to procedure (g) in the previous section, were reacted with trifluoromethanesulfonic anhydride ( $\text{Tf}_2\text{O}$ ) as follows: (a) 15 mL of pyridine was transferred to each of two Schlenk tubes containing PCTFE-diMe-OH film samples. The tubes were cooled to -20°C (Haake bath) and 0.5 mL (1 mmol) of  $\text{Tf}_2\text{O}$  was added, resulting in a clear orange solution. After 42 hours, the reagent was removed from one tube and the film sample was washed with three 20 mL portions of dichloromethane; 0.15 mL of 2,2,2-trichloroethanol (1 mmol) was added to the second tube and the reaction was allowed to proceed at room temperature for 2 hours. The solution (bright red, no precipitate) was removed, and the films were washed with three 20 mL portions each of dichloromethane, methanol and dichloromethane. (b) A solution of 0.8 mL (10 mmol) of pyridine in 15 mL of dichloromethane was transferred to each of two Schlenk tubes containing PCTFE-diMe-OH films and the tubes were cooled to 0°C. 5 mmol (0.8 mL) of  $\text{Tf}_2\text{O}$  was added to each tube. After 45 hours, the reagent was removed from the first tube and the films were washed with three 20 mL portions of dichloromethane. 1.1 mL (12 mmol) of 3-bromo-1-propanol was added

to the second tube and the reaction was allowed to proceed for 20 hours; a precipitate formed, and then redissolved, resulting in a bright yellow solution. The films were washed with three 20 mL portions each of dichloromethane, methanol, and dichloromethane, and dried at room temperature under vacuum.

Reaction of PCTFE-diMe-OH with Trifluoromethanesulfonyl Chloride. (b4p45,49) Relatively deeply modified PCTFE-diMe-OH surfaces were prepared according to procedure (g) in the previous section and reacted with TfCl as follows: (a) 20 mL of pyridine was transferred to each of two Schlenk tubes containing PCTFE-diMe-OH film samples and the tubes were cooled to 0°C. 5 mmol (0.55 mL) of TfCl was added via syringe, resulting in a pale yellow solution. The reaction was allowed to proceed at 0°C for 43 hours. The reagent was removed from the first tube, and the film was washed with three 10 mL portions of dichloromethane at room temperature and dried at room temperature under vacuum. 1.1 mL (12 mmol) of 3-bromo-1-propanol was added to the second tube and the reaction was allowed to proceed for 24 hours. The solution remained bright yellow but a large amount of white precipitate (pyridinium hydrochloride) was formed. The films were washed with two 20 mL portions of dichloromethane, four 20 mL portions of methanol (dissolved the solid), and three 20 mL portions of dichloromethane, and dried at



room temperature under vacuum. (b) A solution of 3.2 mL (40 mmol) of pyridine in 20 mL of dichloromethane was added to each of two tubes and the tubes were cooled to 0°C. 20 mmol (2.1 mL) of TfCl was added via syringe to each tube. The reaction was allowed to proceed for 50 hours. One of the films was isolated and the second was reacted with 3-bromo-1-propanol, as described in (a).

### Cationic Ring Opening Polymerization of 2-Methyloxazoline

#### Reaction of PCTFE-OH with Toluenesulfonyl Chloride

(PCTFE-OTos). (b3p12-14;b4p68-69,84-85) PCTFE-OTos surfaces for the initiation of 2-methyloxazoline were prepared as follows: (a) PCTFE-OH films (prepared at -15°C, 45 minutes) along with 0.79 g (4 mmol) of toluenesulfonyl chloride (TosCl) were loaded into a Schlenk tube in a dry box and 20 mL of pyridine was added at room temperature. The films were allowed to react for 48 hours at approximately -5°C (freezer); the solid TosCl dissolved readily, resulting in a clear yellow solution. The reagent was removed and the films were washed with three 20 mL portions each of THF, methanol and THF, and then dried at 50°C under vacuum. No precipitate had formed and the film's appearance was unchanged. (b) Very shallow PCTFE-OH surfaces were prepared by reaction at -45°C for 2 hours and then reacted with TosCl as described in (a). (c) Deeper PCTFE-OH surfaces were

prepared by reaction at  $-20^{\circ}\text{C}$  for 45 minutes and reacted with  $\text{TosCl}$  as described in (a).

Reaction of PCTFE-diMe-OH with  $\text{TosCl}$  (PCTFE-diMe-OTos).

(b4p26,57) PCTFE-diMe-OH surfaces were prepared according to procedure (g) and reacted with  $\text{TosCl}$  as follows: 0.8 g of  $\text{TosCl}$  and the PCTFE-diMe-OH film samples were loaded into a Schlenk tube in a dry box. 20 mL of pyridine was added (at room temperature), and the reaction was allowed to proceed for 48 hours at  $0^{\circ}\text{C}$ . The reagent was removed and the films were washed with three 20 mL portions each of THF, methanol and THF, and then dried at room temperature under vacuum.

Reaction of Tosylate Surfaces with 2-Methyloxazoline.

(b3p15,17;b4p64-65,71,87-88) Graft polymerizations of 2-methyloxazoline (2MO) were carried out as follows: (a) 15 mL of 2MO was added to a Schlenk tube containing a PCTFE-OTos sample, prepared according to procedure (a), and the tube was heated to  $75^{\circ}\text{C}$  (Haake constant temperature bath) for 47 hours. The initially clear, colorless films turned black and nearly opaque. The reagent was removed and the films were washed with five 20 mL portions each of THF and dichloromethane, and then dried at  $50^{\circ}\text{C}$  under vacuum (0.03 mm). (b) Two PCTFE-diMe-OTos samples, prepared according to procedure (b), were placed in nitrogen-purged Schlenk tubes, necked down to allow a blown-glass seal. 20 mL of acetonitrile

trile was stirred over calcium hydride in a Schlenk-type bulb equipped with a stir bar, and then distilled (trap-to-trap) into the reaction tube. 5 mL of 2MO was distilled into the tube from calcium hydride and the tube was sealed under vacuum and immersed in an oil bath at 80°C. The second tube was treated in the same way. The reaction was allowed to proceed for (1) 24 hours and (2) 6 days at 80°C. At the end of the reaction time, the tube was cooled to room temperature, the seal was broken and the reagent was removed and then 20 mL of dilute aqueous potassium carbonate was added. After approximately 10 minutes, the film was transferred to a Schlenk tube and washed with five 20 mL portions each of water, methanol and THF, and then dried at room temperature under vacuum. Both films were less colored than those prepared by procedure (a), but the 6 day reaction product appeared to have lens shaped surface features. (c) A sample of PCTFE-diMe-OTos prepared by procedure (b), a deeply modified sample of PCTFE-OTos prepared by procedure (a), and a very lightly modified sample of PCTFE-OTos, prepared by procedure (b), were placed in a nitrogen-purged Schlenk tube, necked down to allow a blown-glass seal. 20 mL of 2MO was distilled directly into the reaction tube (trap-to-trap) and the tube was sealed under vacuum. The tube was immersed in an oil bath at 80°C for 5 days and the films were isolated and washed as described for procedure (b), above. (d) A deeply modified PCTFE-OTos sample, pre-



pared according to procedure (c), and a sample of PCTFE film were reacted with neat 2MO in a sealed tube at 90°C for 45 hours and washed as described in procedure (c). A portion of each sample was also washed with five 20 mL portions each of dilute methanolic HCl, methanol and THF, prior to analysis.

## Group Transfer Polymerizations

### Reaction of PCTFE-OH with Isobutyryl Chloride

(PCTFE-OC(=O)-iBu). (b3p50-52) Isobutyryl ester surfaces were prepared as follows: Relatively shallow modified PCTFE-OH surfaces were prepared by reaction at -45°C (dry ice/acetone) for 1 hour. 0.5 mL (5 mmol) of isobutyryl chloride (i-BuCOCl) was transferred via syringe to a Schlenk tube containing the PCTFE-OH film samples in 20 mL of pyridine. The reaction was allowed to proceed for 24 hours. The solution became yellow-orange and a white solid (pyridinium hydrochloride) precipitated out. The reagent was removed and the films were washed with four 20 mL portions each of THF, methanol (dissolves the solid) and THF, and then dried at room temperature under vacuum.

Reaction of PCTFE-OC(=O)-iBu with Trimethylsilyl Chloride and LDA. (b3p53-54) A solution containing 0.25 mL (2 mmol) of trimethylsilyl chloride in 10 mL of THF was trans-

ferred into a nitrogen-purged Schlenk tube containing PCTFE-OC(=O)-*i*Bu film samples and the tube was cooled to 0°C. 0.1 g (1 mmol) of LDA was loaded into a graduated cylinder in a dry box and the cylinder was capped with a septum. 10 mL of THF was added to dissolve the solid, resulting in a pale orange solution. This solution (at room temperature) was added dropwise to the reaction tube. After 18 hours at 0°C, the reagent was removed and the films were washed with five 20 mL portions each of THF and dichloromethane, and then dried at room temperature under vacuum.

Reaction of PCTFE-OC(=O)-*i*Bu with Trimethylsilyl Chloride and Triethylamine in DMF. (b3p58-59) A solution of 3.9 mL (3 mmol) of trimethylsilyl chloride (TMSCl) in 20 mL of DMF was transferred to a Schlenk tube containing PCTFE-OC(=O)-*i*Bu film samples. 8.6 mL (60 mmol) of triethylamine (TEA) was added, resulting in the formation of some cloudy white precipitate (likely due to the reaction of TEA with HCl, generated by the hydrolysis of TMSCl). The tube was heated to 100°C in an oil bath. As the temperature was increased, the films began to discolor. After approximately 2 hours the tube was cooled to room temperature. The reaction was allowed to proceed at room temperature for another 22 hours. The reagent was removed and the dark black-orange films were washed with five 20 mL portions of THF and dried at room temperature under vacuum.

Reaction of PCTFE-OC(=O)-iBu with TEA and Trimethylsilyl Triflate. (b3p74-76,82) (a) A PCTFE-OC(=O)-iBu film sample was loaded into a Schlenk tube in the dry box and 10 mL of benzene was added. The tube was cooled to 0°C and 0.8 mL (6 mmol) of TEA was added via syringe, followed by 0.9 mL (5 mmol) of trimethylsilyl trifluoromethanesulfonate (TMSOTf). The reaction was allowed to proceed at 0°C for 18 hours. The reagent was removed and the film was washed with three 10 mL portions of benzene and dried at room temperature under vacuum. (b) Two film samples were reacted as described above, substituting 8 mmol (1.2 mL) of DBU for TEA. One film was washed as described above. After 18 hours, 2 mL of D<sub>2</sub>O was added to the second tube; an emulsion formed. As a result, this solution was removed and the film was reacted with 1 mL of D<sub>2</sub>O in 10 mL of THF for 15 minutes, and then washed with four 20 mL portions each of methanol and THF.

Reaction of Ethyl Phenylacetate with TEA and TMSOTf. (b3p87-88;b4p103-104,108-109) 1-ethoxy-1-(trimethylsilyloxy)-2-phenylethylene was prepared from ethyl phenylacetate using the following conditions: (a) 3.6 mL (2.5 mmol) of ethyl phenylacetate was dissolved in 25 mL of benzene in a nitrogen-purged round bottom flask, that had been capped with a septum. 5.5 mL (40 mmol) of TEA was added via syringe and the flask was cooled to 0°C. 4.5 mL (25 mmol) of



TMSOTf was added and the solution was stirred. A pale yellow, denser-liquid phase began to appear after approximately 15 minutes. After 3.5 hours, the denser phase was removed using a separatory funnel and the less dense phase was distilled. Benzene, TEA and unreacted TMSOTf were removed at 52°C at a pressure of 17 mm. The residue was distilled at 0.7 mm (attached directly to the vacuum line); the majority was collected as a liquid at 88°C. Analysis of this product by IR revealed both a TMS enol band (1650  $\text{cm}^{-1}$ ) and a weaker ester band (1738  $\text{cm}^{-1}$ ). Latter, the product was analyzed by capillary GC (150°C, isothermal) and GC-MS.

(b) The reaction was repeated using 1.6 mL (11 mmol) of the ester, 3.1 mL (22 mmol) of TEA and 2 mL of TMSOTf in 15 mL of benzene for 6 hours and the products were isolated by distillation (72°C, 0.2 mm). The product was analyzed by capillary GC (150°C, isothermal).

(c) 1.6 mL (11 mmol) of the ester was dissolved in 15 mL of 1,1,1-trichloroethane (TCE), 3.1 mL (22 mmol) of TEA was added and the flask was cooled to 0°C. 2.0 mL (11 mmol) of TMSOTf was added with stirring. After 15 minutes the flask was warmed to room temperature and the reaction was allowed to proceed for 4 hours. As in the previous reaction, a two phase system was formed. The product was isolated by distillation (77-80°C, 0.12 mm) and analyzed by capillary GC (150°C, isothermal). Substitution of DBU for TEA under comparable conditions resulted in no reaction.

1-Ethoxy-1-(Trimethylsilyloxy)-2-Phenyl Ethylene Initiated Polymerization of MMA. (b3p89-90) Approximately 20 mg of TAS·TMSF<sub>2</sub> was added to a Schlenk tube in the dry box. 15 mL of THF was added to dissolve the solid. 0.4 g of 1-ethoxy-1-(trimethylsilyloxy)-2-phenylethylene (and ethyl phenylacetate) prepared by procedure (a) was added. The clear, colorless solution became bright yellow. The tube was cooled to 0°C and methyl methacrylate (MMA) was added, slowly, via syringe. Initially, heat was evolved and the yellow color remained intense, but after the addition of 1 mL of MMA, the color faded and heat no longer evolved. The viscosity of the solution remained low; apparently, the MMA was wet. An additional 0.44 g of the initiator was added; the yellow color was restored and polymerization resumed. After the addition of 5 mL of MMA, polymerization stopped again. An additional 0.4 g of the initiator was required to polymerize the remaining 5 mL of MMA. The final product was a viscous solution, somewhat paler yellow than immediately after initiator addition. Addition of 1 mL of methanol killed the yellow color. The product was characterized by GPC; a very broad PDI was observed.

Reaction of PCTFE-OH with Phenylacetyl Chloride (PCTFE-OC(=O)CH<sub>2</sub>Ph). (b3p91-93) PCTFE-OH surfaces were prepared by reaction at -45°C for 3 hours and reacted with 0.5 mL of phenylacetyl chloride in 20 mL of pyridine for 24 hours.



The reagent was removed and the films were washed with four 20 mL portions each of methanol and THF, and then dried at room temperature under vacuum.

Reaction of PCTFE-OC(=O)CH<sub>2</sub>Ph with TEA and TMSOTf.

(b3p93-95) A solution of 0.8 mL (6 mmol) of TEA in 10 mL of benzene was transferred into a nitrogen-purged Schlenk tube containing esterified film samples. 0.9 mL (5 mmol) of TMSOTf was added and the reaction was allowed to proceed at room temperature for 23 hours. The reagent was removed and the films were washed with three 10 mL portions of benzene and three 20 mL portions of THF. The films were slightly darkened and hazy in appearance.

Reaction of PCTFE-diMe-OH with Phenylacetyl Chloride

(PCTFE-diMe-OC(=O)CH<sub>2</sub>Ph). (b4p76,93-94) Deeply modified PCTFE-diMe-OH surfaces, prepared according to procedure (g), were esterified under the following conditions: (a) 20 mL of pyridine was added to a Schlenk tube containing PCTFE-diMe-OH film samples. 1 mL of phenylacetyl chloride was added via syringe, resulting in a white precipitate that dissolved to yield a bright orange solution. The reagent was removed after 44 hours. The films were washed with five 20 mL portions each of THF, methanol and THF and dried under vacuum at room temperature. The resulting films were clear and colorless. (b) A solution containing 0.08 g of DMAP and



1.3 mL of pyridine in 20 mL of THF was transferred onto PCTFE-diMe-OH film samples in a nitrogen-purged Schlenk tube. 1 mL of phenylacetyl chloride was added via syringe, resulting in a white precipitate. Some of this precipitate dissolved, resulting in a pale yellow solution. After 24 hours, the reagent was removed and the films were washed with three 20 mL portions each of THF, methanol (dissolves the solid) and THF, and then dried at room temperature under vacuum. The films were clear, but slightly discolored. Reaction under these conditions for 48 hours resulted in significant darkening of the film.

Reaction of PCTFE-diMe-OC(=O)CH<sub>2</sub>Ph with TEA and TMSOTf. (b4p77-78,109) The reaction was carried out using one of the following procedures: (a) A solution of 0.8 mL (6 mmol) of TEA in 20 mL of benzene was transferred to a Schlenk tube containing PCTFE-diMe-OC(=O)CH<sub>2</sub>Ph samples prepared according to procedure (a). 0.9 mL (5 mmol) of TMSOTf was added via syringe and the reaction was allowed to proceed for 23 hours at room temperature. The reagent was removed and the films were washed with three 15 mL portions each of benzene and THF, and then dried at room temperature under vacuum. The resulting films were slightly yellow in color. (b) A solution of 0.8 mL of TEA in 15 mL of 1,1,1-trichloroethane was transferred to a nitrogen-purged Schlenk tube containing PCTFE-diMe-OC(=O)CH<sub>2</sub>Ph film samples prepared

according to procedure (b). 0.9 mL of TMSOTf was added via syringe and the reaction was allowed to proceed at room temperature for 23 hours. The films were significantly discolored. The films were washed with three 20 mL portions of dichloromethane and dried at room temperature under vacuum.

Attempted Initiation of MMA from Surfaces Treated with TMSOTf and TEA. (b4p79-83) Group transfer polymerization was attempted using PCTFE-diMe-OC(=O)CH<sub>2</sub>Ph surfaces reacted with TMSOTf and TEA according to procedure (a), using both nucleophilic and electrophilic (Lewis acid) catalysis. A film sample and ~20 mg of TAS·TMSF<sub>2</sub> were loaded into a Schlenk tube in a dry box. A solution of 10 mL of freshly distilled MMA in 10 mL of THF was added. No sign of a color change was observed on the film or in the solution. The reagent was removed after 24 hours. The films were washed with three 20 mL portions each of methanol and THF and dried at room temperature under vacuum. Lewis acid catalyzed reaction was carried out as follows: A solution of 5 mL of MMA in 15 mL of dichloromethane was added to a Schlenk tube containing the film sample and the tube was cooled to -78°C (dry ice/acetone). 0.2 mL (1.7 mmol) of diethylaluminium chloride was added; the solution and film remained clear and colorless. After 19 hours at -78°C, 2 mL of methanol was added, resulting in the formation of a white solid. The



reagent was removed and the film was washed with three 20 mL portions each of THF, dilute methanolic HCl, methanol and THF and dried at room temperature under vacuum.

Preparation of 3-Bromo-2,2-Dimethyl-1-Propyl Iso-  
butyrate (BrPriBu). (b5p37-38) 50 mL (0.22 mole) of 3-bromo-2,2-dimethyl-1-propanol and 1.5 g of DMAP were added to a 500 mL round bottom flask and the flask was capped with a septum. The flask was purged with nitrogen and 100 mL of dichloromethane, followed by 24 mL (0.3 mole) of pyridine, was added and the flask was cooled to 0°C in an ice bath. 31 mL (0.3 mole) of isobutyryl chloride was transferred to a nitrogen-purged graduated cylinder that was capped with a septum. Dichloromethane was added to bring the total volume to 75 mL. This solution was slowly added (via cannula) to the reaction flask with vigorous stirring. Heat was evolved and a large amount of white precipitate (pyridinium hydrochloride) was formed. After 7 hours, the solution was filtered and washed (in a separatory funnel) with water (NaCl added to prevent emulsion), dilute aqueous HCl (to remove unreacted pyridine) and dilute aqueous potassium carbonate (to remove isobutyric acid); the organic layer was dried over calcium chloride. The solvent was removed under vacuum using a rotary evaporator. The reaction proceeds to 80% yield by GC (packed column, 100°C for 2 minutes, 10°C per minute). Fractional distillation was used to isolate



the ester. The ester was isolated in 90% yield (117-120°C, 15 mm) and stored under nitrogen.

Reaction of BrPriBu with LDA and Trimethylsilyl Chloride (BrPrTMSKA). (b5p41-44) 11.2 mL (80 mmol) of diisopropylamine was dissolved in 100 mL of dry THF in a septum-capped, nitrogen-purged 250 mL round bottom flask equipped with an immersed thermometer, and the flask was cooled to 3-5°C in an ice bath. 40 mL of 2.0 M (80 mmol) *n*-butyllithium was cooled to 3-5°C and added dropwise via cannula over a 45 minute period, being careful not to allow the temperature of the solution to increase above 10°C. The clear colorless LDA solution was maintained at 0°C under nitrogen prior to use. 15 mL of BrPriBu (52 mmol) and 20.3 mL of trimethylsilyl chloride were dissolved in 75 mL of THF in a septum-capped, nitrogen-purged 500 mL round bottom flask equipped with an immersed thermometer, and the flask was cooled to 3-5°C in an ice bath. The LDA solution was added to the ester and TMSCl dropwise over a 30 minute period, taking care to keep the solution temperature under 10°C. After 1 hour, the clear colorless solution, was warmed to 35°C (hot water bath), resulting in precipitation of a large amount of LiCl. The solution was transferred via cannula to a nitrogen-purged sidearm flask, a distillation head was added, and the solvent was removed under nitrogen. The high boiling fraction was distilled under vacuum (short path stillhead, 0.1-

0.2 mm). Analysis of the clear colorless product by capillary GC (110°C for 2 minutes, 5°C per minute) and GC-MS revealed 85% conversion to the trimethylsilyl ketene acetal. Fractional distillation allowed isolation of about 5 mL of TMS ketene acetal in 95% purity (125-127°C, 5 mm). The clear colorless liquid was stored under nitrogen in a refrigerator.

Reaction of LiPrTMSKA with PCTFE. (b5p51-53) Approximately 1 mL of BrPrTMSKA was added to a tared, nitrogen-purged 100 mL round bottom flask that had been capped with a septum. The exact amount of BrPrTMSKA was determined (3.4 mmol), 15 mL of THF was added, and the flask was cooled to -78°C. An equimolar amount of 0.8 M *t*-butyllithium solution (4.3 mL) was transferred to a nitrogen-purged Schlenk storage tube and cooled to -78°C. The *t*-butyllithium solution was transferred into the reaction flask with vigorous stirring, resulting in short lived, bright yellow color. After 15 minutes, the reaction was warmed to -20°C for 15 minutes, and then cooled back to -78°C. This clear, colorless solution was transferred to a nitrogen-purged Schlenk tube containing PCTFE film samples equilibrated at -20°C. After 2 hours, the reagent was transferred to a nitrogen-purged septum-capped round bottom flask containing 0.7 mL (20 mmol) of acetone at -78°C. The films were washed with three 20 mL portions of THF and dried at room temperature under vacuum. The reaction with acetone was allowed to proceed at -78°C

for 15 minutes, and then warmed to room temperature for 20 minutes. 0.25 mL (4 mmol) of methyl iodide was added via syringe and the resulting product was analyzed by capillary GC and GC-MS.

Reaction of LiPrTMSKA with PEEK. (b5p54-55) PEEK film samples were reacted with LiPrTMSKA for 8.5 hours at 0°C as described above for the reaction with PCTFE. After the reaction, the LiPrTMSKA produced was reacted with acetone as described above.

#### Polymerization of $\epsilon$ -Caprolactam from Isocyanate Surfaces

(b4p141-142,147-149) The following procedures were employed to polymerize  $\epsilon$ -caprolactam (CL) from FEP(TDI)-NCO surfaces, prepared as described in part I, chapter 2: (a) 4 g of CL was transferred to a graduated cylinder in a dry box and the cylinder was capped with a septum. 40 mL of THF was added. 20 mL of this solution was transferred to each of two Schlenk tubes containing FEP(TDI)-NCO film samples. The reaction was allowed to proceed for 48 hours in the first tube, the reagent was removed, and the film was washed with five 20 mL portions of THF, and then dried at 60°C under vacuum. After 48 hours, 0.25 mL of 1.6 M *n*-butyllithium was added to the second tube. A small amount of white solid formed. The reaction was allowed to proceed for an additional 24 hours and the film was washed and dried as de-



scribed above. (b) In a dry box, 8 g of CL and FEP(TDI)-NCO film samples were transferred to each of two Schlenk tubes. The tubes were transferred to an oil bath and allowed to react at  $105 \pm 10^\circ\text{C}$ . After 24 hours, 3 mL of 1.6 M *n*-butyllithium was added dropwise, via syringe, to one of the tubes. A large amount of white solid was formed, which quickly dissolved. The second tube was allowed to cool to  $\sim 50^\circ\text{C}$ , and 20 mL of THF was added to dissolve the CL. This solution was removed and the films were washed with four 20 mL portions of THF and dried at  $50^\circ\text{C}$  overnight. After an additional 24 hours at  $105^\circ\text{C}$ , a small amount of white solid, presumably polymer, was observed in the second tube. The film in the second tube was washed and dried as described above.

#### Attempted Room Temperature Polymerization of $\epsilon$ -Caprolactam

(b4p145-146) 2 g (18 mmol) of CL was loaded into a Schlenk tube in a dry box and 20 mL of THF was added to dissolve the solid. 1.8 mmol (0.20 mL) of phenylisocyanate was added and the reaction was allowed to proceed for 1 hour. 3 mL of 1.6 M *n*-butyllithium (4.8 mmol) was added via syringe with vigorous stirring. A flocculent white solid was formed; the solid did not redissolve. The reaction is predicted to yield polymer with a  $\langle\text{DP}\rangle$  of 10,000. After 15 hours, the product was poured into a large volume of methanol. All of the solid dissolved, suggesting that the lithi-

um salt of caprolactam was formed, but failed to polymerize, due to it's insolubility in THF. The solvent was removed. The product was dissolved in diethyl ether and washed with water. The ether layer was dried and the ether was removed, resulting in a pale yellow oil. GPC analysis revealed that only oligomers with molecular weights of less than 1200 were formed.

## CHAPTER VII

### RESULTS AND DISCUSSION

Before more elaborate means of initiating polymerization from the surface were investigated a few of the more straightforward approaches were attempted. Based on EPR studies of PTFE-C<sup>1</sup>, relatively stable radicals are expected to be present in FEP-C surfaces. It was of interest to determine whether or not these radicals are capable of initiating polymerization. FEP-C films were washed with as little THF as possible, to remove the sodium naphthalide without killing reactive sites, then, the films were exposed to methyl methacrylate (MMA), a monomer that is readily polymerized both radically and anionically. There was no evidence of reaction by XPS or ATR-IR, indicating that the radical sites are either inaccessible to the reagent or too extensively resonance stabilized to function as initiators.

Attempts were also made to sequentially treat FEP-OH surfaces with a strong base (*n*-butyllithium) and MMA. There was no evidence of reaction by XPS or ATR-IR. It seemed likely that even minimal exposure to dry THF introduced enough adventitious moisture to kill the lithium alkoxides formed on the surface. Unlike the ethylene oxide reaction described in part I, when a similar reaction was carried out using LDA in the presence of MMA, polymerization occurred preferentially in solution; XPS and ATR-IR indicate that little, if any, MMA was incorporated. Attempts were also made to polymerize ethylene oxide from the surface using in-



situ generation of the alkoxide under conditions that allow polymerization to occur. Substitution of potassium triphenylmethide for LDA resulted in no reaction with the surface, and complexation of the lithium counterion by 18-crown-6 resulted in rapid polymerization in solution. Unlike ethylene oxide, ethylene sulfide polymerized rapidly in the presence of LDA. These results confirmed that sufficient exclusion of moisture to allow efficient graft polymerization would be difficult to achieve. The research that will be discussed in the following section focuses on compensating for this problem. The systems that will be studied fall into three general classes: systems that are expected to be tolerant of adventitious moisture, systems that involve relatively stable initiator species and systems that allow in-situ preparation of the initiator species.

#### $\text{Ce}^{\text{IV}}$ Initiated Polymerization of Acrylamides

Initiation by radicals produced on polymer surfaces offers a significant advantage in that radical polymerizations are not affected by water; radical polymerizations of water soluble monomers occur facilely in deoxygenated water. Radicals can be generated by ceric ion oxidation of a variety of functional groups. This procedure has been used to graft water soluble monomers to hydroxyl group-containing polymers in solution (Dextran<sup>2</sup> and poly(vinylalcohol)<sup>3</sup>),



centrations, based on conditions that gave a high yield of graft polymer from carbon black surfaces<sup>8</sup>.

Table 8 summarizes the XPS atomic composition data for graft reactions using acrylamide. A significant amount of nitrogen was introduced and the oxygen:carbon ratio increased using both conditions. Significantly more acrylamide appeared to be present on the surfaces that were reacted at a high ceric ion concentration. However, the N:C ratio was too low to be the result of an acrylamide monolayer (1:3) and fluorine was clearly observed at both 15° and 75° takeoff angles, suggesting that the surface was not completely covered by the graft polymer. The ATR-IR spectrum, shown in figure 20, was also consistent with polymerization. Absorbances were observed at 3500-3200  $\text{cm}^{-1}$  and at 1660  $\text{cm}^{-1}$ , consistent with the presence of primary amide N-H and amide carbonyl groups respectively. As shown in figure 20, these features were more intense for the films prepared using a high ceric ion concentration. In addition, the films appeared rough; white solid material appeared to be deposited on the surface. This was especially pronounced for the films prepared at a high ceric ion concentration. Extraction of these films with THF failed to remove all of the solid, but XPS (table 8) revealed that the amount of nitrogen on both surfaces decreased to the same value. The final N:C ratio was approximately equal to the value observed for films prepared under milder conditions prior to extraction.



**Table 8.** XPS atomic composition data for Ce<sup>IV</sup> initiated graft polymerizations.

Sample	Takeoff Angle	C	F	O	N	Q <sub>c</sub>	Mass increase (mg) <sup>c</sup>
g-AA, dilute Ce <sup>IV</sup>	150°	100	2	30	7	--	
	75°	100	2	25	8	--	
g-AA, dilute Ce <sup>IV</sup> a	150°	100	2	30	7	--	
	75°	100	2	25	8	--	
g-AA, conc. Ce <sup>IV</sup>	150°	100	2	55	20	--	
	75°	100	6	39	14	--	
g-AA, conc..Ce <sup>IV</sup> a	150°	100	3	34	7	1	
	75°	100	6	32	6	--	
g-dMAA, dilute Ce <sup>IV</sup> b	150°	100	1	20	8	--	0.026 (0.018) <sup>b</sup>
	75°	100	1	21	7	--	
g-dMAA, conc. Ce <sup>IV</sup> b	150°	100	3	30	3	--	0.057 (0.004) <sup>b</sup>
	75°	100	5	29	5	--	

<sup>a</sup> extracted (Soxhlet) 24 hours with THF

<sup>b</sup> extracted (Soxhlet) with water (24 h) and THF (24 h)

<sup>c</sup> 1.5 X 1.5 cm<sup>2</sup> film sample

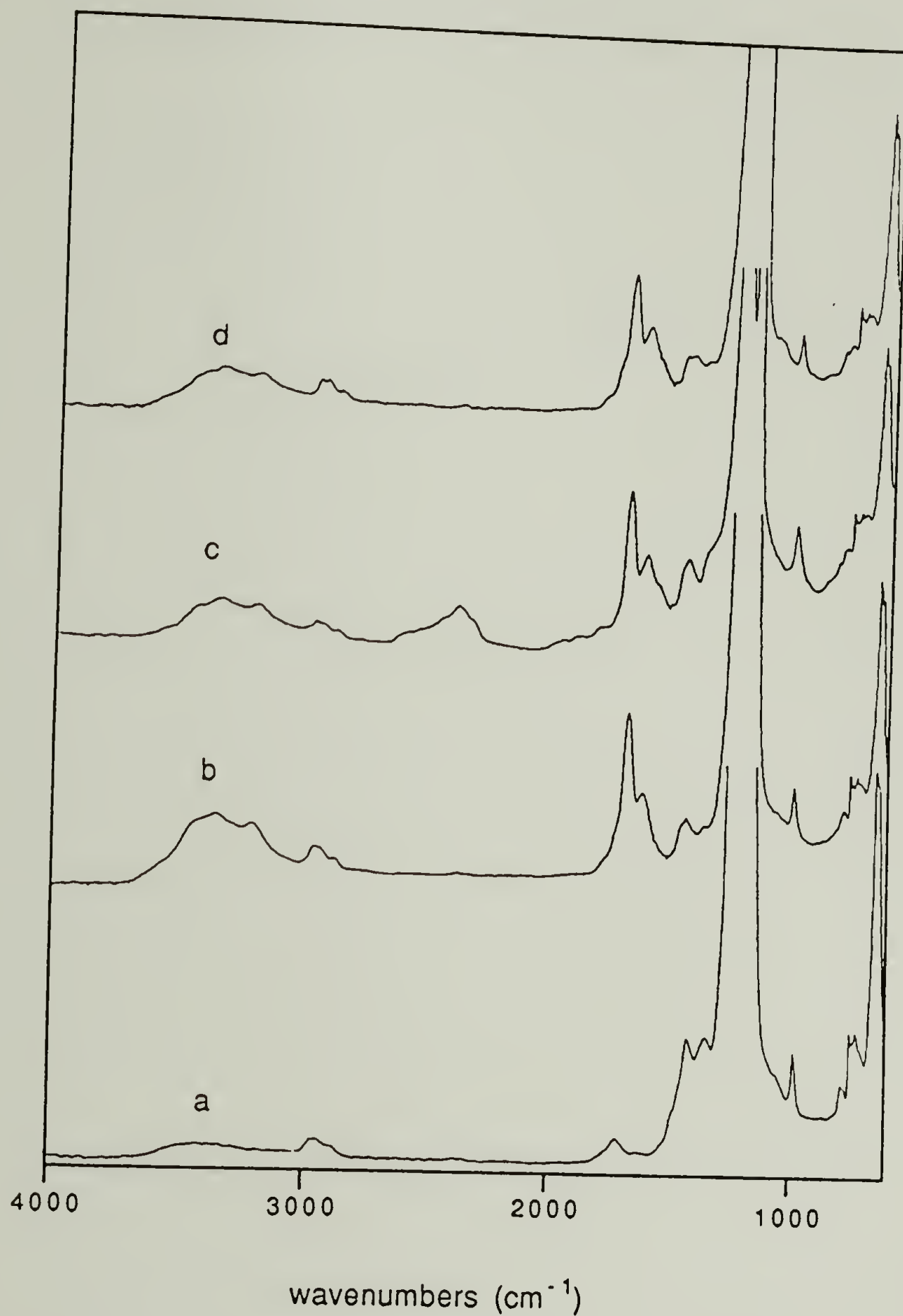


**Figure 20.** ATR-IR spectra of (a) FEP-OH; (b) FEP-g-pAA, high [Ce<sup>IV</sup>]; (c) FEP-g-pAA, low [Ce<sup>IV</sup>]; (d) FEP-g-pAA, high [Ce<sup>IV</sup>], extracted.

The intensity of the acrylamide features in the ATR-IR spectrum (see figure 20d) decreased as well. Comparison of the results obtained using both conditions suggests that a substantial amount of chain transfer<sup>9</sup> occurs at high ceric ion concentrations, resulting in polymer being formed in solution and then adsorbing to the surface. This adsorbed material was removed by THF extraction. Increasing the ceric ion concentration does not increase the amount of polymer that is actually grafted to the surface. The appearance of the surface and the intensity of the ATR-IR absorbances suggested that a substantial amount of polymer had been grafted to the surface, despite the fact that XPS detected FEP-C in the outer 15° Å. One possible explanation is that active protons on acrylamide graft polymer chains initiate polymerization in competition with surface hydroxyl groups, resulting in "clumps" made up of highly branched poly(acrylamide). Work with poly(ether urethane) surfaces suggests that reaction with the carbamate N-H bond results in nitrogen-centered radicals capable of initiating polymerization.<sup>10</sup> A similar reaction may occur involving the amide group of poly(acrylamide).

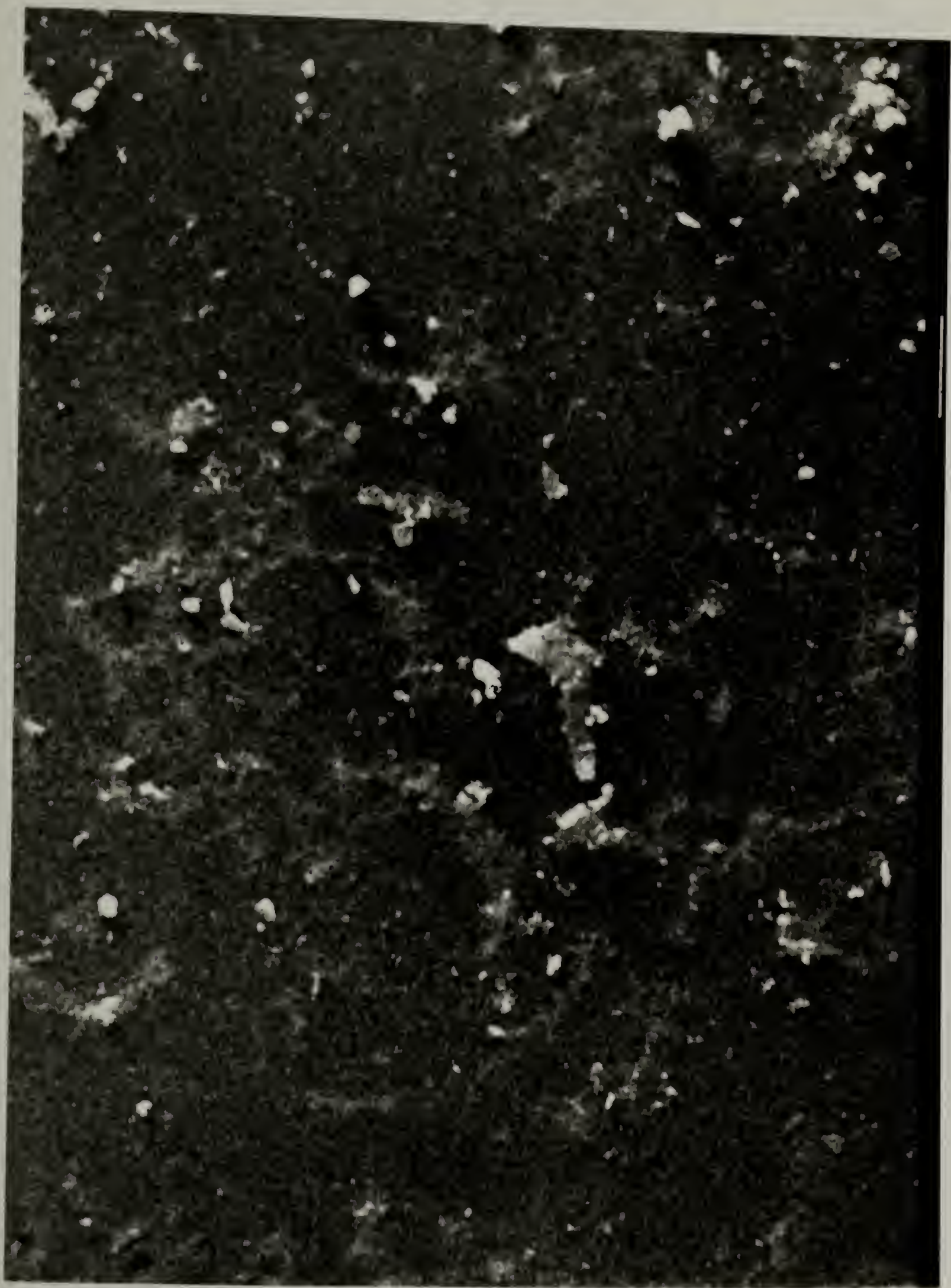
In an attempt to minimize this reaction, N,N-dimethylacrylamide was polymerized under the same conditions. Gravimetric analysis was employed to quantify the amount of polymer that was added to the surface. Samples were weighed before and after THF extraction. The resulting films also



appeared to have white solid deposited on the surface. The gravimetric results, summarized in table 8, indicate that a large amount of polymer was present on both surfaces prior to extraction. Extraction resulted in substantial weight loss for both samples, but nearly all of the graft polymer was removed from the surface produced at a high ceric ion concentration. These results indicate that the grafting efficiency was actually lower under these conditions. This is not surprising since the ceric ion complex is known to participate in termination reactions.<sup>11</sup> The XPS data for this product (after extraction) was similar to that obtained from the acrylamide polymerization. An SEM micrograph (figure 21) of the poly(dimethylacrylamide) graft surface prepared using a low ceric ion concentration confirmed earlier suspicions about the surface morphology. The graft polymer is segregated into clumps, rather than uniformly dispersed over the film surface. Active sites on the graft polymer, possibly protons on the N-methyl groups, appear to form radicals in competition with the hydroxyl surface.

These results confirmed that polymerization could be initiated from surface-confined functional groups on modified fluoropolymer films, however, the results left much to be desired. Although the appropriate choice of conditions allowed the control of side reactions that reduce the yield of graft polymer and result in polymerization in solution, the redox initiation system was not selective enough to

**Figure 21.** SEM micrograph of FEP-g-pdMAA.

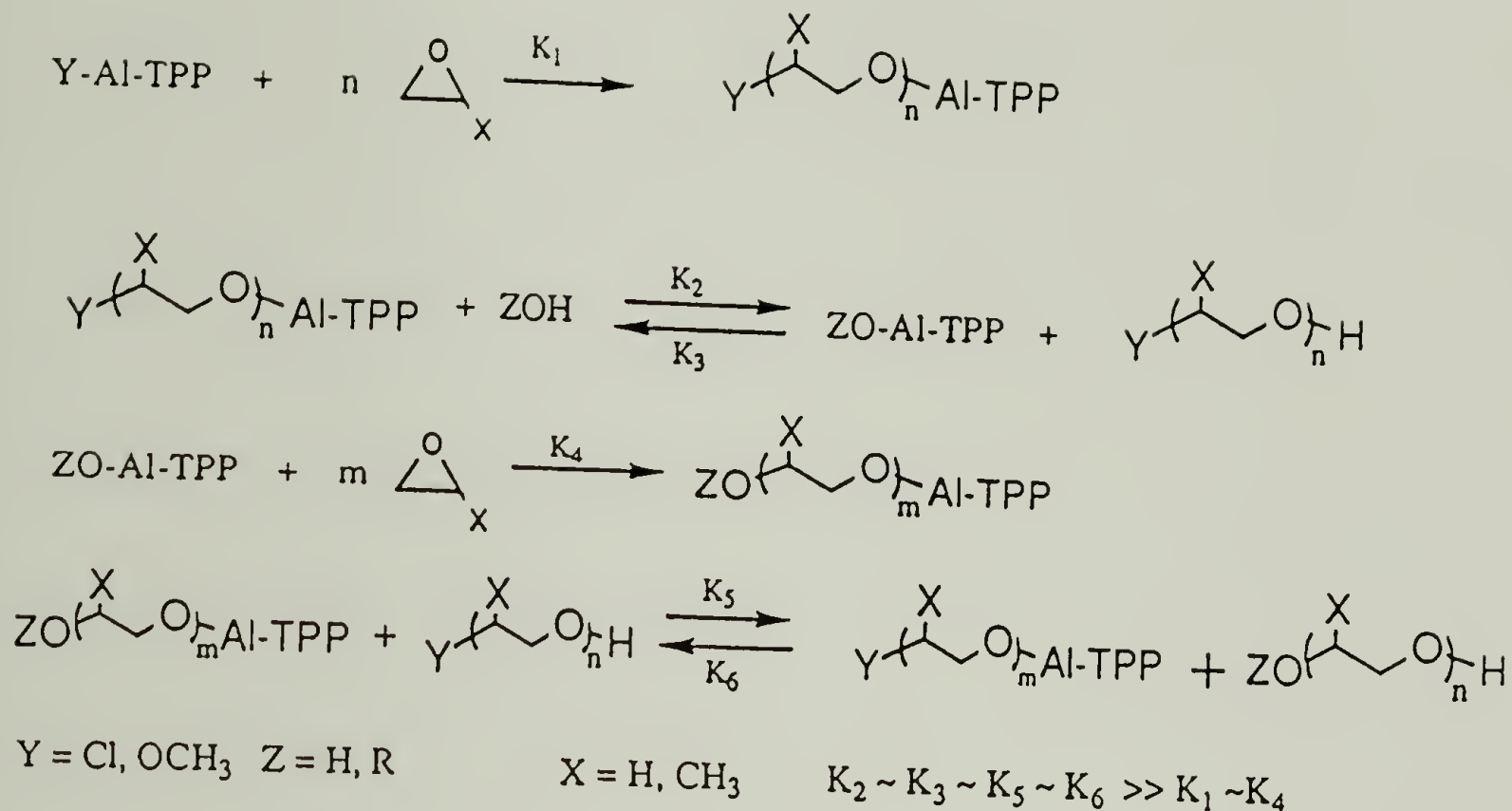




avoid competitive reactions with the graft polymer. It is possible that similar problems were not encountered for poly(ether urethane) surface graft polymerizations because the carbamate group is more reactive than the alcohols on FEP-OH. Model reactions support this conclusion<sup>12</sup>. Although the use of other monomers, such as hydroxyethyl methacrylate, may decrease the reactivity of the graft polymer, ceric ion redox conditions are harsh enough that side reaction will likely remain a problem. In addition, it is difficult to follow the initiation process since the functional groups involved in initiation remain essentially unchanged to XPS and ATR-IR. Further research focused on identifying systems in which initiation and propagation would be cleaner and changes in the surface composition as a result of initiation would be easier to follow.

#### Aluminoporphyrin-Initiated Ring Opening Polymerization

The so called "immortal" aluminoporphyrin-initiated polymerization developed by Inoue has a number of potential advantages as a method of surface-initiated graft polymerization. In this reaction, summarized in equation 3, chain transfer to protic impurities is reversible and occurs at a much faster rate than propagation. As a result, protic impurities initiate new chains that grow at the same rate as those undergoing normal propagation.<sup>13</sup> If these characteristics are preserved in a surface graft reaction, protic

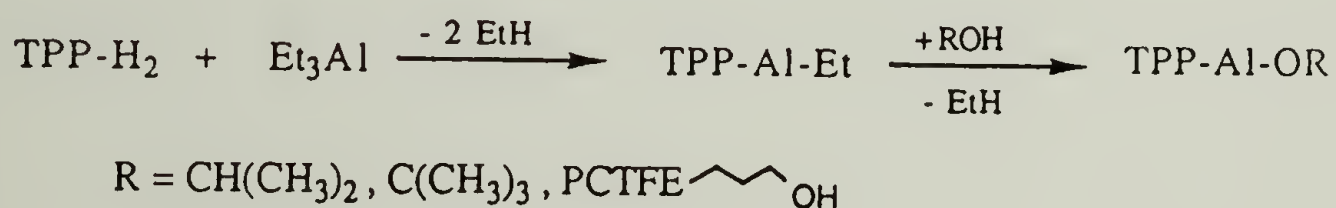


**Equation 3.** Aluminoporphyrin initiated "immortal" polymerization of epoxide monomers

impurities would result in the growth of chains of equal length in solution and on the surface. Indeed, chain transfer to a protic surface should be equivalent to initiation by an aluminoporphyrin-containing surface. Both strategies were investigated; surfaces containing initiator sites were prepared and reacted with epoxide monomers, and epoxide

monomers were polymerized by soluble initiator species in the presence of hydroxyl surfaces.

Although (5,10,15,20-tetraphenylporphinato)aluminum chloride (TPP-Al-Cl) has become the most commonly employed initiator for these polymerizations<sup>14</sup>, successful polymerizations have been reported using the corresponding methoxide (TPP-Al-OMe)<sup>15</sup>. Based on these results, research was carried out with the goal of preparing the corresponding alkoxyaluminumporphyrin from PCTFE-OH surfaces. While hydroxyl groups on PCTFE-OH are primary, the large size of the porphyrin ring gives reason to suspect that steric hindrance due to the interaction of the porphyrin ring with the surface may complicate the preparation of the initiator surface or the subsequent polymerization. As a result, model reactions were carried out using isopropanol and *t*-butanol, as outlined in equation 4. Following the procedure of



**Equation 4.** Preparation of TPP-Al-Et and reaction of TPP-Al-Et with alcohols



Inoue<sup>16</sup>, 5,10,15,20-tetraphenyl-21H,23H-porphine (TPP-H<sub>2</sub>) was reacted with triethylaluminum. While the product of the reaction with methanol is reported to be dark green, the crystalline solid that was isolated appeared much more purple in color. The proton NMR of the product shows a triplet at -3.5 ppm (TPP-CH<sub>2</sub>CH<sub>3</sub>) and a quartet at -6.4 ppm (TPP-CH<sub>2</sub>-CH<sub>3</sub>), consistent with TPP-Al-Et. Comparison of the integral of this methylene signal to the integral of the signal due to 1,5-phenyl protons on the porphyrin (8.2 ppm) suggests approximately 75% of the TPP-H<sub>2</sub> reacts to form TPP-Al-Et<sup>17</sup>. However, a signal at -2.8 ppm is present, suggesting that some other aluminoporphyrin species, possibly TPP-Al-OH, is present. Also, unlike previous reports, the signal due to the protons of the porphyrin ring (9.1 ppm) appears to be split into two signals of differing size, one at 9.2 ppm (larger) and a second at 9.0 ppm. The addition of methanol to TPP-Al-Et was reported to restore the purple color. The TPP-Al-Et solutions prepared here appeared more purple than green and the addition of the alcohol resulted in no significant color change. Proton NMR of this product revealed that the reaction with isopropanol was incomplete. The quartet at -6.4 ppm was present, as well as the triplet at at -3.5 ppm, indicative of TPP-Al-Et. In addition, what appeared to be a doublet at approximately -2 ppm was observed, consistent with the presence of TPP-AlO-*i*Pr<sup>18</sup>. Analysis of the areas of these peaks suggests that less than

half of the TPP-Al-Et reacted to form TPP-AlO-iPr. In addition to the three singlets upfield of TMS associated with the porphyrin, a broad singlet was observed at ~1.0 ppm. When this product was used to initiate the polymerization of ethylene oxide, the expected polymeric product was not obtained. Three closely spaced, monodisperse peaks were observed by GPC, just below the calibration range of the column (~1200 amu). It was clear that the polymerization was nowhere near complete, despite reports that 10,000 molecular weight poly(ethylene oxide) could be prepared under comparable conditions<sup>19</sup>. Reaction with three different initiator species, for example TPP-AlO-iPr, TPP-Al-Et and TPP-Al-Cl (up to 7% Et<sub>2</sub>AlCl is present in Et<sub>3</sub>Al) or chain transfer to water or isopropanol may have resulted in oligomeric species of different lengths due to differences in the initiation rates of the different aluminumporphyrin species.

A similar study was carried out using t-butanol. Despite the addition of excess Et<sub>3</sub>Al, no green color developed. In an effort to increase conversion to the alkoxide, the TPP-Al-Et solution was refluxed for a longer period of time. The results of proton NMR analysis were consistent with the complete conversion of TPP-Al-Et to TPP-AlO-tBu; only a singlet at -2.2 ppm is observed in the region downfield from TMS. Comparison of the area of the t-Bu proton signal with the areas of porphyrin proton signals suggests

that not all of the porphyrin was present as TPP-AlO-tBu; some unreacted TPP-H<sub>2</sub> may have been present. However, the predominant signals are three large singlets at 1.0, 1.3 and 1.4 ppm, with the signal at 1.4 ppm being by far the largest. While the two weaker signals are consistent with t-butanol<sup>20</sup>, the large signal at 1.4 ppm remained unaccounted for. The use of this initiator for the polymerization of ethylene oxide also yields unexpected results. GPC revealed that a very high molecular weight, highly polydisperse polymer was formed ( $\langle M_n \rangle \sim 122,000$ , PDI=7.6). It is clear that a different initiator species, probably the same species responsible for the 1.4 ppm signal, was responsible for the polymerization. The best explanation for these results is that the excess Et<sub>3</sub>Al reacted with t-butanol and/or methanol to form the aluminum trialkoxide. Zinc alkoxides are known to initiate the ring opening polymerization of epoxides by a coordinate mechanism<sup>21</sup>. Aluminum alkoxides also polymerize lactones by a similar mechanism<sup>22</sup>. For epoxides, these polymerizations generally result in highly polydisperse products. Taken together, these results suggest that propagation through the TPP-Al-OR species is quite slow, substantially slower than literature results would suggest, and that polymerization due to the alkoxide competes effectively; excess Et<sub>3</sub>Al should be avoided. The results of reactions with TPP-Al-Et also suggest that relatively long reaction times are required to form the alumino-



porphyrin adduct from hindered alcohols in good yield. Despite the fact that the results of polymerizations using these alkoxy aluminumporphyrins were not consistent with those reported for methoxy or chloro aluminumporphyrin initiation, it was apparent that such species could be prepared and that these species would react with epoxide monomers. Rather than attempt to optimize the solution reaction conditions, it was decided that the reaction would be attempted on the surface. It remained to be established that any reaction would occur between TPP-Al-Et and hydroxyl surfaces.

PCTFE-OH surfaces were reacted with TPP-Al-Et under conditions comparable to those used to prepare the alkoxy aluminumporphyrins in solution. Although the films appeared colored to the naked eye, there was no evidence of reaction by ATR-IR, indicating that the reagent does not penetrate deep into the modified region. The XPS atomic composition data are summarized table 9. The C:N ratio indicates that far less than quantitative reaction of the surface hydroxyl groups had occurred. In addition, the O:N and Al:N ratios indicate an excess of both oxygen and aluminum; the O:C ratio for the porphyrin surface should be lower than that of the starting hydroxyl surface and the N:Al ratio should be 4:1. This, combined with the hazy color of the surface, suggests the presence of aluminum oxides. It was not clear if any PCTFE-OAl-TPP groups were formed. Increasing the

**Table 9.** XPS atomic composition data for aluminoporphyrin  
surfaces and aluminoporphyrin initiated  
graft polymerizations.

#	Sample	L (hrs.)	Monomer	Takcoff Angle	Σ	E	Q	N	Q	Al
1	PCTFE-OAl-TPP	24	-----	150 750	100 100	6 10	44 33	7 5	9 8	-- 3
2	PCTFE-OAl-TPP	39	-----	150 750	100 100	4 9	42 36	5 3	9 10	2 4
3	PCTFE-OAl-TPP	65	-----	150 750	100 100	6 15	27 25	3 --	6 7	4 4
4	PCTFE-OAl-TPP	24	-----	150 750	100 100	1 3	16 15	7 7	-- 2	3 2
5	PCTFE-OAl-TPP (#4) extracted w. CH <sub>2</sub> Cl <sub>2</sub>	24	-----	150 750	100 100	4 8	47 46	5 4	-- 2	9 9
6	PCTFE-OAl-TPP (#4) wash w. MeOH/HCl	24	-----	150 750	100 100	51 29	11 12	-- --	19 10	-- --
7	PCTFE-OAl-TPP (#3)	44	EO	150 750	100 100	13 14	28 25	0.7 --	2 3	3 3
8	PCTFE-OAl-TPP (#1)	44	EO	150 750	100 100	18 33	72 73	4 5	5 6	16 20
9	PCTFE-OAl-TPP (#4)	65	PO	150 750	100 100	16 10	21 20	-- --	-- --	-- --
10	PCTFE-OH, TPP-Al-Cl	42	PO	150 750	100 100	15 19	29 27	2 2	-- --	3 3
11	PCTFE-OH, TPP-Al-Cl wash w. MeOH/HCl	43	PO	150 750	100 100	15 19	23 21	-- --	10 11	-- --
12	PCTFE-OH, TPP-H	24	-----	150 750	100 100	4 8	13 14	5 4	-- --	-- --



reaction time had no significant effect on the yield, although the 65 hour product appeared to have less oxide on the surface. Exposure of these surfaces to ethylene oxide failed to produce any clear evidence of polymerization by ATR-IR or XPS, although it should be recognized that the addition of a small amount of ethylene oxide would be difficult to detect. The reaction was repeated, taking care this time to avoid excess  $\text{Et}_3\text{Al}$ , but the same results were obtained; see table 9, entry 4. The oxygen-aluminum bond in the TPP-Al-OR species is reported to be cleaved by  $\text{HCl}$ <sup>23</sup>. When the TPP-Al-Et treated films were washed with dilute methanolic  $\text{HCl}$ , all of the nitrogen and aluminum was removed (see table 9, entry 6). Surface rearrangement also occurred, as evidenced by the increase in the F:C and Cl:C ratios and the evolution of a high binding energy carbon ( $\text{CF}_2$ ) peak in the  $\text{C}_{1s}$  region of the XPS spectrum. Surprisingly, more PCTFE appeared to be present in the outer angstroms than deeper in the XPS sampling depth. This surface was used to initiate the polymerization of propylene oxide and the product was washed with methanolic  $\text{HCl}$ . A small amount of monomer addition should be easier to identify under these conditions. The presence of methyl groups in the ATR-IR spectrum would provide clear evidence of monomer incorporation and removal of the aluminum oxides should allow the identification of any significant increase in the O:C ratio. No change was observed in the ATR-IR spectrum. Once again,

acid washing appeared to result in surface rearrangement; see table 9, entry 9. Although it is possible that there was some reaction between the surface and the epoxide monomers, it is clear that the yield of graft polymer is, at best, very poor. Part of the problem may be that clean PCTFE-OAl-TPP surfaces could not be prepared. Although it was unclear if aluminum oxide formation was the result of the reaction of the surface with  $\text{Et}_3\text{Al}$  that had failed to react with TPP- $\text{H}_2$  or some subsequent reaction of the porphyrin surface with adventitious impurities, it did not seem likely that a practical way of avoiding oxide formation would be found. As a result, no further work was done in this area.

Given the mechanism of immortal polymerization, no loss of grafting efficiency should be observed if the polymerization is initiated in solution in the presence of a hydroxyl surface, at least if steric interactions between the film and the porphyrin are not so great as to dramatically restrict chain transfer to the surface. A number of experiments were performed in which initiation was carried out using TPP-Al-Cl in solution. TPP-Al-Cl was prepared as described by Inoue<sup>24</sup>. The polymer that was formed in solution was characterized by GPC. Reactions were carried out using ethylene oxide, with the appropriate monomer:initiator ratio to produce a molecular weight of 28,000 amu, and using propylene oxide, with monomer:initiator ratios chosen to

produce polymers of the following molecular weights: 19,500, 7,500 and 11,600. In all of these reactions, the products were monodisperse, but only low molecular weight polymers (1,400-3,000 amu) were obtained. Only low molecular weight polymers were obtained when the reaction was run in the absence of the PCTFE-OH film as well. As shown in figure 22, a relatively weak methyl absorbance was observed in the ATR-IR spectrum of surfaces reacted with propylene oxide. While some incorporation of the monomer occurred, the yield of graft polymer was obviously very poor. Unlike the films prepared from PCTFE-OAl-TPP, these films were clear and colorless. However, XPS results indicate that some porphyrin and aluminum oxide were present on the surface prior to acid washing (compare table 9, entry 10 to entry 11). IR spectra of the oligomeric products reveal that a substantial number of hydroxyl end groups are present. In the absence of water, only Cl and O-Al-TPP end groups should be present for reactions initiated with TPP-Al-Cl. However, it seems unlikely that enough protic impurities were present to result in such low molecular weights. It is not clear why the polymerizations did not proceed to completion. Further, it appears likely that even less polymerization occurred on the surface. One possible reason for this is the difficulty of inserting the monomer into the aluminum-oxygen bond. This requires the monomer to be between the plane of the porphyrin and the polymer film. A control experiment was



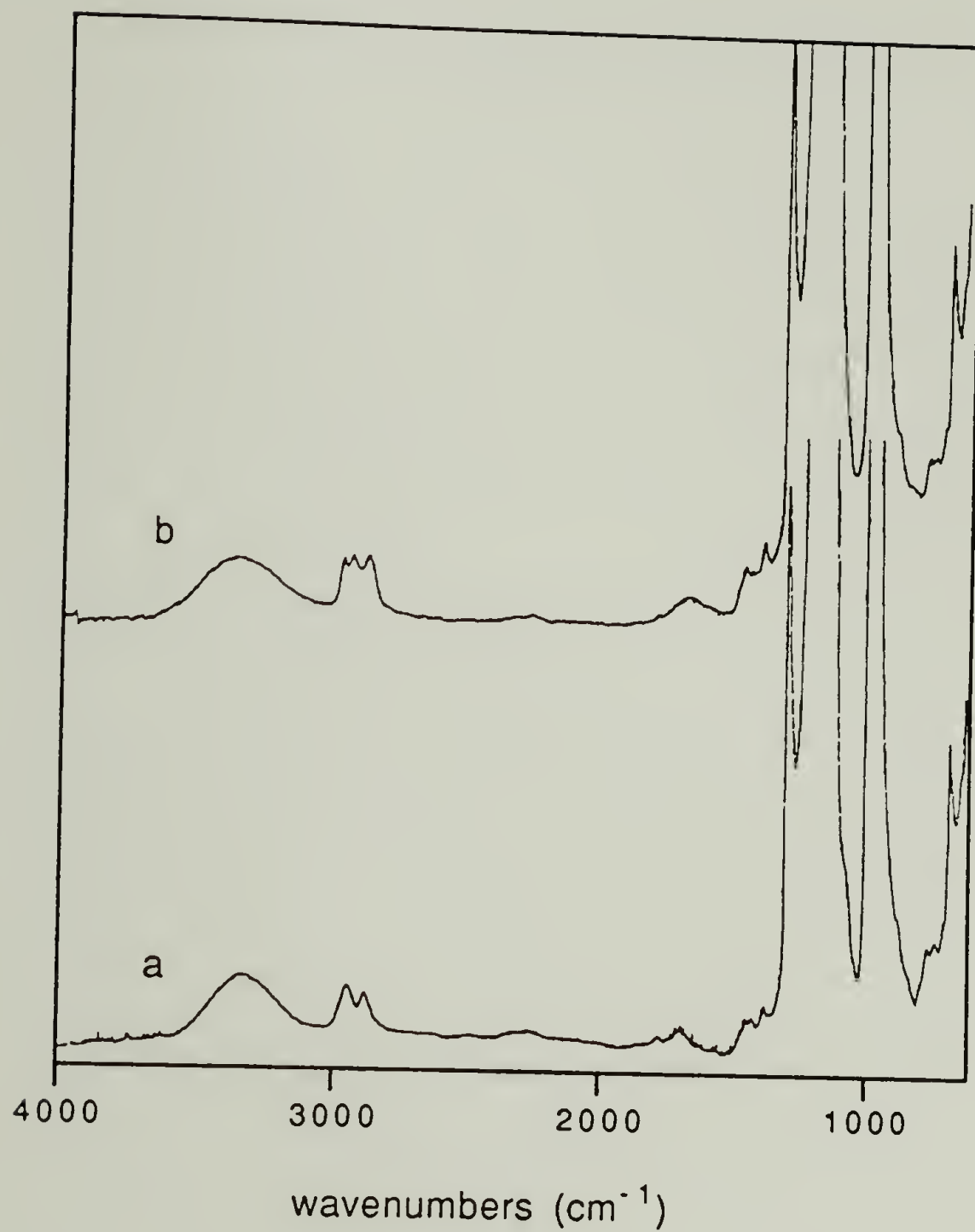


**Figure 22.** ATR-IR spectra of (a) PCTFE-OH; (b) PCTFE-OH + TPP-Al-Cl/P.O.

performed in which PCTFE-OH films were soaked in a solution of TPP-H<sub>2</sub>. Despite extensive washing the films remained green; XPS (table 9, entry 12) verified the presence of adsorbed porphyrin. If strong interactions exist between the porphyrin molecule and the polymer surface, they would further hinder monomer insertion. It is clear from these results that the formation of a well behaved catalyst species and the polymerization from these species to yield polymers with predictable molecular weights may be more difficult to achieve than the literature suggests. However, even if the chain lengths were as small as those formed in solution, more polymer should have been present on the surface if "immortal" kinetics were followed in reactions with the polymer surface. As a result, no further research was carried out on this system.

#### Polymerization of THF from Halogenated Surfaces

One alternative to using a water-insensitive polymerization system is to initiate the polymerization under strictly anhydrous conditions. It would be most desirable to use a system in which initiation and polymerization are fast. Unfortunately, reactive initiator species are likely to be killed by adventitious impurities before the monomer can be introduced, as was observed for the attempted polymerization of MMA from alkoxide surfaces. In situ generation of lithium alkoxides from LDA has proven to be of

little use in polymerizations. Another promising in situ-generated initiator is the triflate group. Treatment of polymers containing allylic or benzylic halogens at chain ends (or along the polymer backbone) with silver salts possessing non-nucleophilic counterions ( $\text{CF}_3\text{SO}_3^-$ ,  $\text{ClO}_4^-$ ) in the presence of tetrahydrofuran (THF) results in the formation of the block<sup>25</sup> (or graft<sup>26</sup>) copolymer. Cationic polymerization of THF under these conditions is rapid and the polymerization is living. These results led to the investigation of the polymerization of THF from halogenated surfaces in the presence of silver triflate.

Reduced PTFE films (PTFE-C) react with chlorine and bromine to form halogenated surfaces<sup>27</sup>. The reaction of FEP with sodium naphthalide results in an eliminated surface (FEP-C) with similar reactivity (see part I). These surfaces were reacted with chlorine under conditions comparable to those used to chlorinate PTFE-C. The XPS results, summarized in table 10, indicate that chlorine is incorporated in high yield without significant oxidation of the film. The presence of residual unsaturation, as evidenced by residual intensity in the  $1600\text{ cm}^{-1}$  and  $1450\text{ cm}^{-1}$  regions (see figure 23) suggests that the halogens on the resulting surface should react like allylic or benzylic halogens. Initially, the surfaces were reacted under condition used to graft THF to chlorinated poly(butadiene) in solution.<sup>28</sup> The reactions were carried out using silver triflate dissolved in



**Table 10.** XPS atomic composition data for room temperature-initiated graft polymerizations of THF.

#	Sample	Polymerization Conditions	Takeoff Angle	C	F	Q	Q	Ag	contact Angle
--	FEP-Cl	-----	150	100	3 +/-2	12 +/-3	34+/-5	--	750/350
			750	100	5 +/-3	11 +/-3	31+/-6	--	
1	FEP-Cl	0.026 M AgOTf, 66 h	150	100	3	17	16	--	720/430
			750	100	5	18	18	1	
2	FEP-Cl	0.26 M AgOTf, 72 h	150	100	15	28	12	--	
			750	100	32	28	13	--	
2	FEP-Cl	0.26 M AgOTf, 72 h extracted w. THF	150	100	4	20	16	--	
			750	100	6	19	15	--	
3	FEP-Cl	0.26 M AgOTf, 4 days sealed tube	150	100	6	24	3	--	900/580
			750	100	13	22	4	--	
4	FEP-Cl	0.26 M AgOTf, 4 days dist. into sealed tube	150	100	11	28	4	2	720/500
			750	100	25	22	4	1	

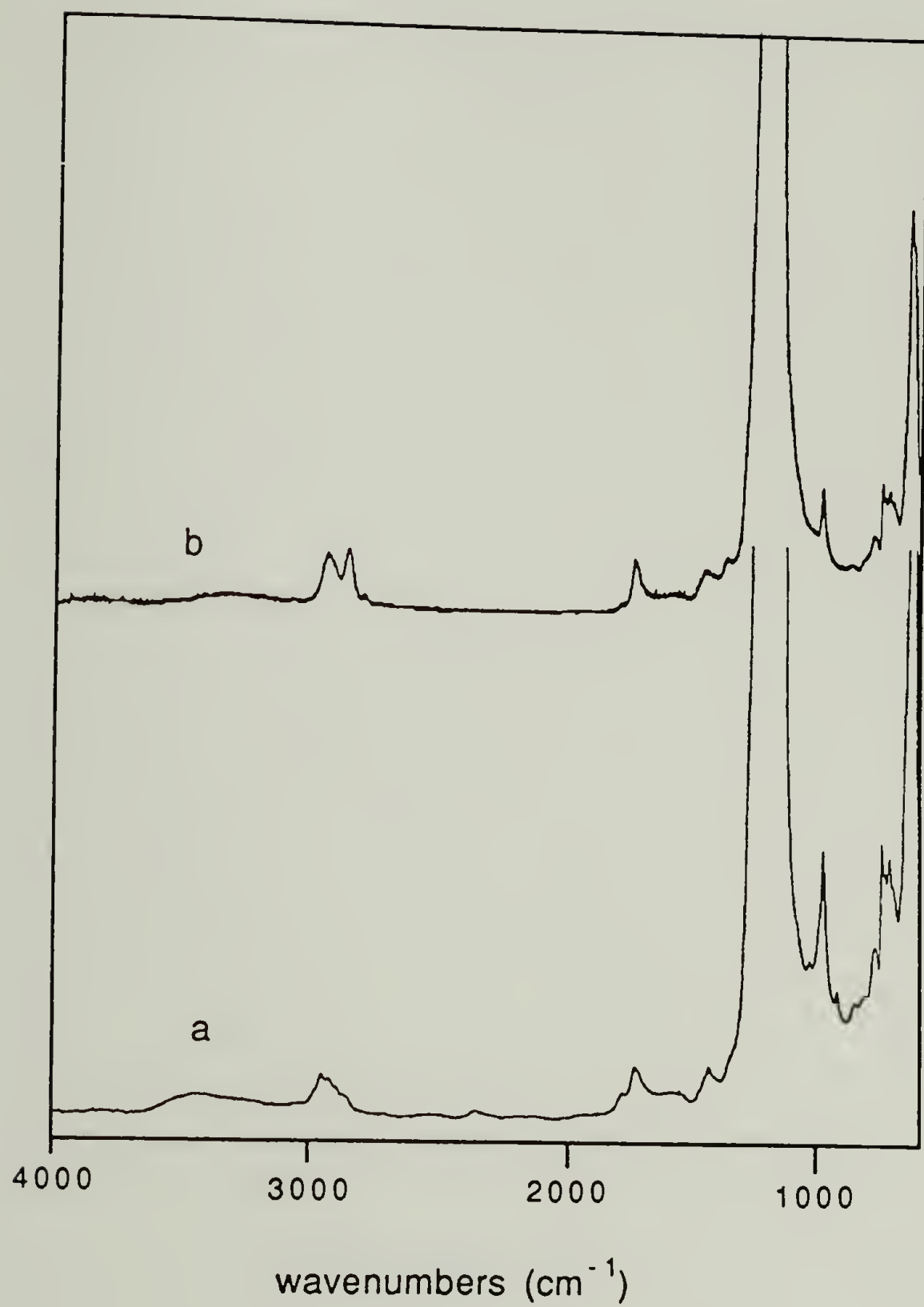


**Figure 23.** ATR-IR spectra of (a) FEP-Cl; (b) FEP(Cl)-g-THF, reacted at room temperature.

THF at room temperature. The ATR-IR spectrum of the resulting product, shown in figure 23, provides clear evidence of reaction with THF. The methylene intensity increased substantially relative to that of the carbon-fluorine bands. The XPS data (table 10) shows an increase in the oxygen to carbon ratio, as expected (poly(tetrahydrofuran) has an O:C ratio of 1:4), but fluorine and unreacted chlorine were clearly present in the outer angstroms. Several polymerizations were carried out. Higher concentrations of silver triflate and longer reaction times (up to 4 days) were used. Attempts were made to minimize contamination by performing the reaction in a sealed tube. As shown in table 10, increasing the concentration and reaction time had the effect of increasing the O:C ratio and decreasing the amount of unreacted chlorine. However, the polymer substrate clearly had not been covered by the graft polymer. The high fluorine content of some of the surfaces suggests that some of the triflate remained in the film, possibly as trifluoromethanesulfonic acid. The ATR-IR spectra of these surfaces showed no further increase in the relative intensity of the methylene absorbance. Gravimetric analysis indicated that no significant mass increase had occurred. This result does imply that enough THF was added (MW=72) to replace the chlorine that was lost (MW=35). The contact angles for the surfaces (with the exception of #3) were similar to each other and essentially the same as FEP-C. Clearly, the



overall efficiency of grafting was low. It is interesting to note that there was no significant increase in the intensity of the hydroxyl absorbance in the ATR-IR spectra of these samples. The reaction of triflate groups with water prior to THF initiation should result in the introduction of secondary hydroxyl groups to the polymer backbone. The reactivity of these hydroxyl groups should be similar to that of hydroxyl groups introduced by hydroboration and oxidation. The reaction of the propagating cyclic oxonium ion with water should result in the formation of hydroxy-terminated oligomers. This surface should react much like the PCTFE-OH surface, which also contains primary hydroxyl groups separated from the surface by a number of methylene groups. In order to determine how many of each type of hydroxyl group was introduced in the graft reaction, hydroxyl groups on the surface of chlorinated and graft polymer samples were labeled with HFBC. The reaction was carried out in THF with pyridine catalysis to label primary hydroxyl groups, and in pyridine in the presence of DMAP, to label more hindered hydroxyl groups.<sup>29</sup> The XPS atomic composition data for the labeled surfaces, summarized in table 11, confirms the ATR-IR results. No increase in the reactivity of the surface towards HFBC occurred due to the reaction with THF and silver triflate. The high fluorine content in entry 3 was due to the appearance of virgin FEP in the outer angstroms, as a result of surface degradation or rearrange-

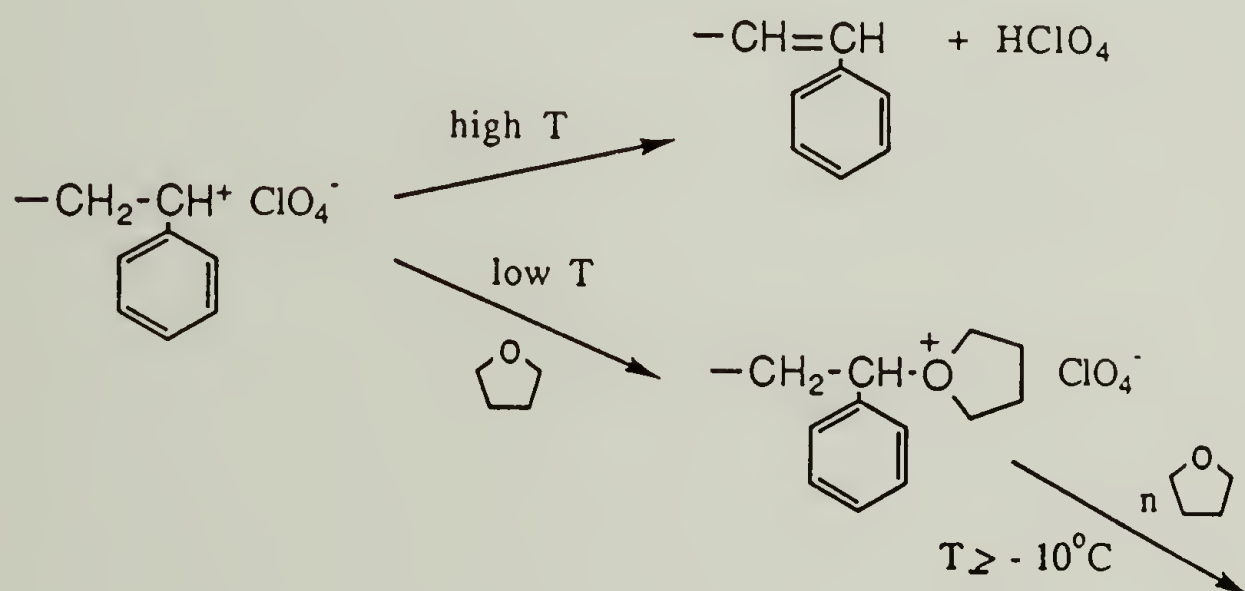
**Table 11.** XPS atomic composition data for HFBC labeling  
of graft THF surfaces.

#	Sample	Conditions	Takeoff Angle	C	F	O	Q
1	FEP-g-THF #3	a, 30 h	150 750	100 100	18 19	26 22	16 13
2	FEP-g-THF #4	a, 47 h	150 750	100 100	9 10	21 21	6 6
3	FEP-g-THF #4	b 48 h	150 750	100 100	26* 36*	20 16	8 8
4	FEP-Cl	a, 47 h	150 750	100 100	14 12	14 13	19 16
5	FEP-Cl	b, 48 h	150 750	100 100	10 11	20 17	10 9 (2 N) (2 N)

(a) 0.2 ml. pyridine, 10 ml. THF      (b) 0.082 g. DMAP, 20 ml. pyridine      \* virgin FEP present in the C<sub>1s</sub> spectrum

ment. A single high binding energy carbon signal was observed in the  $C_{1s}$  region, unlike the combination of  $CF_3$ ,  $CF_2$  and  $C=O$  signals observed for surfaces containing substantial amounts of HFBC.

While these results could conceivably be explained by the reaction of the propagating end of one chain with a neighboring "dead" hydroxy-terminated chain to form a cyclic ether surface, a closer study of the literature revealed a more likely explanation, illustrated by equation 5. When bromine-terminated polystyrene (PsBr) was reacted with THF and silver perchlorate at room temperature  $\beta$ -hydride elimination was found to be the predominant reaction, resulting in the formation of a small number of high molecular weight poly(tetrahydrofuran) graft copolymer chains and a large



**Equation 5.** The effect of temperature on the reaction of AgOTf and THF with PSBr.



number of vinyl-terminated polystyrene chains<sup>30</sup>. In the case of reaction with FEP-Cl at room temperature, the removal of chlorine should result in regeneration of the eliminated surface and the addition of a few high molecular weight graft polymer chains. This would explain why chlorine was removed without introducing a significant number of hydroxyl groups. The absorbances due to unsaturation in FEP-Cl were broad and were not completely eliminated by chlorination, making the identification of further elimination due to the graft reaction by ATR-IR difficult. For the PsBr system, it was found that the extent of elimination could be controlled by decreasing the reaction temperature. If initiation (formation of the perchlorate and reaction with THF to form the cyclic oxonium ion) was carried out at a low temperature, elimination was greatly reduced. The initiation efficiency (calculated from the ratio of PS to PS-g-p(THF) chains) was increased to 75% for initiation at -78°C. As a result, low temperature initiation was studied.

The difficulty encountered in removing chlorine from the surface at room temperature suggested that a more reactive halogenated surface would be advantageous. It was found that benzyl bromides were much more reactive than benzyl chlorides towards silver perchlorate.<sup>31</sup> FEP-Br surfaces could be prepared by reaction with bromine under conditions similar to those used to brominate PTFE-C. Slightly less bromine was incorporated than chlorine. These

surfaces were reacted with silver triflate in a sealed tube using initiation temperatures of (1)  $-78^{\circ}\text{C}$  and (2)  $-23^{\circ}\text{C}$ , and then the polymerization was allowed to proceed at  $-10^{\circ}\text{C}$  (propagation does not occur below  $-10^{\circ}\text{C}$ ). The results were dramatic; the polymer surfaces exhibited an iridescent sheen, suggesting that a layer of poly(THF) thick enough to produce interference effects had been deposited on the surface. The ATR-IR spectrum, shown in figure 24, exhibits very intense methylene stretching ( $2945$ ,  $2860\text{ cm}^{-1}$ ) and C-O ( $1115\text{ cm}^{-1}$ ) absorbances, along with weaker absorbances at  $1490\text{ cm}^{-1}$  and  $1370\text{ cm}^{-1}$ , that were also present in spectra of commercial dihydroxy-terminated poly(THF) (Terathane 2900, DuPont). Very little change occurred as a result of extracting the  $-23^{\circ}\text{C}/-10^{\circ}\text{C}$  product for 24 hours with THF. Extraction of the film reacted at  $-78^{\circ}/-10^{\circ}\text{C}$  with THF for 24 hours resulted in removal of some poly(THF), as evidenced by ATR-IR. The washing procedure used for this sample had resulted in some solution polymerization. Adsorption of this polymer probably accounts for this result. A second extraction resulted in little decrease in the intensity of the poly(THF) bands. The spectra of both products were nearly identical after extraction, indicating that the initiation efficiency was comparable at both temperatures. The XPS atomic composition data, summarized in table 12, indicates that the atomic composition of the outer 40 Å is also the same for both samples. More important, essentially no

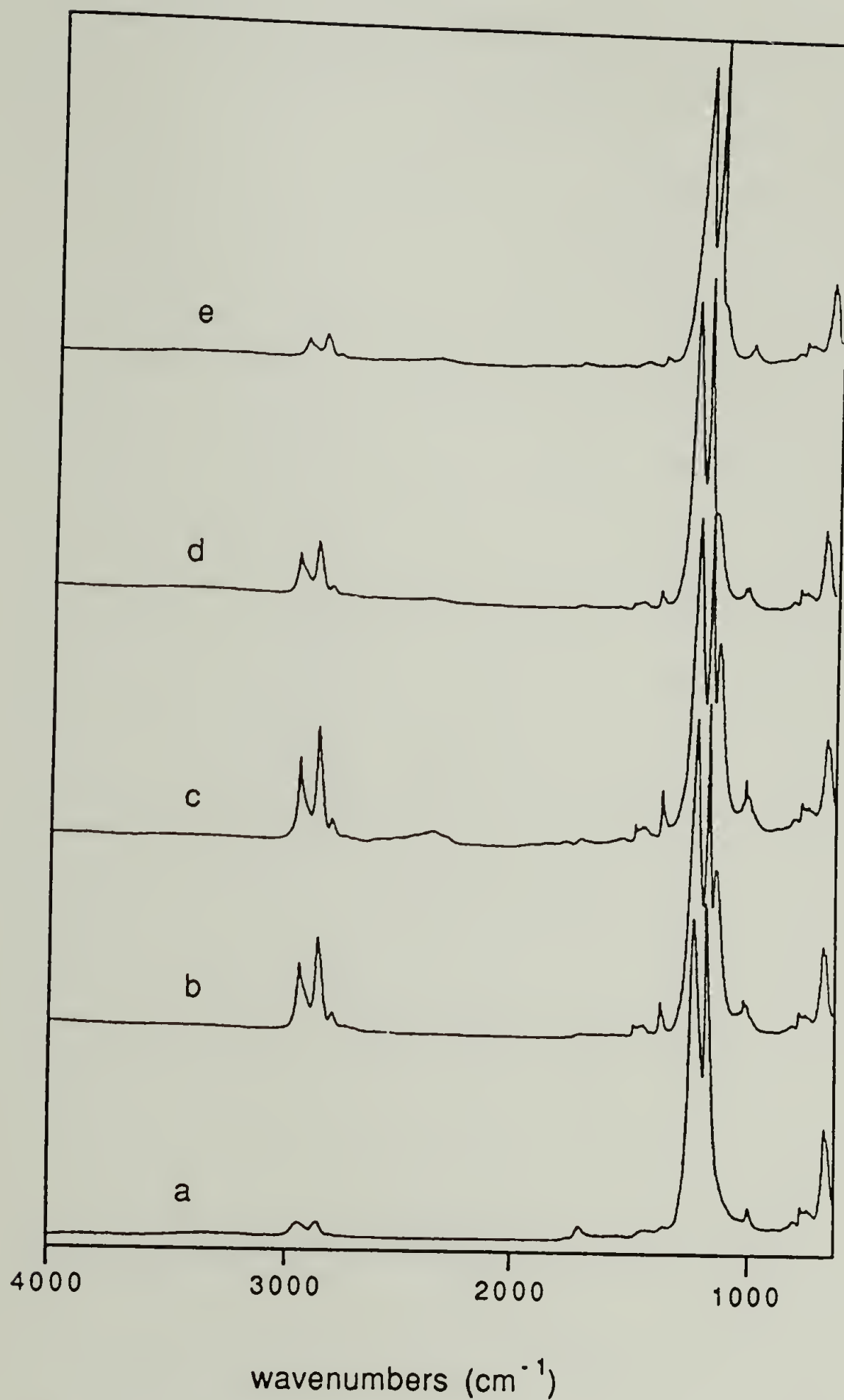


**Figure 24.** ATR-IR spectra of (a) FEP(Cl)-g-THF, reacted at room temperature; FEP(Br)-g-THF reacted at: (b)  $-78^{\circ}\text{C}/-10^{\circ}\text{C}$ , (c)  $-23^{\circ}\text{C}/-10^{\circ}\text{C}$ , (d)  $-10^{\circ}\text{C}$ ; (e) FEP(Cl)-g-THF, reacted at  $-23^{\circ}\text{C}/-10^{\circ}\text{C}$ .



**Table 12.** XPS atomic composition data for low temperature-initiated THF graft polymerizations.

#	Sample FEP-Br	Polymerization Conditions	Takeoff		C	F	O	Br	Contact Angle 60°/35°
			Angle	Angle					
--		-----	150		100	2	11	28	
			750		100	5	11	28	
1	FEP-Br	0.43 M AgOTf, -78°C 20 h, -10°C 72 h	150		100	3	24	<.1	80°/44°
			750		100	<.5	25	<.1	
2	FEP-Br	0.43 M AgOTf, -23°C 18 h, -10°C 72 h	150		100	1	26	<.1	82°/50°
			750		100	1	22	<.1	
3	FEP-Br	0.13 M AgOTf, -10°C 70 h	150		100	3	28	<.1	-----
			750		100	1	25	<.1	
4	FEP-Cl	0.13 M AgOTf, -23°C 70 h	150		100	<.1	23	<.1	-----
			750		100	<.1	23	<.1	

bromine and very little fluorine was present. In fact, for the  $-78^{\circ}\text{C}/-10^{\circ}\text{C}$  product (entry 1), more fluorine was present at a  $15^{\circ}$  takeoff angle (10 Å) than at a  $75^{\circ}$  takeoff angle (40 Å). The O:C ratio is very close to 1:4 at both takeoff angles. In addition, the contact angles for both films are identical and substantially higher than those obtained for the halogenated (hydroxyl contaminated) starting materials. All of these results, including the peculiar appearance of the film samples, can be explained by the presence of a relatively thick, relatively uniform (no large areas of the surface containing less than 40 Å of poly(THF)) graft polymer overlayer. Examination of the  $\text{C}_{1s}$  region, shown in figure 25, supports this conclusion. The spectrum of FEP-Br is clearly asymmetrical, possessing a distinct high binding energy shoulder due to carbon bonded to bromine. The spectrum of the graft polymer is identical at both  $15^{\circ}$  and  $75^{\circ}$  takeoff angles and is symmetrical, but very broad. Curve fitting (figure 26) shows that this spectrum can be represented by two curves of equal area with maxima separated by approximately 2 eV. This is precisely what is expected for poly(THF), which has two carbons bonded only to other carbon and two carbons bonded to oxygen.

Further confirmation of overlayer structure was obtained by  $^3\text{He}^+$  ion beam etching. The etching parameters and changes in the XPS atomic composition ( $75^{\circ}$  takeoff angle) are summarized in figure 27. After very mild etching the

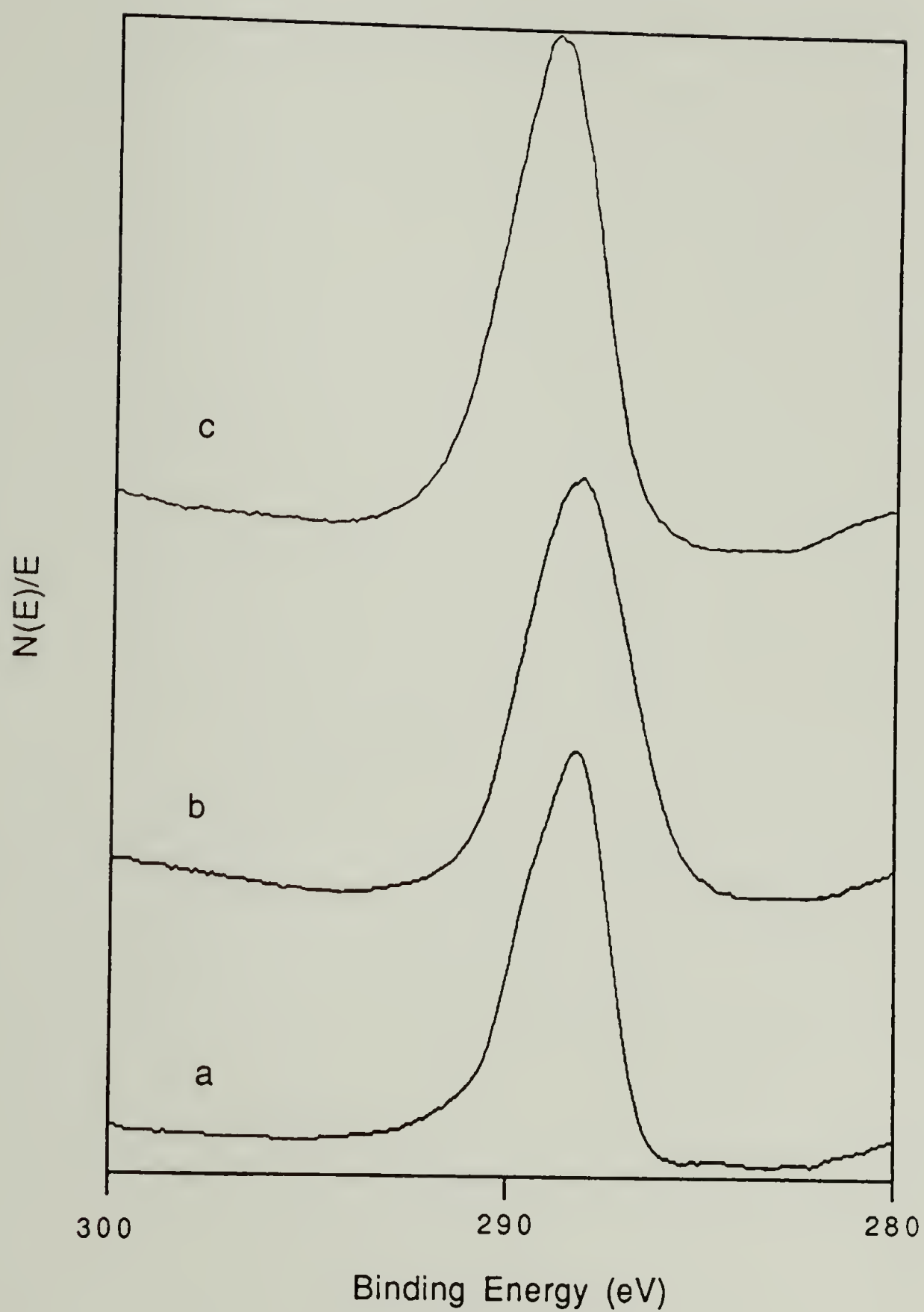
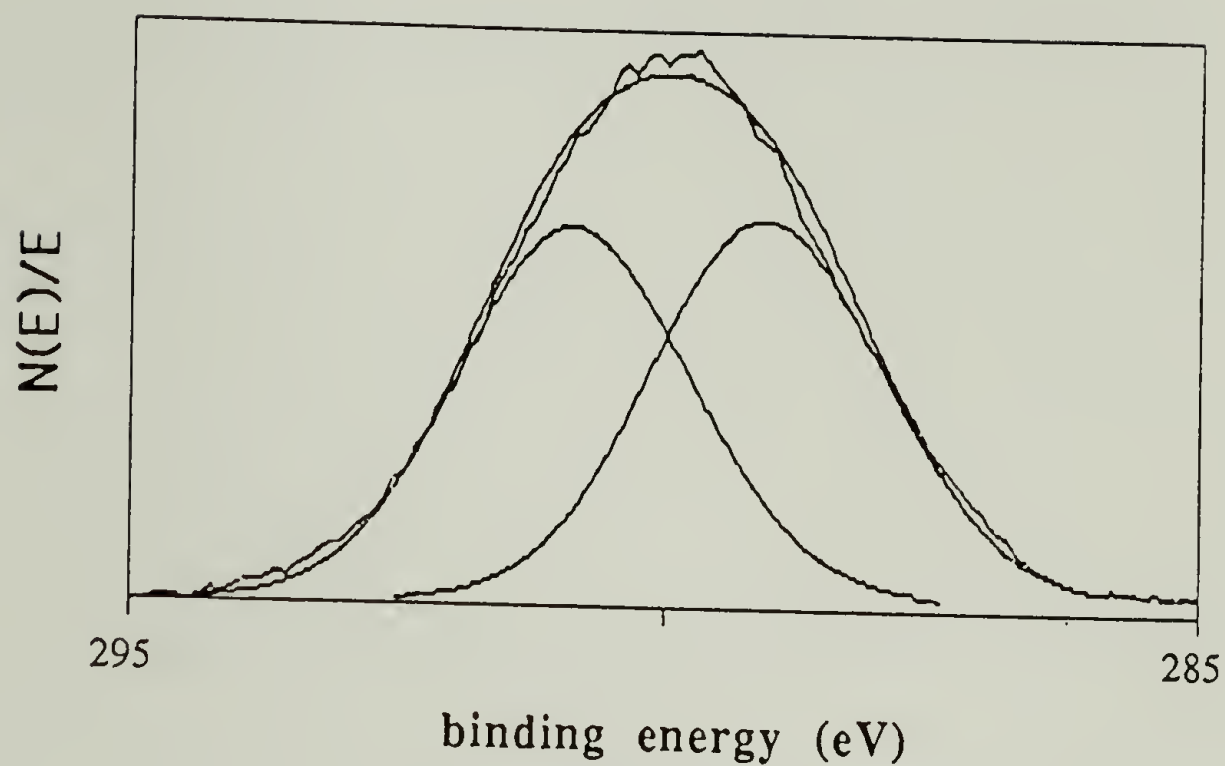


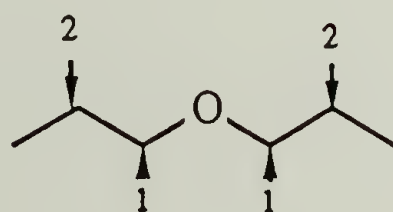
**Figure 25.** XPS spectra (C<sub>1s</sub> region) of (a) FEP-Br; (b) FEP(Br)-g-THF, -78°C/-10°C; (c) FEP(Br)-g-THF, -78°C/-10°C, <sup>3</sup>He<sup>+</sup> ion etched.





<u>Band#</u>	<u>Position</u>	<u>Delta (eV)</u>	<u>% of Total Area</u>
1	290.85	1.84	49.7
2	289.01	0	50.3

Expect:



2 peaks of equal area,  $\Delta$  eV = 2

Figure 26. Curve fitting results (XPS,  $C_{1s}$  region) for FEP(Br)-g-THF,  $-78^{\circ}\text{C}/-10^{\circ}\text{C}$ .

# $^3\text{He}^+$ Ion Beam Etching

#	$V_e$	$I_e$	$I_t$	time
1-2	1 Kv	10 mA	80 nA	20 sec.
3	1 Kv	10 mA	130 nA	30 sec.
4	3 Kv	10 mA	1.2 $\mu\text{A}$	60 sec.
5	3 Kv	10 mA	1.5 $\mu\text{A}$	2 min.
6	3 Kv	25 mA	2.3 $\mu\text{A}$	5 min.

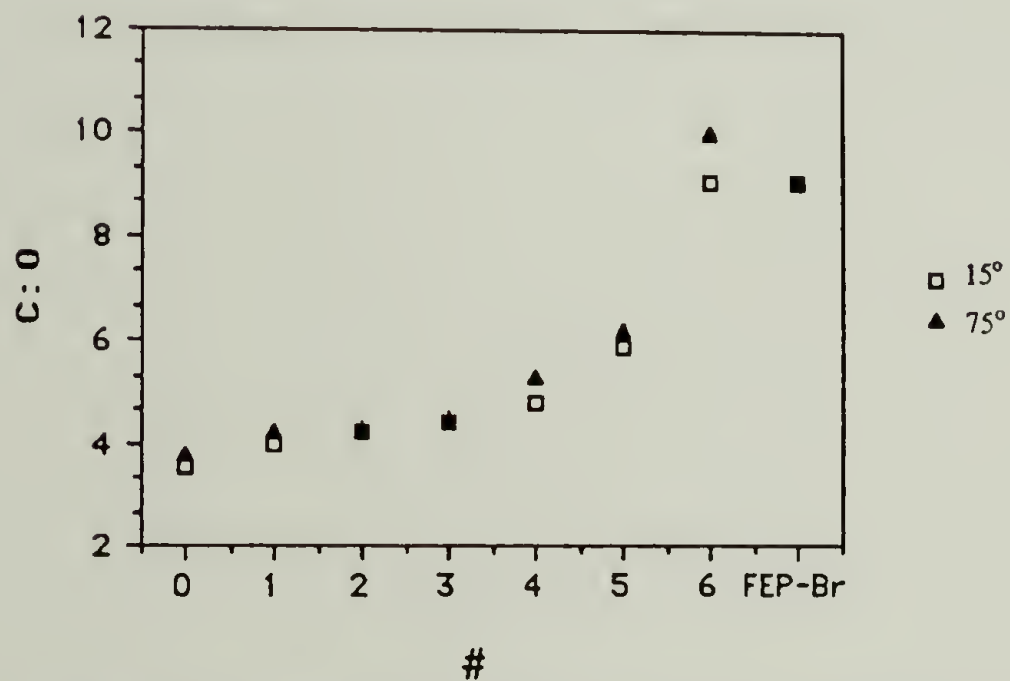
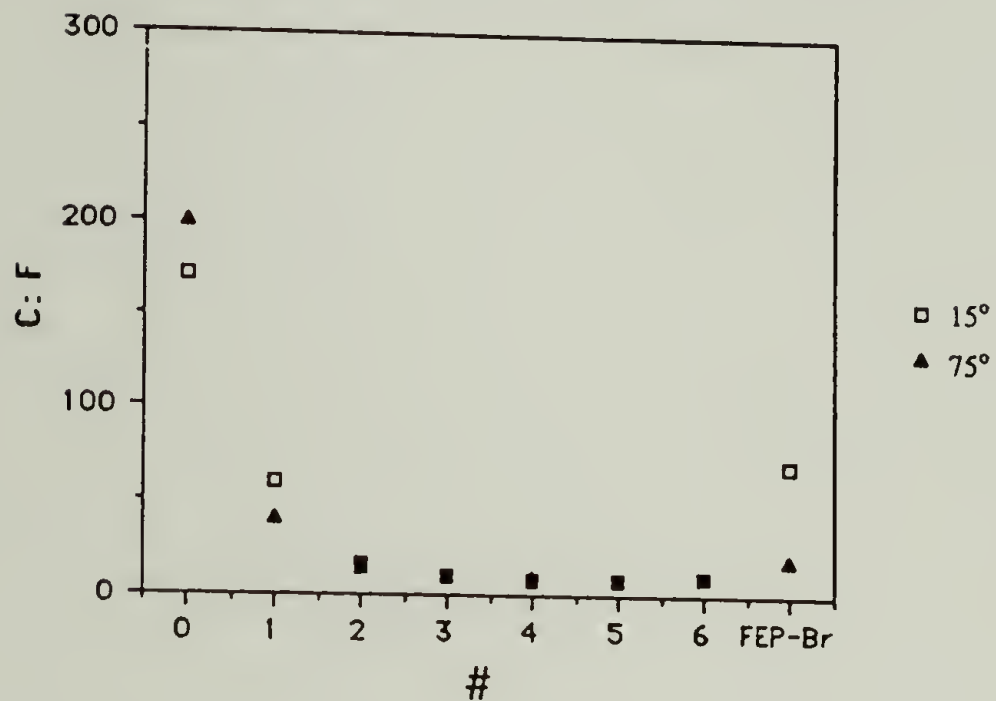
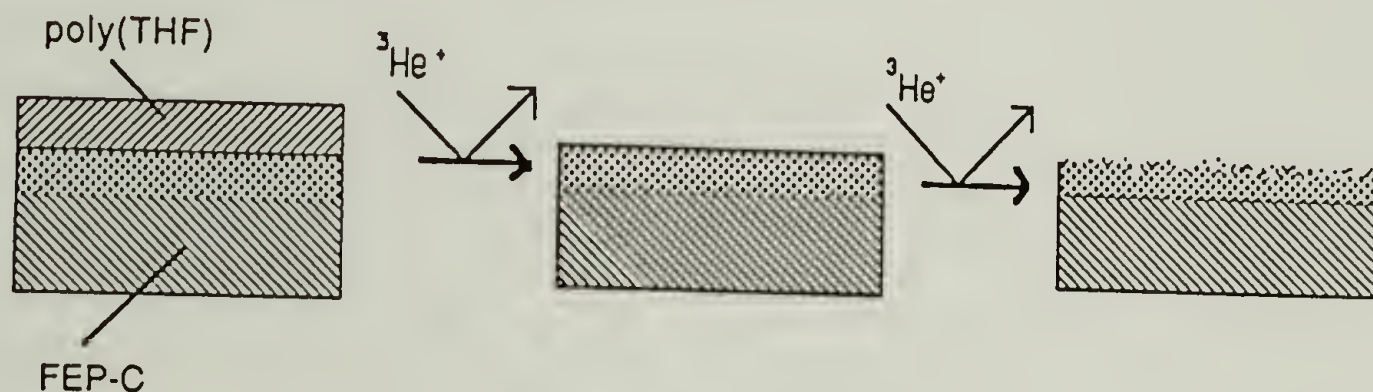


Figure 27.  $^3\text{He}^+$  ion etching results for FEP(Br)-g-THF, reacted at  $-78^\circ\text{C}/-10^\circ\text{C}$ .

C:F ratio returns to the value observed for FEP-Br. As more extensive etching occurs, the C:O ratio slowly increases to the value observed for FEP-Br. No bromine was present, indicating that the reaction with silver triflate was complete. The changes in the C:F and C:O ratios can be explained as shown in equation 6. Relatively mild etching removes the poly(THF) overlayer, exposing the fluorine-containing subphase. Polymerization of THF takes place deeper in the FEP-Br layer as well, resulting in an oxygen rich interpenetrating network-like interphase region consisting of poly(THF) and FEP-C. The crosslinked FEP-C is resistant



**Equation 6.** Effect of ion etching on low temperature-initiated THF graft surfaces.

to ion beam etching, so changes occur more slowly in this region. This explanation is also consistent with the changes in the  $C_{1s}$  region. Throughout the experiment the  $C_{1s}$  peak remained relatively broad and much more symmetrical than was



observed for FEP-C, although at the end of the experiment, a definite decrease in the carbon due to C-O is observed (see figure 25c). It is worth mentioning that the iridescent sheen was absent where the etching had occurred. A line was clearly visible separating areas where the beam had hit from those areas outside the raster lines.

SEM micrographs were taken of the graft surface before and after etching. Unlike the acrylamide graft surfaces, the graft surface is featureless (identical to FEP). Etched films appeared to have deep rounded furrows plowed into the surface, even in areas outside of the raster lines. The lack of FEP by XPS in these samples indicates that rearrangement occurred deep in the film, leaving the surface composition relatively unchanged. This rearrangement may be a result of local heating. In any case, these changes were enough to obscure any evidence of a "shelf" corresponding to the area from which the graft overlayer was removed.

Further experiments were performed to clarify the role of the reaction temperature and the choice of the halogen surface. When initiation was carried out from FEP-Br surfaces at  $-10^{\circ}\text{C}$  the reaction was much more efficient than at room temperature, but the relative intensity of the methylene bands (figure 24d) was substantially smaller than had been observed for surfaces initiated at lower temperatures. Once again, the XPS atomic composition data and the  $\text{C}_{1s}$  peak shape were consistent with a relatively thick poly(THF)

overlayer. When FEP-Cl was substituted for FEP-Br and the reaction was initiated at  $-23^{\circ}\text{C}$ , the product exhibited no visual evidence of reaction, but the ATR-IR spectrum (figure 24e) showed substantial methylene intensity. The XPS atomic composition and  $\text{C}_{1s}$  peak shape were identical to those of surfaces prepared from FEP-Br. In order to determine if chlorine removal was complete, as opposed to chlorine being shielded by the poly(THF) overlayer,  $^3\text{He}^+$  etching was performed on this surface. Etching resulted in an increase in fluorine and oxygen relative to carbon, as was observed for films prepared from FEP-Br. Even for extensively etched surfaces (cumulative time of 20 min at 25 mA, 3 kV) only traces of chlorine were observed. While it is not clear why, the initial reaction of silver triflate with the chlorinated surface appeared to have been faster at reduced temperatures.

While all of the evidence suggests that low temperature-initiated cationic polymerization of THF from halogenated precursor surfaces results in a reasonably thick and uniform graft polymer overlayer, it is important to note that the differences between the composition of the graft polymer and the reduced fluorocarbon subphase are rather subtle. It can not be concluded definitively from the XPS data that only poly(THF) is present in the outer 40 Å. In addition, the scope of this reaction is limited. Only poly(THF) graft copolymers have been reported, although other cyclic ethers

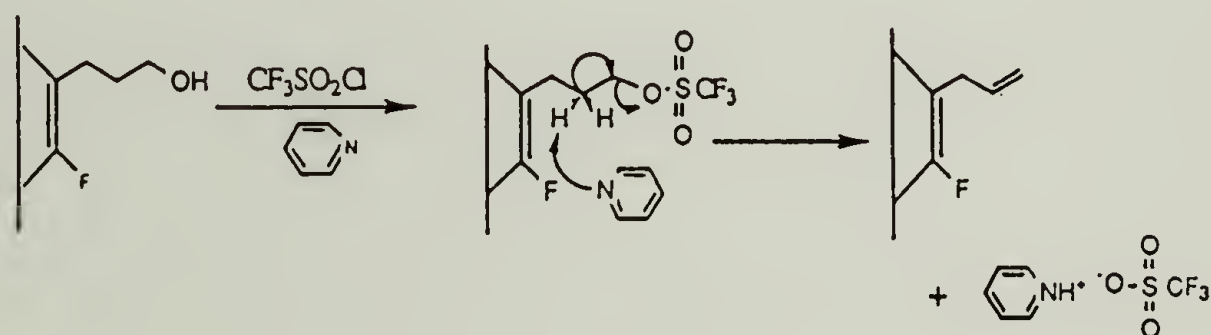
may polymerize under these conditions. The cationic polymerization reactions of other oxygen-containing monomers, such as cyclic acetals and lactones, suffer from side reactions that would probably limit their success. As a result, other graft polymerizations were studied in an effort to find a more generally applicable system.

#### Attempted Preparation of Triflate Surfaces and Preparation of Neopentyl Alcohol Surfaces

The results of the previous section demonstrate the viability of surface-initiated graft polymerization using triflate groups, but the in-situ initiation conditions limit the scope of the reaction. Triflate groups have the potential to polymerize a variety of monomers (cyclic sulfides, vinyl monomers) that may be initiated by contact with silver triflate. In addition, competitive elimination makes the initiation efficiency difficult to determine. If triflate surfaces could be prepared, isolated, and then used to polymerize the monomer in a subsequent step, some of these problems could be avoided. Previous work has shown that PCTFE-OH surfaces can be converted to the corresponding tosylate by reaction with tosyl chloride in pyridine.<sup>32</sup> It was of interest to determine if the corresponding triflate surface could be prepared. When PCTFE-OH surfaces were treated with trifluoromethanesulfonyl chloride (TfCl) in pyridine the results were disappointing. The XPS atomic



composition data (table 13) indicates the presence of sulfur and an increase in the O:C and F:C ratios, but nitrogen is also present, suggesting that at least some of the nitrogen and fluorine is due to pyridinium trifluoromethanesulfonate. Very little  $\text{CF}_3$  was present in the  $\text{C}_{1s}$  region. The ATR-IR spectrum, shown in figure 28, revealed that the problem was more severe. The hydroxyl band had disappeared, but, instead of an intense  $\text{S}=\text{O}$  band at  $\sim 1400\text{ cm}^{-1}$ , vinyl C-H absorptions were observed at  $3138$  and  $3067\text{ cm}^{-1}$ , vinyl C=C stretching bands were observed at  $1635\text{ cm}^{-1}$  and vinyl C=C deformation bands were observed at  $\sim 1000\text{ cm}^{-1}$  and  $670\text{ cm}^{-1}$ . The origin of the  $1490\text{ cm}^{-1}$  band is unclear, although it is consistent with C-H bending. These results indicate that the triflate was formed, but pyridine catalyzed elimination ( $\text{E}_2$ ), as shown in equation 7 occurs,



**Equation 7.** Elimination of PCTFE-OH in the presence of  $\text{TfCl}$  and pyridine.

resulting in terminal vinyl groups. Bond migration may also have occurred, resulting in cis C=C bonds. There are many

**Table 13.** XPS atomic composition data for reactions of PCTFE-OH with TfcCl.

Conditions	Takeoff Angle	C	F	O	Q	S	N
pyridine, -5°C, 55 h.	15°	100	41	31	3	6	3
	75°	100	32	26	3	3.5	3
CH <sub>2</sub> Cl <sub>2</sub> , pyridine -78°C, 2 h.	15°	100	27	35	--	--	--
	75°	100	22	21	--	--	--
CH <sub>2</sub> Cl <sub>2</sub> , pyridine -15°C, 15 h <sup>a</sup>	15°	100	47	36	--	7	--
	75°	100	43	29	2	5	--
theoretical <sup>b</sup>		100	69	46	--	15	--

<sup>a</sup> A large CF<sub>3</sub> peak was observed in the C<sub>1s</sub> region

<sup>b</sup> based on reaction of (CF=CF)(CF=C(C<sub>3</sub>H<sub>6</sub>OH))<sub>4</sub>, see K.-W. Lee and T.J. McCarthy, Macromolecules, **21**, 2318 (1988)

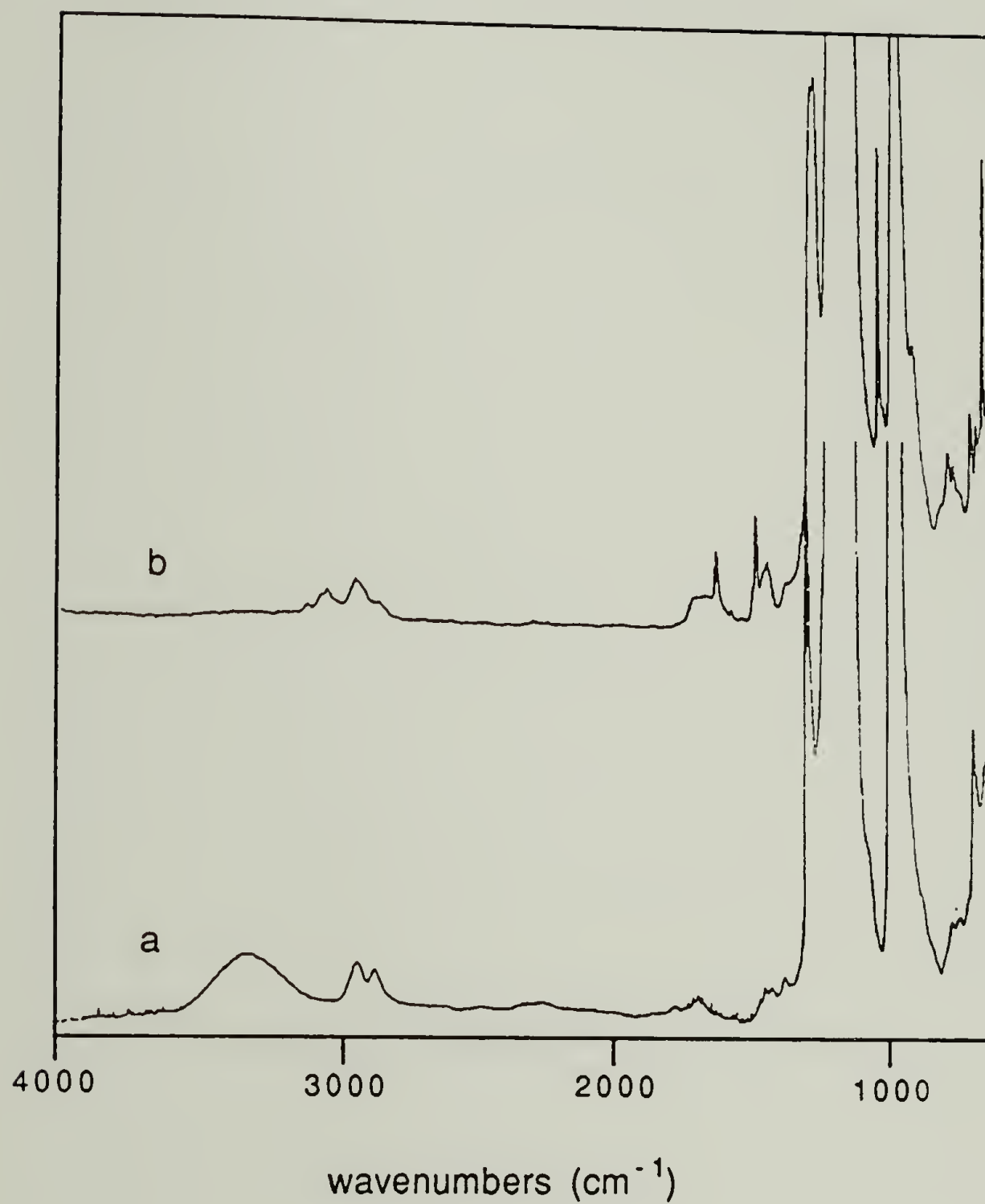


**Figure 28.** ATR-IR spectra of (a) PCTFE-OH, (b) PCTFE-OH + TfCl in pyridine.



reported preparations of alkyl triflates from alcohols possessing  $\beta$ -protons. In general, the alcohols were treated with trifluoromethanesulfonic anhydride in the presence of equimolar pyridine in halogenated hydrocarbons solvents. Most of these species are reported to be stable below 0°C.<sup>33</sup> PCTFE-OH films were treated with 1:1 TfCl and pyridine in dichloromethane at low temperatures. The films were not allowed to warm to room temperature until all of the solvent was removed. Some triflate groups appeared to be formed at -15°C by XPS, but no significant S=O absorbance was observed by ATR-IR. Clearly, relatively forceful conditions are required to form the triflate in reasonable yield on the surface.

A neopentyl alcohol surface would have the advantage of lacking the  $\beta$  proton site, substantially stabilizing the triflate. Triflates have been prepared from hindered alcohols using trifluoromethanesulfonic anhydride (Tf<sub>2</sub>O) in the presence of triethylamine or pyridine.<sup>34</sup> Preparation of the neopentyl alcohol surface was expected to be straightforward and analogous to the preparation of the n-propyl alcohol surface (PCTFE-OH). The corresponding bromo acetal was prepared in good yield from 3-bromo-2,2-dimethyl-1-propanol following the procedure of K.-W. Lee.<sup>35</sup> The lithium reagent was prepared by metal-halogen exchange with *t*-butyllithium in heptane; the product was dissolved in THF and then reacted with PCTFE under conditions known to pro-

duce deeply-modified PCTFE-OH films. The XPS atomic composition data, summarized in table 14, and the ATR-IR results (figure 29) indicate that a very shallow reaction occurred. Oxygen was introduced, but chlorine and large amounts of fluorine were present in the outer angstroms. Examination of the 15° takeoff angle C<sub>1s</sub> spectrum revealed a significant amount of CF<sub>2</sub>. Only weak methyl, methylene and hydroxyl bands were observed by ATR-IR. It was unclear at that time if shallow reaction was a result of some reagent or film-intrinsic factor such as the lower reactivity of the neopentyl lithium or the lower mobility of the reagent, or decomposition of the lithium reagent. The latter was suspected because of the transient color that was observed when THF was added. Similar observations have been noted for the decomposition of THF by lithium reagents.<sup>36</sup> Generally, primary lithium alkyls are stable in THF at these temperatures, but the neopentyl lithium reagent prepared here might be more reactive. In order to verify the stability of the lithium reagent, metal-halogen exchange was carried out as described previously and the product reacted with acetone. Diethyl ether was substituted for THF in order to eliminate the possibility of reaction with THF. The products were analyzed by GC-MS and GC-IR; the results are summarized in Appendix I. The majority of the bromoacetal remained unreacted and the LidiMePrOP that was formed reacted to yield

**Table 14.** XPS atomic composition data for PCTFE-diMe-OH surfaces.

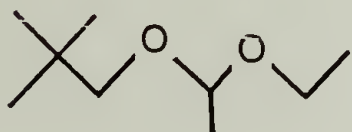
#	Time, Temp.	Solvents (ratio)	Takeoff Angle	C	F	O	Q	Contact Angle
1	2 h., -45°C	THF/hept. (0.7:1)	15° 75°	100 100	31 38	16 11	3 9	
2	45 min., -20°C	THF/hept. (0.7:1)	15° 75°	100 100	35 51	25 19	3 10	
3	24 h., -45°C	THF/hept. (0.7:1)	15° 75°	100 100	36 56	18 18	10 14	
4	2 h., -45°C	Et <sub>2</sub> O/hept. (4:1)	15° 75°	100 100	57 80	14 9	8 26	85°/55°
5	4 h., -20°C	Et <sub>2</sub> O/hept. (5:1)	15° 75°	100 100	21 20	12 10	1 4	74°/53°
6	6.5 h., -30°C	Et <sub>2</sub> O/hept. (1.7:1)	15° 75°	100 100	20 25	12 12	6 5	
7	3-4 h., -20°C	THF/hept. (5:1)	15° 75°	100 100	14+/-3 15+/-2	16+/-3 15+/-2	-- --	83°/55°





**Figure 29.** ATR-IR spectra of PCTFE-diMe-OH prepared by reaction for (a) 5.5 h at 0°C in 0.7:1 THF/hept.; (b) 6.5 h at -30°C in 1.7:1 Et<sub>2</sub>O/hept.; (c) 4 h at -20°C in 5:1 THF/hept.

comparable amounts of three major products. The low retention time product was identified as the acetal (I) produced by reaction with adventitious moisture. The

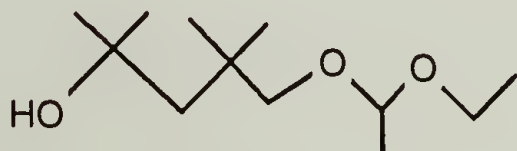


I



II

product that elutes just before the starting bromide has been tentatively identified as the dimer (II), resulting from coupling of the radical intermediate during metal-halogen exchange. The higher retention time product was identified as the acetone addition product (III). The

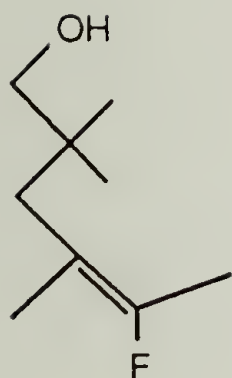


III

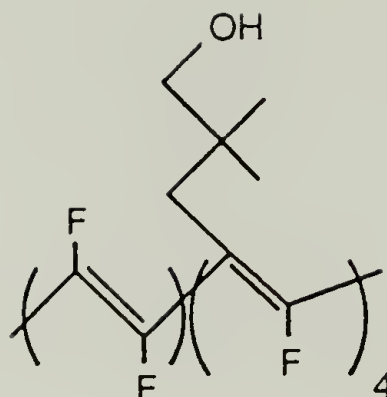
presence of a hydroxyl band in the IR spectrum of this product confirmed the assignment. Additional information was provided by reacting the lithium reagent with water; products I and II were isolated, III was not. It was clear that the lithium reagent could be prepared in reasonable yield and was stable, at least in diethyl ether/hydrocarbon solvent mixtures.

Several PCTFE film reactions were attempted using diethyl ether/hydrocarbon solvent systems. In every case, the XPS atomic composition data (table 14) and the ATR-IR results (figure 29) were consistent with shallow reaction. GC analysis of the reagent, after reaction with acetone, confirmed that LidiMePrOP was present at the end of all of the reactions. These results suggest that film related factors, such as access of the reagent to PCTFE, not the stability of the reagent, play the critical role in limiting the extent of reaction. If this is the case, the use of a THF-rich solvent system should increase the reaction depth, as THF swells PCTFE. When *t*-butyllithium in hexanes was added to a solution of BrdiMePrOP in THF (final hydrocarbon:THF ratio of 1:5), the usual transient yellow color was observed. This reagent was allowed to react with PCTFE at -20°C for 3 to 5 hours. XPS and ATR-IR analysis of the film products revealed that deep modification had occurred. The ATR-IR spectrum, shown in figure 29c exhibits methyl, methylene and hydroxyl bands that are much more intense relative to C-F bands than those in previous films. XPS atomic compositions of approximately  $C_{100}F_{15\pm2}O_{15\pm2}$  (15° and 75° takeoff angles) were reproducibly obtained. These results are more consistent with structure IV shown below, in which all of the repeat units are substituted, than structure V, in which substitution is incomplete<sup>37</sup>. Curve fitting results are also more consistent with IV. 74% of the carbon peak





IV



V

consists of low binding energy carbon (bonded to other carbon) while 25% consists of higher binding energy carbon (bonded to oxygen or fluorine). Structure IV predicts 28% C-O + C-F and 71% C-C, while structure V predicts 33% C-O + C-F and 66% C-C. The contact angles for this surface were essentially the same as those obtained for shallower surfaces, indicating that the reaction was complete in the outer angstroms for all of the systems studied. The contact angles are substantially higher than those observed for PCTFE-OH ( $70^\circ/20^\circ$ ), indicating that the methyl groups influence the surface polarity. The reactivity of this surface towards electrophiles appears to be comparable to PCTFE-OH. Reaction with HFBC in pyridine resulted in an atomic composition of  $C_{100}F_{66}O_{18}$ , corresponding to nearly quantitative reaction of IV ( $C_{100}F_{72}O_{18}$ ).

Unfortunately, the results of reacting these surfaces with  $\text{TfCl}$  and  $\text{Tf}_2\text{O}$  were disappointing. The reaction was carried out in THF at low temperature for up to 50 hours. The XPS atomic composition data, summarized in table 15, indicates that little sulfur and fluorine were added to the surface. Examination of the  $\text{C}_{1s}$  region revealed little, if any,  $\text{CF}_3$  and no changes could be observed by ATR-IR. In an attempt to determine if triflate groups had been introduced to the surface, and then hydrolysed during workup of the film, an excess of an alcohol containing halogen substituents was added to the reaction mixture. It was hoped that triflate groups would be labeled in-situ. There was no evidence of label incorporation by XPS (table 15) or ATR-IR. These results suggest that  $\text{TfCl}$  and  $\text{Tf}_2\text{O}$  are not reactive enough towards PCTFE-diMe-OH surfaces to allow preparation of the triflate.

#### Ring Opening Polymerization of 2-Methyloxazoline

Although tosylate esters are substantially less electrophilic than triflate esters, some polymerizations can be initiated by these species. Tosylate esters initiate the living cationic ring opening polymerization of 2-alkyl and 2-aryl oxazolines, as shown in equation 8.<sup>38</sup> Reactions of tosylate terminated and tosylate substituted polymers have been used to prepare a variety of block and graft copolymers.<sup>39</sup> The chief drawback to this system is that the

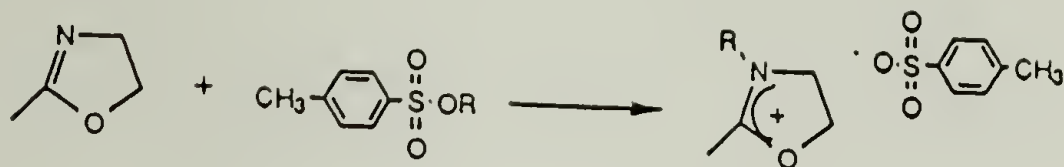
**Table 15.** XPS atomic composition data for reactions of  
PCTFE-diMe-OH surfaces with TfCl and Tf<sub>2</sub>O.

#	Conditions	Takeoff Angle	C	F	O	Q	S	Label	C	F	O	Q	S	Br
1	Tf <sub>2</sub> O, pyr. -20°C	15° 75°	100 100	17 13	15 13	-- 4	-- --	CCl <sub>3</sub> CH <sub>2</sub> OH	100 100	18 16	16 14	-- --	-- --	-- --
2	TfCl, CH <sub>2</sub> Cl <sub>2</sub> , pyr., 0°C	15° 75°	100 100	18 28	16 17	-- --	2 2	BrPrOH	100 100	44 27	17 17	11 3	-- 3	-- --
3	TfCl, pyr, 0°C	15° 75°	100 ---	27 --	28 --	-- --	4 2	BrPrOH	100 100	22 22	20 24	-- --	2 4	.9 --
4	Tf <sub>2</sub> O, CH <sub>2</sub> Cl <sub>2</sub> , 0°C	15° 75°	100 100	53 37	27 19	-- --	2 2	BrPrOH	100 100	37 28	20 10	-- --	-- --	.5 --
Theoretical <sup>a</sup>			100	50	37	--	12		100	10	10	--	--	10

<sup>a</sup> Based on reaction of structure IV



Initiation:



Propagation:



Termination:



Equation 8. Polymerization of 2-methyloxazoline.

polymerization is very slow and high temperatures are required. Temperatures in excess of 100°C and reaction times as long as 2 days are required to obtain high molecular weight polymer in solution. The results of initiating 2-methyloxazoline (2MO) from tosylate surfaces will be reported in this section.

The XPS atomic composition results for the reaction of hydroxyl surfaces with p-toluenesulfonyl chloride (TosCl) are summarized in table 16. PCTFE-OH reacted nearly

Table 16. XPS atomic composition data for tosylate surfaces.

#	Sample	Takeoff Angle	Alcohol			Tosylate			S
			C	F	O	C	F	O	
1	PCTFE-OH	150	100	26	18	100	19	24	1
		750	100	98	9	100	17	21	1
2	PCTFE-diMe-OH <sup>a</sup>	150	100	15	17	100	10	22	--
		750	100	15	16	100	11	21	--
3	PCTFE-OH	150	100	40	19	--	--	--	--
		750	100	50	17	--	--	--	--
4	PCTFE-OH <sup>b</sup>	150	100	21	19	100	22	30	8
		750	100	21	17	100	19	26	--

<sup>a</sup> Predicted atomic composition of the tosylate C<sub>100</sub>F<sub>7</sub>O<sub>21</sub>S<sub>7</sub>

<sup>b</sup> Predicted atomic composition of the tosylate C<sub>100</sub>F<sub>15</sub>O<sub>27</sub>S<sub>7</sub>

quantitatively with TosCl while reaction with PCTFE-diMe-OH was less extensive. The ATR-IR spectrum of a relatively deeply modified tosylate surface (figure 30) exhibits a substantially decreased hydroxyl absorbance, a methyl absorbance at  $2965\text{ cm}^{-1}$  and a very intense S=O band at  $1365\text{ cm}^{-1}$ . Initial investigations were carried out using shallow surfaces, as it was suspected that the harsh reaction conditions would result in dissolution of the modified layer.

Initially, a shallow-modified PCTFE-OTos sample was reacted with neat 2MO at  $75^{\circ}\text{C}$  for 47 hours. It was readily apparent that some reaction had occurred. The initially clear, colorless films became opaque and black. ATR-IR revealed a rather intense absorbance in the C-H region and broad, intense absorbances at  $1642\text{ cm}^{-1}$  and  $1742\text{ cm}^{-1}$ , as well as a weak S=O band at  $1365\text{ cm}^{-1}$ . The band at  $1642\text{ cm}^{-1}$  is consistent with the amide carbonyl in the resulting polymer and the absorbance at  $1742\text{ cm}^{-1}$  could be due to the kinetic termination product resulting from the reaction of the propagating oxazolinium ion with water (see equation 8). However, the  $1642\text{ cm}^{-1}$  band is also consistent with the C=N absorbance of the monomer and the carbonyl band could be explained by oxidation of the modified substrate. The XPS atomic composition data, summarized in table 17, revealed evidence of some surface rearrangement (increased Cl:C and F:C ratios) as well as unreacted tosylate groups (sulfur) and nitrogen. It appeared likely that PCTFE was being



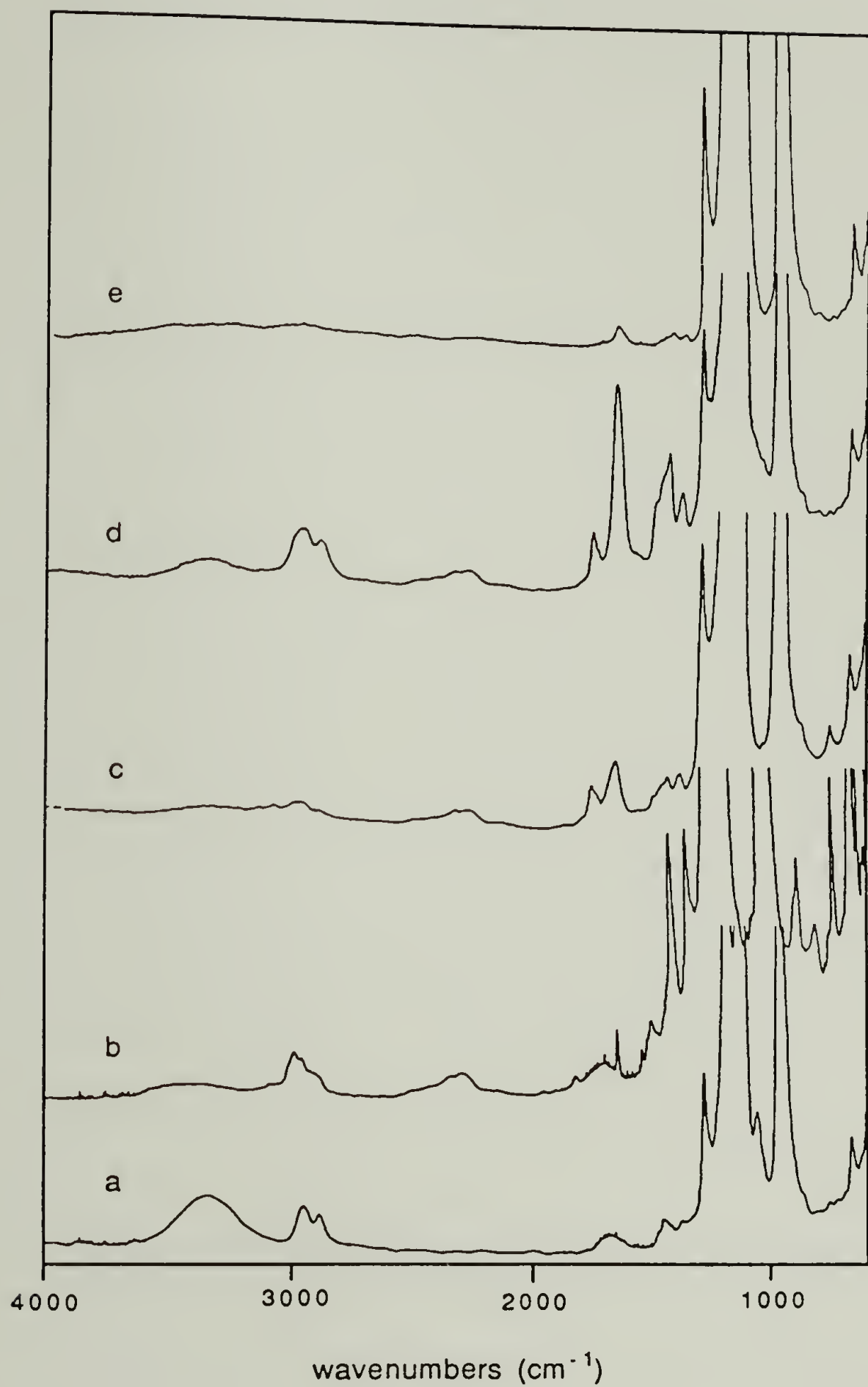


**Figure 30.** ATR-IR spectra of (a) PCTFE-OH; (b) PCTFE-OTos, #4; (c) PCTFE-g-2MO, #1; (d) PCTFE-g-2MO, #4; (e) PCTFE control.

**Table 17.** XPS atomic composition data for 2-methyloxazoline graft polymerizations.

<u>-OTos Sample #</u>	<u>Conditions</u>	<u>Takeoff Angle</u>	<u>C</u>	<u>F</u>	<u>O</u>	<u>S</u>	<u>N</u>	<u>O</u>
1 <sup>a</sup>	neat, 80°C, 24 h	15°	100	60	19	2	8	13
		75°	100	47	18	1	8	12
2 <sup>b</sup>	CH <sub>3</sub> CN, 80°C, 24 h	15°	100	11	20	3.2	--	--
		75°	100	11	19	3.2	--	--
2 <sup>b</sup>	CH <sub>3</sub> CN, 80°C, 6 days	15°	100	10	19	2.4	.8	--
		75°	100	9	15	2.5	.8	--
2 <sup>b</sup>	neat, 80°C, 5 days	15°	100	12	21	2	<5	--
		75°	100	11	17	2	<5	1
PCTFEC	neat, 80°C, 5 days	15°	100	105	14	.7	4	19
		75°	100	101	9	.7	3	19
4 <sup>a</sup>	neat, 80°C, 5 days	15°	100	23	18	.7	2	3
		75°	100	30	16	.6	2	6
5 <sup>a</sup>	90°C, 45 h; wash HCl	15°	100	22	30	--	9	5
		75°	100	32	21	--	9	8
PCTFE Control	90°C, 45 h; wash HCl	15°	100	106	18	--	5	54
		75°	100	135	13	--	2	62

<sup>a</sup> PCTFE-OTos

<sup>b</sup> PCTFE-diMe-OTos

<sup>c</sup> XPS of the starting material contained < 1% sulfur and < 1% oxygen

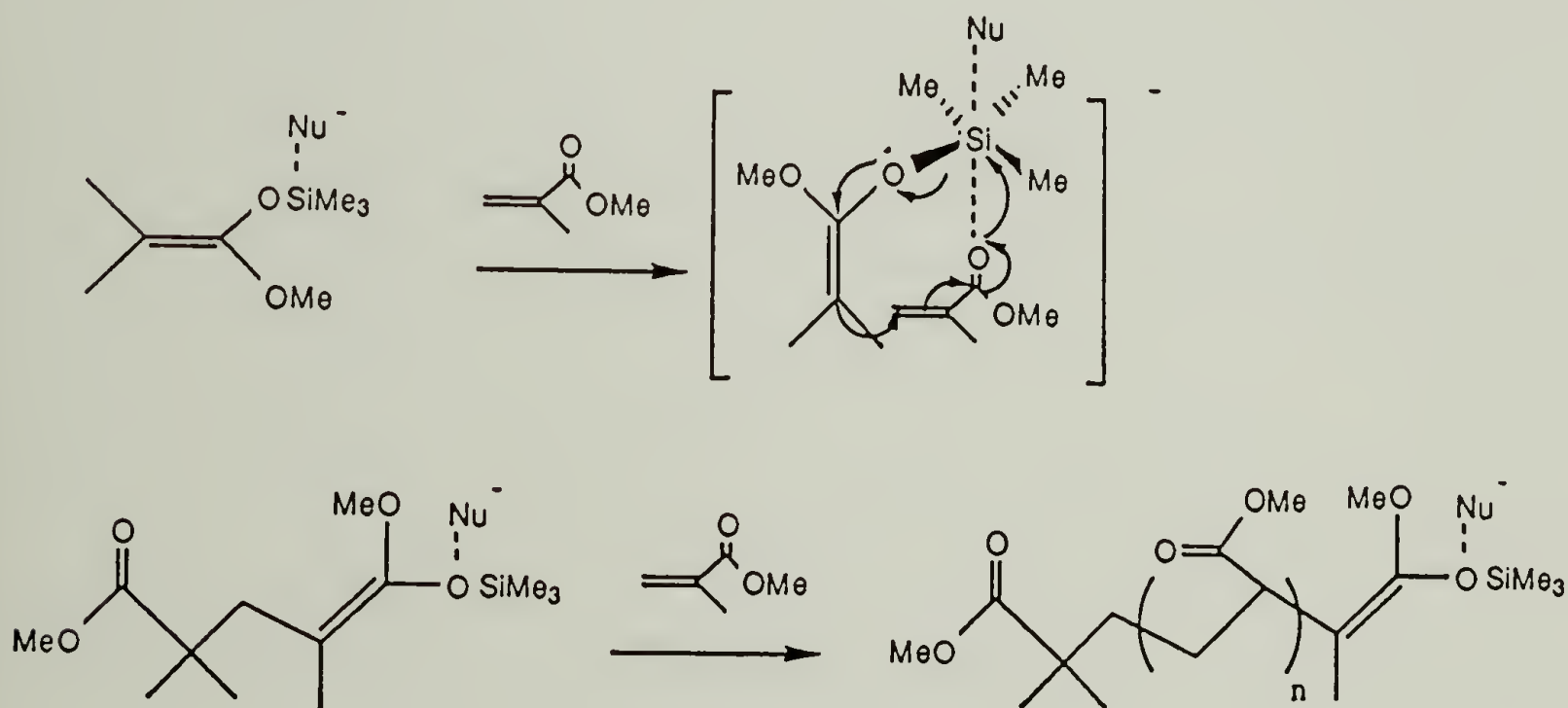
reduced by the amine monomer under these condition, but it was not clear if any polymerization was taking place. The reaction was attempted using surfaces derived from PCTFE-diMe-OH in acetonitrile in a sealed tube. Very little change occurred in the first 24 hours by XPS and ATR-IR, although the film was quite black. After 6 days, the same features observed previously were apparent by ATR-IR. Absorbances due to the reaction were surprisingly intense considering the small amount of nitrogen observed by XPS (see table 17, 3rd. entry), suggesting that monomer or polymer may be present deeper in the film. Using aqueous potassium carbonate to kill the polymerization appeared to decrease the intensity of the  $1740\text{ cm}^{-1}$  absorbance.<sup>40</sup> Reaction of PCTFE-OH and PCTFE-diMe-OH derived surfaces was carried out in a sealed tube with neat monomer for 5 days at  $80^{\circ}\text{C}$ . Inadvertently, one film sample was included in which so little hydroxyl group formation had occurred that the sample was essentially unmodified. Surprisingly, the ATR-IR spectrum of this sample exhibited absorbances associated with the graft polymerization of comparable intensity to those observed for the other film samples. A large amount of nitrogen was also present in the XPS sampling depth. From these results it was clear that monomer absorption had occurred. The fluorine and chlorine contents of the essentially unmodified film also decreased, indicative of reduction. The following experiments were performed in order to



determine if any polymerization occurs: A deeply modified PCTFE-OTos sample (table 16, tosylate sample #4) was reacted with neat 2MO at 95°C for 45 hours. The sample was washed with dilute methanolic HCl, and then analyzed. The ATR-IR spectrum (figure 30) retained the absorbances attributed to the polymer and nitrogen was still detected by XPS. Both hydroxyl (compare the hydroxyl intensities in figure 30d to 30b) and ester end groups are readily detected. A PCTFE control sample was reacted with 2MO under identical conditions. Prior to washing with acid, intense features ascribed to the polymer were observed. After acid washing, only a broad, weak absorbance at 1600  $\text{cm}^{-1}$  was observed, although nitrogen remained in the XPS sampling depth. Reduction of the PCTFE film is extensive, as evidenced by the loss of chlorine, the development of the 1600  $\text{cm}^{-1}$  absorbance (due to unsaturation) and the dark color. These results indicate that some reaction of tosylate groups with 2MO occurs, however, unlike the THF graft polymerization discussed previously, only low molecular weight oligomers are formed. In addition, the conditions are harsh enough to cause extensive reaction with the PCTFE substrate. Attempts to prepare the more chemically-resistant FEP-OTos surface from FEP-OH failed; FEP-OH is too unreactive. These results suggest that reactions that are slow and require forceful conditions in solution should be considered poor candidates for surface-initiated graft polymerizations.

## Group Transfer Polymerizations

Group transfer offers a number of potential advantages as a mechanism for surface-initiated graft polymerization. The initiator species is a relatively stable functional group, polymerizations are living (free of side reactions) and, unlike the tosyl ester/2MO system, initiation and propagation are rapid and occur under mild conditions. Silyl ketene acetal groups are activated in the presence of anionic (nucleophilic) catalysts, as shown in equation 9. Initiation occurs by the addition of the monomer and transfer of the TMS group, resulting in a new trimethylsilyl ketene acetal end groups. Propagation continues in this



**Equation 9.** Group transfer polymerization.

fashion. This mechanism has been used to polymerize a variety of acrylate monomers,<sup>41</sup> although the best results have been obtained for methyl methacrylate. Electrophilic (Lewis acid) catalysts can also be used, although the mechanism is somewhat different. In this case, the catalyst coordinates with the carbonyl of the monomer, activating the monomer towards nucleophilic attack by the TMS ketene acetal. This system is particularly well suited for acrylate monomers.<sup>42</sup> This mechanism has been used to prepare a variety of block and star block copolymers,<sup>43</sup> as well as graft polymer from TMS ketene acetal-functionalized polystyrene gels.<sup>44</sup> While the environment presented by these crosslinked gels is expected to be much more solution-like than that of the modified polymer surface, these results suggest that a TMS ketene acetal-containing surface would initiate polymerization. The research described in this section was focused on introducing TMS ketene acetal groups to polymer surfaces.

The usual procedure for preparing GTP initiators is to treat the appropriate isobutyrate ester with a strong non-nucleophilic base, such as LDA, and trap the enol by reaction with trimethylsilyl chloride (TMSCl).<sup>45</sup> While the isobutyrate surface was expected to be easily obtained by the reaction of PCTFE-OH surfaces with isobutyryl chloride, sequential treatment of this surface with LDA and TMSCl would result in extensive reduction of the PCTFE substrate.



One promising alternative appeared to be the reaction of LDA with the polymer surface in a solution containing  $\text{TMSCl}$ . It was hoped that this would minimize the amount of time that the surface would have to be exposed to LDA. The successful use of this addition sequence is reported in the literature.<sup>46</sup> A relatively shallow PCTFE-OH surface (prepared at  $-45^\circ\text{C}$ , 1 h) with an XPS atomic composition represented by  $\text{C}_{100}\text{F}_{40}\text{O}_{19}\text{Cl}_{10}$  at a  $15^\circ$  takeoff angle and  $\text{C}_{100}\text{F}_{61}\text{O}_{16}\text{Cl}_{15}$  at a  $75^\circ$  takeoff angle was treated with isobutyryl chloride in pyridine. The atomic composition of the product was found to be  $\text{C}_{100}\text{F}_{21}\text{O}_{21}\text{Cl}_2$  at a  $15^\circ$  takeoff angle and  $\text{C}_{100}\text{F}_{25}\text{O}_{20}\text{Cl}_5$  at a  $75^\circ$  takeoff angle. The ATR-IR spectrum, shown in figure 31, is consistent with quantitative reaction. The hydroxyl band has been replaced by an intense ester carbonyl at  $1735\text{ cm}^{-1}$  and a methyl absorbance at  $2960\text{ cm}^{-1}$ . When this surface was treated with LDA in the presence of  $\text{TMSCl}$ , no clear evidence of reaction was obtained. Although a small amount of silicon was present by XPS (see table 18), no enol  $\text{C}=\text{C}$  ( $\sim 1700\text{ cm}^{-1}$ ) was present in the ATR-IR spectrum (figure 31b). It is likely that this silicon represents surface contamination or TMS ethers formed by the reaction of  $\text{TMSCl}$  with residual hydroxyl groups. One consistent explanation for the failure of this reaction is that LDA reacts with  $\text{TMSCl}$  to form the silyl amide  $(i\text{-Pr})_2\text{NTMS}$  and  $\text{LiCl}$  before it can react with ester groups on the surface. The fact that there was no evidence of PCTFE reduction, such as film discoloration or

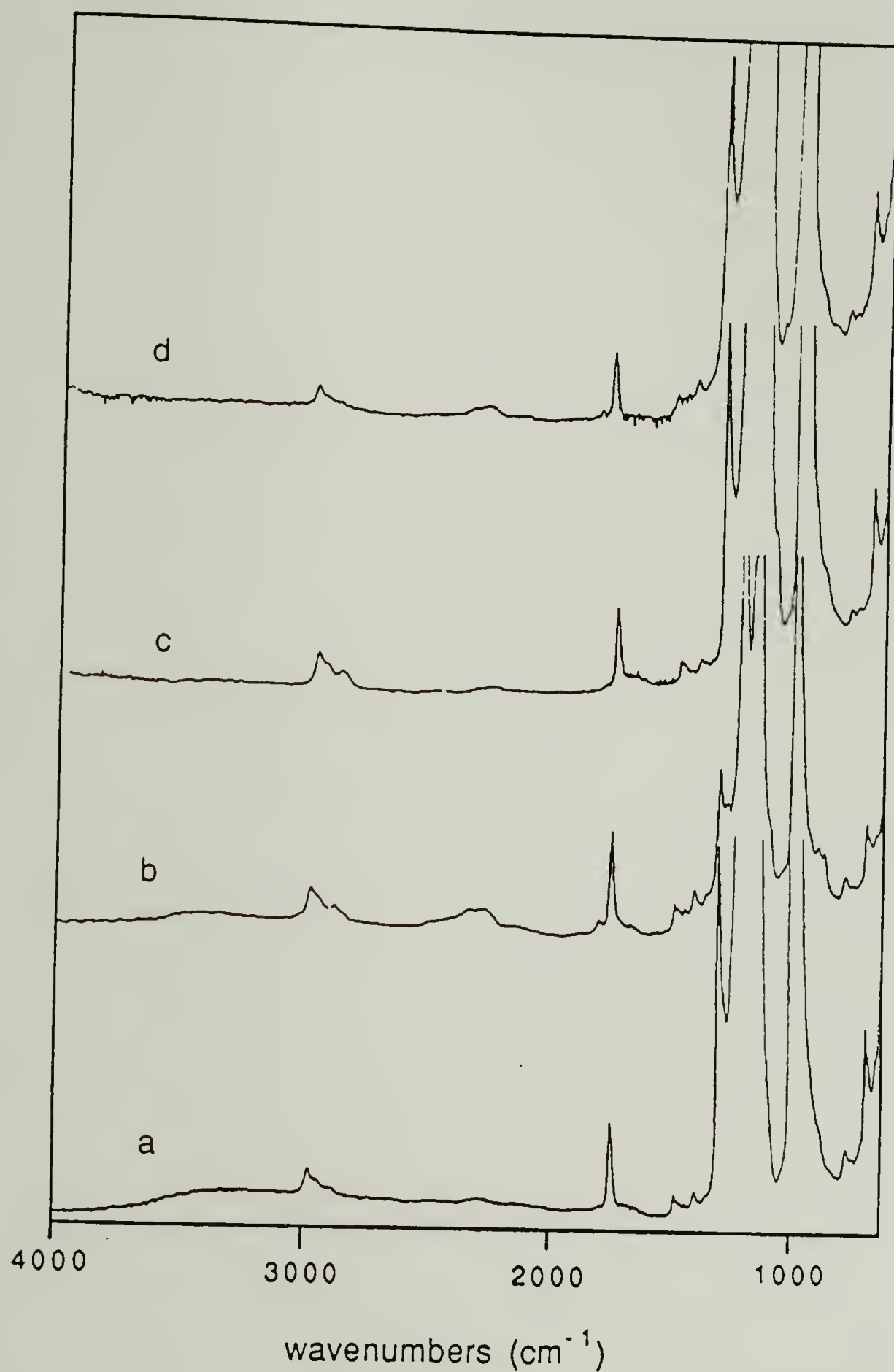


**Figure 31.** ATR-IR spectra of (a) PCTFE-OC(=O)iBu; PCTFE-OC(=O)iBu reacted with (b) LDA/TMSCl, (c) TEA/TMSCl, (d) TEA/TMSOTf.

**Table 18.** XPS atomic composition data for reactions of isobutyrate surfaces.

<u>Sample #</u>	<u>Reaction Conditions</u>	<u>Takeoff Angle</u>	<u>C</u>	<u>F</u>	<u>O</u>	<u>Q</u>	<u>Si</u>
1	LDA + TMSCl, THF 18 h, 0°C.	15° 75°	100 100	16 21	21 17	-- 12	2 1
2	Et <sub>3</sub> N + TMSCl, DMF 22 h, room temp. <sup>a,b</sup>	15° 75°	100 100	25 26	22 21	2 3	2 1
3	Et <sub>3</sub> N + TMSOTf, PhH 0°C, 18 h	15° 75°	100 100	21 25	33 26	-- 4	9 3

<sup>a</sup> films were badly discolored

<sup>b</sup> reacted at 100°C for the first 2 hours



loss of fluorine and chlorine by XPS (particularly at a 75° takeoff angle) suggests that some other reaction had consumed the LDA.

Silyl enol ethers have been prepared by treating ketones with an organic base and TMSCl in a polar aprotic solvent. In a typical procedure, the ketone is treated with triethylamine and TMSCl in refluxing DMF for 48 hours<sup>47</sup>. The reaction of the film with triethylamine (TEA) and TMSCl in DMF was initially carried out at 100°C. Almost immediately, the films showed signs of discoloration. At the end of two hours the films were dark black. The reaction was continued overnight at room temperature. When the films were analyzed by XPS and ATR-IR, no evidence was found for TMS ketene acetal formation (see table 18 and figure 31c). It was clear that milder reaction conditions would be required to avoid extensive damage to the subphase. The use of a more reactive silylating agent, such as trimethylsilyl trifluoromethanesulfonate (TMSOTf) allows the reaction to be carried out in a less polar solvent at room temperature. Relatively acidic esters, such as ethyl phenylacetate, have been converted to the corresponding TMS ketene acetal using these conditions.<sup>48</sup> The isobutyrate surface was treated with TEA and TMSCl in benzene at room temperature. The XPS atomic composition of the product (table 18) suggests that some reaction had occurred; a large amount of silicon was present. However, the ATR-IR spectrum (figure 31d) showed

no evidence of enol C=C. Resonance with the phenyl group increases the  $pK_a$  of the enol of phenylacetyl esters substantially relative to the enol of the isobutyrate. It is likely that the isobutyrate ester is not acidic enough to be converted to the TMS ketene acetal under these conditions.

In order to gain a better understanding of the reaction and evaluate the effectiveness of the resulting TMS ketene acetal as a GTP initiator, 1-ethoxy-1-(trimethylsilyloxy)-2-phenyl ethylene was prepared according to the procedure of Simchen and Kober,<sup>49</sup> and the product was used to initiate GTP polymerization. Ethyl phenylacetate was reacted with TEA and TMSOTf in benzene. As expected, triethylammonium trifluoromethanesulfonate separated into a denser phase during the course of the reaction. The product could not be analyzed by GC using a packed column, substantial decomposition occurred. However, the IR spectrum was consistent with the conversion of a substantial amount of the ester to the TMS ketene acetal. In addition to the ester carbonyl at  $1738\text{ cm}^{-1}$ , an intense absorbance consistent with the enol C=C was observed at  $1650\text{ cm}^{-1}$ . The mixture was stored under nitrogen until some time later, when capillary GC and GC-MS became available. At this time, the majority of the sample consisted of the starting ester. However, GC-MS did detect a high retention time product with an M/e spectrum consistent with the TMS ketene acetal (see Appendix II). A large signal was observed at an M/e of 73, characteristic of TMS,

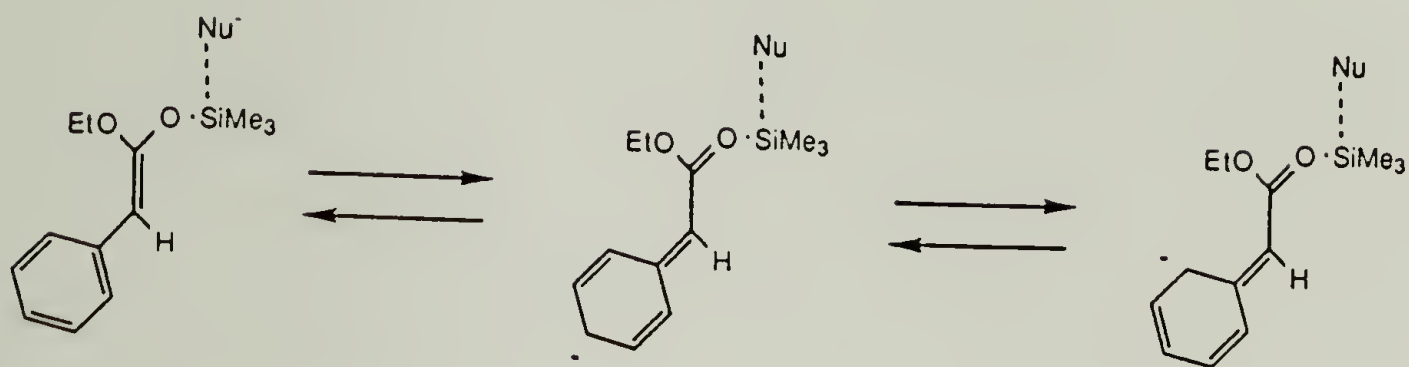
and a molecular ion at 237, equal to the molecular weight of the expected product, was observed. The intensity of the enol C=C in the IR spectrum of the mixture had decreased substantially, indicating that the product had reacted with adventitious moisture during storage.

The reaction was repeated and the product was analyzed immediately by capillary GC. These results indicate that only 19% of the the ester remained unreacted; 74% was converted to the previously identified TMS ketene acetal and 7% to a product that appeared at a slightly lower retention time. If the former is identified as the Z-isomer and the latter as the E-isomer the results are in excellent agreement with the literature.<sup>50</sup>

Initiation was attempted using the product of the first reaction, immediately after preparation. While difficulty was encountered in performing the polymerization due to contaminated MMA, it was clear that the  $\beta$ -phenyl TMS ketene acetal could initiate polymerization. It was also clear that the polymerization mechanism differs substantially from previously published work. If the reaction had occurred as expected, three monodisperse polymer fractions (due to initiation that occurred during each of the three charges of initiator) would have been detected by GPC. Instead, a very broad distribution was observed. These results are consistent with a polymerization in which the rate of initiation is substantially lower than the rate of propagation. The



origin of this effect is shown in equation 10. The partial



**Equation 10.** Charge delocalization in 1-ethoxy-1-(trimethylsilyloxy)-2-phenyl ethylene.

negative charge that develops during catalysis with  $\text{TMSF}_2^-$  is delocalized throughout the phenyl ring, decreasing the reactivity of the initiator; this also explains the yellow color. Once reaction with MMA had occurred, the TMS ketene acetal group was no longer stabilized in this way; the color faded and propagation was able to proceed at the normal rate. The persistence of color during the polymerization indicated that unreacted initiator was present throughout the course of the polymerization. This should have no effect on the "livingness" of the system.

As a result, phenylacetyl surfaces were prepared and reacted with TEA and  $\text{TMSOTf}$ . Treatment of a relatively shallow PCTFE-OH surface with phenylacetyl chloride in pyridine resulted in changes in the XPS atomic composition (table 19) consistent with esterification. The carbon content increased substantially. The ATR-IR spectrum, shown

in figure 32, is consistent with quantitative reaction. The hydroxyl band is absent, phenyl C-H bands are present at  $3060\text{ cm}^{-1}$  and  $3030\text{ cm}^{-1}$ , an intense ester carbonyl band is present at  $1736\text{ cm}^{-1}$ , and C=C aromatic bands are present at  $1500\text{ cm}^{-1}$  and  $1450\text{ cm}^{-1}$ . The absorbance at  $1670\text{ cm}^{-1}$  may be due to pyridinium phenylacetate deep in the film. No nitrogen was observed by XPS, indicating that no such species were present in the outer 40 Å. The effect of treating this surface with TEA/TMSOTf in benzene was rather surprising. The ATR-IR spectrum of the product is shown in figure 32b. All of the features associated with the phenylacetate group disappeared. New bands appear at  $1670\text{ cm}^{-1}$ , consistent with C=C, and at  $1286\text{ cm}^{-1}$  and  $1055\text{ cm}^{-1}$  consistent with Si-CH<sub>3</sub> and Si-O-C respectively. The origin of the absorbance at  $638\text{ cm}^{-1}$  is unclear; this is much lower than expected for Si-CH<sub>3</sub> or cis alkene bands. The best explanation for these observations is that base assisted ( $E_2$ ) elimination has occurred. It is unclear why a terminal vinyl surface did not result, as was observed when PCTFE-OH was reacted with TfCl in pyridine. TEA may catalyze bond rearrangement to allow conjugation with the surface. In all likelihood, the silyl groups that are present belong to surface contaminants. Washing with benzene alone was probably insufficient to remove all of the adsorbed silicon-containing species.

The use of ester surfaces derived from PCTFE-diMe-OH provides a potential solution to this problem. The XPS

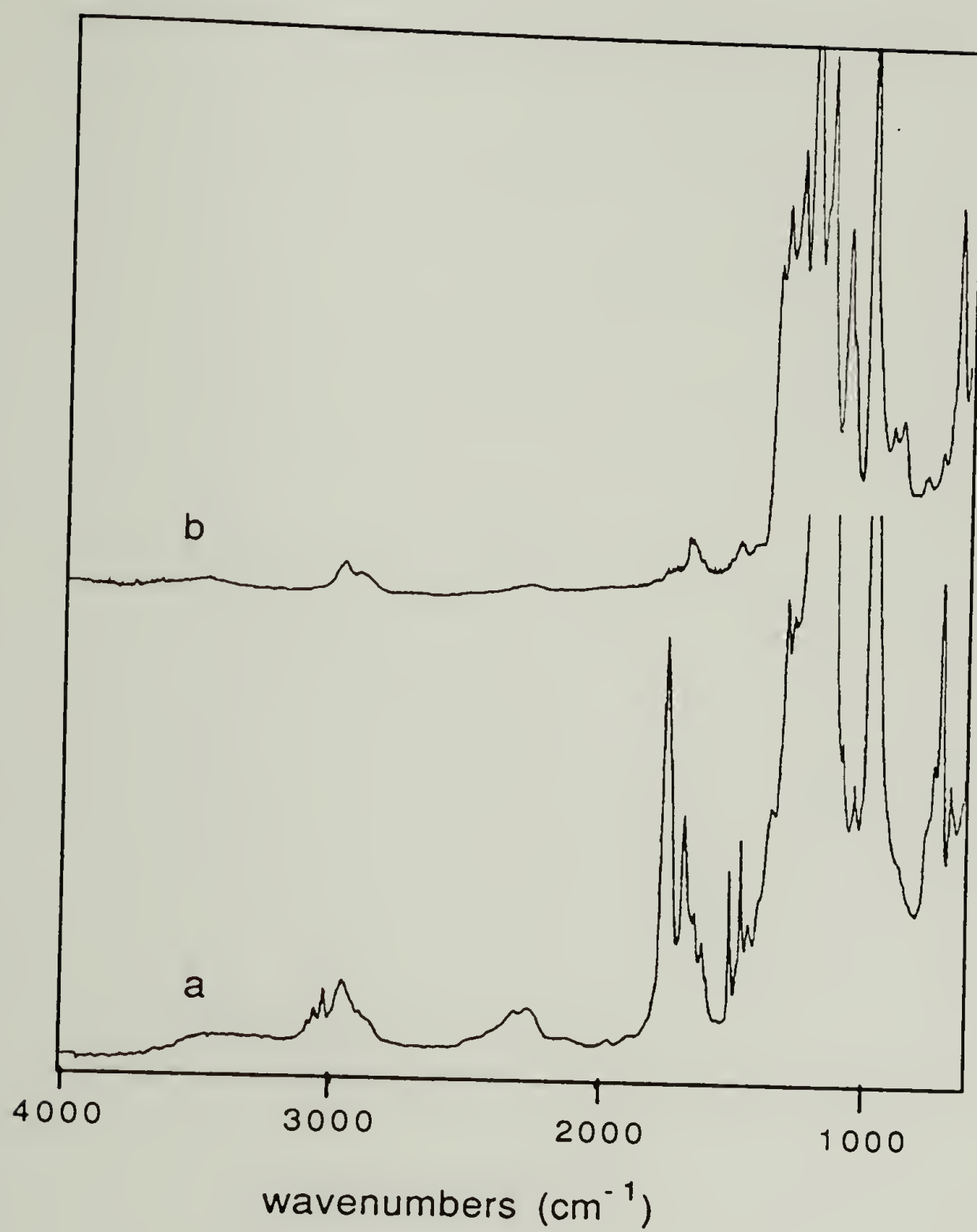


**Figure 32.** ATR-IR spectra of (a) PCTFE-OC(=O)CH<sub>2</sub>Ph, (b) PCTFE-OC(=O)CH<sub>2</sub>Ph + TEA/TMSOTf.



atomic composition data is summarized in table 19. Since the atomic composition of the ester differs little from that of the PCTFE-diMe-OH surface, little information can be gained from this data. Examination of the ATR-IR spectrum (figure 33a) indicates that the ester was formed, but unreacted hydroxyl groups remained on the surface. A somewhat higher yield was obtained when the reaction was carried out using DMAP catalysis, as evidenced by the decrease in the hydroxyl intensity in figure 33b. The phenylacetate surface obtained by reaction in pyridine was treated with TEA and TMSOTf in benzene under conditions identical to those used to react the PCTFE-OC(=O)CH<sub>2</sub>Ph surface. The XPS atomic composition data is summarized in table 20. As in earlier experiments, the surface contained a large amount of silicon. The ATR-IR spectrum of the product, shown in figure 33c, was quite complicated. Aromatic C-H and C=C bands were clearly present, indicating that displacement of the phenylacetate group had not occurred, but a number of absorbances between 1800 and 1600 cm<sup>-1</sup> were observed, including the original ester band (1740 cm<sup>-1</sup>) and bands at 1713 cm<sup>-1</sup> and 1650 cm<sup>-1</sup>. It was not clear if the ester carbonyl absorbance had decreased in intensity. If any TMS ketene acetal groups were produced, the yield was very low. The polarity of benzene is very low, making it unlikely that the interphase region is significantly swollen during the course of the reaction. This may result in a very shallow reaction,

Table 19. XPS atomic composition data for phenylethyl ester surfaces.

#	Sample	takeoff		Esterification				
		Angle	C	F	O	O	C	Si
1	PCTFE-OH	15°	100	40	19	4	100	9
						4	13	.5
		75°	100	50	17	10	100	9
						10	12	.8
2	PCTFE-diMe-OH	15°	100	14	16	--	100	6
						--	15	--
		75°	100	12	13	--	100	6
						--	13	--
3	PCTFE-diMe-OH	15°	100	15	15	--	100	8
						--	17	--
		75°	100	15	15	--	100	10
						--	13	--

<sup>a</sup> Theoretical composition C<sub>100</sub>F<sub>7</sub>O<sub>13</sub> based on structure IV

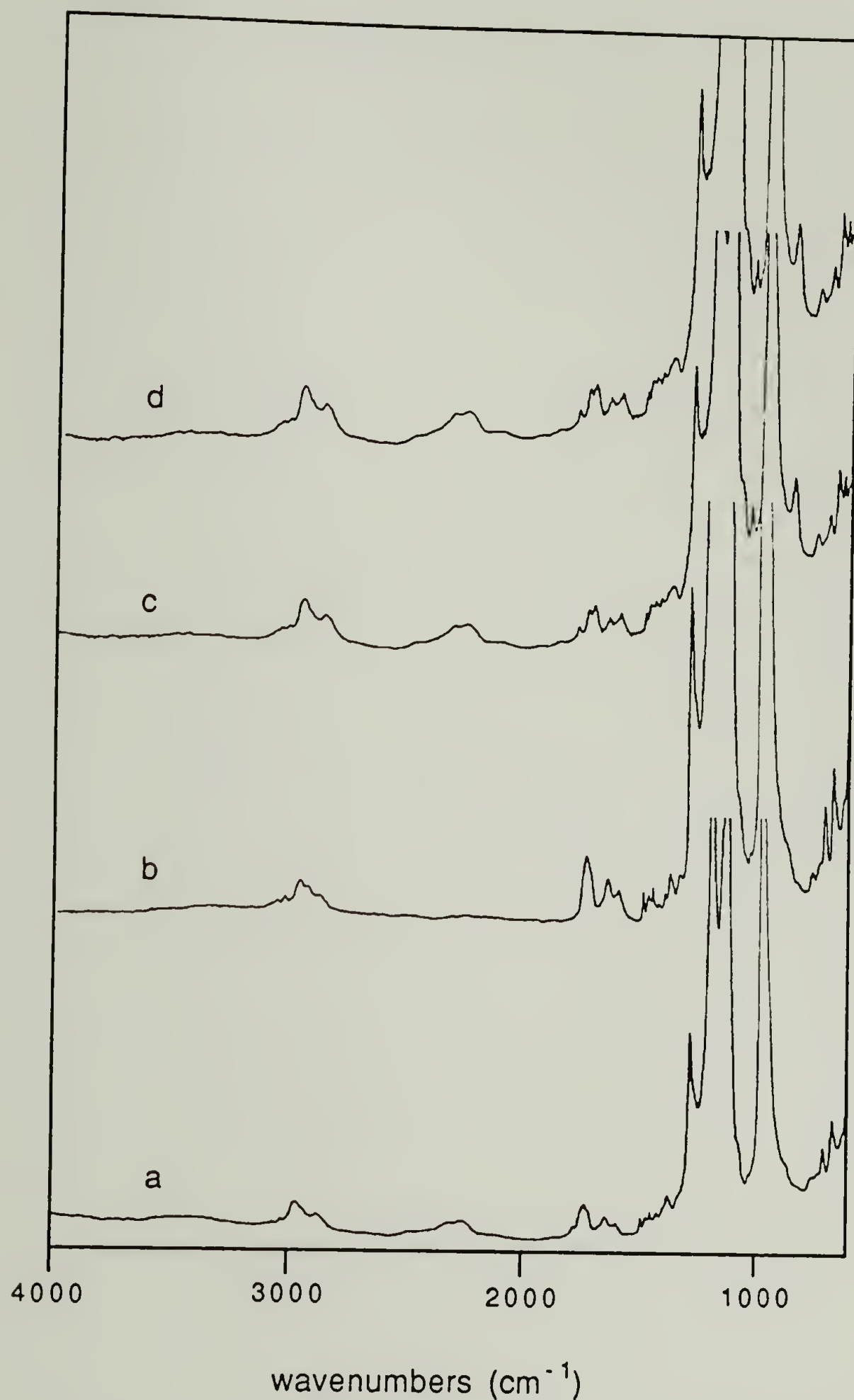


**Figure 33.** ATR-IR spectra of PCTFE-diMe-OC(=O)CH<sub>2</sub>Ph prepared in (a) pyridine, (b) THF/pyridine/DMAP; (c) reaction of product (b) with TMSOTf/TEA in benzene, (d) reaction of product (b) with TMSOTf/TEA in TCE.



**Table 20.** XPS atomic composition data for reactions of phenylethyl ester surfaces.

<u>Ester Sample</u>	<u>Reaction Conditions</u>	<u>Takeoff Angle</u>	<u>C</u>	<u>F</u>	<u>O</u>	<u>Q</u>	<u>Si</u>
#2	Et <sub>3</sub> N, TMSOTf, PhH	150	100	5	30	2	9
	room Temp., 24 h.	750	100	14	21	4	6
#3	Et <sub>3</sub> N, TMSOTf, PhH	150	100	8	23	--	5.7
	room Temp., 20 h.	750	100	9	19	--	3
#3	Et <sub>3</sub> N, TMSOTf, CH <sub>3</sub> CCl <sub>3</sub>	150	100	11	28	--	3.3
	room Temp., 23 h.	750	100	11	22	--	1.7

<sup>a</sup> Theoretical Predicted composition of C<sub>100</sub>F<sub>5.5</sub>O<sub>11</sub>Si<sub>5.5</sub> based on structure IV

as was observed for the reaction of LidiMePrOP with PCTFE in low THF solvent mixtures. THF could not be used because cationic ring opening polymerization would occur in the presence of TMSOTf. As a result, the reaction was run in 1,1,1-trichloroethane, which has a similar dielectric constant to THF and is inert to TMSOTf. A model reaction was carried out using ethyl phenylacetate. The TMS ketene acetal was obtained in high yield. However, when the reaction was carried out on the film surface, the XPS (table 20) and ATR-IR (figure 33d) results were nearly identical to those obtained for the reaction in benzene.

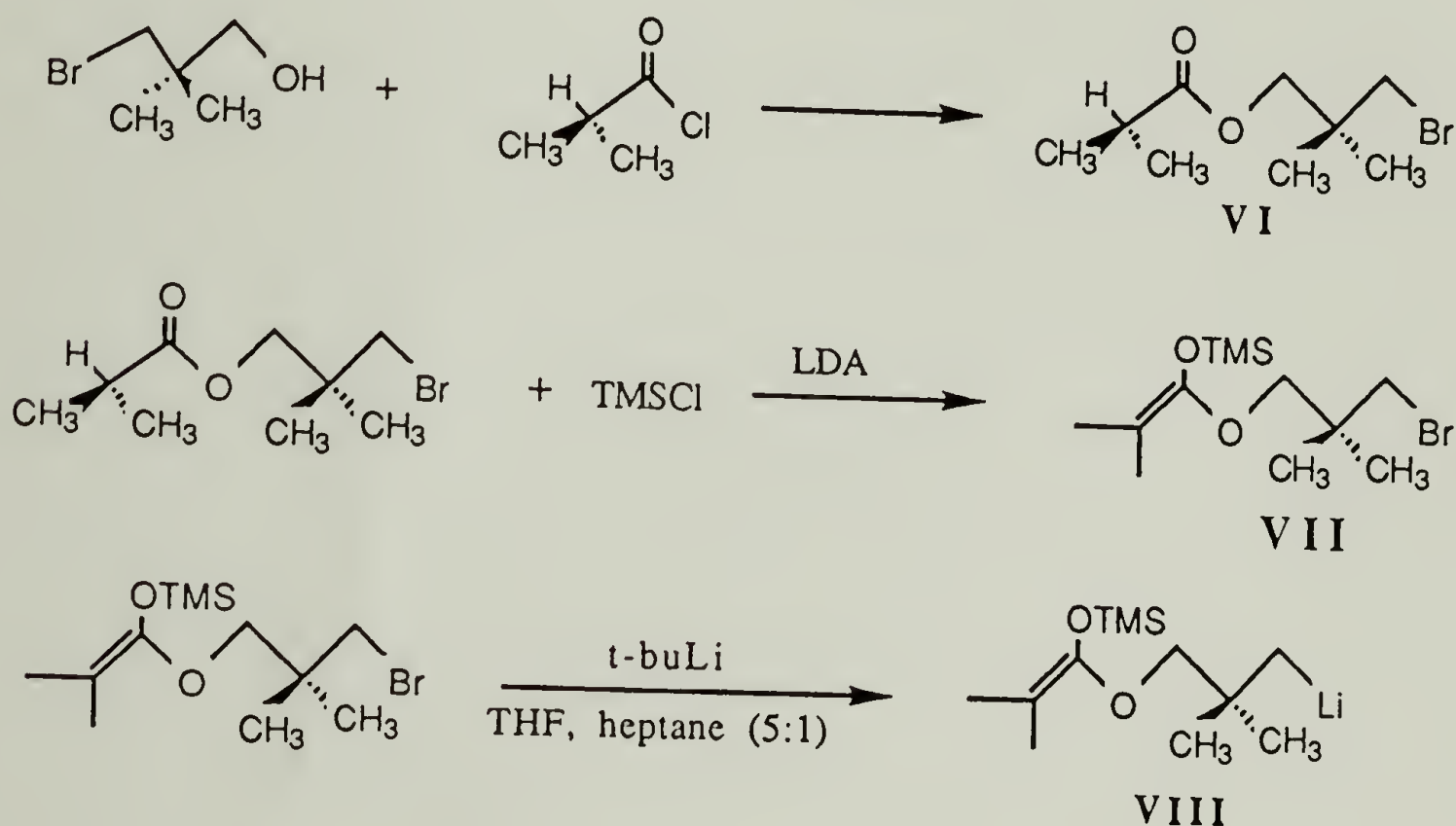
These results do not rule out the formation of some TMS ketene acetal groups. As a result, the polymerization of methyl methacrylate was attempted with nucleophilic catalysis using  $\text{TAS} \cdot \text{TMSF}_2$ . The XPS atomic composition data, summarized in table 21, shows that the O:C ratio increased, but a large amount of silicon was present. There was no change in the ATR-IR spectrum. Polymerization was also attempted using electrophilic catalysis. The use of diethylaluminum chloride at  $-78^\circ\text{C}$  has been reported in the literature. This system has the advantage that the products resulting from the reaction of  $\text{Et}_2\text{AlCl}$  with water also function as initiators.<sup>51</sup> There was no evidence of polymerization by XPS or ATR-IR. There appears to be no practical means of converting esters on PCTFE surfaces to TMS ketene acetals.

**Table 21.** XPS atomic composition data for attempted surface-initiated GTP polymerizations.

<u>TMSOTf Product</u>	<u>Conditions</u>	<u>Takeoff Angle</u>	<u>C</u>	<u>F</u>	<u>O</u>	<u>Q</u>	<u>Si</u>
#3	MMA, (Me <sub>2</sub> N) <sub>3</sub> SF <sub>2</sub> TMS	15°	100	4	31	--	7.3
		75°	100	5	21	--	4
#3	MMA, Et <sub>2</sub> AlCl	15°	100	6	13	--	--
		75°	100	6	13	--	--



The preparation of a lithium reagent containing the TMS ketene acetal group was investigated as an alternative route to a GTP initiator surface. Although the TMS ketene acetal group is not generally considered a protecting group for esters, it should have little electrophilic reactivity and may be stable towards alkyllithium reagents. Preparation of the reagent is outlined below. The bromo ester VI was



**Equation 11.** Preparation of LiPrTMSKA.

obtained in good yield by esterification of 3-bromo-2,2-dimethyl-1-propanol with isobutyryl chloride. Initial attempts to prepare the TMS ketene acetal (VII) by sequential reaction with LDA and TMSCl failed. Cyclization occurred as a result of displacement of the bromine by the enolate, as evidenced by the presence of a species possessing a molecu-

lar ion with an M/e ratio of 156. A similar problem was reported in the preparation of a difunctional GTP initiator capable of cyclizing to form a 6 member ring. The problem was solved by adding LDA to a solution containing the ester and TMSCl.<sup>52</sup> Commercial LDA solutions were cloudy and orange colored, indicating contamination. Commercial solutions of (TMS)<sub>2</sub>NLi, another strong non-nucleophilic base, were more stable, but addition of this reagent to a solution containing the ester and TMSCl resulted primarily in the formation of (TMS)<sub>3</sub>N. Addition of freshly prepared LDA in THF to a solution of BrPriBu and TMSCl results in VII in good yield as evidenced by GC-MS and GC-IR (see Appendix III). No side reactions occurred and the product was easily separated from the unreacted ester by fractional distillation. The product was reacted with t-butyllithium in THF under the conditions that had been used previously to prepare LidiMePrOP. PCTFE film modification was attempted using conditions that resulted in relatively deeply-modified PCTFE-diMe-OH. As in previous work, the presence of the lithium reagent was confirmed by reaction with acetone. In this case, methyl iodide was added to react with the alkoxide rather than water, and the ether was isolated; the TMS ketene acetal was expected to be moisture sensitive. The film modification results were disappointing. The XPS atomic composition data is summarized in table 22 and the ATR-IR spectrum is shown in figure 34. While some oxygen

**Table 22.** XPS atomic composition data for reactions with  
LiPrTMSKA.

<u>Sample</u>	<u>Takeoff</u>		<u>Conditions</u>				
	<u>Angle</u>	<u>C</u>	<u>F</u>	<u>O</u>	<u>N</u>	<u>C</u>	<u>O</u>
PCTFE	15°	100	150	--	50	100	46
	75	100	150	--	50	100	67
PEEK	15°	100	--	20	--	100	0°C, 8 h
	75	100	--	16	--	100	--



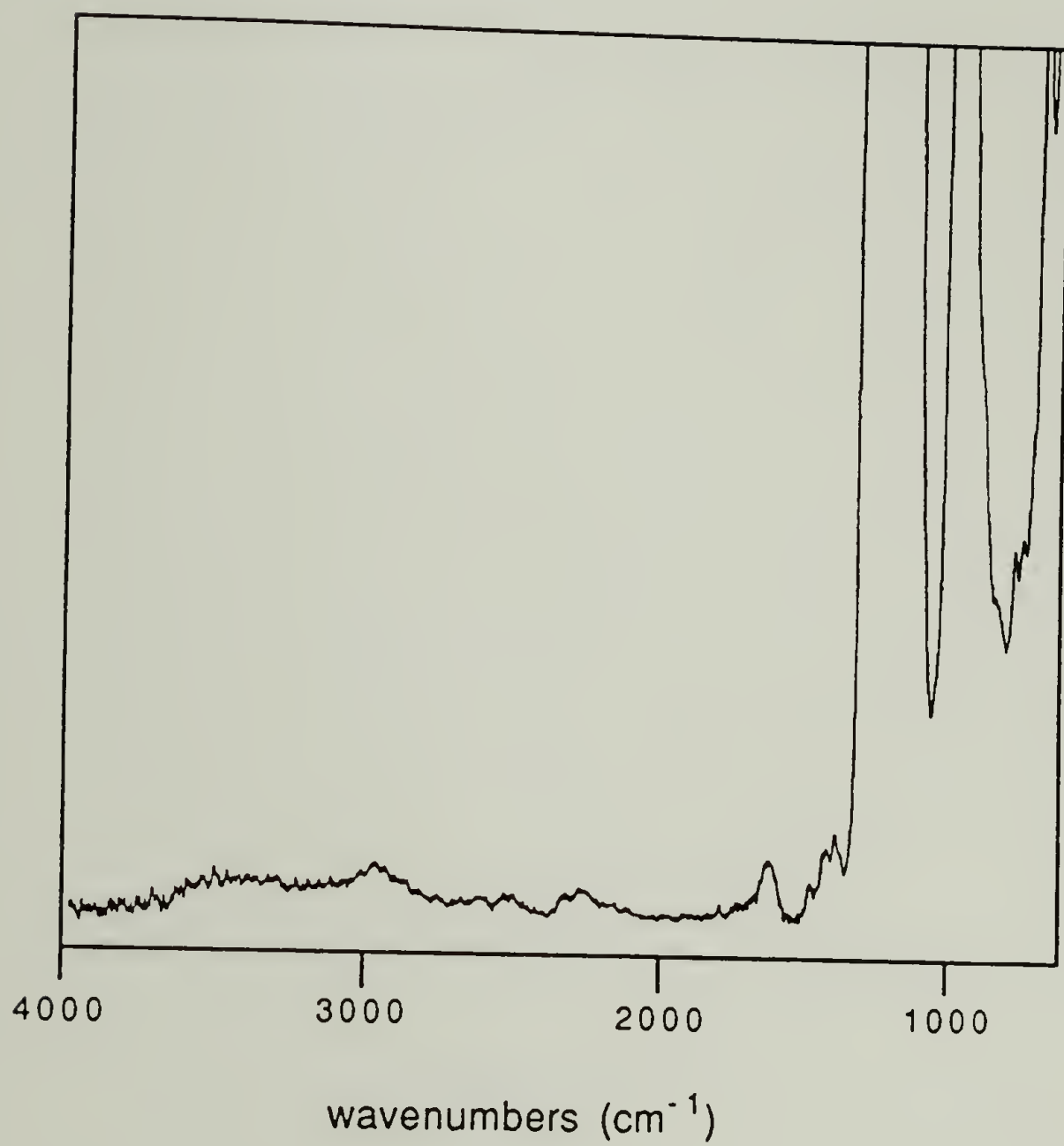
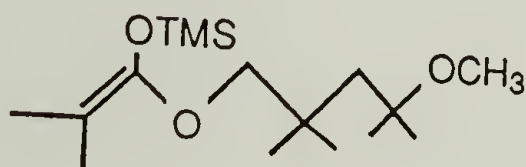


**Figure 34.** ATR-IR spectrum of PCTFE reacted with LiPrTMSKA.

was introduced, no ester or enol absorbances, are present in the IR spectrum. Only weak bands at  $1610\text{ cm}^{-1}$ ,  $1470\text{ cm}^{-1}$  and  $1380\text{ cm}^{-1}$  are observed. These results suggest that reduction occurred. Unlike the the reaction of LidiMePrOP with acetone, the reaction of VIII resulted in a complex mixture of products. GC-MS analysis (see Appendix III) revealed the presence of some of the addition product, IX, as well as a fairly large amount of VI and VII, but the structures of most of the products could not be determined.



IX

Clearly, side reactions involving the TMS ketene acetal group are occurring. Reduction of this group by *t*-butyllithium in the early stages of the reaction is a strong possibility. One of the low retention time products was identified as hexamethyldisilane, one of the expected reduction products. Enough of the addition product (IX) was formed to suggest that addition to the surface might still be feasible under the right conditions. While lowering the reaction temperature may decrease the extent of reduction relative to substitution, previous work suggests that this would result in only very shallow modification. It was decided to try the reaction using poly(ether ether ketone)

(PEEK). The ketone groups of this surface have been shown to react with LiPrOP to give the corresponding *n*-propanol/tertiary alcohol surface. While only shallow modification is expected, the extent of reaction is easily monitored by XPS; the loss of carbonyl oxygen in the  $O_{1s}$  region is a particularly sensitive indicator.<sup>53</sup> A solution containing VIII was prepared as described above and reacted with PEEK for 8 hours at 0°C. No significant change in the atomic composition or the  $O_{1s}$  peak shape were observed. Despite substantial effort, surfaces containing TMS ketene acetal groups could not be prepared.

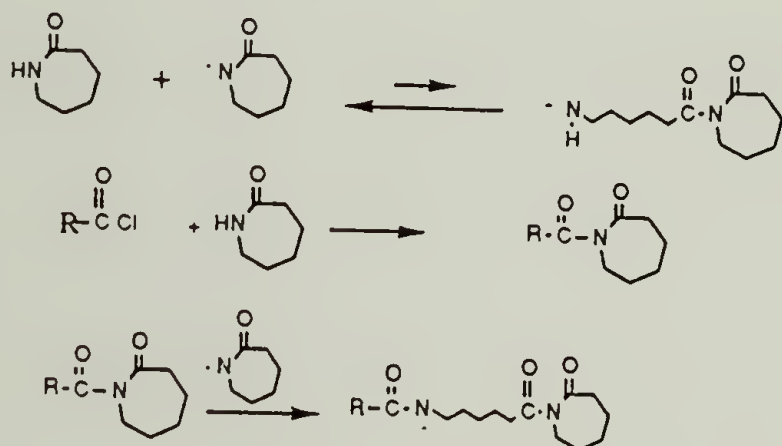
#### Polymerization of $\epsilon$ -Caprolactam from Isocyanate Surfaces

Activated monomer-type polymerizations represent another potentially useful system for surface initiated graft polymerization. While propagation usually involves a reactive, moisture-sensitive species, the concentration of these species is determined by the amount of "activator" added rather than the amount of the initiator species present. The activator reacts with the monomer, while propagation occurs by the reaction of the activated monomer with the relatively stable propagating chain end. The best studied example of this mechanism is the anionic ring opening polymerization of  $\epsilon$ -caprolactam.<sup>54</sup> The polymerization mechanism is shown in equation 12, below. Reaction with the base results in the generation of the lactam ion (activated

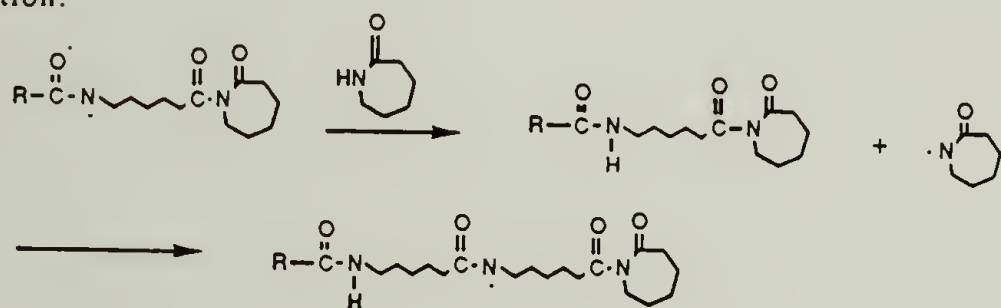


monomer). In the absence of N-acyllactam, initiation requires the formation of the more basic (primary amine) dimer. As a result, a substantial induction period is required. If a portion of the monomer is acylated first, this species acts as the initiator. Since the reaction of this species with the activated monomer results in a stabilized anion, the induction period is eliminated. Proton transfer occurs between the open-chain amide group and the lactam, regenerating the lactam ion. Propagation continues by attack of the lactam ion on the terminal N-acyllactam.

Initiation:



Propagation:



**Equation 12.** Activated monomer polymerization of  $\epsilon$ -caprolactam.

If small amounts of protic impurities are present, the lactam ion concentration is reduced but propagation can

continue. A variety of side reactions complicate this polymerization, resulting in chain degradation (depolymerization), branching and termination.<sup>55</sup> Many of these reactions become more important as the polymer concentration increases. This could be a significant drawback for surface-initiated graft polymerization since high local chain concentrations will occur early in the reaction. Despite these problems, block copolymers have been prepared by the anionic polymerization of  $\epsilon$ -caprolactam. One successful technique is to acylate caprolactam with polymeric isocyanates and use these species to initiate polymerization.<sup>56</sup> These results suggest that isocyanate surfaces could be used in a similar way to prepare graft polymer surfaces.

FEP(TDI)-NCO surfaces were chosen because of the high reactivity of the isocyanate group (see part I) and the resistance of FEP to reduction. The films were reacted first with  $\epsilon$ -caprolactam (CL), and then *n*-butyllithium was added to generate the lactam ion in-situ. The reaction was initially carried out in THF at room temperature. The XPS atomic composition data is summarized in table 23 and ATR-IR spectra are shown in figure 35. Due to the similarity of the atomic composition of the monomer to that of the isocyanate surface, the formation of the N-acyl urea is difficult to monitor by XPS. Examination of the ATR-IR spectrum shows that the isocyanate absorbance is substantially diminished, indicating that reaction of the isocyanate had oc-

**Table 23.** XPS atomic composition data for reactions of isocyanate surfaces with  $\epsilon$ -caprolactam.

<u>Sample #</u>	<u>Takeoff Angle</u>	<u>Starting Material</u>				<u>Conditions</u>			
		<u>C</u>	<u>F</u>	<u>O</u>	<u>N</u>	<u>C</u>	<u>F</u>	<u>O</u>	<u>N</u>
1	15°	100	--	27	10	100	1	25	13
	75°	100	--	28	10				
1	15°	100	--	27	10	100	2	30	10
	75°	100	--	28	10				



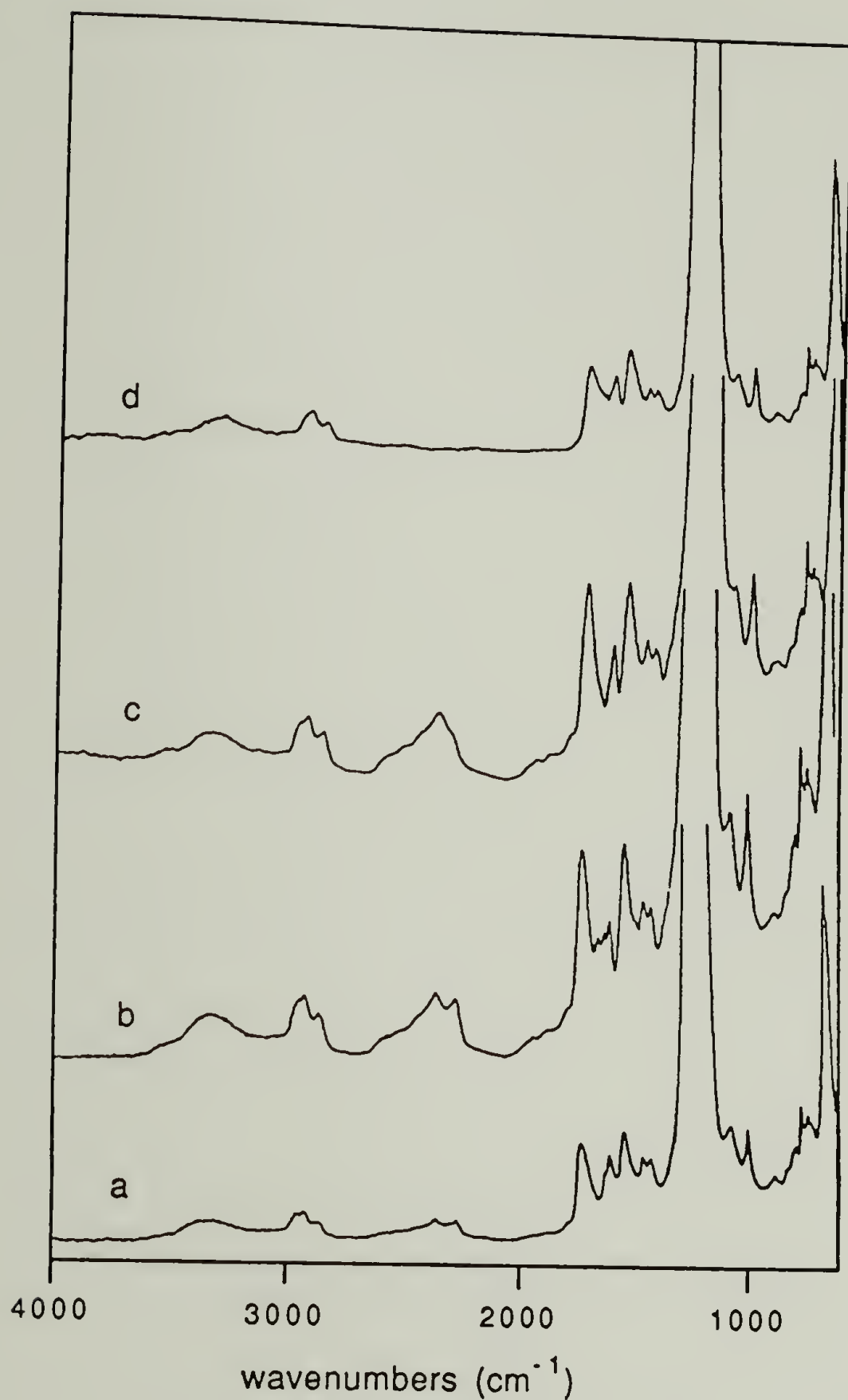


**Figure 35.** ATR-IR spectra of (a) FEP-CL, prepared in THF, (b) FEP-g-CL prepared in THF, (c) FEP-CL prepared in the melt, (d) FEP-g-CL prepared in the melt.

curred. However, no clear evidence of CL incorporation (increased methylene intensity, amide carbonyl at  $\sim 1650\text{ cm}^{-1}$ ) was observed. Analysis of the sample that had been treated with *n*-butyllithium showed no evidence of additional reaction. Fluorine remained in the XPS sampling depth and no significant changes occurred in the ATR-IR spectrum. Caprolactam is generally polymerized in the melt, suggesting that room temperature solution polymerization may not occur. As a result, a model reaction was carried out using the product of phenyl isocyanate and CL as the initiator. Polymerization was allowed to proceed for a comparable period of time in THF at room temperature. Only low molecular weight oligomers were produced. The presence of methanol-soluble salts at the end of the reaction suggests that poor solvation of the anion may decrease its reactivity. The polymerization was attempted using CL in the melt. The reaction was carried out at  $105^{\circ}\text{C}$  in order to maximize polymerization while minimizing decomposition of the urea linkage.<sup>57</sup> The ATR-IR spectrum of the product of reaction with CL (2-3-16c) exhibits no isocyanate absorbance, an intense absorbance at  $1653\text{ cm}^{-1}$  and enhanced methylene intensity. However, extraction with THF resulted in a substantial decrease in the intensities of bands associated with CL, indicating that most of the CL observed in the previous spectrum was adsorbed, not covalently bonded, to the surface. Reaction of this surface with caprolactam ion result-

ed in a small increase in the intensity of the CL bands, but it was clear that little polymer was grafted to the surface. These results indicate that the activated monomer polymerization of caprolactam from isocyanate surfaces is not a practical way to produce a relatively thick graft polymer layer.



## References

1. Costello, C.A.; McCarthy, T.J. *Macromolecules* **1987**, *20*, 2823.
2. McCormick, C.L.; Park, L.S. *J. Polym. Sci., Polym. Chem. Ed.* **1984**, *22*, 49.
3. Gonen, S.; Kohn, D.H. *J. Polym. Sci., Polym. Chem. Ed.* **1981**, *19*, 2215.
4. Tsubokawa, N.; Fujiki, K.; Sone, Y. *J. Polym. Sci., Polym. Chem. Ed.* **1986**, *24*, 191.
5. Qiu, K.Y.; Fang, F.L.; Huang, Z.X.; Feng, X.J. *Polym. Commun.* **1982**, *2*, 81.
6. Mino, G.; Kaizerman, S.; Rasmussen, E. *J. Polym. Sci.* **1959**, *39*, 523.
7. See reference 3.
8. See reference 4.
9. See reference 4, pp 193-194.
10. See reference 5.
11. See reference 2, p 52.
12. Feng, X.D.; Sun, Y.H.; Qiu, K.Y. *Macromolecules* **1985**, *18*, 2105.
13. Asano, S.; Aida, T.; Inoue, S. *J. Chem. Soc. Chem. Commun.* **1985**, 1148.
14. Yasuda, T.; Aida, T.; Inoue, S. *Macromolecules* **1983**, *16*, 1792.
15. Takeda, N.; Inoue, S. *Makromol Chem.* **1978**, *179*, 1377.
16. Inoue, S.; Takeda, N. *Bull. Chem. Soc. Jpn.* **1977**, *50*, 984.
17. Aida, T.; Maekawa, Y.; Asano, S.; Inoue, S. *Macromolecules* **1988**, *21*, 1195.; Inoue, S.; Takeda, N. *Bull. Chem. Soc. Jpn.* **1977**, *50*, 984.
18. The spectrum of *i*-PrOH consists of a doublet and a weak heptet; see Pouchert, C.J. *Aldrich Library of NMR Spectra*, 2nd Ed., Vol. 1 Aldrich Chem. Co.: Milwaukee Wis. 1983; p 109c.

19. See reference 13.
20. See reference 18, p 117.
21. Inoue, S.; Aida, T. In *Ring Opening Polymerizations*, vol. 1, Ivin, K.J.; Sagegusa, T. eds., Elsevier: New York, 1984, pp 239-241, 267-271.
22. Ouhadi, T.; Stevens, C. Teyssie, Ph.; *Makromol Chem, Suppl.* 1975, 1, 191.
23. Aida, T.; Maekawa, Y.; Asano, S.; Inoue, S. *Macromolecules* 1988, 21, 1195.
24. See reference 14, p 1793.
25. Burgess, F.J.; Cunliffe, A.V.; MacCallum, J.R.; Richards, D.H. *Polymer* 1977, 18, 719.
26. See reference 21, pp 225-228.
27. Costello, C.A.; McCarthy, T.J. *Macromolecules* 1987, 20, 2819.
28. Dreyfuss, P.; Kennedy, J.P. *J. Polym. Sci., Polym. Symp.* 1976, 56, 129.
29. See part I, this thesis.
30. See reference 25.
31. See reference 25, p 721.
32. Lee, K.-W.; McCarthy, T.J. *Macromolecules* 1988, 21, 2318.
33. Stang, P.J.; Hanack, M.; Subramanian, L.R. *Synthesis* 1982, 85.
34. See reference 33 pp 103-105.
35. See reference 32.
36. Jung, M.E.; Blum, R.B. *Tetrahedron Lett.* 1977, 43, 3791.
37. This structure has been proposed for PCTFE-OH, see reference 32, p 2321.
38. Kobayashi, S.; Masuda, E.; Shoda, S.-I.; Shimano, Y. *Macromolecules* 1989, 22, 2878.

39. Kobayashi, S.; Saegusa, T. In *Ring Opening Polymerizations*, vol 2., Ivin, K.J.; Saegusa, T. eds., Elsevier: New York, 1984; pp 783-786.
40. See reference 38, p 2879.
41. Webster, O.W.; Hertler, W.R.; Sogah, D.Y.; Farnham, W.B.; RajanBabu, T.V. *J. Amer. Chem. Soc.* **1983**, *105*, 5706.
42. Hertler, W.R.; Sogah, D.Y.; Webster, O.W.; Trost, B.M. *Macromolecules* **1984**, *17*, 1415.
43. Sogah, D.Y.; Hertler, W.R.; Webster, O.W.; Cohen, G.M. *Macromolecules* **1987**, *20*, 1473.
44. Hertler, W.R.; Sogah, D.Y.; Boettcher, F.P. *Macromolecules* **1990**, *23*, 1264.
45. See reference 43, p 1474 and reference 44, p 1265.
46. Yu, H.-S.; Choi, W.-J.; Lim, K.-T.; Choi, S.-K. *Macromolecules* **1988**, *21*, 2894.
47. House, H.O.; Czuba, L.J.; Gall, M.; Olmstead, H.D. *J. Org. Chem.* **1969**, *34*, 2324.
48. Emde, H.; et. al. *Synthesis* **1982**, 6-8.
49. Simchen, G.; Kober, W. *Synthesis* **1976**, 259.
50. See reference 48, p 7.
51. See reference 42, p 1416.
52. See reference 46.
53. Franchina, N.L.; McCarthy, T.J. *Polym. Prepr. (Am. Chem. Soc., Div. Polym. Chem.)* **1990**, *31(1)*, 416.
54. Sekiguchi, H. In *Ring Opening Polymerization*, vol. 2, Ivin, K.J.; Saegwa, T.P. eds., Elsevier:New York, 1984, pp 832-858.
55. See reference 54, pp 842-844, 852-855.
56. Allen, W.T.; Evans, D.E. *Angew Makromol Chem.* **1977**, *58/59*, 321.
57. Hergenrother, W.L.; Ambrose, R.J. *J. Polym. Sci., Polym. Chem. Ed.* **1974**, *12*, 2613.



## CHAPTER VIII

### CONCLUSIONS AND SUGGESTIONS

The research presented in this section has demonstrated the viability of the concept of surface-initiated graft polymerization from initiator species generated by specific organic reactions on the polymer surface. The best results were obtained for the polymerization of THF from halogenated surfaces. Treatment of eliminated-then-brominated FEP surfaces with silver trifluoromethanesulfonate in THF resulted in the introduction of substantial amounts of poly(THF), as evidenced by ATR-IR, if initiation (formation of the triflate followed by reaction with THF to form the cyclic oxonium ion) was allowed to occur below the "floor temperature" of THF polymerization ( $\sim -10^{\circ}\text{C}$ ). The iridescent appearance of the films suggested that a layer of poly(THF) thick enough to produce interference effects was grafted to the polymer surface. The XPS results are consistent with complete coverage of the eliminated fluorocarbon substrate to a depth of at least 40 Å. The changes in the atomic composition of the surface (by XPS) resulting from helium ion etching also support the existence of a poly(THF) overlayer.

The results of other attempted graft polymerizations were less satisfactory. Application of ceric ion redox initiation, one of the most studied means of initiation from specific functional groups, to eliminated-then-hydroxylated fluorocarbon surfaces resulted in a significant yield of the

graft copolymer. However, the relatively unselective nature of the initiation resulted in the formation of "clumps" of polymer rather than the production of a uniform overlayer. The so called "immortal" polymerization of epoxide monomers by aluminoporphyrin initiators proved to be unsuitable for surface initiated graft polymerization. Aluminoporphyrin-containing surfaces could not be successfully prepared by the reaction of hydroxyl surfaces with TPP-Al-Et and chain transfer to the hydroxyl surface resulted in the addition of only a small amount of monomer. While it is probable that the steric demands of the initiator are primarily responsible for the failure of this reaction to proceed on the surface as it does in solution, there is evidence that attractive, non-covalent interactions between the surface and the porphyrin ring exist. These interactions would be expected to further hinder monomer insertion. It should also be noted that difficulty was encountered in reproducing the results that have been reported for solution polymerization using TPP-Al-Cl. The reaction of 2-methyloxazoline with tosylate surfaces derived from poly(chlorotrifluoroethylene) resulted in some monomer incorporation, but only low molecular weight oligomers were formed and reaction with the tosylate groups was incomplete, even for long reaction times. In addition, the reaction conditions were harsh enough to result in damage to the PCTFE substrate. While group transfer polymerization seemed promising<sup>1</sup>, no suc-

cessful means of introducing the TMS ketene acetal initiator group to the surface was found. While  $\epsilon$ -caprolactam appeared to react with isocyanate surfaces prepared from hydroxyl surfaces (FEP-OH) and 2,4-toluene diisocyanate, the reaction of the  $\epsilon$ -caprolactam ion and these surfaces resulted in very little polymerization.

Comparison of the key features of each of these polymerizations reveals several that were unique to the THF graft polymerization system. In-situ generation of the actual initiator species in the presence of the monomer allowed the use of a very reactive initiator species under strictly anhydrous conditions. With proper control of the reaction temperature, initiation and propagation were fast and appeared to be relatively free of side reactions. Since the initiator surface could be prepared from FEP (among the most generally chemically-resistant polymer substrates) and the polymerization occurred under mild conditions, side reactions involving the polymer substrate were not encountered. The interface between the polymer substrate and the graft surface was reasonably sharp, being determined primarily by the thickness of the initial FEP-C modified region. Simplicity appears to be a virtue in surface initiated graft polymerizations. Polymerizations that involved complex, sterically demanding initiator species failed, as did those that sacrificed mechanistic simplicity for tolerance of adventitious impurities. Polymerizations that require long



reaction times and harsh conditions to reach high molecular weight in solution, such as the cationic ring opening polymerization of oxazolines, also appear to be poor candidates. Under these conditions, it is difficult to produce high molecular weight chains and avoid side reactions with the substrate. Comparison of the results of the silver triflate-initiated polymerization of THF with the results of the ceric ion-initiated polymerization of acrylamides clearly demonstrates the value of generating the initiator species via a more selective reaction. The former case resulted in uniform coverage of the polymer surface rather than formation of "clumps" of graft polymer.

A number of features identified for an ideal system were not realized in the triflate-initiated polymerization of THF. The actual initiator species could not be isolated on the surface and the initiation efficiency was difficult to determine. Although problems with  $\beta$ -hydride elimination were overcome, the preparation of a stable triflate surface from the hydroxyl precursor proved impossible. In addition, molecular parameters relevant to the graft polymer, such as the number of chains grafted to the surface and their average length, could not be determined, although block copolymerization results suggest that the polydispersity of the grafted poly(THF) chains should be low.<sup>2</sup> It seems unlikely that any surface-initiated graft polymerization will allow much control over chain length; if the control of this

variable is critical, the grafting of end-functionalized polymers to the surface would be expected to yield more satisfactory results.

The research reported here has identified one successful system for graft polymerization from chemically-well defined initiator species on polymer surfaces and is of sufficient scope to provide some guidance in choosing systems for further study. It does not, however, represent a complete treatment of the subject. Initiator surfaces have been limited to those that can be derived from halogenated and hydroxylated fluorocarbons. These surfaces were chosen because their preparation and reactivity were relatively well understood. Polymer surfaces containing other functional groups such as amines are potentially useful as initiators<sup>3</sup>. In addition, most of the polymerizations that were studied employed the ring opening of cyclic monomers. While most of the polymerizations that were studied here were reported to be living in solution, it has not been established that this is necessary. The polymerizations of a vinyl monomer that is not initiated by AgOTf using in-situ generated triflate groups may help to determine if there is any advantage to using polymerizations that are living in solution. A number of other systems appear to be promising candidates based on this work. One example is silyl aldol condensation polymerization from aldehyde-containing surfaces<sup>4</sup> and another is living ring-opening metathesis polymer-

ization from metalocyclobutane-containing surfaces<sup>5</sup>. While the results for the activated monomer polymerization of  $\epsilon$ -caprolactam were disappointing, activated monomer polymerizations in which reactions with the polymer leading to chain degradation are less important, such as the cationic ring-opening of lactones initiated by an acylating agent in the presence of alcohols<sup>6</sup> (in this case, the hydroxyl surface), may yield more satisfactory results.

The fundamental physical aspects of the polymer-polymer interface in these systems remain unexplored. It would be of interest, for example, to compare well-defined polymer graft surfaces prepared by grafting from surface-confined initiators to comparable surfaces prepared by grafting functionalized polymers to the surface. It is conceivable, for example, that the density of the grafting sites would be much greater in the former case since the reaction involves diffusion of low molecular weight species to the surface while the latter involves diffusion of the polymer. Such a study would require more quantitative information about such factors as chain end concentration, polymer layer thickness and polymer layer density. Radioactive labeling and ellipsometry experiments may provide this type of information. The effect of the graft polymer overlayer on the physical properties of the surface also warrants further study. The importance of the formation of chemical bonds between the separate components in the strengthening of adhesion between



dissimilar materials by coupling agents is the subject of some controversy. One theory holds that the rheological properties of the intervening layer formed by the silane coupling agent, not covalent interconnections formed between the two layers through the coupling agent, are primarily responsible for the observed enhancement in the adhesive joint strength<sup>7</sup>. Well-defined graft polymer overlayers may prove to be useful model surfaces for studying the rheological properties of thin polymer layers made up of chains covalently attached to polymeric substrates.

## References

1. Hertler, W.R.; Sogah, D.Y.; Boettcher, F.P. *Macromolecules* **1990**, *23*, 1264.
2. Burgess, F.J.; Cunliffe, A.V.; MacCullum, J.R.; Richards, D.H. *Polymer* **1977**, *18*, 719.
3. Polymerization of N-carboxy- $\alpha$ -amino acid anhydrides, for example, is initiated by primary amines, See Imanish, Y. In *Ring Opening Polymerizations*, vol. 2, Ivin, K.J.; Saegusa, T. eds., Elsevier: New York, 1984, pp 523-555.
4. Sogah, D.Y. *Polym. Prepr. (Am. Chem. Soc., Div. Polym. Chem.)* **1986**, *27(1)*, 163.
5. Gilliam, L.R.; Grubbs, R.H. *J. Amer. Chem. Soc.* **1986**, *108*, 733.
6. Okamoto, Y. *Polym. Prepr. (Am. Chem. Soc., Div. Polym. Chem.)* **1990**, *31(1)*, 10.; Okamoto, Y. *Polym. Prepr. (Am. Chem. Soc., Div. Polym. Chem.)* **1984**, *25(1)*, 264.
7. Gent, A.N.; PSE department seminar, University of Massachusetts, Amherst, April 1988.

PART III  
SURFACE CHEMISTRY OF FIBRILLAR CARBON



## CHAPTER IX

### INTRODUCTION

Much of the work in this dissertation has been concerned with the surface-selective introduction of organic functional groups to the surface of chemically resistant polymers. Graphitic carbon surfaces represent another type of chemically resistant organic surface. Understanding and being able to control the surface properties of graphitized carbon materials is of paramount importance to their technological applications, whether it is as reinforcing fibers and fillers,<sup>1</sup> adsorbents<sup>2</sup>, or electrochemical substrates.<sup>3</sup> The research reported here describes the chemical modification of Graphite Fibrils by oxidation and reactions with carbenes. The functional group composition of the oxidized surface was also probed using XPS labeling techniques and the effect of oxidation on the fibril morphology was examined. The following sections will describe briefly what is meant by fibrillar graphite, why this material was chosen for this study, and what is known about the modification and characterization of graphitic carbon surfaces.

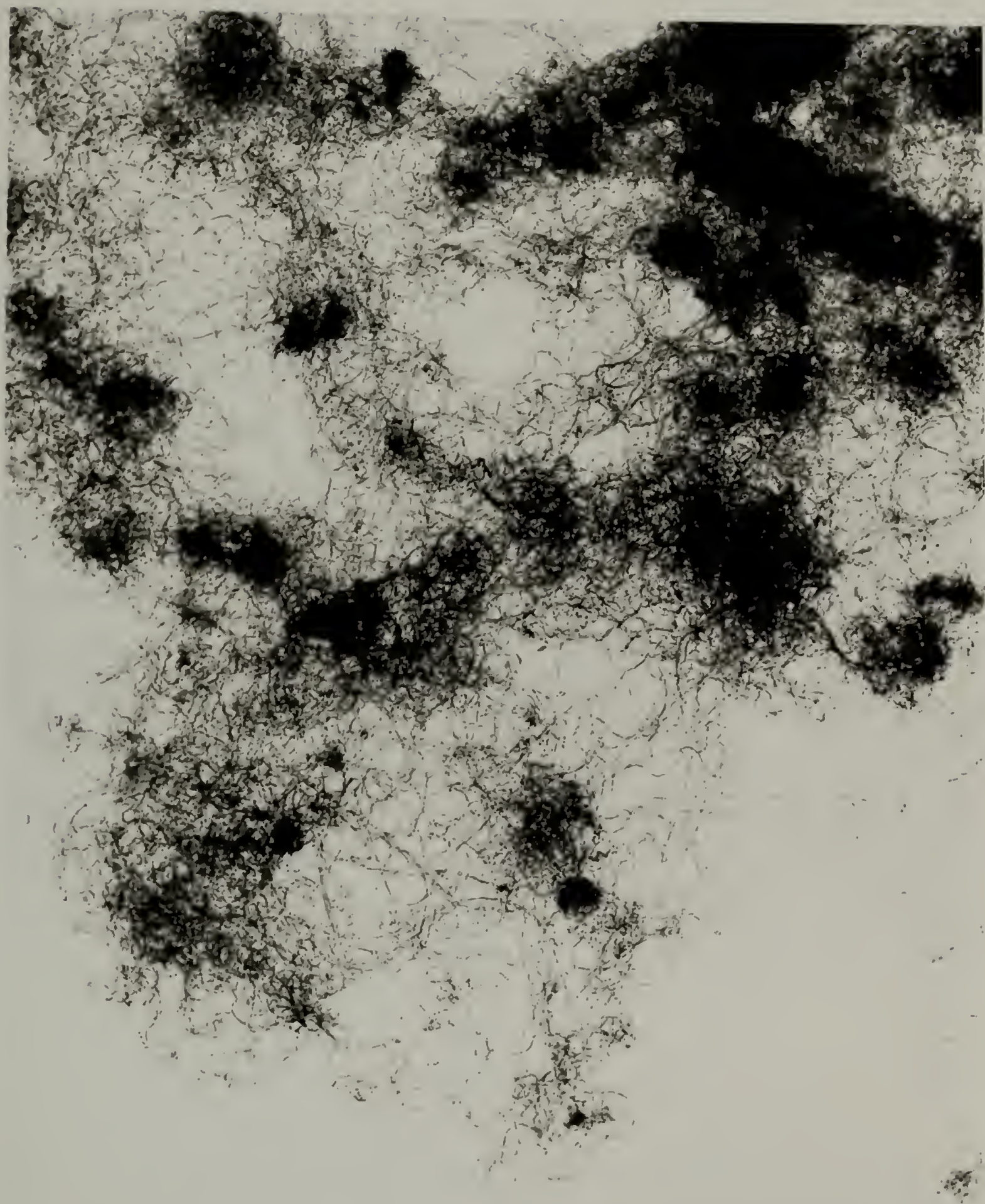
#### Fibrillar Carbon

Recently graphitic carbon has been prepared in a fibrillar morphology<sup>4</sup> consisting of hollow, approximately 100 Å diameter tubes, microns in length. The fibrils are grown from metal catalyst particles at high temperatures in the

presence of a hydrocarbon feedstock. Graphite layers form in concentric rings parallel to the fibril axis (like tree rings). TEM results indicate that the fibril walls are comprised of 15-20 graphite layers. As shown in figure 36, the fibrils grow in a contorted morphology, forming highly entangled mats. The shape indicates that some defects must be present to allow for the curvature. High resolution end-on micrographs indicate that the fibrils are faceted, not cylindrical in cross section. Dark field microscopy detects defects that are formed by mismatching of these polygonal regions along the fibril axis. Other defects such as the incomplete connection of individual graphite layers (like a partially peeled onion) or changes in the number of layers along the fibril axis may be present as well. These defects result in exposed graphite plane edges and are expected to be important as reaction sites. Electron diffraction results indicate that the fibrils are highly graphitic (little amorphous carbon). Elemental analysis results are consistent with this conclusion; very little oxygen (1-2%) and very little hydrogen (<0.2%) is present. Apart from the obvious technological interest in objects of this morphology, the fibrils offered a number of advantages as substrates for carbon surface modification studies. The fibrils could be prepared with a high, reproducible, surface area, low oxygen content and the vast majority of the carbon in a well defined, primarily graphitic, state. Most other carbon

**Figure 36.** TEM micrograph of graphite fibrils.





materials (carbon blacks, charcoals, carbon fibers) are prepared by pyrolysis of synthetic or natural polymeric materials; the properties of the resulting material are very sensitive to the preparation conditions.<sup>5</sup> In most cases, these materials are less graphitic and contain more oxygen, hydrogen and often nitrogen, making the changes due to chemical modification harder to follow. In addition, it was hoped that the unique morphology of the materials would allow the detection of the morphological effects of corrosive reaction. Ideally, it was thought that the location of the reaction sites, and the nature of the reaction (corrosive, at well defined sites versus randomly along the fibril) could be identified by changes in the fibril shape resulting from reaction.

#### Chemical Modification of Graphitic Carbon

An extensive literature exists on the modification of graphitic carbon. Most methods rely on oxidation to introduce functional groups to the surface. A variety of oxidation methods have been employed, including exposure to air, nitrous oxide and water vapor at high temperatures<sup>6</sup>, exposure to RF plasmas<sup>7</sup> and reaction with chemical (wet) oxidants, including  $\text{KClO}_3$  in sulfuric acid<sup>8</sup>, potassium permanganate, sodium hypochlorite, and nitric acid.<sup>9</sup> Except in unusual cases<sup>10</sup>, it is generally accepted that reaction is confined to the edges of the graphite planes, present at



crystalite borders and defects. Although a variety of further reactions have been performed on these surfaces, the chemical structure of the oxidation product remains an area of considerable controversy. The following section will attempt to summarize what is known about the chemistry of oxidized carbon surfaces and discusses in some detail some of the most important experimental evidence.

### Chemical Composition of Oxidized Carbon

Despite an ongoing effort that has produced numerous review articles and several books, a definitive description of the functional group composition and the reactivity of oxidized carbon surfaces has remained elusive. A number of problems have complicated the study of these materials. In general, the specific properties depend strongly on the sample preparation conditions, especially the thermal history, making the comparison of the results obtained by different investigators difficult<sup>11</sup>. The physical and spectroscopic properties of these materials makes analysis difficult. The complexity of these surfaces may ultimately limit the extent to which their chemical composition can be described. A variety of techniques have been applied to the study of oxidized carbons, including thermal desorption (pyrolysis), titration, polarography, derivitization, infrared spectroscopy (IR), X-ray photoelectron spectroscopy (XPS) and electron paramagnetic resonance (EPR) spectroscopy.



py. Data consistent with the presence of a wide variety of functional groups, including carboxylic acids, phenols, enols, lactones, quinones, anhydrides, ketones, and free radicals has been obtained.<sup>12</sup> Often the conclusions based on the results obtained using one technique contradict the results obtained by other experimental techniques. Some of the experimental results that provide background relevant to the research in this dissertation will be described in detail in the following sections.

Titrametric Studies. It has been recognized for some time that oxidized carbon surfaces are acidic. One of the oldest and most widely used techniques for studying these surfaces is titration with aqueous base. Direct potentiometric titrations yield rather flat curves with no identifiable inflection points.<sup>13</sup> Direct titration has been reported to be successful in non-aqueous media, but the results are far from convincing.<sup>14</sup> As a result, the titration of surface acidic groups is generally performed by equilibrating standard base solutions over carbon samples and titrating the base solution to determine the amount of base consumed. Boehm determined that the amount of sodium bicarbonate, sodium carbonate, sodium hydroxide and sodium ethoxide neutralized was related by a ratio of 1:2:3:4 for air-oxidized carbons, and 2:3:4:5 for chemically (wet) oxidized carbons, indicating an increase in the highly acidic groups

using chemical oxidation.<sup>15</sup> Based on this data, functional groups of various acidities (carboxylic acids, phenols, lactones) were proposed. Puri has questioned the validity of this approach, stating that titrations of weak acids with weak bases will not proceed to completion, allowing for the possibility that the same acid groups could have neutralized varying amounts of each base<sup>16</sup>. It was found (by pyrolysis and titration of the product) that the highly acidic oxygen-containing species were eliminated as CO<sub>2</sub> at high temperatures (other oxygen containing functional groups are eliminated as CO). However, derivitization results indicate that these groups are not simple carboxylic acids. A variety of "macro" functional groups, including hydroxyl lactones, and lactones similar in structure to fluorescein (f-lactones, I) have been proposed to explain this data<sup>17</sup>.



I

Spectroscopic Studies. It would seem that many of the questions posed above could be answered by IR spectroscopy, however, obtaining spectra poses many experimental problems. Most carbons are hard to grind and disperse, making transmission IR experiments difficult. Scattering problems have been avoided by using attenuated total reflectance (ATR)<sup>18</sup> and photoacoustic IR<sup>19</sup>. Some of the best data has been obtained by transmission IR of thin carbonized films<sup>20</sup>. In most cases, broad absorbances are observed in the 1750-1550  $\text{cm}^{-1}$  region indicating carbonyl functionality and the 3000-3600  $\text{cm}^{-1}$  region, indicating phenolic functionality. Based on the positions of the absorbances in the 1750-1550  $\text{cm}^{-1}$  region and changes in this region resulting from chemical derivitization, a variety of carbonyl-containing functional groups have been proposed, including cyclic anhydrides,  $\epsilon$ -lactones, lactones and  $\beta$ -hydroxyketones. As expected, the features observed for a given sample depend in a complex fashion on the conditions under which the sample was prepared.<sup>21</sup> The application of X-ray photoelectron spectroscopy to the study of carbon surfaces will be reviewed briefly in the "Results and Discussion" section.

Derivitization Experiments. A wide variety of reactions have been studied as a means of derivitizing specific functional groups on carbon surfaces. Most of these reactions have been carried out in conjunction with base neu-



tralization studies, although changes have also been followed by IR spectroscopy and microanalysis. Results consistent with the presence of carboxylic acids, phenols, quinones, and lactones have been obtained. Functional group composition estimates based on the yield for these reactions leave most of the oxygen unaccounted for. In addition, many functional groups could not be differentiated by this technique. Acidic enols and carboxylic acids, for example, would yield products that are indistinguishable by most of the techniques that have been used to follow these reactions.<sup>22</sup> The principle advantage of this approach is that it provides direct information about the reactivity of the surface, which is of primary interest if the oxidized surface is to be used as a reactive substrate for further modification.

Overall Conclusions. The chemistry of oxidized carbon surfaces clearly defies a simple and general explanation. While the chemistry appears to be dominated by the reactions of acidic, oxygen-containing functional groups, no combination of simple, independently reacting functional groups is capable of explaining all of the data. The trend has been to propose increasingly complex lactonic structures that possess carboxylic and phenolic reactivity.

In light of the expected close steric and electronic association of oxygen on the surface, it is probably most

realistic to view the oxygen as part of a "macro" functional group with it's own unique chemistry that depends on the preparation of the sample. Some investigators have gone so far as to dismiss the concept of functional groups entirely, preferring to describe the surface oxygen as part of an acidic complex consisting of two oxygen atoms attached to an "active" carbon, similar to chemisorbed oxygen on catalyst metal surfaces.<sup>23</sup>

## Objectives

The overall goal of the research that will be presented here was to introduce reactive functional groups to the surface of fibrillar carbon. Oxidation was studied initially, despite the fact that this was expected to result in chemically complex surfaces. XPS labeling experiments were employed to characterize the resulting surfaces. These results allow comparison to be made between surfaces derived from the fibril samples and "traditional" carbon surfaces. It was hoped that this new approach to carbon surface characterization would clarify the chemistry of oxidized carbon surfaces to some degree. Ideally, this work would lead to identification of a reaction or class of reactions capable of proceeding in high yield on the surface or converting the surface to one with simple reactivity. This latter approach has proven successful for "carbonaceous" surfaces prepared by the reduction of fluoropolymers.<sup>24</sup> Functional group

introduction by reaction with carbenes and the effect of varying oxidation conditions on the fibril morphology were also investigated.



## References

1. Donnet, J.-B.; Bansal, R.C.; *Carbon Fibers*, Marcel Dekker: New York, 1984.
2. Bansal, R.C.; Donnet, J.-B.; Stoeckli, F. *Active Carbon*, Marcel Dekker: New York, 1988.
3. Murray, R.W. *Electroanal. Chem.* **1984**, *13*, 191.
4. Tennet, H. U.S. Pat. No. 4,663,230.
5. See, for example, reference 2, pp 1-25, and reference 1, pp 1-44.
6. Puri, B.R. *Chem. and Phys. of Carbon* **1970**, *6*, 194-201.
7. Evans, J.F.; Kuwana, T. *Anal. Chem.* **1977**, *49*, 1632.
8. Smith, R.N. *Quarterly Rev.* **1959**, *13*, 287.
9. See reference 1, pp 120-124.
10. Evans, J.F.; Kuwana, T. *Anal. Chem.* **1979**, *51*, 358.
11. See, for example, reference 6, pp 191-242, and reference 2, pp 60- 67.
12. For recent reviews, see (a) reference 2, pp 27-118; (b) Boehm, H.P. *Adv. in Catalysis* **1966**, *16*, 181-225.; (c) Mattson, J.S.; Mark, H.B. Jr. *Activated Carbon*, Marcel Dekker: New York, 1971, pp 25-86.
13. Villars, D.S. *J. Amer.Chem. Soc.* **1947**, *69*, 214.
14. Studebaker, M.L. In *Proceedings of the Fifth Conference on Carbon*, Penn. State, 1961, vol. II, Pergamon Press: New York, 1963, p 189.
15. Boehm, H.-P.; Diehl, E.; Heck, W.; Sappok, R. *Angew. Chem. Int. Ed.* **1964**, *3*, 669.
16. See reference 6, pp 233-237.
17. For a recent review of this subject, see reference 2, pp 35-49.
18. See reference 12c, pp 61-83.
19. See reference 2, pp 87-92.
20. Zawadzki, J. *Chem. and Phys. of Carbon* **1989**, *21*, 147.

21. For a recent review of this subject, see reference 2, pp 67-87.
22. For reviews of this subject see reference 2, pp 60-67, and Donnet, J.B. *Carbon* **1968**, 6, 161-167.
23. See reference 6, pp 228-229.
24. Bening, R.C.; McCarthy, T.J. *Macromolecules* **1990**, 23, 2648.

## CHAPTER X

### EXPERIMENTAL SECTION

#### Methods

The work described in this section involved samples that behaved essentially as powders; as a result, the techniques for sample handling differed somewhat from the techniques used to handle polymer films. In general, fibril samples were reacted in Schlenk tubes and transferred to a fritted filter funnel (10-20  $\mu$ ) in air. The solution was removed using a vacuum (Gast pump). In most cases, little, if any, of the fibril sample was not retained. The fibrils were washed by transferring the desired solvent into the funnel. The suspension was stirred (usually for 2-5 minutes) and the solvent was removed using a vacuum. The samples were returned to Schlenk tubes for drying under vacuum. When the product was expected to be air sensitive, filtrations were performed in a Schlenk-type filtration apparatus, shown in figure 37. The reaction was carried out in the round end of the tube. When the reaction was over, the tube was inverted to transfer the contents to the filter side. After the samples were dried, they were handled under inert atmosphere in a dry box or using Schlenk techniques. Dry samples were difficult to handle due to static build up. Neutralization with a Zerostat (Aldrich) helped, but, in



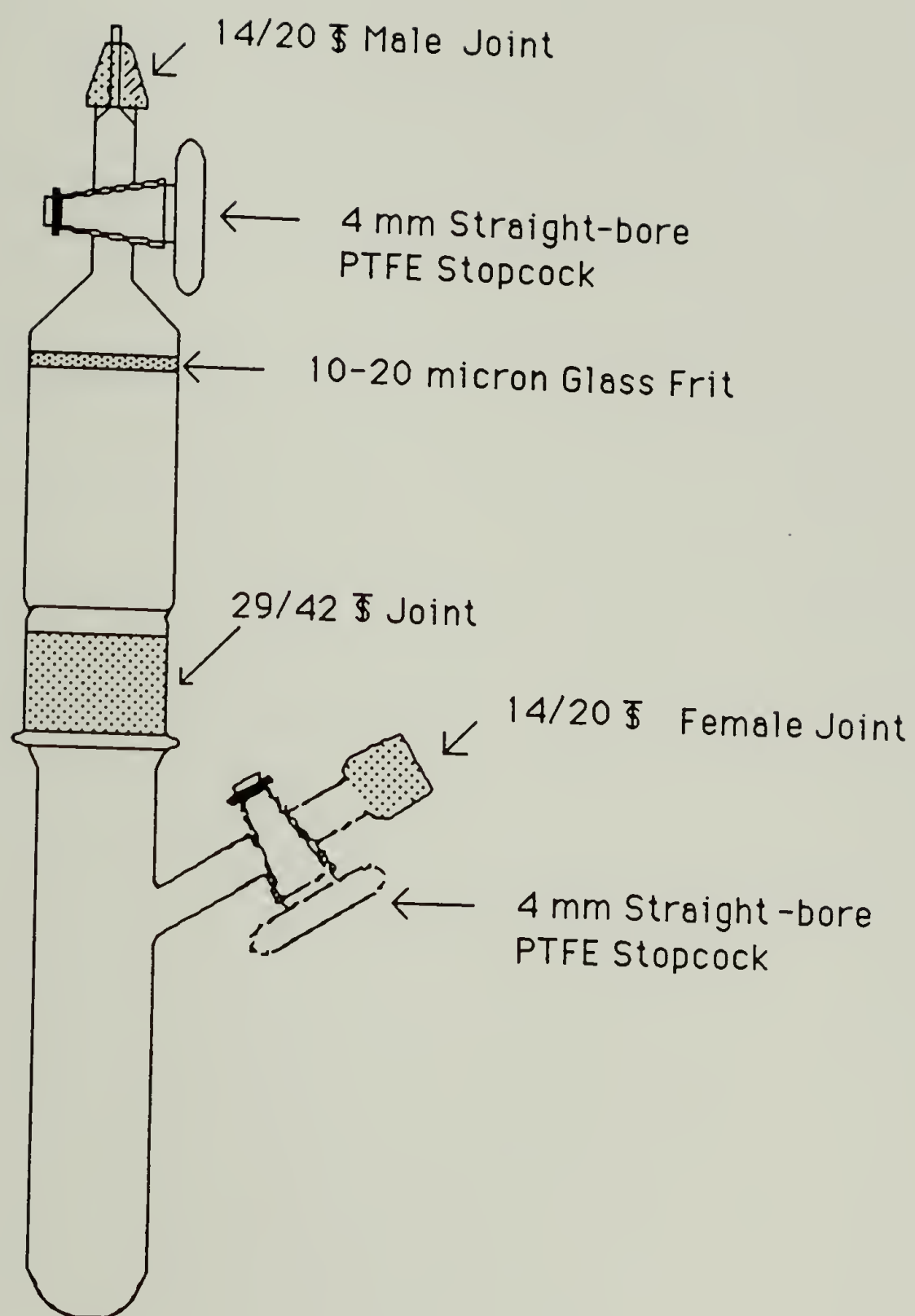


Figure 37. Schlenk-type filter apparatus.

general, the samples were easier to handle on a conductive surface such as aluminum foil.

X-ray photoelectron spectra (XPS) were recorded on a Perkin-Elmer-Physical Electronics 5100 spectrometer ( $\text{MgK}_\alpha$  excitation, 300 W) using a pass energy of 71.5 eV. The powder samples were attached to Mylar films using double stick tape and mounted to the sample holder. In general, atomic composition results were reported for analysis at a  $15^\circ$  takeoff angle. Analysis at a grazing angle minimizes the contribution due to the tape. In general, identical results were obtained at a  $75^\circ$  takeoff angle. Because the fibers were randomly oriented, angle dependent XPS could not be used to determine the composition profile as a function of depth as it had been for film samples. For objects of these dimensions, XPS atomic compositions represent essentially bulk values. TEM micrographs of the fibril samples were provided by Hyperion Catalysis International. Packed column gas chromatography of reagents and model reaction products was performed using an Analabs Superpak II column and a Perkin Elmer 5790A gas chromatograph equipped with an FID detector.

#### Purification of Solvents and Reagents

The purification of the following solvents and reagents is described in part I, chapter 2: tetrahydrofuran, water,

methanol, ethanol, pyridine, heptafluorobutyryl chloride, 2,4-dinitrophenylhydrazine, DBU.

The purification of the following solvents and reagents is described in part II, chapter 2: dichloromethane, diethyl ether, benzene, dimethylformamide, 3-bromo-1-propanol.

**Thallium ethoxide** (Aldrich) was filtered through an 0.2  $\mu$  filter under nitrogen, to remove oxides, immediately prior to use.

**Dibutyl ether** (Aldrich) was distilled from sodium benzo-phenone dianion and stored under nitrogen.

**0.1 N HCl solution** was standardized relative to dry potassium carbonate by potentiometric titration.

**0.5 N and 0.1 N NaOH solutions** were standardized by titration with standard HCl solution using bromothymol blue indicator.

**Decahydronaphthalene** (Decalin, Aldrich) was stirred over and distilled from calcium hydride under reduced pressure.

**n-Butylamine** (Aldrich) was refluxed over and distilled from calcium hydride under reduced pressure (trap-to-trap) and stored under nitrogen.

The following reagents were used without further purification: Graphite Fibrils® (Hyperion Catalysis International, lot 066-04), calcium hydride (Aldrich), sodium hydroxide (Fisher), 4-dimethylaminopyridine (DMAP, Aldrich), calcium



chloride (Fisher), potassium chlorate ( $\text{KClO}_3$ , Alfa), sulfuric acid (ACS conc., Fisher), isopropanol (Fisher), boron trifluoride etherate (Aldrich), 2,2,2-trifluoromethylamine hydrochloride (Aldrich), sodium nitrite (Aldrich), benzoic acid (Fisher), acetic acid (Aldrich), dicyclohexylcarbodiimide (Aldrich), p-bromophenylethanol (Aldrich), carbonyldiimidazole (Aldrich), 3-fluorobenzyl bromide (Aldrich), chloromethyl methyl sulfide (Aldrich), sodium methoxide (Aldrich), thionyl chloride (Aldrich), bromothymol blue (0.04 wt.% in water, Aldrich), copper(II) acetate monohydrate (Aldrich), ethyl diazoacetate (Aldrich), potassium hydroxide (Fisher), ammonium chloride (Fisher).

#### $\text{KClO}_3$ Oxidation

(b1p4-8,31-34,55,73,86) Carbon fibrils were oxidized using one of the following conditions: (a) 1.0 g  $\text{KClO}_3$  was dissolved in 50 mL of  $\text{H}_2\text{SO}_4$ , resulting in a dark red solution. The solution was transferred to approximately 1 to 2 g of fibrils in a beaker, in air. Gas (presumably chlorine) was evolved. The black, gel-like slurry was stirred for the desired time (30 minutes, 60 minutes, 24 hours) at room temperature. The slurry was transferred to a fritted (10-20  $\mu$ ) filter funnel, the reagent was removed, and the product was washed with copious amounts (~1 liter each) of water and methanol. The  $\text{KClO}_3$  solution was somewhat dark in color, suggesting that some of the fibrils were too small to be

retained. The fibrils were dried under vacuum (0.03 mm) at 90-100°C. (b) 5 g of carbon fibrils was reacted with 3.4 g of  $\text{KClO}_3$  in 170 mL of  $\text{H}_2\text{SO}_4$  for 1 hour, as described in (a). (c) Approximately 1 to 2 g of fibrils were reacted with 5 g of  $\text{KClO}_3$  in 50 mL of  $\text{H}_2\text{SO}_4$ . The addition of acid to the  $\text{KClO}_3$  resulted in the copious evolution of chlorine. Gas evolution continued after the solution was transferred to the fibrils. After the desired amount of time (3 hours, 24 hours, 95 hours) the samples were isolated and washed as described above. The solution was darker, suggesting that fewer of the fibrils were retained on the frit.

#### Lithium Triethylborohydride Reduction

(bIp21-22,73) 0.2 g (~2-3 mmol of surface oxygen) of oxidized fibrils and 0.2 g of "as received" fibrils were placed in separate nitrogen-purged Schlenk tubes and 10 mL (10 mmol) of a 1.0 M THF solution of lithium triethylborohydride was added to each tube. The reaction was allowed to proceed at room temperature for 18 hours. 5 mL of isopropanol was added to each tube, to kill any unreacted hydride, and the fibrils were collected on a glass frit. The sample was washed with water, methanol (~100 mL of each) and THF (~30 mL) and then dried at 120°C under vacuum. The filtrate that was removed from the "as received" sample was clear and colorless, while the filtrate that was removed from the oxidized sample was dark colored. The reduction

was also performed using 2.5 g of oxidized fibrils (~21 mmol of oxygen) in 50 mL (50 mmol) of 1.0 M lithium triethylborohydride for 25 hours. The fibrils were isolated and washed as described above.

#### Reaction with Thallium Ethoxide

(bIp17-20,56,74,116) The fibril samples (~0.1 g) were placed in a Schlenk-type filter apparatus. Enough TlOEt was added, through an 0.2  $\mu$  HPLC preparation filter cartridge via gastight syringe, to cover the fibrils. The reaction was allowed to proceed for 2-3 minutes and nitrogen pressure was applied to remove the reagent. The samples were washed with ten 10 mL portions of dry ethanol under nitrogen, and then washed with an additional 100-200 mL of dry ethanol in air. Great care must be taken to avoid leaving behind adsorbed TlOEt. The absence of TlOEt in the ethanol rinse could be verified by the addition of a small amount of HCl; HCl reacts with TlOEt to form white, insoluble TlCl. Washing was continued until no white precipitate was observed when HCl was added to the last volume of the filtrate. The samples were dried under vacuum at 120°C.

#### Reaction of Tl-Labeled Surfaces with Heptafluorobutyryl Chloride

(bIp56,58-60) Thallium-labeled surfaces were reacted with heptafluorobutyryl chloride (HFBC) under the following



conditions: (a) 0.2 g of oxidized carbon fibrils (0.02 g/mL  $\text{KClO}_3$ , 1 hour) was reacted with  $\text{TlOEt}$  as described above, and loaded into the reaction tube end of a Schlenk-type filter apparatus (described in the "methods" section), in a dry box. The fibrils were suspended in 10 mL of THF and 0.5 mL of HFBC was added via syringe. A white precipitate formed immediately. The tube was covered with foil and the reaction was allowed to proceed for 18 hours at room temperature. At the end of the reaction, the precipitate had dissolved, resulting in a clear, dark solution. The fibrils were washed with five 20 mL portions of THF and dried at room temperature under vacuum. (b) 0.2 g of the Tl-labeled oxidized fibril sample was prepared as described above and reacted with 1 mL of HFBC in 10 mL of THF in the dark. Once again, a white precipitate formed immediately. Within 10 minutes, the precipitate had dissolved to yield a dark, clear solution. After 15 minutes the reagent was removed and the product was washed and dried as described above.

#### Preparation of Trifluoromethyldiazomethane

(bIp94-99,101-102) Trifluoromethyldiazomethane ( $\text{CF}_3\text{CH-N}_2$ ) was prepared as a diethyl ether solution as follows: 13.5 g (0.1 mole) of trifluoroethylamine hydrochloride was dissolved in 50 mL of distilled water in a 250 mL round bottom flask. 75 mL of diethyl ether was added and 7.5 g (0.103 mole) of sodium nitrite was added, slowly with vigor-

ous stirring. Gas was evolved and a yellow color developed in the ether layer. A Teflon stopper was placed on the flask and the flask was cooled to  $-10^{\circ}\text{C}$  (Haake bath). After 10 to 15 minutes, the solution was transferred to a separatory funnel; the ether layer was removed and stored, tightly capped, in a refrigerator. The aqueous solution was returned to the flask, an additional 50 mL of ether was added, and the flask was shaken and allowed to stand for 10 to 15 minutes at  $-10^{\circ}\text{C}$ . The ether layer was removed in a separatory funnel and combined with the previous ether solution. The aqueous phase was extracted with an additional 50 mL of ether as described above. The final volume of ether was very pale yellow colored. The clear, bright yellow ether solution was washed with two 25 mL portions of aqueous potassium carbonate, dried over calcium chloride (2 h,  $-10^{\circ}\text{C}$ ) and distilled. The product codistilled with the ether resulting in a clear, bright yellow solution. When refrigerated under nitrogen, the product is reported to be stable for at least 6 weeks. Neat  $\text{CF}_3\text{CHN}_2$  was prepared by substituting dibutyl ether for diethyl ether in the procedure described above and using 6.75 g of 2,2,2-trifluoroethylamine hydrochloride and 3.75 g of sodium nitrite. The product was distilled (bp  $\sim 13^{\circ}\text{C}$ ) into a cold trap (dry ice/acetone) under reduced pressure ( $\sim 500$  mm) with the pot at room temperature. Distillation was considered to be complete when all of the yellow color was gone from the dibutyl

ether solution. Approximately 3 to 5 mL of the bright yellow solution was collected. The product was dissolved in 20 mL of dichloromethane and stored under nitrogen in a refrigerator.

#### Reaction of $\text{CF}_3\text{CHN}_2$ with Benzoic Acid in Dichloromethane

(bIp102-103) 0.85 g (7 mmol) of benzoic acid was dissolved in 10 mL of dichloromethane in a nitrogen-purged, septum-capped round bottom flask. 5 mL of  $\text{CF}_3\text{CHN}_2$  in dichloromethane (~1.75 mmol) was added. Addition of 0.05 mL (0.4 mmol) of boron trifluoride etherate resulted in rapid gas evolution and loss of the yellow color. After 2 hours, the colorless dichloromethane solution was washed with aqueous potassium carbonate, dried over calcium chloride, concentrated to ~5 mL (rotary evaporator) and analyzed by GC.

#### Boron Trifluoride Etherate Catalyzed Reaction with $\text{CF}_3\text{CHN}_2$

(bIp103-105, 109-110) 0.25 g of the carbon fibril sample was suspended in 10 mL of dichloromethane in a nitrogen-purged Schlenk tube. 5 mL of  $\text{CF}_3\text{CHN}_2$  in dichloromethane (prepared as described above), followed by 0.05 mL of boron trifluoride etherate, was introduced to the reaction tube. Gas evolution began immediately and continued for several hours after the addition of the  $\text{BF}_3 \cdot \text{OEt}_2$ . After 24 hours, the fibrils were collected on a frit and washed with five 10



mL portions each of dichloromethane, methanol and THF. The reagent remained somewhat yellow in color, indicating incomplete reaction of the diazoalkane. One portion of each sample was washed with aqueous potassium carbonate and water prior to washing with THF and a third was refluxed in 1 N aqueous HCl for 24 hours, and then washed with water, methanol and THF. All of the samples were dried under vacuum at 110°C.

#### Reaction with 2,4-Dinitrophenylhydrazine

(bIp8-9,11-12) Carbonyl groups were labeled with 2,4-dinitrophenylhydrazine (DNPH) using one of the following procedures: (a) 0.1 to 0.2 g of each of "as received" and oxidized fibril (24 h, 30 min) samples were placed in nitrogen-purged Schlenk tubes. 0.6 g (3 mmol) of DNPH was dissolved in 3 mL of distilled water and approximately 1 mL of HCl in a nitrogen-purged graduated cylinder, 60 mL of THF was added, and 20 mL of the bright orange solution was transferred to each of the tubes. After 24 hours, the fibrils were collected on a frit and washed with approximately 200 mL of THF (until no further orange color was observed in the rinse), 100 mL of methanol and 30 mL of THF, and then dried at 70°C under vacuum. (b) 2.0 g (10 mmol) of DNPH was dissolved in a mixture of 40 mL of ethanol and 25 mL of THF. The solution became bright orange, but some of the hydrazine remained suspended. 30 mL of this mixture was

added to each of three Schlenk tubes containing approximately 0.2 g of "as received", oxidized or oxidized/reduced fibril samples. 0.25 mL of acetic acid was added to each tube. The reaction was allowed to proceed at room temperature for 45 hours. Some of the hydrazine remained undissolved. After 45 hours, the samples were isolated, washed and dried as described in (a). Washing with THF removed all of the remaining hydrazine.

#### Reaction with Heptafluorobutyryl Chloride

(bIp13,24,44-46) Hydroxyl groups were labeled using one of the following procedures: (a) The carbon fibril sample (0.1-0.2 g) was placed in a nitrogen-purged Schlenk tube and 10 mL of pyridine was added. 0.5 mL (3.3 mmol) of HFBC was added via syringe with rapid stirring, resulting in a bright yellow solution. After 24 hours, the fibrils were collected on a frit (in air) and washed with approximately 150 mL each of THF and methanol, and then dried at 70°C under vacuum.

(b) The carbon fibril sample (0.1-0.2 g) was placed in a nitrogen-purged Schlenk tube and a solution of 0.05 g (0.4 mmol) of DMAP in 15 mL of pyridine was added. 0.5 mL of HFBC was added via syringe. A white precipitate formed, some of which dissolved to yield an orange solution. After 46 hours, the fibrils were collected on a frit and washed and dried as described above. The remaining white solid dissolved in methanol.

### Reaction with DCC and p-Bromophenylethanol

(bIp35-36,41) 1.27 g (6 mmol) of dicyclohexylcarbodiimide (DCC) was dissolved in 30 mL of THF; half of this solution was transferred into each of two Schlenk tubes containing (1) "as received" and (2) oxidized carbon fibrils (0.1-0.2 g). 1.7 mL (12 mmol) of p-bromophenylethanol and 1 mL of pyridine were added to each tube via syringe. After 17 hours at room temperature, the samples were collected on a glass frit and washed with 60 mL each of THF, methanol and THF, and then dried at approximately 150°C under vacuum.

### Reaction with Carbonyldiimidazole

(bIp47-50,88) The acyl imidazole surface was prepared as follows: 0.8 g of carbonyldiimidazole (CDI) was dissolved in 20 mL of THF and the solution was transferred onto approximately 0.1 g of the fibril sample in the reaction tube end of a Schlenk-type filter apparatus. A small amount of gas evolution occurred upon addition of the CDI solution. After 18 hours, the solution was removed and the fibrils were washed with five 20 mL portions of THF under nitrogen, and then dried at room temperature under vacuum. The acyl imidazole surface was reacted with p-bromophenylethanol as follows: An oxidized fibril sample (approximately 0.1 g) was reacted with CDI as described above. After the fibrils were washed, they were transferred back to the reaction tube side and a solution of 1.4 mL (10 mmol) of p-bromophenylethanol



in 10 mL of THF was added and the tube heated to 50°C. After 20 hours the reagent was removed and the fibrils were washed with four 10 mL portions of THF (in air), and then dried at 120°C under vacuum.

#### DBU Catalyzed Reactions with Electrophiles

(bIp68,84-85,89-90) The fibril sample (approximately 0.2 g) was placed in a nitrogen-purged Schlenk tube equipped with a water jacket around the top half. 20 mL of benzene, followed by 0.2 mL (1.5 mmol) of DBU was added to the tube and the tube was heated in order to reflux the solution. After 2 hours, 0.4 mL (3 mmol) of 3-fluorobenzyl bromide was added via syringe. After refluxing for 45-50 hours, the solution was cooled to room temperature, the fibrils were collected on a glass frit, and the sample was washed with five 10 mL portions each of benzene, methanol and THF, and then dried at room temperature under vacuum. The reaction was also carried out using 3 mmol (0.25 mL) of chloromethyl methyl sulfide.

#### Reaction with Sodium Methoxide

(bIp61-62) 0.54 g of sodium methoxide was loaded into a graduated cylinder in a dry box and dissolved in 10 mL of dry methanol. The solution was transferred to a Schlenk tube containing approximately 0.2 g of oxidized carbon fibrils. The reaction was allowed to proceed for 24 hours,

the product was collected on a glass frit (in air), washed with three 10 mL portions of methanol and then dried at 180°C under vacuum.

#### Reaction with Thionyl Chloride

(bIp64-65) Approximately 0.2 g of oxidized fibrils were placed in the reaction tube side of a Schlenk-type filter apparatus. 10 mL of thionyl chloride was added, along with 50  $\mu$ L of dimethylformamide. After 29 hours at room temperature, the solution was removed and the fibrils were washed with three 20 mL portions of THF (under nitrogen) and then dried under vacuum at room temperature. A portion of the product was reacted with 3-bromo-1-propanol (0.2 mL) in pyridine (10 mL) in the presence of DMAP (0.04 g) for 26 hours. The product was collected on a frit, washed with five 10 mL portions each of THF, methanol and THF, and then dried at room temperature under vacuum.

#### Titration

(bIp72-77,79,80,86-87) The fibril samples were titrated with aqueous sodium hydroxide by one of the following procedures: (a) 100.0 mL of 0.465 N NaOH solution was transferred by volumetric pipet to each of round bottom flasks containing (1) 0.95 g "as received", (2) 0.48 g oxidized fibril samples; 100 mL of the base solution was also transferred to an empty round bottom flask, to serve as a control. The

flasks were capped with septa, the headspace was purged briefly with nitrogen, and the fibrils were stirred for 46 hours at room temperature. When the stirring was discontinued the "as received" sample settled out, but the oxidized fibril sample remained suspended. A 25 mL aliquot of the base solution was removed from the control flask and the "as received" sample and titrated with 0.116 N HCl using bromothymol blue as the indicator. The oxidized fibril sample was separated from the base solution by vacuum filtration and a 25 mL aliquot of the filtrate was titrated. (b) A 1.88 g sample of oxidized fibrils and a 1.99 g sample of "as received" fibrils were equilibrated with 0.086 N aqueous sodium hydroxide as described above. All three samples (including the blank) were forced through a fritted glass filter using positive nitrogen pressure, to avoid concentrating the base solution, and a 25 mL aliquot of the filtrate was titrated as described above.

## Reactions of Fibrillar Carbon with Carbenes

### Cu Catalyzed Reaction with $\text{CF}_3\text{CHN}_2$ . (bIp106-107)

Approximately 0.01 g of copper acetate monohydrate ( $\text{CuAc}_2 \cdot \text{H}_2\text{O}$ ) and 0.2 g each of "as received", oxidized and oxidized/reduced fibrils were added to Schlenk tubes and 20 mL of trifluoromethyldiazomethane (in ether) was added to each tube at room temperature. Gas evolution began immedi-



ately. After 20 hours, the fibrils were collected on a glass frit; the filtrate was clear and pale blue, indicating complete reaction of the diazoalkane. The samples were washed with approximately five 10 mL portions each of diethyl ether, aqueous  $K_2CO_3$ , water and THF. All of the samples did not wet as easily as they did prior to the reaction; the fibrils tended to float on the surface. The addition of a small amount of methanol helped to disperse the products. A small amount of an extremely hydrophobic white solid was also present. The fibrils were dried under vacuum at  $100^\circ C$ . A portion of each sample was also refluxed for approximately 24 hours in 1 N aqueous HCl and washed and dried as described above.

Cu Catalyzed Reaction with Ethyl Diazoacetate. (bI-p114-116) 0.014 g of  $CuAc_2 \cdot H_2O$  and 0.2 g each of oxidized and "as received" fibril samples were added to Schlenk tubes, 10 mL of diethyl ether was added and the tubes were cooled to  $0^\circ C$ . 0.8 mL (4 mmol) of ethyl diazoacetate was dissolved in 20 mL of diethyl ether and 10 mL of this pale orange solution was transferred to each of the tubes. When the solutions were warmed to room temperature, the reaction began to bubble vigorously; gas evolution continued for about one hour. After 24 hours, the products were collected on a glass frit; the filtrate was pale blue colored, indicating complete reaction of the diazoacetate. The products

were washed with five 10 mL portions each of diethyl ether, water, methanol and THF, and then dried at 100°C under vacuum. A portion of each sample was also refluxed in a solution containing 20 mL of water, 20 mL of methanol and 4 mL HCl for 23 hours, and then washed with five 20 mL portions each of water and methanol, and dried at 120°C under vacuum.

Thermal Decomposition of Ethyl Diazoacetate in the Presence of Fibril Samples. (bIp118-119) One gram of "as received" fibrils was suspended in 20 mL of decalin in a 3 neck round bottom flask, a septum was added to one arm, a thermometer was immersed in the suspension through an adapter and a condenser was attached to the third arm. The flask was purged with nitrogen and heated to 135°C in an oil bath. 5 mL of ethyl diazoacetate was added via a needle through the septum at a rate of 1 mL per hour using a syringe pump. Gas was evolved when the diazoacetate came in contact with the hot solvent. After all of the reagent was added, the flask was heated to 160°C for 2 hours. The suspension was cooled to room temperature and the fibrils were collected on a glass frit. 0.5 g of the product was washed with five 10 mL portions each of THF, water and methanol, and dried at 100°C under vacuum. 0.5 mL of the product was hydrolyzed overnight in a refluxing solution of 10 g of KOH in 80 mL of ethanol and 20 mL of water. The base was removed, the

fibrils were stirred in a solution of 5 mL of HCl, 20 mL of water and 25 mL of ethanol and then dried at 100°C under vacuum.

Amidation of Ester Surfaces. (bIp120) The surface that resulted from the reaction of the fibrils with ethyl diazoacetate at 135°C in decalin was reacted with n-butylamine as described below. Approximately 0.2 g of the product and 0.1 g of ammonium chloride were loaded into a reflux condenser-equipped Schlenk tube, 10 mL of n-butylamine was added and the suspension was refluxed for 21 hours. The tube was cooled to room temperature, the fibrils were collected on a glass frit, washed with five 20 mL portions each of methanol, water, methanol and THF, and then dried at 120°C under vacuum. A sample of "as received" fibrils was subjected to the same reaction conditions as a control.



## CHAPTER XI

### RESULTS AND DISCUSSION

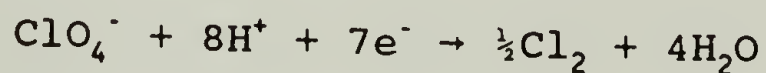
#### Oxidation and Reduction

Oxidation has been the most widely studied means of introducing functional groups to carbon surfaces. Of the variety of oxidation techniques that have been reported, chemical (wet) oxidation appeared to be best suited for functionalization of the fibrils. Choice of the reagent and variation of the reagent concentration offers more control over the harshness of the oxidation conditions than is offered by RF plasmas and thermal oxidation. In addition, wet oxidation is reported to result in a higher yield of the most acidic (expected to be the most reactive) functional groups<sup>1</sup>. The highly graphitic nature of the fibrils suggested that relatively harsh conditions would be required. Potassium chlorate in sulfuric acid has been shown to be reactive towards carbon materials<sup>2</sup>; it is easy to prepare and, unlike  $\text{KMnO}_4$  and  $\text{Cr}_2\text{O}_7$ , insoluble oxides are not formed as a biproduct of oxidation. At concentrations below 2 g in 50 mL, chlorate ion is the species primarily responsible for oxidation and the half-reaction can be written as:



Equation 13. Half reaction for chlorate oxidation.

At higher concentrations, some of the potassium chlorate is oxidized to potassium perchlorate; under these conditions, the primary oxidant is the perchlorate ion<sup>3</sup> and the relevant half-reaction for oxidation can be written as:



**Equation 14.** Half reaction for perchlorate oxidation.

However, the complexity of the substrate that is being oxidized and incomplete understanding of the oxidation mechanism makes an a priori prediction of the product stoichiometry from the oxidant concentration impossible.

The fibrils were oxidized as described in the experimental section and examined by XPS and TEM. TEM micrographs of the product retained on the frit revealed no evidence of physical damage, although a small amount of the fibrils were not retained, suggesting that some cleavage had occurred. The XPS atomic composition data is summarized in table 24. A significant increase in the oxygen content occurred as a result of the reaction. A control reaction (1 h,  $\text{KClO}_3$  omitted) resulted in no change in the atomic composition.

**Table 24.** XPS atomic composition data for fibril oxidations.

<u>Time</u>	<u>Concentration (g/mL)</u>	<u>C</u>	<u>O</u>
As Recv.	--	100	1.6
30 min.	0.02	100	8.8
1 hour	0.02	100	9 ± 2
24 hours	0.02	100	10
95 hours	0.1	100	15
24 hours	0.1	100	15

It is also interesting to note that there was little change in the extent of oxidation as a result of increasing the reaction time and the reagent concentration. These results are consistent with the rapid introduction of a large amount of oxygen to the reactive sites, presumably the graphite plane edges at defects. Unless otherwise specified, reactions were performed on fibrils that had been oxidized for 1 hour using 0.02 g/mL  $\text{KClO}_3$  in  $\text{H}_2\text{SO}_4$ . The XPS spectra of the  $\text{C}_{1s}$  and  $\text{O}_{1s}$  regions, before and after oxidation, are shown in figures 38 and 39, respectively. Very little change was observed in the  $\text{C}_{1s}$  region, despite the introduction of a large amount of oxygen; similar results have been reported for other carbon surfaces<sup>4</sup>. There are two reasons for this: the oxidation reaction results in the formation of a variety of oxygen-containing functional groups with a nearly continuous range of carbon binding energies, the net result



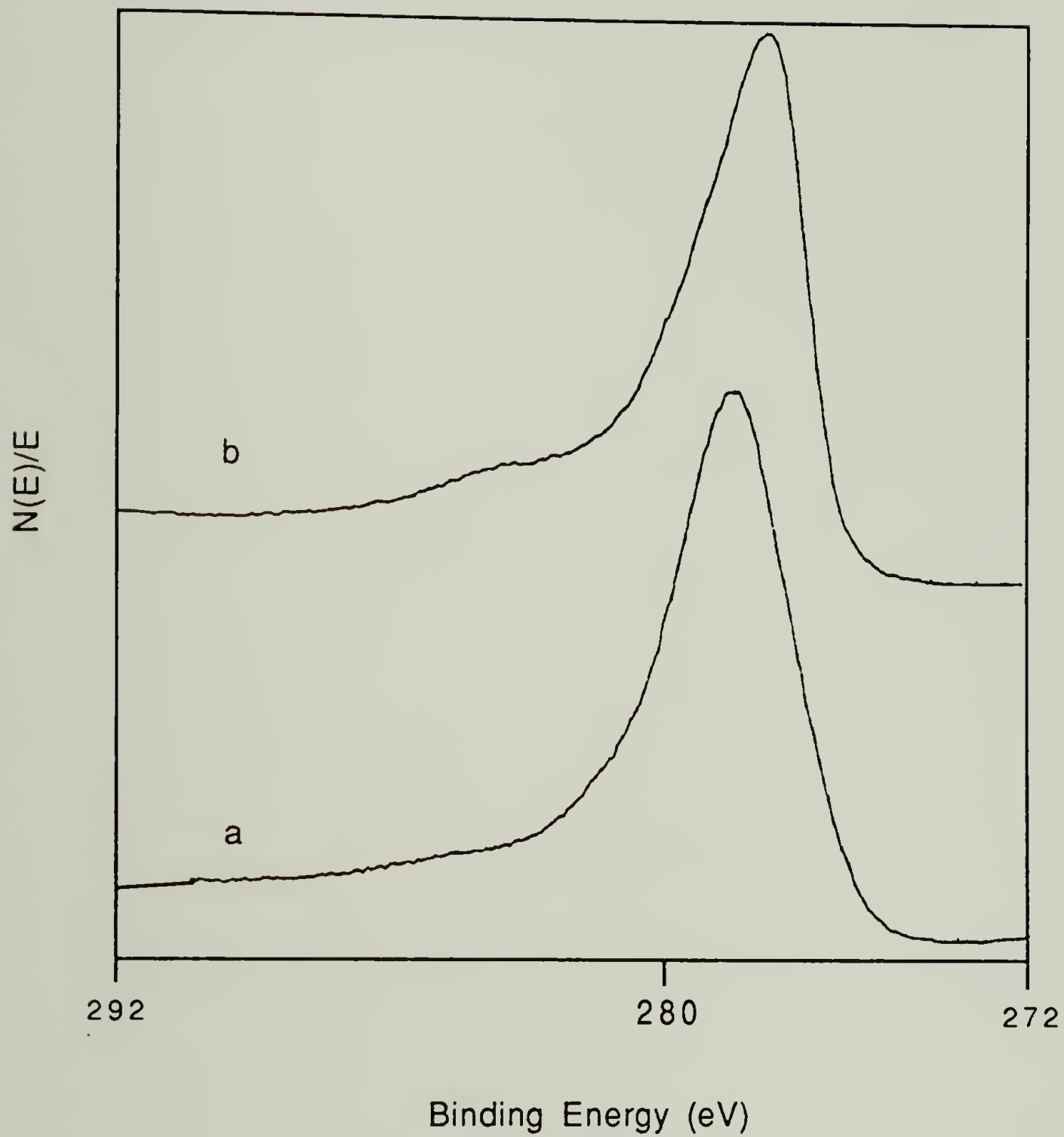


**Figure 38.** XPS spectra ( $C_{1s}$  region) of (a) "as received" and (b) oxidized carbon fibrils.

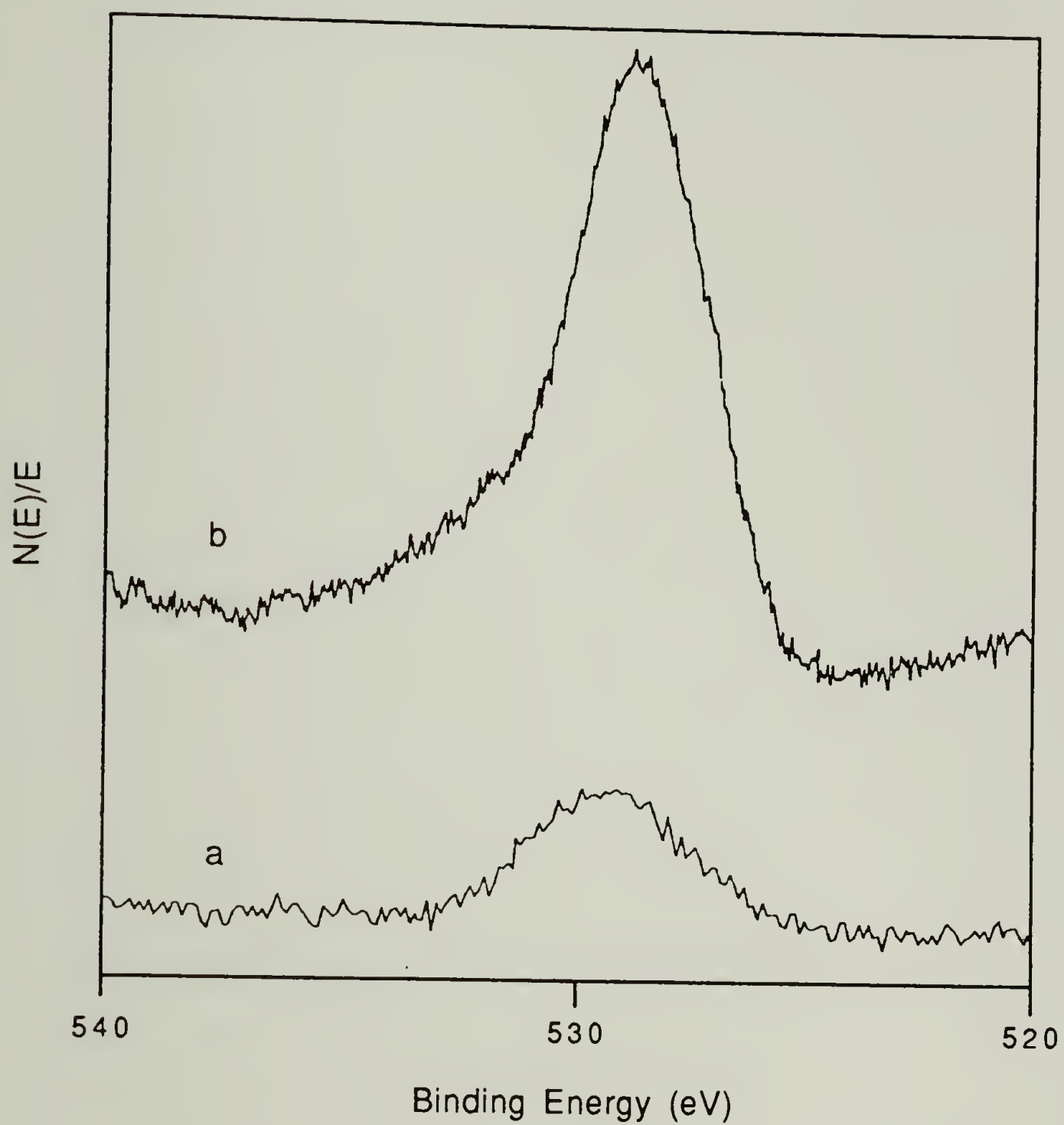


**Figure 39.** XPS spectra ( $O_{1s}$  region) of (a) "as received" and (b) oxidized carbon fibrils.

being tailing into the high binding energy region rather than well defined peaks. In addition, the existence of a variety of  $\pi-\pi^*$  transitions of differing energies results in a high binding energy tail, even in the nearly complete absence of oxygen-containing functional groups, as shown in figure 38a. The spectrum of the  $O_{1s}$  region prior to oxidation is rather broad and noisy due to the low abundance of oxygen on the surface. Oxidation results in a very broad peak with a distinct high binding energy shoulder. Numerous attempts have been made to assign the functional group composition of carbons based on curve fitting of the  $C_{1s}$  and  $O_{1s}$  regions and using the expected binding energy shifts for various oxygen-containing functional groups. Even when subtraction of the contribution of the starting material is used to identify features due to oxidation, the peaks were generally broad and relatively symmetrical, making the unique assignment of the contribution from each functional group difficult. In addition, estimates based on fitting of the  $C_{1s}$  region rarely agreed with those based on fitting of the  $O_{1s}$  region.<sup>5</sup>

Reduction of oxidized carbons has been used to enhance their reactivity towards electrophiles,<sup>6</sup> presumably by increasing the hydroxyl group content. Oxidized fibril samples were reduced with lithium triethylborohydride in THF. The atomic composition data is summarized in table 25. No significant change in the atomic composition occurred



**Table 25.** XPS atomic composition data for reduced fibrils.

<u>Sample</u>	<u>C</u>	<u>O</u>
As Recv.	100	2.5
Ox. (30 min)	100	8.5
Ox. (1 hour)	100	9
Ox. (24 hours)	100	9.4

for any sample and the shape of the  $C_{1s}$  and  $O_{1s}$  regions was unchanged. These results were surprising, especially for the oxidized sample, as the reduction of carboxylic acids to methylol groups would be expected to decrease the O:C ratio, and the reduction of any C=O groups would be expected to increase the amount of carbon occurring at a lower binding energy and oxygen occurring at a higher binding energy. Assuming the reduction occurs to a significant extent, these results suggest that few simple functional groups, especially carboxylic acids, are present. These results are more consistent with the expectations based on the reduction of complex lactonic functional groups proposed by some investigators<sup>7</sup>.

### Labeling Reactions

The results of the previous section clearly indicate that oxygen-containing functional groups could be introduced to the fibril surface. In order to develop rational surface chemistry for this substrate, the functional group composi-

tion must be better understood. It is clear that XPS data alone is insufficient to characterize the surface. A variety of infrared spectroscopic techniques, including transmission (KBr mull) diffuse reflectance (DRIFT) and Fourier transform attenuated total reflectance (FT ATR-IR, Ge IRE) were attempted on the oxidized fibrils with very poor results. Due to their entangled morphology, the fibrils could not be dispersed homogeneously (on the order of the wavelength of IR radiation), resulting in severe scattering problems in transmission, and, to a lesser extent, in DRIFT experiments. The high absorbtivity of the fibrils and the their relatively low functional group content further hindered efforts to obtain lucid spectra. Even the use of an "as received" carbon background in the DRIFT experiment<sup>8</sup> did not allow identification of bands due to oxidation. These difficulties were compounded by the fact that the bands are expected to be broad. Even if lucid spectra could be obtained, it is unlikely that much information would be provided about the functional group composition beyond verifying the presence of carbonyl groups.<sup>9</sup>

One way to obtain additional information about the chemistry of these surfaces is to determine the extent of reaction for a series of functional group-specific reactions. A variety of such derivitization reactions have been reported for carbon surfaces.<sup>10</sup> Estimates of functional group composition from this data must be made with caution.

A number of assumptions must be made that are difficult to verify for such a complex, difficult-to-analyze surface. It must be assumed that the reaction is specific to the functional group of interest, quantitative for this group, and does not induce changes in the surface chemistry that are not readily accounted for. Predicting the reactivity of complex lactonic functional groups, such as those proposed by Garten, Weiss and Willis,<sup>11</sup> may not be straightforward. However, when, as in this case, the principle objective is to determine what types of reactions proceed to high yield, this type of study will give the most useful results. The problem of analyzing the resulting surface remains. In most previous studies, changes in the carbon surface were monitored by indirect methods, such as titration or pyrolysis. Bulk microanalysis has been used but the small changes in the atomic composition make such data difficult to obtain with high precision<sup>12</sup>. In some cases, changes in the IR spectrum have been successfully used to follow reactions. In general, this has been most successful for highly oxidized carbons<sup>13</sup>.

XPS labeling experiments have not been extensively applied to this problem. XPS has a number of advantages for studying carbon surfaces. Powder samples do not present a sample preparation problem. The high sensitivity of XPS to certain elements (fluorine, many metals) can be a significant advantage. The selection of a label containing the



appropriate elements allows the detection and quantitative determination of very small amounts of the label on the surface.<sup>14</sup> In this study a variety of XPS labeling reactions were performed on "as received", oxidized and oxidized-then-reduced carbon fibril samples. Based on the carbon black literature, reactions of acidic oxygen-containing functional groups are expected to offer the most promise for subsequent surface modification. As a result, the majority of the work was aimed at labeling these groups. The stoichiometry of the surface can be represented by two extreme cases, one in which all of the oxygen possesses phenolic reactivity, that is, one acidic proton per oxygen, or one in which all of the surface oxygen possesses carboxylic reactivity (one acidic proton for every two oxygens). For oxidized and oxidized-then-reduced fibrils possessing an average atomic composition of  $C_{100}O_{9.2}$ , this leads to empirical formulas of  $C_{11}-OH$  and  $C_{21}-CO_2H$ , respectively. It will become apparent in the remainder of this section that finding labeling reactions that clearly distinguish between phenols (or acidic enols) and carboxylic acids was not possible. As a result, the extent of labeling will be given relative to the reaction of both of these theoretical models. The actual stoichiometry of the reaction of acidic oxygen on the surface is probably somewhere between these two extremes. Unless otherwise specified, no significant change occurred in the shape of the  $C_{1s}$  or  $O_{1s}$  spectrum.

Thallium ethoxide labels acidic functional groups with  $pK_a$  values less than that of phenol. This would include carboxylic acids, phenols and acidic enols; lactones may also react by ring opening due to attack by the ethoxide ion. The resulting salts are stable to air, moisture and light.<sup>15</sup> The high sensitivity of XPS to thallium allows relatively precise quantitation of very small amounts of thallium on the surface. The XPS atomic composition data is summarized in table 26. Although the amount of Tl on

**Table 26.** XPS atomic composition data for Tl-labeled fibrils.

<u>Sample</u>	<u>C</u>	<u>O</u>	<u>Tl</u>	<u>%Carboxylic Acid</u>	<u>%Phenol</u>
As recv.	100	3	0.4	40	20
C <sub>50</sub> -OTl	100	2	2		
C <sub>100</sub> -CO <sub>2</sub> H	100	2	1		
Oxid	100	11±.1	4.3±.6	95	48
Ox./Red	100	10	3.6	80	40
C <sub>11</sub> -OTl	100	9	9		
C <sub>21</sub> -CO <sub>2</sub> Tl	100	9	4.5		

the "as received" surface is low, it is enough to account for at least 20% of the oxygen on the surface. Oxidation

resulted in a very large increase in the Tl uptake. Enough Tl is present to account for at least 40% and as much as 80% of the surface oxygen. These results were surprising, considering that no other derivitization reaction has been reported to account for more than about 30% of the surface oxygen<sup>16</sup>. Reduction resulted in very little change in the Tl uptake; if reduction had occurred, very little change occurred in the surface acidity. This is also consistent with expectations for some of the proposed lactonic structures, in which reduction would be expected to result in phenolic (enolic) species, rather than alcohols.

Thallium salts of carboxylic acids and phenols react with acid chlorides to form anhydrides and esters, respectively<sup>17</sup>. The high yield of the reaction with TlOEt suggested that this might be a useful step in the further modification of the oxidized surface. As a result, oxidized fibrils were reacted with TlOEt and then reacted with heptafluorobutyryl chloride (HFBC) in THF for 18 hours. The XPS atomic composition data is summarized in table 27. The reaction should result in the replacement of each Tl by  $C_4F_7O$ . As expected, all of the surface Tl was converted to TlCl, but far too little  $C_4F_7O$  (approximately 20% of the predicted amount) was added. TlCl seemed to be converted to some soluble species on standing. Inorganic thallium salts are easily oxidized and sensitive to light, suggesting that



**Table 27.** XPS atomic composition data for reactions of Tl-labeled surfaces with HFBC.

#	<u>Reaction Time</u>	<u>C</u>	<u>O</u>	<u>F</u>	<u>Tl</u>	<u>Cl</u>
1	18 hours	100	12	5	.7	1
2	15 minutes	100	18	6	9	9
C <sub>fib</sub> -[Ox], Tl		100	12	--	4	--
Theoretical <sup>a</sup>		100	14	24	--	--

<sup>a</sup>Tl replaced by C<sub>4</sub>F<sub>7</sub>O

the formation of thallium oxides accounts for this observation. If the anhydride was formed with HFBC, the product would be expected to be extremely moisture sensitive. Hydrolysis may have occurred on standing, resulting in the loss of a significant amount of the C<sub>4</sub>F<sub>7</sub>O that has been added. As a result, the reaction time was decrease to 15 minutes. More of the insoluble TlCl remained, but the extent of C<sub>4</sub>F<sub>7</sub>O incorporation remained essentially unchanged. If it is assumed that only the esters formed by the relatively weakly acidic phenols and enols were hydrolytically stable enough to isolate, these results suggest that approximately 10% of the oxygen on the oxidized fibrils is present in this form. Assuming phenolic reactivity,

about 50% of the oxygen reacts with TlOEt; about 20% of this oxygen forms a stable HFBC adduct.

Oxidized fibril samples were also reacted with sodium methoxide in methanol. The product initially contained large amounts of oxygen as well as sodium, suggesting the presence of adsorbed NaOMe. Extraction with methanol and drying at 180°C resulted in a product with the following atomic composition by XPS:  $C_{100}O_9Na_{1.2}$ . This corresponds to the reaction of 13 to 26% of the surface oxygen, substantially less than was observed for the reaction with TlOEt.

Reaction with diazomethane has been one of the most commonly used derivitization reactions for studying the composition of oxidized carbon. Changes in the surface have been followed by titration, bulk microanalysis and IR spectroscopy<sup>18</sup>. Only subtle changes in the O:C ratio are expected to occur upon methylation, making this reaction unsuitable for use in an XPS study. As a result, the use of a fluorine-containing diazoalkane was investigated. Tri-fluoromethyldiazomethane was prepared by diazotization of 2,2,2-trifluoroethylamine according to the procedure of Gilman and Jones.<sup>19</sup> The diazoalkane was found to react cleanly with benzoic acid in the presence of boron trifluoride etherate in dichloromethane. The diazoalkane was too stable to react in the absence of the catalyst (due to the electron withdrawing effect of the  $CF_3$  group) and reaction in diethyl ether resulted in the formation of the ethyl

ester, presumably by reaction with the ylide type intermediate formed by the reaction of the diazoalkane with ether<sup>20</sup>. The XPS atomic composition data for the  $\text{BF}_3 \cdot \text{OEt}_2$  catalyzed (electrophilic) reaction of  $\text{CF}_3\text{CHN}_2$  with "as received", oxidized and oxidized-then-reduced fibril samples is summarized in table 28. Under these conditions,

**Table 28.** XPS atomic composition data for  $\text{BF}_3 \cdot \text{OEt}_2$  catalyzed reactions of fibril samples with  $\text{CF}_3\text{CHN}_2$

<u>Sample</u>	<u>Rinsing Procedure</u>	<u>C</u>	<u>O</u>	<u>F</u>	<u>%Carbox. Acid</u>	<u>%Phenol</u>
As Recv.	A	100	3	3.2	100	50
AS Recv.	B	100	3	2.3	80	40
$\text{C}_{50}\text{-OCH}_2\text{CF}_3$		100	2	5.8		
$\text{C}_{100}\text{-CO}_2\text{CH}_2\text{CF}_3$		100	2	2.9		
Oxid.	A	100	11	8.5	65	37
Oxid.	B	100	13	4.4	35	18
Oxid.	C	100	9	6.6	52	26
Ox./Red.	A	100	8	6.6	53	26
Ox./Red.	B	100	8	6	46	23
$\text{C}_{11}\text{-OCH}_2\text{CF}_3$		100	8	23		
$\text{C}_{21}\text{-CO}_2\text{CH}_2\text{CF}_3$		100	8	12.5		

(A)  $\text{CH}_2\text{Cl}_2$ , MeOH, THF

(B)  $\text{CH}_2\text{Cl}_2$ , aqueous  $\text{K}_2\text{CO}_3$ , water, MeOH, THF

(C)  $\text{CH}_2\text{Cl}_2$ , water, MeOH, THF

reaction would be expected to occur for alcohols as well as phenols and carboxylic acids. "As received" samples reacted



more extensively with this reagent than with TlOEt; at least 50% of the surface oxygen reacts. These results suggest that a substantial amount of the surface oxygen is present as alcohols or weakly acidic phenols (enols). The extent of reaction with the oxidized surface was less for this reagent, but still substantial. Somewhat less reaction occurred with the oxidized-then-reduced sample. When the fibrils were washed with dilute aqueous sodium carbonate (to insure complete removal of 2,2,2-trifluoroethanol and fluoroboric acid), the amount of fluorine decreased only slightly for the "as received" and the oxidized-then-reduced samples, while nearly half of the fluorine was removed from the oxidized surface. Rinsing of the oxidized sample with water resulted in significantly less fluorine loss. These results suggest that extremely hydrolytically labile species account for a significant amount of the product of the reaction with the oxidized fibrils. Hydrolysis of the diazomethane adduct with aqueous acid has been used in the past to distinguish between esters (derived from carboxylic acids) and ethers (derived from phenols)<sup>21</sup>. The changes in the atomic composition due to hydrolysis for these surfaces are summarized in table 29. It should be noted that  $\text{CF}_3\text{CH}_2\text{O}^-$  is a much better leaving group than methoxide, as a result, ethers derived from relatively acidic phenols may be hydrolyzed under these conditions. Substantial fluorine loss occurred for all of the samples. The fluorine loss was

**Table 29.** XPS atomic composition data for hydrolysis  
(1N HCl) of  $\text{CF}_3\text{CHN}_2$  labeled fibrils.

<u>Sample</u>	<u>C</u>	<u>O</u>	<u>F</u>	<u>% of Oxygen as Ether<sup>a</sup></u>
As Recv.	100	3	1.8	22
Oxid.	100	10	2.4	9
Ox./Red.	100	8	3.2	12

<sup>a</sup>Calculated from the O:C ratio, assuming all fluorine present as  $\text{OC}_2\text{F}_3$

lowest for the sample derived from the "as received" fibrils, consistent with the presence of a substantial number of weakly acidic phenol and alcohol-type functional groups. If it assumed that this fluorine is present in ether groups, these results indicate that approximately 22% of the oxygen on the surface is present as the ether. Only about 9% of the oxygen was present as the hydrolytically-stable ether in the sample derived from the oxidized fibrils, indicating a lower percentage of weakly acidic functional groups. Reduction resulted in little, if any, increase in the number of weakly acidic functional groups, as expected based on the Tl labeling results. Unlike a number of previous reports for reactions with diazomethane, no nitrogen was observed in the product. Nitrogen incorporation has been attributed to reaction with quinones to form the pyrazoline ring.<sup>22</sup>

Hydroxyl groups capable of nucleophilic reaction were labeled with HFBC. The reaction was carried out with and without DMAP cataysis in an attempt to distinguish between relatively reactive (primary) and less reactive (secondary, tertiary) hydroxyl groups<sup>23</sup>. The XPS atomic composition data (summarized in table 30) indicates that very little

**Table 30.** XPS atomic composition data for HFBC labeled fibrils.

<u>Sample</u>	<u>Acylation Conditions</u>	<u>C</u>	<u>O</u>	<u>F</u>	<u>%PhOH</u>
As Recv.	pyridine	100	2	0.9	7
As Recv.	pyr., DMAP	100	3	1	8
As Recv./Red.	pyridine	100	2.4	0.8	6
$C_{50}-OCOC_3F_7$		100	3.7	13	
Ox. (24 h.)	pyridine	100	10	2	6
Ox. (30 min.)	pyridine	100	11	4	8
Ox. (30 min.)	pyr., DMAP	100	4	0.4	0.8
Ox. (30 min.)/Red	pyridine	100	8.3	5	11
Ox. (30 min)/Red.	pyr., DMAP	100	6.8	4.5	9
Ox. (24 h.)/Red.	pyridine	100	8	4.3	9
$C_{11}-OCOC_3F_7$		100	13	47	

reaction occurred with any of the fibril samples under



either of the conditions. It is unclear why so little fluorine was observed in the product of DMAP-catalyzed reaction with carbon oxidized for 30 minutes; no other experiments revealed any difference in the reactivity as a function of oxidation time. Little, if any, increase in the reactivity occurred due to reduction. If any reduction occurred, the products were poor nucleophiles. These results suggest that nucleophilic hydroxyl groups account for only about 10% of the surface oxygen; any other OH groups that are present are highly deactivated by steric and/or electronic factors.

Carbonyl groups (aldehydes and ketones) were labeled with 2,4-dinitrophenylhydrazine (DNPH). The XPS atomic composition data is summarized in table 31. HCl catalyzed

**Table 31.** XPS atomic composition data for DNPH labeled fibrils.

<u>Sample</u>	<u>Conditions</u>	<u>C</u>	<u>O</u>	<u>N</u>	<u>%C=O</u>
As Recv.	A	100	3	0.2	3
As Recv.	B	100	3	0.3	4
$C_{50}-C_6O_4N_4$		100	7	7	
Oxid.	A	100	14	2	9
Oxid.	B	100	14	2	9
$C_{11}-C_6O_4N_4$		100	23	23	

(A) THF/HCl

(B) THF/EtOH/CH<sub>3</sub>CO<sub>2</sub>H

reaction resulted in a very poor yield; less than 5% of the oxygen on the "as received" fibrils and only about 10% of the oxygen on the oxidized sample were labeled. The reaction of other carbonyl-containing surfaces under these conditions has failed to go to completion<sup>24</sup>. Protonation of the hydrazine (decreases the reaction rate) is reported to be less extensive when acetic acid is used as the catalyst and the reaction is run in ethanol<sup>25</sup>. The solubility of DNPH in ethanol was quite low; addition of THF as co-solvent resulted in dissolution of most of the hydrazine. However, no increase in the yield was observed.

A number of electrophilic reactions were attempted using activated derivatives of surface carboxylic acids. The formation of the acid chloride on the surface of oxidized carbons using thionyl chloride has been reported by a number of investigators<sup>26</sup>. Treatment of oxidized fibrils with thionyl chloride resulted in the introduction of very little chlorine; the empirical formula of the product was  $C_{100}O_{12}Cl_{1.2}$ . Treatment of this surface with a label nucleophile (3-bromo-1-propanol) resulted in no reaction. Dicyclohexylcarbodiimide (DCC) has been used to activate carboxylic acids on carbon surfaces.<sup>27</sup> "As received" and oxidized fibrils were esterified with 4-bromophenylethanol using DCC; the XPS atomic composition results are summarized in table 32. It should be noted that etherification

**Table 32.** XPS atomic composition data for reactions of fibrils using CDI and DCC.

<u>Sample</u>	<u>Conditions</u>	<u>C</u>	<u>O</u>	<u>N</u>	<u>Br</u>	<u>%Carbox.</u> <u>Acid</u>	<u>%Phenol</u>
As Recv.	DCC/BrPhEtOH	100	2	--	--	0	0
Oxid	DCC/BrPhEtOH	100	9	--	0.6	18	9
Oxid.	CDI/BrPhEtOH	100	9	--	0.65	20	10
C <sub>21</sub> -CO <sub>2</sub> EtPhBr		100	6.7	--	3.3		
C <sub>11</sub> -OEtPhBr		100	5.3	--	5.3		
Oxid.	CDI	100	9	1.4	--	17	11
Ox./Red.	CDI	100	7	1	--	12	8
C <sub>21</sub> -COC <sub>3</sub> N <sub>2</sub>		100	4	8	--		
C <sub>11</sub> -OCOC <sub>3</sub> N <sub>2</sub>		100	13	13	--		

of phenols may have occurred as well<sup>28</sup>. No reaction occurred for the "as received" fibrils and only a small amount of bromine was incorporated for reaction of the oxidized sample. A similar reaction is expected to occur using carbonyldiimidazole. The XPS atomic composition data (table 32) indicates that the acyl imidazole on the surface could be isolated and quantitatively converted to the ester. These results were in good agreement with the results of reaction using DCC. About 10-20% of the oxygen on the surface reacts with nucleophiles in the presence of activating agents.



The use of carboxylate salts as nucleophiles often results in a better yield for acylations of sterically hindered carboxylic acids. Very good yields have been reported for the reaction of hindered acids in solution with electrophiles in the presence of DBU<sup>29</sup>. The results of treatment of "as received", oxidized and oxidized-then-reduced fibril samples with chloromethyl methyl sulfide and 3-fluorobenzyl bromide in the presence of DBU are summarized in table 33. Very little reaction occurred with any of

**Table 33.** XPS atomic composition data for DBU catalyzed reactions of fibrils with electrophiles.

<u>Sample</u>	<u>Label</u>	<u>Rinsing Procedure</u>	<u>C</u>	<u>O</u>	<u>F</u>	<u>S</u>	<u>N</u>
As Recv.	FBzBr	PhH, MeOH, THF	100	4	<.5	--	<.5
As Recv.	FBzBr	MeOH, HCl	100	3	<.5	--	<.5
Oxid.	FBzBr	PhH, MeOH, THF	100	9	1.5	--	1
Oxid.	FBzBr	extract w. THF	100	9	1	--	1
Oxid.	FBzBr	PhH, MeOH, THF	100	9	2	--	1
Oxid.	FBzBr	MeOH, HCl	100	7	1	--	<.5
Ox./Red.	FBzBr	MeOH, HCl	100	7	.7	--	<.5
As Recv.	CH <sub>3</sub> SCH <sub>2</sub> Cl	PhH, MeOH, THF	100	3	--	<.5	--
Oxid.	CH <sub>3</sub> SCH <sub>2</sub> Cl	PhH, MeOH, THF	100	9	--	<.5	--
Ox./Red.	CH <sub>3</sub> SCH <sub>2</sub> Cl	PhH, MeOH, THF	100	8	--	<.5	--

the surfaces using chloromethyl methyl sulfide. There appears to have been some reaction with 3-fluorobenzyl bromide, but DBU remained adsorbed to the sample, even after washing with acidic methanol. Clearly, this procedure results in no improvement over activation with DCC or CDI.

### Titration Results

Acidic functional groups on the surface of "as received" and oxidized fibril samples were titrated with aqueous sodium hydroxide using the "equilibration" method<sup>30</sup>. The results of the first titration are summarized in table 34. A small increase in base concentration was observed

**Table 34.** Results of titration #1.

<u>Sample</u>	<u>Base Consumed (meq.)</u>	<u>Base Consumed (meq./100 g)<sup>a</sup></u>
As Recv.	0.3	34
Oxid.	-0.13	-35
Control	-.03	

<sup>a</sup> Corrected for base consumed by the control

in the control (evaporative loss) and base was consumed by the "as received" sample, as expected. Quite unexpectedly, the sample volume that had been exposed to oxidized fibrils

became more basic. Closer examination of the experimental conditions revealed the probable cause. Vacuum filtration, to remove the suspended fibrils, concentrated the base solution. The "as received" sample settled out, allowing the base solution to be removed without filtration. The titration was repeated and the fibrils were removed by filtration using positive nitrogen pressure to force the titrant through the frit. The results are summarized in table 35. The high base concentration of the control

**Table 35.** Results of titration #2.

<u>Sample</u>	<u>Base Consumed (meq)</u>	<u>Base Consumed (meq/100 g)<sup>a</sup></u>
As Recv.	-0.56	22
Oxid.	0.25	66
Control	-1.00	

<sup>a</sup>Corrected for base consumed by the control

sample was disturbing but the results for the "as received" sample are in reasonable agreement with those obtained in the previous experiment. While the experimental data is somewhat sparse, the values are within expectations for surfaces containing relatively little oxygen<sup>31</sup>.



Comparison of the amount of sodium hydroxide consumed, as measured by titration, to the total acidic functional group content predicted from the stoichiometry of the labeled products proved to be very interesting. These results are summarized in table 36. These results indicate that all of the acidic functional groups present on "as received" samples can be titrated with sodium hydroxide. Most, if not

**Table 36.** Summary of titration results.

<u>Sample</u>	<u>Base Consumed (meq/100 g)</u>
As Recv.	22-34
As Recv. TlOEt <sup>a</sup>	33
Oxid.	66
Ox., NaOMe	100
Ox., CDI <sup>a</sup>	60
Ox., TlOEt <sup>a</sup>	360

<sup>a</sup>Predicted from the stoichiometry of the product based on the XPS atomic composition data.

all, of the acidic functional groups on the oxidized sample that react with sodium methoxide in methanol and CDI could also be titrated with sodium hydroxide. For the oxidized sample, however, much more reaction occurred with TlOEt. One consistent explanation is that ring-opening of lactone groups, to yield additional acidic sites, occurs under the

influence of ethoxide, and not methoxide. If this is the case, these results suggest that lactonic functional groups account for the majority of the oxygen that is introduced by  $\text{KClO}_3$  oxidation while relatively few of such groups are present in the "as received" sample.

#### Functional Group Composition

The results of the labeling experiments and titrations, along with what is known about the chemistry of oxidized carbon, lead to the estimates of functional group composition summarized in table 37.

**Table 37.** Summary of chemical composition estimates based on fibril reactivity.

<u>Oxygen Present As:</u>	<u>As Received</u>	<u>Oxidized</u>
Alcohols (nucleophillic)	10%	10%
Aldehydes/Ketones	5%	10%
Weakly Acidic Phenols/Enols	10-15%	5-10%
Acidic Phenol/Enols	10-15%	} 20-40%
Carboxylic Acids	0%	
Lactones	0%	25%-50%

The HFBC labeling results indicate that alcohols that participate in nucleophilic reactions comprise only a small

percentage of the surface oxygen. The DNPH labeling results suggest that ketones account for only a small amount of the surface oxygen in the "as received" sample; oxidation increases the percentage slightly. If the oxygen that reacts with  $\text{CF}_3\text{CHN}_2$  to form a hydrolytically stable product is identified with alcohols and weakly acidic phenols/enols, subtraction of the contribution due to alcohols results in an estimate of 10-15% of the oxygen as being associated with weakly acidic phenols/enols for the "as received" samples. The percentage of these groups on the oxidized samples is slightly lower. While none of the reactions allowed an absolute distinction to be made between acidic phenolic /enolic groups and carboxylic acids, comparison between the amount of the hydrolytically-labile  $\text{CF}_3\text{CHN}_2$  adduct and the extent of TlOEt labeling suggests that most of the acidic oxygen on the "as received" sample possesses phenolic reactivity. The amount of oxygen that forms hydrolytically-labile  $\text{CF}_3\text{CH}_2$  species (assuming phenolic reactivity) is roughly equal to the amount that reacts with TlOEt. No such correlation could be drawn for the oxidized sample but the amount of the hydrolytically-labile  $\text{CF}_3\text{CH}_2$  adduct that is formed suggests that carboxylic acids and acidic phenols /enols combined account for not less than 20% and not more than 40% of the surface oxygen. The extensive reaction with TlOEt suggests that most of the remaining oxygen on the surface of the oxidized fibrils is present as lactones. A

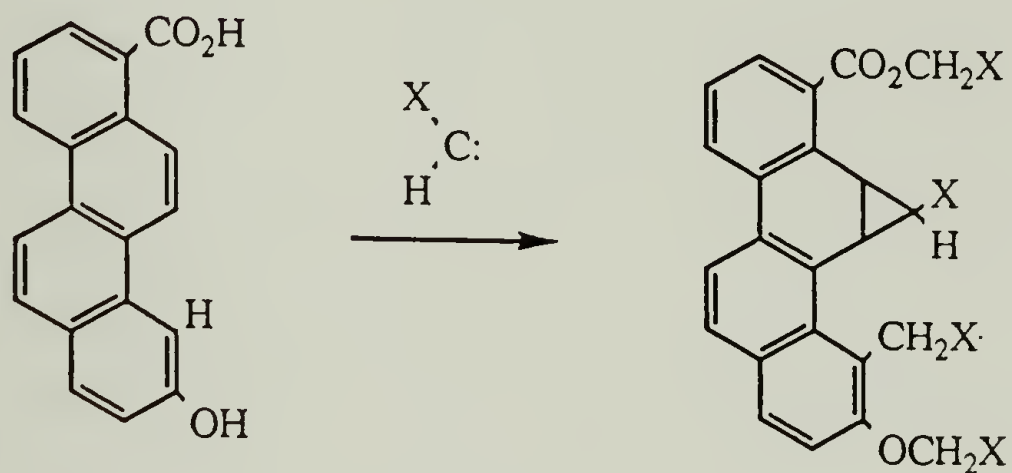


substantial amount of the oxygen on the surface of the "as received" fibrils did not react with any of the labels. The reactivity of the oxidized surface was essentially unchanged by  $\text{LiEt}_3\text{H}$  reduction. If any reduction has occurred, the products are highly acidic and weakly nucleophilic. These estimates are generally consistent with previous reports for carbon surfaces. It is important to realize that these estimates really represent a summary of how the surfaces behaved towards a variety of reagents. Functional groups may be present that do not react, or react very differently due to steric and electronic factors. It is probably most realistic to view the surface as consisting of a combination of oxygen-containing functional groups in a complex steric and electronic environment, reacting as a single "macro" functional group, rather than a composite of independently reacting functional groups. It is also apparent that oxidation failed to introduce a good "reactive handle" for further modification and reduction failed to simplify the reactivity of the product.

#### Reactions of Fibrillar Carbon with Carbenes

It is clear from the results of the previous section that oxidation of the carbon fibrils results in a chemically-complex surface of limited utility for further modification. Although this is typical of oxidized carbon surfaces, surprisingly few other reactions have been studied for

functionalizing graphitic carbon.<sup>32</sup> One promising candidate is reaction with carbenes. Carbenes insert into C-H bonds and add to vinyl and aromatic C=C bonds, all of which are expected to be present at defect sites on graphitic carbon (Equation 15). A variety of functional group



**Equation 15.** Reaction of graphitic carbon with carbenes.

containing carbenes can be prepared by the thermal or transition metal-catalyzed decomposition of diazoalkanes and diazoesters.<sup>33</sup> These reactions were studied as a means of introducing functional groups to carbon fibrils.

"As received", oxidized and oxidized-then-reduced fibril samples were treated with  $\text{CF}_3\text{CHN}_2$  in the presence of copper(II) acetate monohydrate ( $\text{CuAc}_2 \cdot \text{H}_2\text{O}$ ). All of the diazoalkane was decomposed, as evidenced by the loss of the yellow color. The XPS atomic composition data is summarized in table 38. All of the samples contained extremely large

amounts of fluorine, which explains why the fibrils were wet poorly by water. A substantial amount of fluorine

**Table 38.** XPS atomic composition data for reactions with  $\text{CF}_3\text{CHN}_2$  in the presence of  $\text{CuAc}_2 \cdot \text{H}_2\text{O}$ .

<u>Sample</u>	<u>AC</u>			<u>AC (hydrolyzed)</u>		
	<u>C</u>	<u>O</u>	<u>F</u>	<u>C</u>	<u>O</u>	<u>F</u>
As Recv.	100	3	30 <sup>a</sup>	100	4.8	22
Ox.	100	8	23	100	5.5	15
Ox./Red.	100	8.5	32	100	7	25

<sup>a</sup>extraction with  $\text{CH}_2\text{Cl}_2$  or cyclohexanone results in no fluorine loss.

remained after hydrolysis, consistent with the formation of C-C bonds by insertion into C-H and addition to C=C bonds. Examination of the  $\text{C}_{1s}$  region revealed the presence of a small peak at high binding energy, consistent with the introduction of  $\text{CF}_3$  groups (figure 40a), which was present in all of the samples. Surprisingly, two peaks were observed in the  $\text{F}_{1s}$  region of all of the samples, the second being approximately 4 eV lower in energy than the first (figure 40b). The origin of this peak was unclear. There was no reason to suspect that fluoride would be present. Low binding energy fluorine has also been observed for



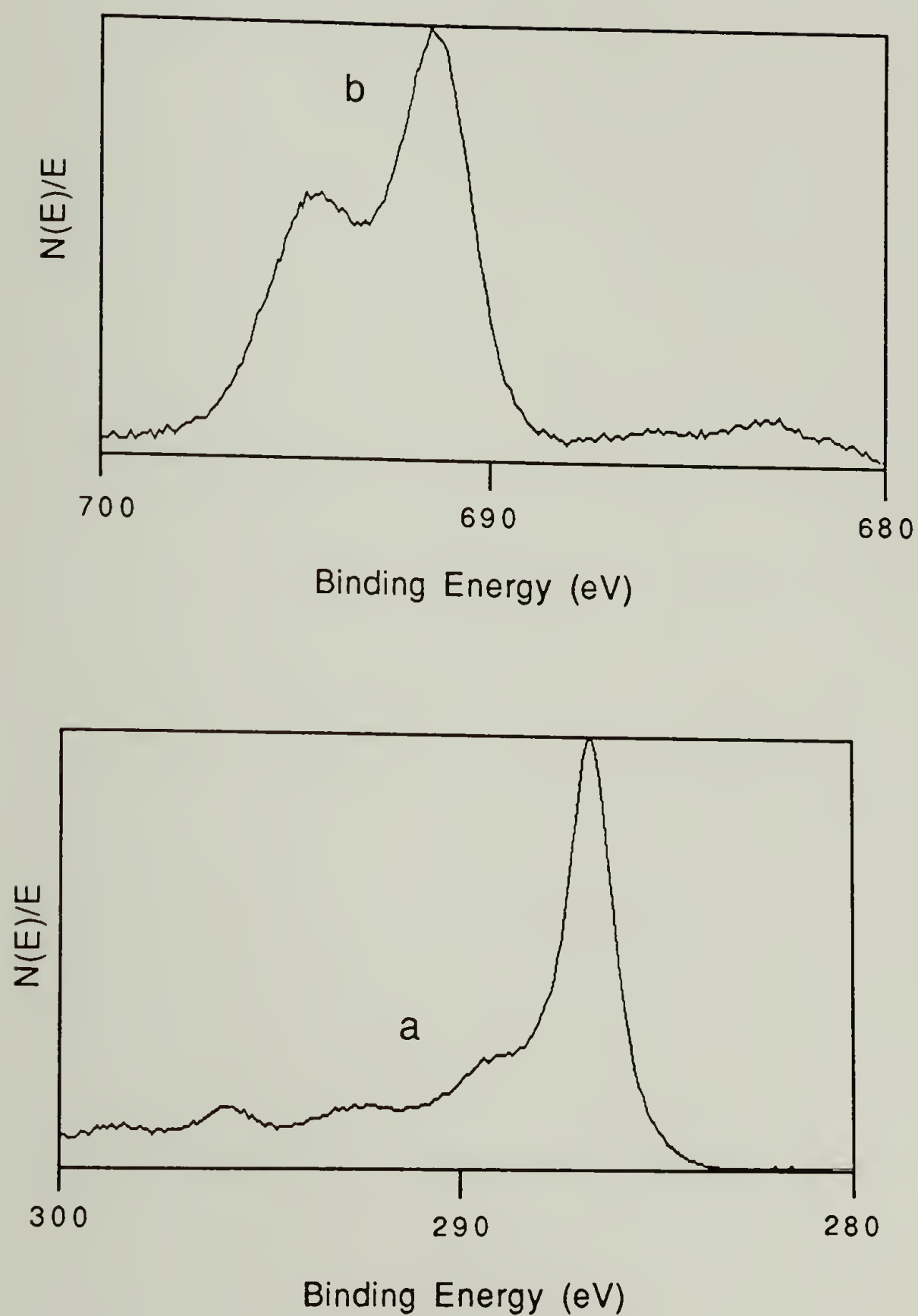


**Figure 40.** XPS spectra of "as received" fibrils reacted with  $CF_3CHN_2$  in the presence of  $CuAc_2 \cdot H_2O$ . (a)  $C_{1s}$  region, (b)  $F_{1s}$  region.

fluorinated graphite<sup>34</sup>, but in this case, fluorine is bonded directly to the aromatic carbon skeleton. There is no mechanism that would explain decomposition of the  $\text{CF}_3$  group to fluorinate the carbon skeleton in this system. Curve fitting results indicate that the  $\text{CF}_3$  peak is too small to account for all of the fluorine present (4-5% of the carbon is present as  $\text{CF}_3$ , leading to a predicted F:C ratio of 12-17:100) and it's area was not consistent with the assignment of either of the  $\text{F}_{1s}$  peaks to fluorine present as  $\text{CF}_3$ .

Despite these rather puzzling results, it was decided to attempt to introduce ester groups by reacting "as received" samples with carbenes generated from ethyl diazoacetate. It was hoped that this would result in a surface of simple reactivity. The ester groups could be hydrolyzed to chemically-versatile carboxylic acid groups. The reaction was initially attempted using copper carbenoid species generated by reacting the diazoester with  $\text{CuAc}_2 \cdot \text{H}_2\text{O}$ . Very little oxygen was introduced and hydrolysis with aqueous acid resulted in a surface that exhibited no increase in reactivity towards  $\text{TlOEt}$ . The carbenoid species generated from ethyl diazoacetate is expected to be less reactive than the carbenoid species generated from trifluoromethyl-diazomethane due to the less electron withdrawing character of the ester group. The true carbene generated by thermal decomposition of ethyl diazoacetate is also known to be more reactive than the metal carbenoid; the former adds to ben-

zene while the latter does not.<sup>35</sup> The diazoester was added to a hot decalin suspension of the fibrils over a long period of time. It was hoped that by keeping the concentration of the carbene low,<sup>36</sup> self-reaction (formal carbene coupling) of the carbenes would be avoided. The XPS atomic composition data (summarized in table 39) initially

**Table 39.** XPS atomic composition data for reaction with ethyl diazoacetate.

<u>Sample</u>	<u>C</u>	<u>O</u>	<u>N</u>
-CO <sub>2</sub> Et	100	17	--
-CO <sub>2</sub> H <sup>a</sup>	100	6.5	--
-CONHC <sub>4</sub> H <sub>9</sub>	100	3	1

<sup>a</sup>The same atomic composition was observed when C<sub>fib</sub>-[CO<sub>2</sub>Et] was washed with dilute KOH/MeOH at room temperature

appeared promising. A large amount of oxygen was added; the O<sub>1s</sub> spectrum exhibited two peaks, characteristic of the ester. However, hydrolysis resulted in the loss of much of the oxygen, as did the attempted amidation of the ester surface. These results are not consistent with the formation of C-C bonds, as expected for insertion into C-H bonds or addition to C=C bonds.



One explanation consistent with the results for both of the systems is the adsorption of self-reaction products. Polymeric side reaction products typically form during reactions that generate carbenes<sup>37</sup>. The initial product of ethyl diazoacetate-derived carbene coupling would be expected to be relatively insoluble, but saponification or amidation would be expected to solubilize the product. A similar reaction of carbenes derived from trifluoromethyl-diazomethane would result in the formation of highly insoluble fluorocarbon polymers. The two peaks in the  $F_{1s}$  region may be the result of charging differences between adsorbed species and  $CF_3$  groups covalently bonded to the graphite skeleton. In any case, reaction with carbenes generated from diazoalkanes does not appear to be a simple way to produce a chemically-well defined carbon surface.

#### Effect of Oxidation on Fibril Morphology

For a variety of technological applications, it would be advantageous to create fibrils that are less entangled. The products would be able to be dispersed homogeneously on the scale of fibril length and, if predominantly straight, could be aligned with shear flow to create novel materials such as fibril reinforced fibers. Since the fibrils grow together in contorted shapes forming entangled mats, and are very stiff, it would seem unlikely that they could be disentangled without cleaving them. The oxidation results,

especially at high  $\text{KClO}_3$  concentrations, indicated that some fibril cleavage occurs, as evidenced by the black color of the reagent after filtration through the glass frit. When these solutions were filtered through an  $0.45\ \mu$  membrane filter (Gelman) a small amount of black solid was collected. Since oxidation is expected to occur exclusively at defect sites, in principle, if the defect sites are localized along the fibril, the appropriate oxidation conditions should result in selective cleavage of the fibrils. A variety of oxidation conditions were employed in an attempt to increase the yield of fibrils that passed through the  $10\text{--}20\ \mu$  frit but were retained by the  $0.45\ \mu$  filter. The fibrils were reacted with 0.1, 0.2, 0.4, 0.6, 0.8, and 1.0 equivalents (assuming oxidation occurs according to equation 13) of  $\text{KClO}_3$  in  $\text{H}_2\text{SO}_4$ ;  $\text{KClO}_3$  was added slowly, using a dropping funnel, to avoid perchlorate formation. Most of the product remained on the frit. Initial results using perchloric acid in  $\text{H}_2\text{SO}_4$  were promising, but these solution are shock-sensitive. After a violent explosion occurred (fortunately there were no serious injuries), this work was discontinued. Reactions were also attempted using aqua regia ( $3:1\ \text{HNO}_3$  in  $\text{HCl}$ ) and  $\text{H}_2\text{O}_2/\text{H}_2\text{SO}_4$  solutions; once again, most of the product remained on the frit. Reaction for 6 hours in refluxing chromic acid ( $\text{H}_2\text{Cr}_2\text{O}_7$ , 5 x molar excess relative to fibrils) resulted in a sample that passed through the glass frit; a large percentage of this sample was retained on the mem-

brane. Attempts to obtain TEM images of this sample have been frustrated by the presence of large amounts of chromate salts. In addition, it was obvious that much of the starting fibril sample had been completely decomposed to soluble products and  $\text{CO}_2$ . Controlled chemical oxidation does not appear to be a viable way to produce large amounts of shorter fibrils.



## References

1. Boehm, H.-P.; Diehl, E.; Heck, W.; Sappok, R. *Angew. Chem. Int. Ed.* **1964**, *3*, 669.
2. Smith, R.N. *Quarterly Rev.* **1959**, *13*, 287.
3. Lenher, V.; Stone, H.W.; Skinner, H.H. *Justus Liebigs Ann. Chem.* **1922**, 143.
4. Xie, Y.; Sherwood, P.M.A. *Appl. Spectrosc.* **1989**, *43*, 1153.
5. Bansal, R.C.; Donnet, J.-B.; Stoeckli, F. *Active Carbon*, Marcel Dekker: New York, 1988, pp 92-103.
6. Evans, J.F.; Kuwana, T. *Anal. Chem.*, **1977**, *49*, 1632
7. See, for example, (a) Barton, S.S.; Harrison, B.H. *Carbon* **1975**, *13*, 283.; (b) Garten, V.A.; Weiss, D.E.; Willis, J.B. *Austral. J. Chem.* **1957**, *10*, 295.
8. Venter, J.J.; Vannice, M.A. *Appl. Spectrosc.* **1988**, *42*, 1096.
9. The features observed for highly graphitic carbons are generally weak and difficult to assign to specific functional groups. See, for example, Mattson, J.S.; Mark, H.B., Jr. *Activated Carbon*, Marcel Dekker: New York, 1971, pp 65-72.
10. See reference 5, pp 60-67.
11. See reference 7b.
12. (a) Boehm, H.P. *Advances in Catalysis* **1966**, *16*, 179-211.; (b) reference 9, pp 46-51.
13. See reference 9, pp 52-63.
14. Everhart, D.E.; Reilley, C.N. *Anal. Chem.* **1981**, *53*, 665.
15. Batich, C.D.; Wendt, R.C. In *Photon, Electron and Ion Probes of Polymer Structure*, Dwight, D.; Fabish, T.; Thomas, H. eds., American Chemical Society: Washington DC, 1981, pp 229-231.
16. Donnet, J.B. *Carbon* **1968**, *6*, 167.

17. Taylor, E.C.; McLay, G.W.; McKillop, A. *J. Amer. Chem. Soc.* **1968**, *90*, 2422.
18. See reference 9, pp 46-50.
19. Gilman, H.; Jones, R.G. *J. Amer. Chem. Soc.* **1943**, *65*, 1458.
20. Wulfman, D.S.; Poling, B. In *Reactive Intermediates*, vol. 1, Abramovitch, R.A. ed., Plenum Press: New York, 1980, 358.
21. See reference 9, pp 46-50.
22. Puri, B.R.; *Chem. and Phys. of Carbon* **1970**, *6*, 216.
23. See part I, this thesis.
24. Franchina, N.L.; McCarthy, T.J. *Polym. Prepr. (Am. Chem. Soc., Div. Polym. Chem.)* **1990**, *31(1)*, 416.
25. *Org. Syn.*, vol III; Horning, E.C. ed.in chief, Wiley: New York, 1955, 102.
26. For example, see reference 1 and Boehm, H.P.; Diehl, E.; Heck, W. *Symp. Carbon Tokyo Prepr.* **1964**, *8*, 10.
27. Murray, R.W. *Electroanal. Chem.* **1984**, *13*, 266-267.
28. Vowinkel, E. *Chem. Ber.* **1962**, *95*, 2997.
29. Ono, N.; Yamada, T.; Saito, T.; Tanaka, K.; Kaji, A. *Bull. Chem. Soc. Jpn.* **1978**, *51*, 2401.
30. See reference 1, pp 670-671.
31. See reference 12a, p 186.
32. See reference 16, pp 168-174.
33. Wulfman, D.S.; Linstrumelle, G.; Cooper, C.F. In *Chemistry of the Diazonium and Diazo Group* pt. 2, Patai, S. ed., Wiley: New York, 1978.
34. Wagner, C.D.; Riggs, W.M.; Davis, L.E.; Moulder, J.F.; Muillerberg, G.E. *Handbook of X-ray Photoelectron Spectroscopy*, Perkin-Elmer: Eden Prairie, Minn., 1979, p 44.
35. Marchand, A.P.; Brockway, N.M. *Chem. Rev.* **1974**, *74*, 431.

36. Badger, G.M.; Cook, J.W.; Gibb, A.R.M. *J. Chem. Soc.* **1951**, 73, 3456.
37. Wulfman, D.S.; Poling, B. In *Reactive Intermediates* vol. 1; Abramovitch, R.A. ed., Plenum Press: New York, 1980, 424.



## CHAPTER XII

### CONCLUSIONS AND SUGGESTIONS

This research has shown that the chemistry of the oxidized fibrils is typical of other graphitic carbon materials, to the extent that such generalizations can be made. Acidic oxygen-containing functional groups are present on the surface. Treatment with an oxidizing solution increases the number of such groups and changes the nature of the surface from one of principally phenolic reactivity to one that is better described by the chemistry of "f-lactones" or similar lactonic functional groups. The chemistry of this surface is much more complex than that of "carbonaceous" surfaces prepared by the reduction of fluorocarbon polymers. No functional group could be identified as a suitable reactive handle. The chemistry of the surface was quite complex and no preparatively useful reaction was found that occurred in high yield. Reduction failed to simplify the reactivity of the surface; the chemistry of the surface was left essentially unchanged.

From these results, it is clear that oxidation is a poor way to selectively introduce functional groups to graphitic carbon surfaces. A more suitable approach would be to introduce a well defined functional group directly to the graphite surface. Reaction with carbenes generated from diazoalkanes offered a promising alternative. Carbenes would be expected to react with a variety of functional groups present at graphite edges and a variety of reactive

functional groups, including carboxylic acids (introduced as the ester) and amines (introduced as the nitro group) could, in principle, be introduced to the surface. In practice, the reactions were found to be more complex. Carbenes generated from ethyl diazoacetate do not appear to form the expected products with the fibrils. No evidence for covalently attached ester groups was obtained. The results of reaction with carbenes generated from trifluoromethyldiazomethane are less clear. Fluorine is present on the surface, but it is not clear if covalent bonds are formed with the surface or if the fluorine results from adsorption of highly insoluble fluorocarbon side reaction products. Functionalization of graphitic carbon using carbenes warrants further study, if for no other reason than the fact that no other methods have shown any promise for introducing well defined functional groups. One promising candidate would be carbenes generated from  $\alpha$ -fluoro or  $\alpha$ -trifluoromethyl diazoesters. The presence of fluorine should result in substantially increased reactivity relative to ethyl diazoacetate and hydrolysis of the ester should solubilize any adsorbed side reaction products.

A number of XPS labeling reactions were applied to carbon materials for the first time in this study. While there is ample evidence that the complexity of oxidized carbon surfaces will defy simple descriptions, it is conceivable that these techniques could clarify some of the

issues. In particular, if the correct substrate, such as graphitized carbon films, was employed, XPS labeling could be used in conjunction with IR spectroscopy. Such an analysis for samples labeled with TlOEt and  $\text{CF}_3\text{CHN}_2$  holds particular promise for clarifying the role of lactones in carbon chemistry.

The "chemical milling" of fibril samples was only a partial success. These results suggest that control of the fibril structure would be best accomplished during fibril growth rather than through subsequent treatment of the product.

It is unlikely that specific functional group chemistry will ever be performed as elegantly on graphitic carbon as it has been for some of the other surfaces studied in this dissertation. The steric and electronic character of graphitic carbon surfaces seems to defy the introduction of chemically distinct functional groups.

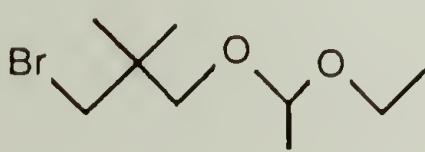
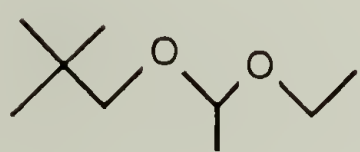
One alternative is to use adsorption to change the behavior of the surface. The ability of carbon materials to tightly adsorb other molecules is well known. Electrons in graphite are highly delocalized, allowing the graphite surface to act as an electron sink or source, resulting in strong adsorption of both electron-rich and electron-poor species. One potential application is in the preparation of composites. The choice of the appropriate diblock copolymer, in which one end adsorbs to the fibril and the

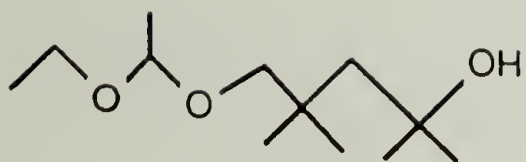


other interacts with the matrix resin, should result in strong ties between the matrix and the fibril.

APPENDIX A  
SUMMARY OF GC-MS AND GC-IR DATA FOR  
LidiMePrOP MODEL REACTIONS

The data in this appendix represent a summary of the characteristic M/e peaks observed by GC-MS and absorbances (in  $\text{cm}^{-1}$ ) observed by GC-IR (gas phase) for the reaction of LidiMePrOP with acetone (see the experimental section, part II). When possible, the most likely origin of each feature is listed.

<u>Product (retention time)</u>	<u>Mass/Charge {origin}</u>	<u>Absorbance {origin}</u>
 SM (11.09 min.)	223, 225 {SM-CH <sub>2</sub> }	2962 {CH <sub>3</sub> }
	195, 193 {SM-EtO}	1480 {CH <sub>2</sub> }
	151, 149 {SM-C <sub>4</sub> H <sub>9</sub> O <sub>2</sub> }	1375 {CH <sub>3</sub> }
	73 {C <sub>4</sub> H <sub>9</sub> O <sub>2</sub> -CH <sub>4</sub> }	1142, 1060
	45 {EtO}	{C(CH <sub>3</sub> ) <sub>2</sub> }
	29 {Et}	1100 {C-O}
 I (5.23 min.)	145 {I-CH <sub>3</sub> }	2964 {CH <sub>3</sub> }
	115 {I-EtO}	1483 {CH <sub>2</sub> }
	103	
	73 {C <sub>4</sub> H <sub>9</sub> O-CH <sub>4</sub> }	1385 {CH <sub>3</sub> }
	57 {(CH <sub>3</sub> ) <sub>3</sub> C}	1143, 1060
	45 {EtO}	{C(CH <sub>3</sub> ) <sub>3</sub> }
	29 {Et}	1096 {C-O}



II (12.74 min.)

157	{ II-HOC(CH <sub>3</sub> ) <sub>2</sub> }	3524	{ OH }
129	{ II-C <sub>4</sub> H <sub>9</sub> O <sub>2</sub> }	2980	{ CH <sub>3</sub> }
113		1480	
73	{ C <sub>4</sub> H <sub>9</sub> O-CH <sub>4</sub> }	1385	{ CH <sub>3</sub> }
59	{ HOC(CH <sub>3</sub> ) <sub>2</sub> }	1347	{ OH }
45	{ EtO }	1141, 1059	
		{ C(CH <sub>3</sub> ) <sub>2</sub> }	
29	{ Et }	1097	{ CH <sub>3</sub> }



III (10.72)

172	{ III-2(C <sub>4</sub> H <sub>9</sub> O) }	2987	{ CH <sub>3</sub> }
127		1480	
103		1386	{ CH <sub>3</sub> }
73	{ C <sub>4</sub> H <sub>9</sub> O <sub>2</sub> -CH <sub>4</sub> }	1254	
57			
45	{ Et <sub>2</sub> O }	1142, 1062	
29	{ Et }	{ C(CH <sub>3</sub> ) <sub>2</sub> }	
		1096	{ C-O }



APPENDIX B

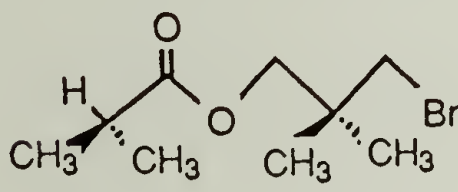
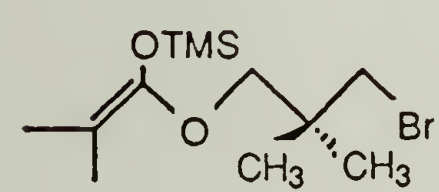
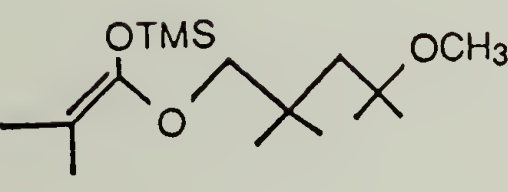
SUMMARY OF GC-MS DATA FOR THE PREPARATION OF  
1-ETHOXY-1-(TRIMETHYLSILYLOXY)-2-PHENYL ETHYLENE

The data in this appendix represent a summary of the characteristic M/e peaks observed by GC-MS for the reaction of ethyl phenylacetate with TEA and TMSOTf (see the experimental section, part II). Where possible, the most likely origin of each feature is listed.

<u>Product</u>	<u>Retention Time (min.)</u>	<u>Mass/Charge {Origin}</u>
ethyl phenylethyl- acetate (A)	8.75	164 {molec.ion}
		135 {A-Et}
		105
		91 {PhCh <sub>2</sub> }
		65
		39
		29 {Et}
1-ethoxy-1-(tri- methysilyloxy)-2- phenyl ethylene (B)	11.05	236 (molec.ion)
		209
		179
		131
		105
		73 {TMS}
		45 {EtO}
		29 {Et}

APPENDIX C  
SUMMARY OF GC-MS AND GC-IR DATA FOR LiPrTMSKA  
PREPARATION AND REACTIONS

The data in this appendix represents a summary of the characteristic M/e peaks observed by GC-MS and absorbances observed by GC-IR (gas phase) for reactions of BrPrTMSKA (see the experimental section, part II). When possible, the most likely origin of each feature is listed.

<u>Product (retention time)</u>	<u>Mass/Charge</u> <u>{origin}</u>	<u>Absorbance</u> <u>{origin}</u>
 VI (7.5 min.)	206, 208 {VI-2 (CH <sub>3</sub> )}	1758 {ester C=O}
	148, 150 {VI-C <sub>4</sub> H <sub>7</sub> O <sub>2</sub> }	2981 {CH <sub>3</sub> }
	127	1153 {C-O}
	89	
	71 {C <sub>4</sub> H <sub>7</sub> O}	
	43 {C <sub>3</sub> H <sub>7</sub> }	
	28 {CO}	
 VII (8.8 min.)	310, 308 {molec. ion}	1704 {enol C=C}
	239, 237 {-TMS, +H}	2970 {CH <sub>3</sub> }
	183, 181	1189 {C-O}
	160 {C <sub>7</sub> H <sub>16</sub> O <sub>2</sub> Si <sup>+</sup> }	
	144 {C <sub>7</sub> H <sub>15</sub> O <sub>2</sub> Si-CH <sub>3</sub> }	
	129	
	73 {TMS}	
	70	
 IX (10.0 min.)	286 {IX-CH <sub>4</sub> }	
	201	
	160 {C <sub>7</sub> H <sub>16</sub> O <sub>2</sub> <sup>+</sup> }	
	144 {C <sub>7</sub> H <sub>15</sub> O <sub>2</sub> Si-CH <sub>3</sub> }	
	129	
	73 {TMS}	
	70	
	57 {CH <sub>3</sub> OC(CH <sub>3</sub> ) <sub>2</sub> -CH <sub>4</sub> }	

## BIBLIOGRAPHY

- Adamson, A. *Physical Chemistry of Surfaces*, 4th ed., Wiley: New York, 1982.
- Aida, T.; Maekawa, Y.; Asano, S.; Inoue, S. *Macromolecules* **1988**, *21*, 1195.
- Allen, W.T.; Eaves, D.E. *Angew Makromol Chem.* **1977**, *58/59*, 321.
- Andrade, J.D. In *Surface and Interfacial Aspects of Biomedical Polymers*, vol. 1. Andrade, J.D. ed., Plenum: New York, 1985.
- Andrade, J.D.; Hlady, V. *Adv. Poly. Sci.* **1986**, *79*, 1.
- Asano, S.; Aida, T.; Inoue, S. *J. Chem. Soc., Chem. Commun.* **1985**, 1148.
- Badger, G.M.; Cook, J.W.; Gibb, A.R.M. *J. Chem. Soc.* **1951**, *73*, 3456.
- Bansal, R.C.; Donnet, J.-B.; Stoeckli, F. *Active Carbon*, Marcel Dekker: New York, 1988.
- Barker, D.J.; Brewis, D.M.; Dahm, R.H.; Hoy, L.R. *Polymer* **1978**, *19*, 856.
- Barton, S.S.; Harrison B.H. *Carbon* **1975**, *13*, 283.
- Batich, C.D.; Wendt, R.C. In *Photon, Electron and Ion Probes of Polymer Structure*, Dwight, D.; Fabish, T.; Thomas, H. eds., American Chemical Society: Washington DC. 1981, pp 221-235.
- Benderly, A.A. *J. Appl. Poly. Sci.* **1962**, *6*, 221.
- Bening, R.C.; McCarthy, T.J. *Macromolecules* **1990**, *23*, 2648.
- Boehm, H.-P. *Advances in Catalysis* **1966**, *16*, 181-225.
- Boehm, H.-P.; Diehl, E.; Heck, W. *Symp. Carbon Tokyo Prepr.* **1964**, *8*, 10.
- Boehm, H.-P.; Diehl, E.; Heck, W.; Sappok, R. *Angew. Chem. Int. Ed.* **1964**, *3*, 669.
- Bonafini, J.A.; Dias, A.J.; Guzdar, Z.A.; McCarthy, T.J. *J. Polym. Sci., Polym. Lett. Ed.* **1985**, *23*, 33.



- Borisova, F.K.; Galkin, G.A.; Kiselev, A.V.; Korolev, A.; Lygin, V.I. *Colloid J. USSR. (Eng.)* **1965**, *27*, 265.
- Britton, R.A.; Merrill, E.W.; Gilland, E.R.; Salzman, E.W.; Austen, W.G.; Kemp, D.S. *J. Biomed. Mater. Res.* **1968**, *2*, 42
- Brown, H.C.; Knights, E.F.; Coleman, R.A. *J. Amer. Chem. Soc.* **1969**, *91*, 2144.
- Burgess, F.J.; Cunliffe, A.V.; MacCullum, J.R.; Richards, D.H. *Polymer* **1977**, *18*, 719.
- Chakrabarti, N.; Jacobus, J. *Macromolecules* **1988**, *21*, 3011.
- Clark, D.T.; Feast, W.J. *Polymer Surfaces*, Wiley Interscience: New York, 1978.
- Costello, C.A. Ph.D. Dissertation.
- Costello, C.A.; McCarthy, T.J. *Macromolecules* **1987**, *20*, 2819.
- Cragg, G. *Organoboranes in Organic Synthesis*, Dekker: New York, 1973.
- Dautartas, M.F.; Evans, J.F.; Kuwana, T. *Anal. Chem* **1979**, *51*, 104
- Dias, A.J.; McCarthy, T.J. *Macromolecules* **1984**, *17*, 2529.
- Dias, A.J.; McCarthy, T.J. *Macromolecules* **1985**, *18*, 1826.
- Dias, A.J.; McCarthy, T.J. *Macromolecules* **1987**, *20*, 2068.
- Donnet, J.-B. *Carbon* **1968**, *6*, 161.
- Donnet, J.-B.; Bansal, R.C. *Carbon Fibers*, Marcel Dekker: New York, 1984.
- Dreyfuss, P.; Kennedy, J.P. *Polym. Sci., Poly. Symp.* **1976**, *56*, 129.
- Dwight, D.W.; Riggs, W.J. *J. Colloid Interface Sci.* **1974**, *47*, 650.
- Emde, H. et. al. *Synthesis* **1982**, *1*.

- Evans, J.F.; Kuwana, T. *Anal. Chem.* **1977**, *49*, 1632.
- Evans, J.F.; Kuwana, T. *Anal. Chem.* **1979**, *51*, 358.
- Everhart, D.E.; Reilley, C.N. *Anal. Chem.* **1981**, *53*, 665.
- Farkas, A.; Mills, G.A. In *Advances in Catalysis* vol 13, Elex, D.D.; Selwood, P.W.; Weisz, P.B. eds., Academic Press: New York, pp 395-447.
- Feng, X.D.; Sun, Y.H.; Qiu, K.Y. *Macromolecules* **1985**, *18*, 2105.
- Ferstandig, L.L.; Scherrer, R.A. *J. Amer. Chem. Soc.* **1959**, *81*, 4838.
- Franchina, N.L.; McCarthy, T.J. *Polym. Prepr. (Am. Chem. Soc., Div. Polym. Chem.)* **1990**, *31(1)*, 416.
- Gangal, S.V. In *Encyclopedia of Polymer Science and Technology*, vol 16, Wiley: New York, 1987, pp 582-599.
- Garten, V.A.; Weiss, D.E.; Willis, J.B. *Austral. J. Chem.* **1957**, *10*, 295.
- Gilliam, L.R.; Grubbs, R.H. *J. Amer. Chem. Soc.* **1986**, *108*, 733.
- Gilman, H.; Jones, R.G. *J. Amer. Chem. Soc.* **1943**, *65*, 1458.
- Gonen, S.; Kohn, D.H. *J. Polym. Sci., Polym. Chem. Ed.* **1981**, *19*, 2215.
- Ha, K.; Garton, A. *Polym. Prepr. (Am. Chem. Soc., Div. Polym. Chem.)* **1990**, *31(1)*, 326.
- Halaska, V.; Lochmann, L.; Lim, D. *Coll. Czech. Chem. Commun.* **1968**, *23*, 3245.
- Harrick, N.J. *Internal Reflectance Spectroscopy*, Harrick Sci. Corp.: New York, 1979.
- Hergenrother, W.L.; Ambrose, R.J. *J. Polym. Sci., Polym. Chem. Ed.* **1974**, *12*, 2613.
- Hertler, W.R.; Sogah, D.Y.; Boettcher, F.P. *Macromolecules* **1990**, *23*, 1264.
- Hertler, W.R.; Sogah, D.Y.; Webster, O.W.; Trost, B.M. *Macromolecules* **1987**, *20*, 1473.

Holland, L. *The Properties of Glass Surfaces*, Chapman and Hall: London, 1966.

Holubka, J.W. *Reactive Oligomers*, ACS Symposium Series, 282, American Chemical Society: Washington DC, p 117.

Horning, E.C. ed. in chief *Organic Synthesis*, vol. II., Wiley: New York, 1955, p 102.

House, H.O.; Czuba, L.J.; Gall, M.; Olmstead, H.D. *J. Org. Chem.* **1969**, 34, 2324.

Imanish, Y. In *Ring Opening Polymerizations*, vol. 2, Ivin, K.J.; Saegusa, T. eds., Elsevier: New York, 1984, pp 523-555.

Inoue, S.; Aida, T. In *Ring Opening Polymerizations*, vol. 1, Ivin, K.J.; Saegusa, T. eds., Elsevier: New York, 1984, pp 185-298.

Inoue, S.; Takeda, N. *Bull. Chem. Soc. Jpn.* **1977**, 50, 984.

Johnson, R.E., Jr.; Dettre, R.H. *J. Phys. Chem.* **1964**, 68, 1744.

Jung, M.E.; Blum, R.B. *Tetrahedron Lett.* **1977**, 43, 3791.

Knights, E.F.; Brown, H.C. *J. Amer. Chem. Soc.* **1968**, 90, 5281.

Kobayashi, S.; Masuda, E.; Shoda, S.-I.; Shimano, Y. *Macromolecules* **1989**, 22, 2878.

Kobayashi, S.; Saegusa, T. In *Ring Opening Polymerizations*, vol. 2., Ivin, K.J.; Saegusa, T. eds., Elsevier: New York, 1984, pp 783-786.

Kolb, B.U.; Patton, P.A.; McCarthy, T.J. *Macromolecules* **1990**, 23, 366.

Lane, C.F.; Brown, H.C. *J. Organometal. Chem.* **1971**, 26, C51.

Lee, K.-W.; McCarthy, T.J. *Macromolecules* **1988**, 21, 2318.

Lenher, V.; Stone, H.W.; Skinner, H.H. *Justus Liebigs Ann. Chem.* **1922**, 143.



- Lin, A.W.C.; Yeh, P.; Yacynych, A.M.; Kuwana, T. *J. Electroanal. Chem.* **1977**, *84*, 411.
- Marchand, A.P.; Brockway, N.M. *Chem. Rev.* **1974**, *74*, 431.
- Mattson, J.S.; Mark, H.B., Jr. *Activated Carbon*, Marcel Dekker: New York, 1971.
- McCormick, C.L.; Park, L.S. *J. Polym. Sci., Polym. Chem. Ed.* **1984**, *22*, 49.
- Miller, M.L.; Postal, R.H.; Sawyer, P.N.; Martin, J.G.; Kaplit, M.J. *J. Appl. Polym. Sci.* **1970**, *14*, 257.
- Mino, G.; Kaizerman, S.; Rasmussen, E. *J. Polym. Sci.* **1959**, *39*, 523.
- Mirabella, F.M. *J. Polym. Sci. Phys. Ed.* **1982**, *20*, 2309.
- Morra, M.; Occhiello, E.; Garbassi, F. *Langmuir* **1989**, *5*, 872.
- Murray, R.W. *Electroanal. Chem.* **1984**, *13*, 263-286.
- Nelson, E.R. Kilduff, T.J.; Benderly, A.A.; *Ind. Eng. Chem.* **1985**, *50*, 329.
- Okamoto, Y. *Polym. Prepr. (Am. Chem. Soc., Div. Polym. Chem.)* **1984**, *25(1)*, 264.
- Okamoto, Y. *Polym. Prepr. (Am. Chem. Soc., Div. Polym. Chem.)* **1990**, *31(1)*, 10.
- Ono, N.; Yamada, T.; Saito, T.; Tanaka, K.; Kaji, A. *Bull. Chem. Soc. Jpn.* **1978**, *51*, 2401.
- Ouhadi, T.; Stevens, C.; Teyssie, Ph. *Makromol. Chem. Suppl.* **1975**, *1*, 191.
- Pouchert, C.J. *Aldrich Library of NMR Spectra*, 2nd Ed. Vol. 1, Aldrich Chemical Co.: Milwaukee Wis., 1983, p 1170.
- Puri, B.R. *Chem. and Phys. of Carbon* **1970**, *6*, 191.
- Qiu, K.Y.; Fang, F.L.; Huang, Z.X.; Feng, X.J. *Feng, X.D. Polym. Commun.* **1982**, *2*, 81.

Quirk, R.P.; Seung, N.S. In *Ring Opening Polymerization*, McGrath, J.E. ed. ACS. No 286: Washington DC, 1985, pp 37-45.

Ramakrishnan, S.; Berluche, E.; Chung, T.C. *Macromolecules* **1990**, *23*, 378.

Reegen, S.L.; Frisch, K.C. In *Advances in Urethane Science and Technology*, vol. 10, Frisch, K.C.; Reegen, S.L. eds., Technomic Pub. Co.: Stamford Conn., pp 49-75.

Sekiguchi, H. In *Ring Opening Polymerization*, vol. 2, Ivin, K.J.; Saegusa, T.P. eds., Elsevier: New York, 1984, pp 809-918.

Shriver, D.F.; Drezdon, M.A. *Manipulation of Air Sensitive Compounds*, 2nd. ed., Wiley Interscience: New York, 1986.

Simchen, G.; Kober, W. *Synthesis* **1976**, 259.

Smith, R.N. *Quarterly Rev.* **1959**, *13*, 287.

Smolin, E.M.; Rapapport, L. *S-Triazenes and their Derivatives*, Interscience Pub.: New York, 1959, pp 48-90.

Sogah, D.Y. *Polym. Prepr. (Am. Chem. Soc., Div. Polym. Chem.)* **1986**, *27(1)*, 163.

Sogah, D.Y.; Hertler, W.R.; Webster, O.W.; Cohen, G.M. *Macromolecules* **1987**, *20*, 1473.

Stang, P.J.; Hanack, M.; Subramanian, L.R. *Synthesis* **1982**, 85.

Steglich, W.; Höfle, G.; *Angew. Chem. Intern. Ed.* **1969**, *8*, 981.

Studebaker, M.L. In *Proceeding of the Fifth Conference on Carbon, Penn. State, 1961*, vol.II, Pergamon Press: New York, 1963, pp 189-197.

Taylor, E.C.; McLay, G.W.; McKillop, A. *J. Amer. Chem. Soc.* **1968**, *90*, 2422.

Takeda, N.; Inoue, S. *Makromol Chem.* **1978**, *179*, 1377.

Tennet, H. U.S. Pat. No. 4,663,230.

- Tse, D.C.S.; Kuwana, T.; Royer, G.P. *J. Electroanal. Chem.* **1979**, *98*, 345.
- Tsubokawa, N.; Fujiki, K.; Sone, Y. *J. Polym. Sci., Polym. Chem. Ed.* **1986**, *24*, 191.
- Varma, A.J.; Jog, J.P.; Nadkarni, V.M. *Makromol. Chem., Rapid Commun.* **1983**, *4*, 715.
- Venter, J.J.; Vannice, M.A. *Appl. Spectrosc.* **1988**, *42*, 1096.
- Villars, D.S. *J. Amer. Chem. Soc.* **1947**, *69*, 214.
- Vowinkel, E. *Chem. Ber.* **1962**, *95*, 2997.
- Wagner, C.A.; Riggs, W.M.; Davis, L.E.; Moulder, J.F. *Handbook of X-ray Photoelectron Spectroscopy*, Muilenberg, G.E. ed., Perkin-Elmer: Eden Prairie Minn., 1979.
- Ward, W.J.; McCarthy, T.J. In *Encyclopedia of Polymer Science and Engineering*, 2nd ed.; Supplement, Wiley: New York, 1989; pp 674-689.
- Webster, O.W.; Hertler, W.R.; Sogah, D.Y.; Farnham, W.B.; RajanBabu, T.V. *J. Amer. Chem. Soc.* **1983**, *105*, 5706.
- Wong, S.-W.; Frisch, K.C. In *Advances in Urethane Science and Technology*, Vol. 10, Frisch, K.C.; Klempner, D. eds., Technomic Pub. Co.: Stamford Conn., pp 49-75.
- Wulfman, D.S.; Linstrumelle, G.; Cooper, C.F. In *Chemistry of the Diazonium and Diazo Group Pt. 2*, Patai, S. ed., Wiley: New York, 1978, pp 821-976.
- Wulfman, D.S.; Poling, B. In *Reactive Intermediates*, Vol. 1, Abromavitch, R.A. ed., Plenum Press: New York, 1980, pp 321-512.
- Xie, Y.; Sherwood, P.M.A. *Appl. Spectrosc.* **1989**, *43*, 1153.
- Yacynych, A.M.; Kuwana, T. *Anal. Chem.* **1978**, *50*, 640.
- Yasuda, T.; Aida, T.; Inoue, S. *Macromolecules* **1983**, *16*, 1792.
- Yoshino, K.; Yanagida, S.; Sakai, T.; Azuma, T.; Inui-shi, Y.; Sakurai, H. *Jpn. J. Appl. Phys.* **1982**, *21*, L301.



Yu, H.-S.; Choi, W.-J.; Lim, K.-T.; Choi, S.-K. *Macromolecules* **1988**, *21*, 2894.

Zawadzki, J. *Chem. and Phys. of Carbon* **1989**, *21*, 147.



